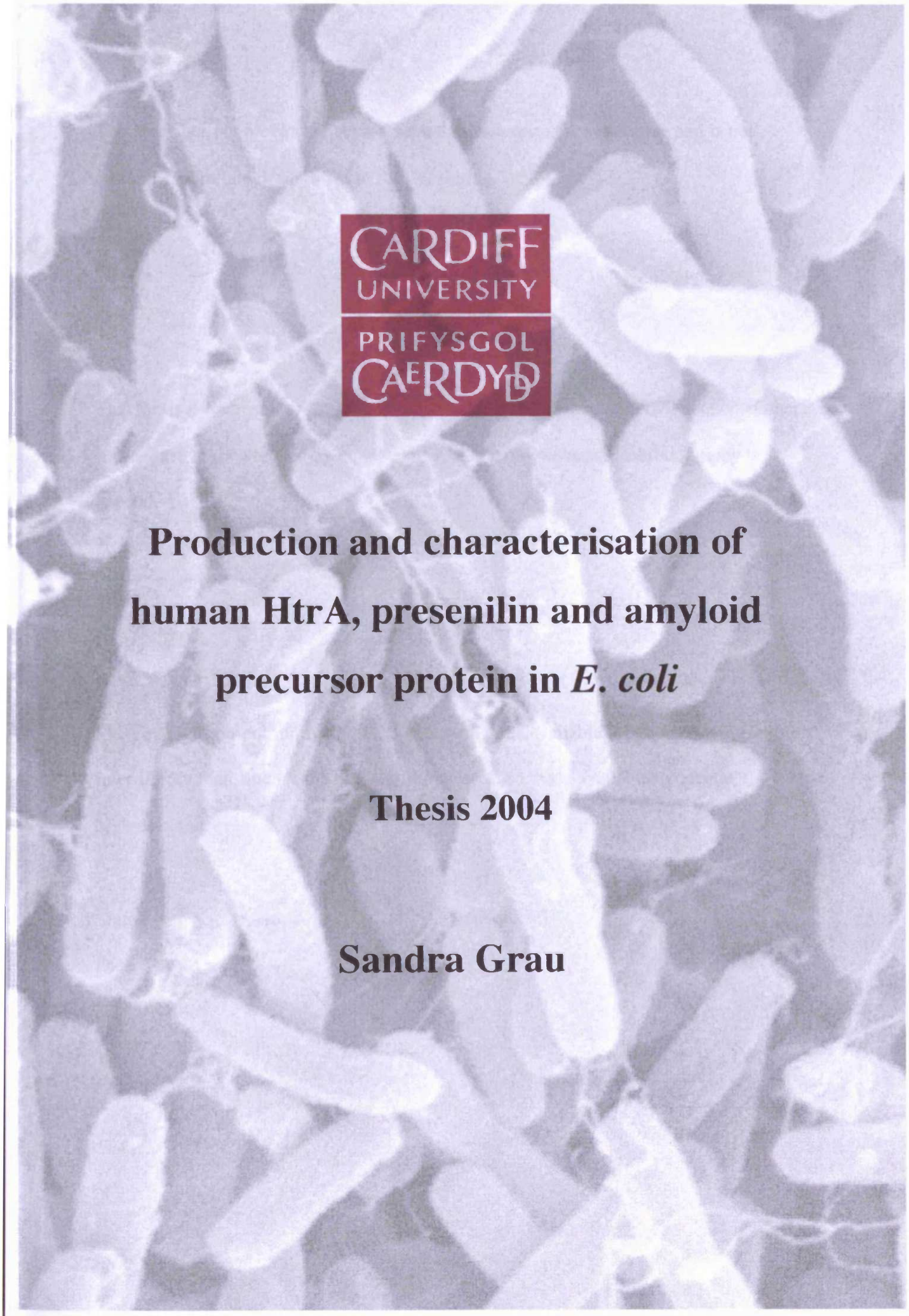

Production and characterisation of human HtrA, presenilin and amyloid precursor protein in *E. coli*

Thesis 2004

Sandra Grau

ProQuest LLC
789 East Eisenhower Parkway
P.O. Box 1346
Ann Arbor, MI 48106-1346

Acknowledgements

Firstly, I would like to take the opportunity to thank Prof. Michael Ehrmann for offering me this interesting project and his encouragement throughout my work during the last four years. I was most appreciative of the fact that he always had time to talk about problems or new ideas. His enthusiasm was most helpful during times when nothing really wanted to work.

I would like to thank Prof. John Kay and Prof. Rob Beynon for reading my reports and agreeing to be my internal and external examiners respectively.

I am grateful to Dr. Simon Jones and Dr. Peter Richards for providing me with all the arthritis samples and for giving me an insight into the processes involved in this disease.

A big thanks goes to my lab mates Alexandra Beil, Mona Harnasch, Tanja Henrichs, Markus Eser, Sarah Amir and Natasha Mikhaleva for the warm and friendly atmosphere in the lab. Thank you Alexandra for providing me with MalS, Markus for providing me with TreA and Mona for brainstorming with me all the time about Alzheimer´s disease.

Further thanks goes to Prof. Christian Haass, Dr. Manuel Than and Prof. Bode for giving me the opportunity to work at the Max-Planck Institut in Munich, Prof. Weiming Xia and Dr. Hans-Rudi Loetscher (LaRoche, Basel) for their collaboration and Dr. Tim Clausen for the pictures of the DegP structure.

Finally, I would like to thank my family, especially my parents, for their financial and emotional support during the last four years.

Table of contents

Abstract

The human serine protease L56 is thought to be a mediator in diseases such as arthritis and cancer although its precise function is unknown. L56 may also play a role in Alzheimer's disease due to an interaction with the γ-secretase component presenilin 1 (PS1) which is thought to cleave C99 (a fragment of the amyloid precursor protein) to produce Aβ peptides. However, information regarding the function of L56 and its interaction with C99 and PS1 is limited. The present report describes the production and characterisation of recombinant L56, PS1 and C99 and their potential involvement in human disease was also investigated. Full-length *l56* and a truncated form (*Δmac25l56*) were cloned and expressed in *E. coli*. Δmac25L56 was purified by affinity and ion exchange chromatography. Subsequent gel filtration chromatography suggested a trimeric oligomerisation state. For initial biochemical characterisation, protease assays were performed using resorufin-labelled casein as a substrate. Δmac25L56 showed a typical biphasic temperature-dependent curve with an optimum of proteolytic activity at 47°C. Proteolytic activity was detected between pH 7.5 and 10.5. Furthermore, proteolytic activity increased with salt concentrations from 0 to 60 mM and remained unchanged up to 1 M NaCl. The ability of L56 to act as both a protease and chaperone was investigated in refolding assays using chemically denatured α-amylase MalS from *E. coli* as a substrate. Chaperone activity could be detected for a proteolytically inactive L56 mutant (the active site serine residue was exchanged to alanine) but not for the wild type protein.

Western blot analysis indicated that full-length L56 is present in synovial fluids from rheumatoid arthritis and osteoarthritis patients and in white blood cells and serum from healthy human donors. Protease assays with synovial fluid and purified Δmac25L56 demonstrated the presence of at least two substrates for L56. In addition to these findings, L56 was also shown to have a potential role in Alzheimer's disease through its interaction with C99 and PS1, both of which are thought to be pivotal in the progression of this degenerative disease. Both C99 and PS1 were produced in *E. coli* and their interaction was verified by a stabilisation assay performed in *E. coli* and by co-purification using affinity chromatography. Interaction of PS1 and Δmac25L56 was also confirmed by co-purification. Protease assays with purified Δmac25L56, purified or membrane bound C99 and solubilised PS1 suggested that C99 is degraded by Δmac25L56. Degradation was not observed in the absence of PS1, suggesting that when C99 is bound to PS1, it is no longer accessible to L56 dependent processing.

These data indicate that recombinant techniques can be used to produce proteolytically active L56 and to identify interaction partners and substrates. Thus, *E. coli* may serve as an alternative model system to advance our understanding of the function of human proteins involved in for example Alzheimer's disease and arthritis.

1.1 Abbreviations

Aβ	β fragment of APP
AD	Alzheimer's disease
ApoE	apolipoproteinE
AP	alkaline phosphatase
APP	amyloid precursor protein
sAPPα and sAPPβ	soluble N-terminal APP fragment
APS	ammonium persulphate
amp	ampicillin
BACE	ß-amyloid cleaving enzyme
BCA	bicinchoninic acid
BSA	bovine serum albumin
C83 and C99	C-terminal fragments of APP
CHAPSO	3-[(3-cholamidopropyl)dimethylammonio]-2-hydroxy-1-propanesulphonate
CIAP	calf intestine alkaline phosphatase
cm	chloramphenicol
COMP	cartilage oligomeric matrix protein
CV	column volumes
DegP	bacterial HtrA
DDM	dodecylmaltoside
DFP	diisopropyl fluorophosphate
DMF	N,N-dimethylformamide
DMSO	dimethyl sulphoxide
DTT	dithiothreitol
dNTP	deoxynucleotides
ECM	extracellular matrix
ER	endoplasmic reticulum
FAD	familial Alzheimer's disease

FCS	foetal calf serum
GST	glutathione-S-transferase
h	hours
IAP	inhibition of apoptosis proteins
IGF	insulin-like growth factor
IGFBP	insulin-like growth factor binding proteins
IPTG	isopropyl-ß-D-thiogalactoside
Kb	kilo basepair
kDa	kilo Dalton
MBP	maltose binding protein
min	minutes
NBT	4-nitroblue-tetrazoliumchloride
neo	neomycin
NGF	neuronal growth factor
NHS	normal human serum
NicA	nicastrin
NICD	Notch intracellular domain
NPG	4-nitrophenyl-α-D-hexa(1-4)-glucopyranoside
OA	osteoarthritis
ODx	optical density
Omi	human HtrA2
o/n	overnight
PAGE	polyacrylamide gel electrophoresis
PMA	phorbol myristate acetate
P1	peptide 1
PCR	polymerase chain reaction
PDZ	protein-protein interaction domain
PS1	presenilin 1
PS2	presenilin 2

PS1Δ9	PS1 with deletion of the exon9 region
PSAP	presenilin associated protein
RA	rheumatoid arthritis
rpm	revs per minute
RT	room temperature
RIP	regulated intramembrane proteolysis
S1	subsite 1
SAP	shrimp alkaline phosphatase
SDS	sodium dodecyl sulphate
SREBP	sterol regulatory element-binding proteins
ss	signal sequence
TAE	Tris acetate EDTA
TACE	tumour necrosis factor-α-converting enzyme
TBS	Tris buffered saline
TBS-T	Tris buffered saline with Tween-20
TCA	trichloroacetic acid
TM	transmembrane segment
TNF	tumour necrosis factor
TSS	transformation and storage solution
TEMED	N,N,N′,N′-tetramethylenediamine
wt	wild type
XP	5-bromo-4-chloro-3-indolylphosphate

2 Introduction

2.1 Proteolysis and proteolytic enzymes

Proteases and chaperones serve in quality control of cellular proteins. Their substrates are misfolded and partially folded proteins, arising from slow rates of folding or assembly, environmental stress, and intrinsic structural instability. The decision as to whether a protein is degraded or repaired, is not completely understood, but the state of misfolding might be critically involved.

2.1.1 Physiological significance of proteolysis

It is useful to distinguish between two functions for protein degradation in growing cells (Maurizi, 1992). Some substrates are degraded to rid the cell of damaged or non-functional proteins or peptides (housekeeping degradation); for other substrates, degradation is used to regulate the level of a functional protein (regulatory degradation).

2.1.1.1 Housekeeping degradation

A few normal cellular processes are known that generate substrates for housekeeping degradation. For example, signal peptides cleaved from secreted proteins are degraded so rapidly that they are difficult to detect experimentally (Miller and Conlin, 1994). Many other processes occurring in growing cells may generate substrates requiring degradation. Translational errors are likely to lead to the formation of misfolded polypeptides that are proteolytic substrates. Other processes (for example heat shock or other stresses that cause folding problems) may damage normally stable proteins, converting them into degradable substrates. A surprisingly large number of processes can lead to protein damage that might generate hyperdegradable proteins (Stadtman,

1990). For example, starvation for any of a variety of required nutrients leads to an elevated rate of degradation of proteins that are stable in growing cells (Miller, 1987). In general, it is thought that misfolded proteins are exposing hydrophobic patches on their surface and that this property is responsible for targeting to one of the many housekeeping proteases. As misfolded proteins tend to aggregate, it is of vital importance for cells to remove damaged proteins (Kopito, 2000).

Proteases that have broad substrate specificity can also be used as tools to identify protein domains or folding intermediates. As many proteases are recognising and cleaving unstructured regions, they are routinely used in so called limited proteolysis experiments (for review see Hubbard, 1998). For example, individual domains of multidomain proteins are connected by linker regions that are susceptible to protease treatment. The same strategy can be applied to identify partly folded states of a given protein (see for example Polverino de Laureto *et al.*, 1999, 2001 and 2002; Tsai *et al.*, 2002). Other applications include probing of conformations of native proteins such as protease inhibitors and avidin (Ellison *et al.*, 1995, Hubbard *et al.*, 1991)

2.1.1.2 Regulation by proteolysis

Several important cellular regulatory systems involve rapidly degraded proteins as a key element. For a protein to function in regulation, either its activity or its level (or both) must respond to a regulatory signal. For regulatory proteins (e.g. the lactose repressor LacI) the activity of the regulator is affected, usually as the result of a conformational change induced by binding an effector. However, in other cases, the level of the regulator responds to the signal, and in a few cases, the level of the regulator is determined mainly by its susceptibility to proteolysis. The regulatory protein (e.g. the regulatory subunits sigma32 or sigmaS of RNA polymerase) is unstable under normal conditions ("constitutively unstable") (Gottesman, 1989) and in response to a regulatory signal, its degradation is inhibited or its rate of synthesis is elevated above the capacity of the degradation apparatus. In other cases, the regulatory protein is normally stable and becomes unstable in response to a regulatory signal. A classic example is the LexA protein, which is a repressor of the promoter region of UV-induced genes (Walker, 1987).

2.1.2 Classification of peptidases

There are three major criteria in use for the classification of peptidases: (1) the reaction catalysed, (2) the chemical nature of the catalytic site, and (3) the evolutionary relationship, as revealed by structure (Barrett, 1994). By these three criteria, it is possible to distinguish between exopeptidases, which act only near the ends of polypeptide chains, and endopeptidases, which act preferentially in the inner regions of peptide chains, away from the termini (Barrett, 1994). The criterion of the chemical nature of the catalytic site leads to a further division of the endo- and exopeptidases into four groups (the serine-type peptidases, the cysteine-type peptidases, the aspartic-type endopeptidases, and the metallopeptidases). The serine-type peptidases have an active site serine involved in the catalytic process, the cysteine-type peptidases have a cysteine residue in the active site, the aspartic-type endopeptidases depend on two aspartic acid residues for their catalytic activity, and the metallopeptidases use a metal ion (commonly zinc) in the catalytic mechanism. The third criterion includes the evolutionary and structural relationships among the enzymes as well as the comparison of the primary amino acid sequences. This method is very useful because the structural similarities within a family of peptidases commonly reflect important similarities in catalytic mechanism and other properties (Barrett, 1994).

2.1.2.1 Families of serine peptidases

Proteolytic enzymes dependent on a serine residue for catalytic activity are widespread and very numerous. Serine peptidases are found in all living organisms and they include exopeptidases as well as endopeptidases. By the criteria mentioned above, it is possible to distinguish between 20 families of serine proteases. On the basis of three-dimensional structures and sequence comparisons, most of these families can be grouped together into about six clans that may well have common ancestors. However, the structures that are known for members of four of the clans, chymotrypsin, subtilisin, carboxypeptidases C, and D-Ala-D-Ala peptidase A from *Escherichia coli*, show them to be totally unrelated. This would imply that there are at least four separate evolutionary origins of serine peptidases (Rawlings and Barrett, 1994).

There are similarities in the reaction mechanism for several of the peptidases with different evolutionary origins. Thus, the peptidases of the chymotrypsin, subtilisin, and carboxypeptidase C clans have in common a "catalytic triad" comprised of the three amino acids: serine (nucleophile), aspartate (electrophile), and histidine (base). The geometric orientations of these are very similar between families, despite the fact that the protein folds are quite different. The way in which certain glycine residues tend to be conserved in the vicinity of the catalytic serine residue in the first serine peptidases to be sequenced, to form the motif Gly-X-Ser-Y-Gly led to an early expectation that this motif would be found in all serine peptidases. Although it is true that most of the families show conserved glycine residues near the essential serine residue, their exact positions are variable (Rawlings and Barrett, 1994).

2.1.2.2 Mechanism of serine proteases and substrate specificity

Most serine proteases contain the typical "histidine, aspartate, serine" catalytic triad. Recently, serine proteases with novel catalytic triads and dyads have been discovered (Blow, 1997; Hedstrom, 2002). The catalytic triad spans the active site cleft with Ser195 on one side and Asp102 and His57 on the other side (using the chymotrypsin numbering). Within the active site, the hydroxyl oxygen of the catalytic serine becomes a more potent nucleophile by the presence of the basic side chain of histidine. Furthermore, the positive charge that develops at the histidine side chain is stabilised by the negatively charged side chain of the aspartate. In the acylation half of the reaction (Fig. 2.1), the active site serine attacks the carbonyl carbon of the peptide substrate with support from the active site histidine to generate a tetrahedral intermediate. The resulting His-H^+ is stabilised by the active site aspartate (Fig. 2.1). The oxyanion of the tetrahedral intermediate is stabilised in the oxyanion hole which is formed by the backbone NHs of Gly193 and the active site serine (Ser195) (Fig. 2.2). Subsequently, the tetrahedral intermediate collapses and forms the acylenzyme intermediate (Fig. 2.1). In the deacylation half of the reaction, water attacks the acylenzyme intermediate supported by the active site histidine and forms a second tetrahedral intermediate. This intermediate disintegrates and releases the active site serine and the carboxylic acid product (Hedstrom, 2002) (Fig. 2.1).

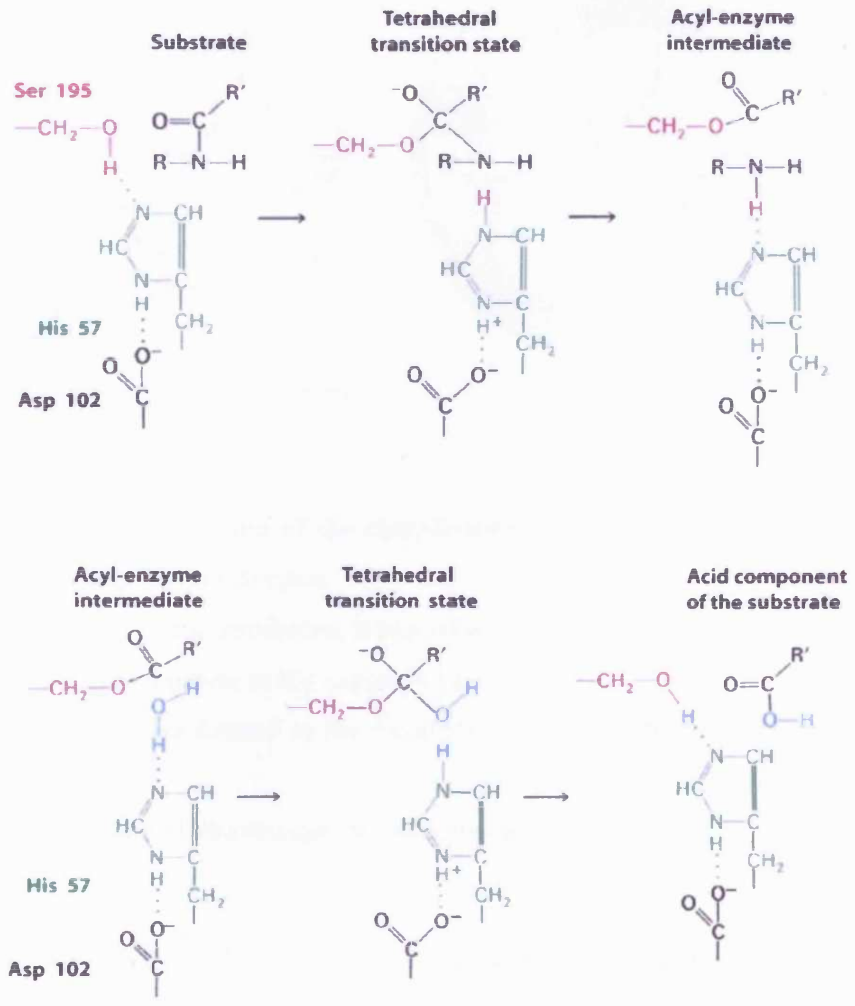

Fig. 2.1 The mechanism of chymotrypsin.

The catalytic cycle is schematically shown. It can be divided into two steps (shown in the upper and lower parts, respectively). Acylation (including extraction of a proton from S195 by H57, attack of the scissile peptide bond by S195 and formation of the tetrahedral intermediate, donation of a proton to the peptide nitrogen by His 57, cleavage of the peptide bond and release of the first product) and Deacylation (including attack of the acyl-enzyme intermediate by H_2O that donates a proton to H57, the remaining OH attacks the acyl carbon and H57 donates a proton to the S195 oxygen. The ester bond is cleaved and the second product is released).

(Taken from srv2.lycoming.edu/~newman/courses/bio44403/catalysis.ppt)

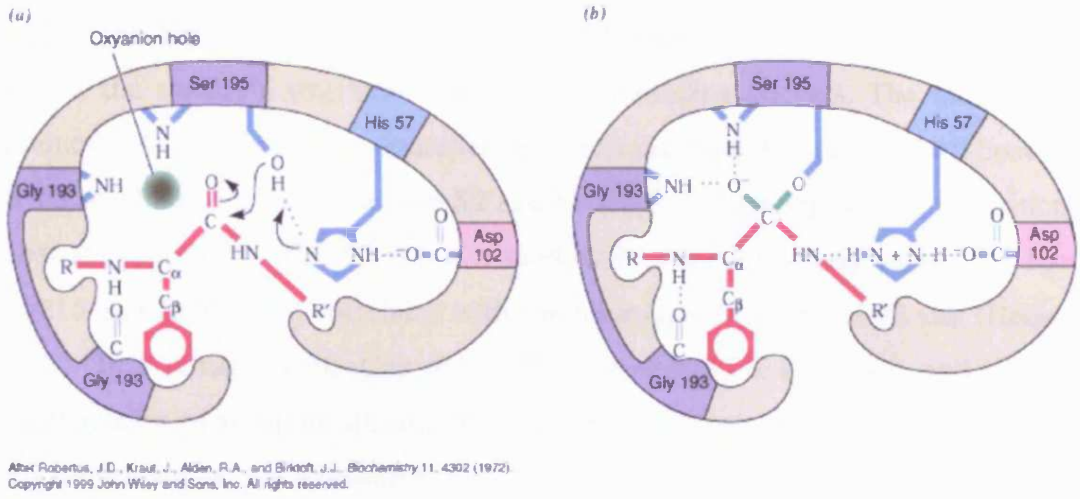

Fig. 2.2 Schematic representation of the contribution of the oxyanion hole to the enzymatic mechanism of chymotrypsin.

a) During the formation of the tetrahedral intermediate, the carbonyl oxygen obtains a partial negative charge and moves to the oxyanion hole.

b) Two hydrogen bonds are formed in the oxyanion hole that stabilise the transition state.

The substrate is shown in red, the residues of chymotrypsin in blue.

Digestive proteases such as trypsin and chymotrypsin cleave their substrate after positively charged or hydrophobic residues, respectively (Blow, 1997; Hedstrom, 2002). The features that determine substrate specificity can be rationalised by the topology of the substrate binding sites that lie adjacent to the active site and the binding pockets for the side chains of the peptide substrate. Studies on protease specificity usually focused on the P1/S1 interaction (based on the nomenclature of Schechter and Berger (1967). P1 (peptide 1) represents the first residue of the N-terminal side of the scissile bond. The subsites on the protease, for example S1 (subsite 1) interact with the substrate. In chymotrypsin, residues 189-192, 214-216 and 224-228 form the S1 pocket and the specificity is determined by residues 189, 216 and 226 (Perona and Craik, 1995; Czapinska and Otlewski, 1999). In chymotrypsin, Ser189, Gly216 and Gly226 create a deep hydrophobic pocket that binds to hydrophobic residues of the substrate. In contrast, in trypsin Asp189, Gly216 and Gly226 create a negatively charged S1 site that

interacts with Arg or Lys at the P1 site in the substrate (Huber *et al.*, 1974; Hedstrom, 2002). Elastase prefers small aliphatic residues at P1 because the S1 site consists of Val216 and Thr226 (Shotton and Watson, 1970; Hedstrom, 2002). Beyond the S1 site pocket, the substrate interacts with additional binding pockets. The main chain of residues 214-216 forms an antiparallel beta sheet and interacts with the backbone of the P1-P3 residues of a substrate. The S2 and S3 sites of chymotrypsin are not critical for substrate specificity. The S2 site is a shallow hydrophobic group formed by His 57, Trp215 and Leu99 and correlates with the hydrophobicity of the P2 site (Hedstrom, 2002). In contrast in elastase the P3/S3 interaction is dominant and critical in determination of substrate specificity (Stein *et al.*, 1987; Bode *et al.*, 1989). Additional structural features that generate variations in substrate specificity and enzyme activity are ions such as Na^+ and Ca^{2+}, surface insertion loops and exosites that are linked to the polypeptide binding sites and active site (DiCera and Krem, 2003).

2.1.2.3 Function of propeptides

Serine proteases are synthesized as inactive proenzymes (zymogens) with an N-terminally localised propeptide (also known as prosegment or activation peptide). These propeptides range in size from dipeptides to units of more than several hundred amino acids (Khan and James, 1998; Kardos *et al.*, 1999; Lazure, 2002). Pancreatic zymogens such as chymotrypsinogen, trypsinogen and proelastase contain short propeptides (6-15 amino acids). Proteases of the coagulation system such as plasminogen have large propeptides with several domains called kringle domains (Kardos *et al.*, 1999). Propeptides suppress enzymatic activity by masking the catalytic machinery (active site residues and oxyanion hole) and preventing the formation of the catalytic intermediate (Khan and James, 1998). Post-translational cleavage of this propeptide is either achieved by peptidases or through autocatalysis. The trigger for cleavage could be an enzymatic or nonenzymatic cofactor or a simple change in pH that results in autocatalysis (Khan and James, 1998). The propeptide is then further degraded or as in the case of chymotrypsinogen and proelastase2, remains attached to the enzyme via a disulphide bond and stabilizes the formed active site (Kardos *et al.*, 1999). Furthermore, propeptides can act as intramolecular chaperones, assisting the peptidase to fold and

target subunit oligomerisation (e.g. in the proteasome) (Lazure, 2002). Propeptide is not required for the correct folding of proteases such as trypsinogen, chymotrypsinogen, proelastase and also viral peptidases such as HIV-1 protease due to its size (Khan and James, 1998).

2.1.2.4 The chymotrypsin subfamily

The members of this family (belonging to the SA clan) are commonly secreted proteins. Each is synthesised with a signal peptide that targets it to the secretory pathway. Proteolytic activation of the proenzymes occurs extracellularly or sometimes in storage organelles. Functions are occasionally intracellular, as in intracellular digestion of bacteria by neutrophils, but most commonly extracellular. Examples of extracellular functions are digestion of food proteins in the intestine by the enzymes from pancreas, and coagulation, fibrinolysis, and complement activation by the enzyme systems in the plasma. Most of these enzymes are monomers, but there are also some oligomers such as tryptase, which is a homotetramer (Bode *et al.*, 1998; Bode *et al.*, 2002).
HtrA is defined within the SA clan as SIC protease. Most of the 180 members of this family contain at least one C-terminal PDZ domain, which is a protein-protein interaction domain (Clausen *et al.* 2002). PDZ domains are named after the three proteins in which they were first identified, postsynaptic density protein-95 PSD-95 (Cho *et al.*, 1992), *Drosophila* discs large tumour suppressor Dlg (Woods and Bryant, 1991), and the tight junction protein ZO-1 (Itoh *et al.*, 1993).

2.1.3 The human serine protease L56

Two groups discovered L56, a human serine protease of unknown function, which is also called ORF480 or HtrA1. Zumbrunn and Trueb (1996) identified L56 as a transformation-sensitive protein, that is, after transformation of normal human fibroblasts with the oncogenic virus SV40, the expression of the protein disappears. Furthermore, Hu *et al.*, (1998) detected a 7-fold increase in L56 mRNA and protein levels in osteoarthritic cartilage.

The L56 mRNA is strongly expressed in placenta, moderately in brain, liver and kidney and weakly in lung, skeletal muscle, heart and pancreas (Zumbrunn and Trueb, 1996). Because of its signal sequence, L56 might be translocated into the ER and transported through the Golgi-network to the extracellular matrix (ECM) (Hu *et al.*, 1998). The gene for L56, called PRSS11, is situated at a single locus on the long arm of chromosome 10 (Zumbrunn and Trueb, 1996).

2.1.3.1 Structure of L56

Mature L56 has a molecular mass of 51 kDa. It is synthesised as a precursor protein with an N-terminal signal sequence of 22 residues (Fig. 2.3). This signal sequence is followed by a 117 residues long domain (residues 23-140) that exhibits high similarity to IGFBPs (Insulin-like growth factor binding proteins) and is called mac25 domain. The identity with IGFBP-3 is 44%. The identity with IGFBP-5 is 42% and the similarity is 55%. One characteristic of this domain is a conserved cluster of 12 cysteine residues which may form several disulphide bonds (Zumbrunn and Trueb, 1996). The following overlapping segment (residues 97-155) shows high similarity to the Kazal-type-inhibitor motif (Fig. 2.3), a serine protease inhibitor motif also found in human pancreatic trypsin inhibitor.

An alignment of the human pancreatic trypsin inhibitor (Horii *et al.*, 1987) with this region of L56 revealed 32% sequence identity or 53% sequence similarity. With human follistatin, which harbours several Kazal-type inhibitor motifs (Shimasaki *et al.*, 1988), the identity was 42% (60% similarity). Follistatin is a specific inhibitor of the biosynthesis and secretion of follicle stimulating hormone. The Kazal-type inhibitor motif contains a conserved tyrosine residue and six cysteine residues, which are arranged in three disulphide bonds. L56 contains four of the six conserved cysteine residues which can form two of the three disulphide bonds, and the conserved tyrosine residue. It is therefore possible that the related segment of the L56 protein will fold into a tertiary structure resembling that of trypsin inhibitor (Zumbrunn and Trueb, 1996).

M Q I P R A A L L P L L L L L L A A P A S A Q L S R A G R

S A P L A A G **C** P D R **C** E P A R **C** P P Q P E H **C** E G G R A

R D A **C** G **C** **C** E V **C** G A P E G A A **C** G L Q E G P **C** G E G L

Q **C** V V P F G V P A S A T V R R R A Q A G L **C** V **C** A S S E

P V **C** G S D A N T Y A N L **C** Q L R A A S R R S E R L H R P

P V I V L Q R G A **C** G Q G Q E D P N S L R H K Y N F I A D

V V E K I A P A V V H I E L F R K L P F S K R E V P V A S

G S G F I V S E D G L I V T N A **H** V V T N K H R V K V E L

K N G A T Y E A K I K D V D E K A **D** I A L I K I D H Q G K

L P V L L L G R S S E L R P G E F V V A I G S P F S L Q N

T V T T G I V S T T Q R G G K E L G L R N S D M D Y I Q T

D A I I N Y G N **S** G G P L V N L D G E V I G I N T L K V T

A G I S F A I P S D K I K K F L T E S H D R Q A K G K A I

T K K K Y I G I R M M S L T S S K A K E L K D R H R D F P

D V I S G A Y I I E V I P D T P A E A G G L K E N D V I I

S I N G Q S V V S A N D V S D V I K R E S T L N M V V R R

G N E D I M I T V I P E E I D P

Fig. 2.3 Amino acid sequence of L56.

L56 protein consists of a signal sequence (red), a mac25 domain (black) and a HtrA domain (blue). The Kazal-type inhibitor like motif and the PDZ domain are underlined in black and yellow, respectively. L56 contains only 5 of the 6 conserved cysteine residues found in Kazal-type inhibitor motifs. The cysteine residues and the amino acids HDS of the catalytic triad are shown in bold.

The C-terminal part of the L56 protein (residues 140-480) contains the catalytic triad (histidine, aspartate and serine residues) and the conserved sequence GNSGG in the active site. This part of L56 was found to be highly related to the family of the HtrA or Do proteases from bacteria (Lipinska *et al.*, 1988; Seol *et al.*, 1991; Skorko-Glonek *et al.*, 1995). A comparison with DegP (bacterial HtrA) from *E. coli* showed 32% sequence identity or 58% similarity.

The PDZ domain of L56 is located at its very C-terminus. These domains have been reported to be involved in a variety of functional protein-protein interactions that can initiate signal transduction and the formation of receptor-membrane complexes (Fanning and Anderson, 1998; Mueller *et al.*, 2000; Ponting, 1997; Songyang *et al.*, 1997).

2.1.3.2 Function of L56

In bacteria, HtrA is a critical component of the universal cellular response to stress which is characterised by the induction of a set of so-called heat-shock proteins (Neidhardt, 1984). In addition to temperature elevation, heat-shock proteins are induced by oxidative stress (Christman *et al.*, 1985), viral phage infection (Bahl *et al.*, 1987), ethanol, and intracellular expression of aberrant proteins. The DegP protein enables bacteria to survive at elevated temperatures. Although L56 does not appear to be inducible by elevated temperatures, it could be upregulated by a more general stress pathway. This model is supported by upregulation of L56 during osteoarthritis (Hu *et al.*, 1998) and ageing (Ly and Handelsman, 2002). Furthermore, there is evidence that L56 might have a tumour suppressor function. Expression of *l56* is absent after transformation of normal human fibroblasts with SV40 (Zumbrunn and Trueb, 1996). In addition, recent studies reported that L56 mRNA was either absent or significantly reduced in ovarian cancer (Shridhar *et al.*, 2002) and overexpression of *l56* inhibited proliferation *in vitro* and tumour growth *in vivo* (Baldi *et al.*, 2002).

When *l56* was expressed in the baculovirus-infected *Drosophila* cell line Sf9 and the human cell line HEK-293, proteolytic activity was detected in both cases (Hu *et al.*, 1998). Incubation of purified L56 with ß-casein results in the generation of specific proteolytic cleavage products of this substrate (Hu *et al.*, 1998). However, natural

substrates of this protease remain to be identified. Because of its hypothetical localisation in the ECM and its proposed involvement in arthritis and tumour progression/invasion, possible substrates for L56 could be other proteases, ECM proteins, growth factors and proteins that modulate growth factors (Hu *et al.,* 1998). Unpublished data showed that L56 is able to degrade the extracellular matrix proteins, COMP (cartilage oligomeric matrix protein), fibronectin and fibromodulin (46th and 47th Annual Meeting, Orthopaedic Research Society, March 2000, Orlando Florida and February 2001, San Francisco California).

L56 contains a mac25 domain related to IGFBPs, which are involved in the binding and storage of insulin-like growth factor (IGF) (Zumbrunn and Trueb, 1998; Baxter, 2000). There are two IGFs (I and II) and their activity is modulated by IGFBPs. Six IGFBPs occurring in most tissues and body fluids have been characterised so far (Baxter, 2000). They bind IGF I and IGF II with similar affinity and appear to function as a reservoir for growth factors. The IGFs are liberated from the complex by specific proteases (Baxter, 2000; Claussen *et al.*, 1997; Fowlkes *et al.*, 1994; Zheng *et al.*, 1998). It is thought that IGFBP-2 and IGFBP-5 are cleaved by serine proteases because DFP and other serine protease inhibitors can prevent cleavage (Clemmons, 1998). There are two mechanisms whereby IGF II and I could activate proteases (Fowlkes and Freemark, 1992). First, the growth factor binds directly to the protease and leads to activity or second, binding of IGFs may enhance the susceptibility of the IGFBP to proteolytic cleavage.

However, Kato *et al.* (1996) noted that mac25 is more closely related to follistatin, an activin-binding protein that is a specific inhibitor of the biosynthesis and secretion of follicle stimulating hormone. Activin and inhibin belong to the tumour growth factor β superfamily and are involved in several processes such as embryogenesis, osteogenesis and reproductive physiology. Therefore, it is possible that L56 is involved in cell growth regulation perhaps via a modulation of growth factor systems other than IGF, e.g. the activin/inhibin system.

Furthermore, the Kazal-type-inhibitor motif, which is conserved in a diverse group of serine protease inhibitors, also occurs within mac25, follistatin and agrin (Hu *et al.,* 1998). Agrin and agrin-related proteins appear to function as extracellular components that bind to and regulate the activity of growth factors (Hu *et al.,* 1998). Recombinant agrin has been shown to inhibit serine proteases of the trypsin class but not the thrombin

class. The presence of this protease inhibitor motif suggests that L56 may be a self-regulating enzyme.

2.1.3.3 The bacterial homologue DegP from *E. coli*

DegP is an ATP-independent serine protease in the periplasm of *E. coli* (Seol *et al.*, 1991). Null mutants of DegP were either unable to grow at elevated temperatures or failed to digest misfolded proteins in the periplasm (Clausen *et al.*, 2002). DegP levels are controlled by the heat-shock factor σ^{24} under stressful conditions (Lipinska *et al.*, 1990; Seol *et al.*, 1991). The main function of DegP is the degradation of unfolded or misfolded proteins in the periplasm. It has been proposed that it preferentially cleaves peptide bonds of Val-X or Ile-X of which X can be any amino acid (Kolmar *et al.*, 1996). Except for DFP, none of the routinely used inhibitors for trypsin and chymotrypsin nor metal chelators inhibit DegP proteolytic activity (Swamy *et al.*, 1983). DegP can function as a protease and as a chaperone and these activities switch in a temperature dependent manner. Below 20°C, almost no proteolytic activity but chaperone activity is detectable whereas above 30°C, the proteolytic activity increases rapidly in a non-linear manner (Skorko-Glonek *et al.*, 1995; Spiess *et al.*, 1999). Only in a proteolytically inactive DegPS210A mutant, is the chaperone activity present at low and high temperatures (Spiess *et al.*, 1999).

2.1.3.3.1 Structure and mechanism of DegP

DegP is synthesised as a 51 kDa precursor protein with an N-terminal signal sequence of 26 residues (Lipinska *et al.*, 1988). After cleavage of the signal sequence, the mature protein has a molecular mass of 48 kDa. A domain of 50 residues of unknown function follows the signal sequence. The next 30 residues are proline-, serine- and glutamine-rich and have characteristics of a Q-linker. A Q-linker is a flexible segment that is able to connect two domains (Wootton and Drummond, 1989). The main part of the protein is the catalytic domain with the active site Ser210 (Lipinska *et al.*, 1990) that is part of the catalytic triad (His105, Asp135, Ser210) (Fig. 2.4), which is typical for trypsin-like

serine proteases (Rawlings and Barrett, 1994). As expected, mutations in Ser210 or His105 lead to a loss of proteolytic activity (Skorko-Glonek *et al.*, 1995). DegP also contains two PDZ domains at the C-terminus that are believed to be involved in substrate recognition.

The crystal structure of DegP indicated a hexameric conformation (Fig. 2.5) that is formed by staggered association of two trimeric rings (Krojer *et al.*, 2002). Trimerisation involves several, mainly hydrophobic residues of the protease domains. The two trimers (Fig. 2.5 B) are connected by a long loop LA (Fig. 2.6) that appears to be essential for hexamer formation. The LA loops of opposing trimers are wound around each other to form the corner pillars of the DegP cage (Fig. 2.5 B).

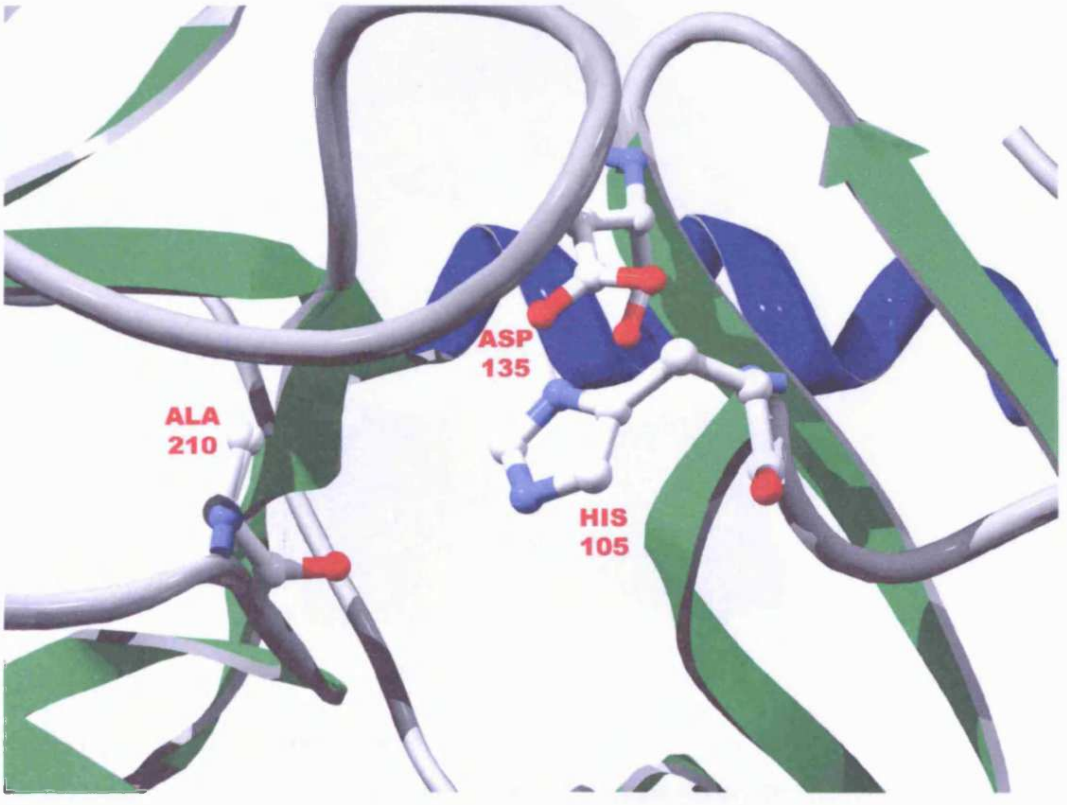

Fig. 2.4 Arrangement of the catalytic triad in DegP

The three residues of the catalytic triad are marked in red. The active Ser210 was exchanged to Ala in the crystallised DegP to prevent autoproteolysis. Picture prepared by Dr. Tim Clausen, IMP, Vienna, Austria.

As in other serine proteases, the active site is located in a crevice between two perpendicular beta-barrel lobes. There are two loops L1 and L2 that together with loop LA from the opposing trimer (termed LA*) block the entrance to the catalytic site, thus rendering it inactive (Fig. 2.6).

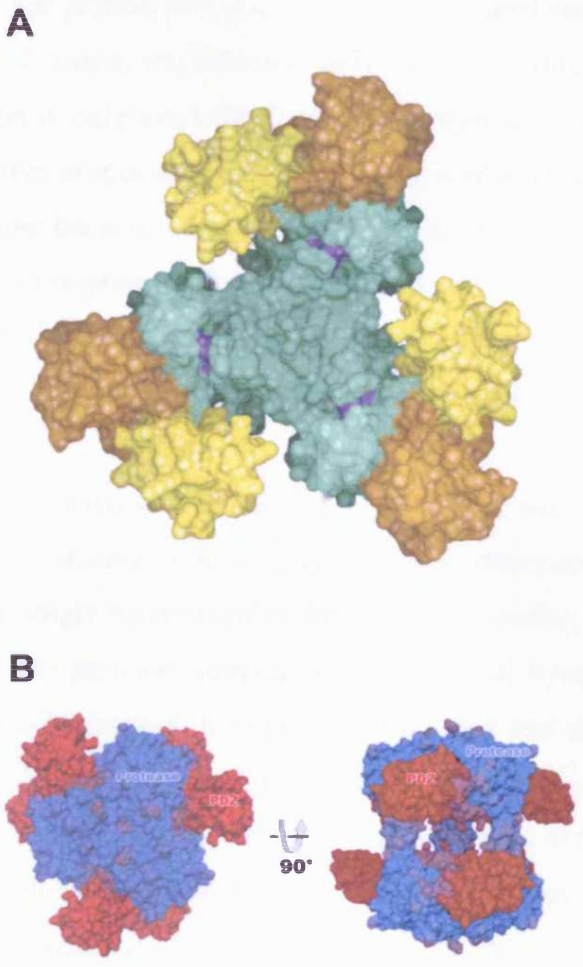

Fig. 2.5 Overall architecture of DegP.

(A) A bottom view of the molecular surface of one trimeric funnel that represents the functional unit of HtrA proteins. The location of different DegP domains (protease in green, PDZ1 in yellow and PDZ2 in orange) and the proteolytic sites (blue) are indicated. (B) Molecular surface of the DegP hexamer (bottom view (left) and side view (right)) coloured by the thermal motion factors (blue: rigid portions; red: flexible portions). The protease domains build up a solid molecular cage with the PDZ domains controlling the lateral access to the inner cavity. The two DegP trimers are connected by the loops LA of opposing trimers which form the pillars of the inner cavity (shown in (B) right) (prepared by Dr.Tim Clausen, IMP, Vienna, Austria).

In addition, the active site Ser210 is tilted away from the other members of the catalytic triad which again contributes to the inactivity of DegP (Fig. 2.4) (Clausen *et al.*, 2002; Krojer *et al.*, 2002). It should be noted that the protein that was crystallised contained a mutation exchanging the catalytic Ser210 to Ala. However, subsequent structural analysis of the wild type protein revealed the same misformed catalytic triad (T. Krojer, M. Ehrmann and T. Clausen, unpublished data). It is therefore apparent that to date structural information is only available for the proteolytically inactive form of DegP. However, it is attractive to speculate that the inactive conformation is not the result of a proform of the enzyme because there are no data available indicating that proteolytic processing of DegP is required for activation. The only requirement appears to be elevated temperature and based on hints from the crystal structure, a reorientation of Ser210 and the loops 1, 2 and LA* might be sufficient to convert the inactive into the active form.

The 12 PDZ domains construct the mobile sidewalls of the DegP particle, which mediate the opening and closing of the cage (Fig. 2.5). Furthermore, it was hypothesised that the PDZ domains might be responsible for the initial binding of substrate. Because the central cavity of the protease domain contains several hydrophobic patches that extend towards the PDZ1 domain, it might be speculated that substrate bound to the PDZ domain could slide into the cage and the active site (Clausen *et al.*, 2002; Krojer *et al.*, 2002). This model, however, has not yet been addressed experimentally. Another peculiarity is that the substrate binding site of PDZ2 is blocked because one loop of PDZ2 mimics a bound substrate in its binding pocket. The reason for this feature is unknown and it remains to be determined if for example substrate can compete with the internal loop for binding to PDZ2.

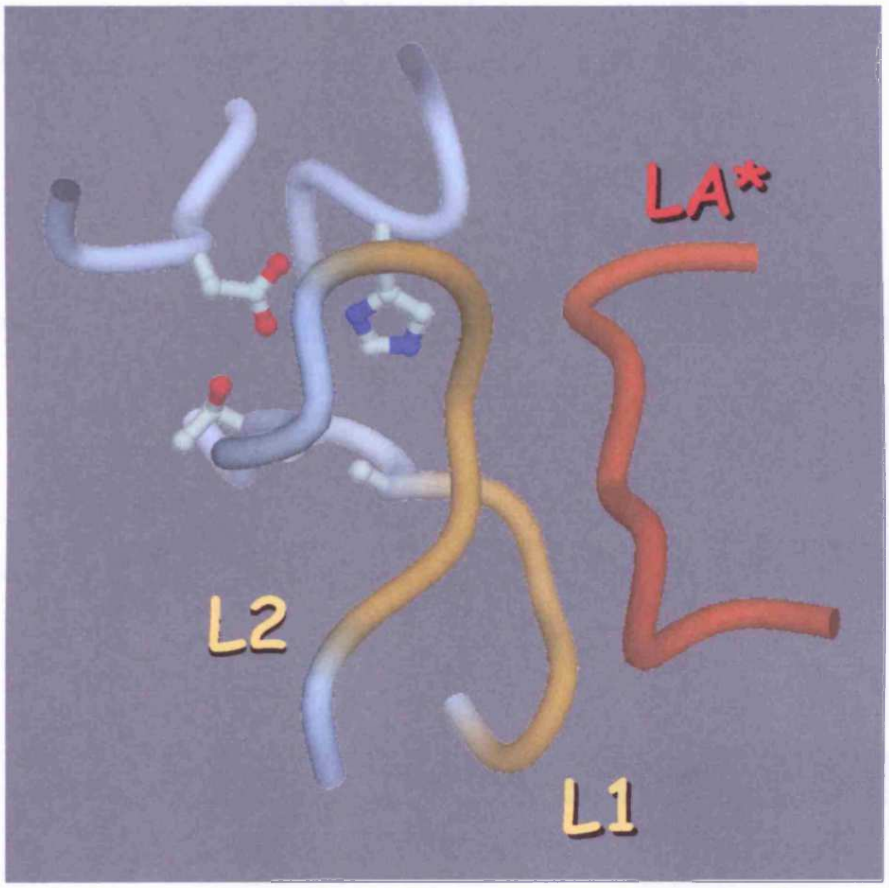

Fig. 2.6 Arrangement of the loops L1, L2 and LA* in DegP.
The residues of the catalytic triad are shown in ball and stick representation. Loops 1, 2 and LA* form a structure that blocks access to the active site. Picture prepared by Dr. Tim Clausen, IMP, Vienna, Austria.

2.1.3.4 The human HtrAs

Beside L56 (HtrA1), three additional human HtrAs have been identified: HtrA2 (Omi) (Gray *et al.*, 2000; Faccio *et al.*, 2000 a,b), HtrA3 (Nie *et al.*, 2003) and HtrA4 (GenBank accession no. AKO75205.1). *htrA3* and *htrA4* are localised on chromosomes 4p16.1 and 8p11.22, respectively (Nie *et al.*, 2003, Clausen *et al.*, 2002). However, the gene products are not yet biochemically characterised (for review see Clausen *et al.*, 2002). The best characterised and crystallised human homologue is HtrA2.

The similarity among HtrA2, L56 and DegP is restricted to the C-terminus of the proteins (Fig. 2.7), each protein having its own unique N-terminus. *HtrA2* is expressed

ubiquitously, but the highest mRNA level is found in placenta and pancreas. The gene for HtrA2 is located on chromosome 2p12 (Faccio *et al.*, 2000b).

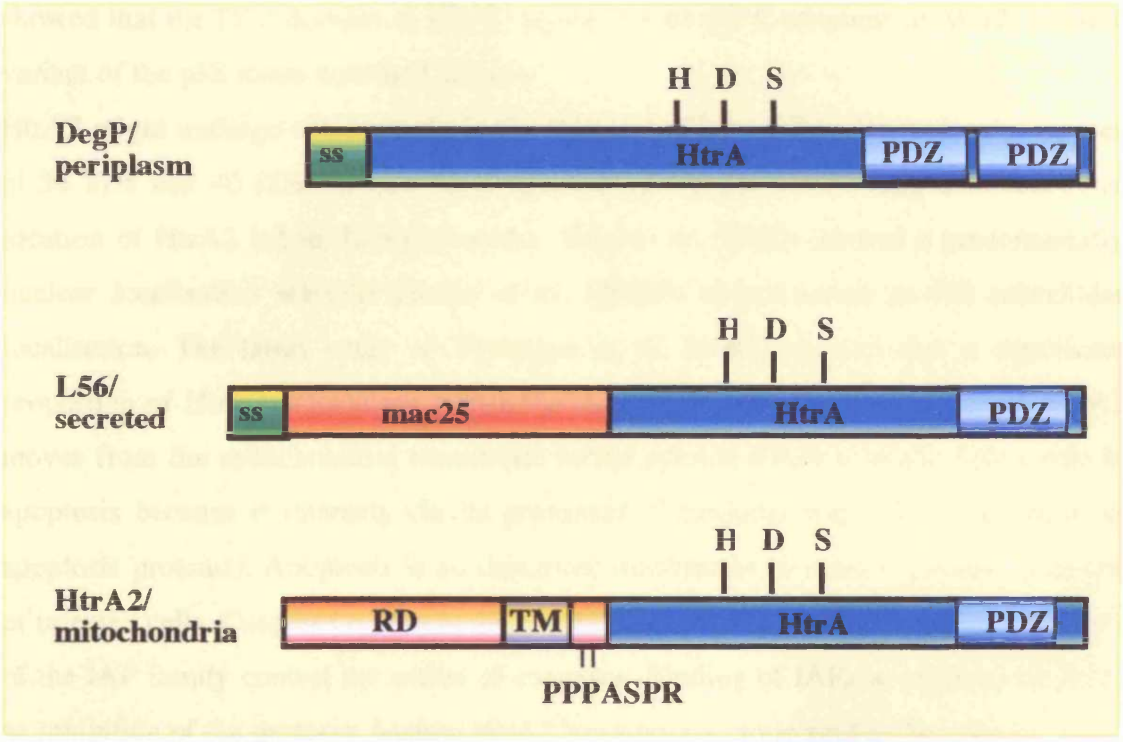

Fig. 2.7 Schematic comparison of L56 and its homologues.
The regions for the signal sequences (ss), HtrA domains (HtrA), PDZ domains (PDZ), mac25 domain (mac25), regulatory domain (RD), transmembrane segment (TM) and the src-homology binding domain and phosphorylation site (PPPASPR) are shown as well as the relative positions of the catalytic triads (H: histidine; D: aspartate; S: serine).

Full-length HtrA2 consists of 458 residues and has an N-terminal domain, proposed to be a regulatory domain, and a C-terminal catalytic domain (Fig. 2.7). The regulatory domain contains a putative transmembrane segment between residues 105-125 (Fig. 2.7) and a potential phosphorylation site, SPRS, for stress-activated kinases at residue 142 (Faccio *et al,*. 2000b). Overlapping the phosphorylation site, there is an SH3 (src-homology)- binding domain, PPPASPR, which is a protein-protein interaction motif. The catalytic domain of HtrA2 has 51% identity and 68% similarity with the corresponding domain of L56 and 36% identity and 58% similarity with DegP from *E. coli*. This domain contains the catalytic triad (HDS) and one PDZ domain (Savopoulos *et al.*, 2000).

HtrA2 might be involved in the cellular response to stress because its activity increases in a mouse model system of kidney ischemia/reperfusion as well as after heat shock and tunicamycin treatment of cells (Gray *et al.*, 2000). Furthermore, Faccio *et al.* (2000a) showed that the PDZ domain of HtrA2 interacts with the C-terminus of Mxi2, a splice variant of the p38 stress activated kinase.

HtrA2 might undergo autoproteolysis yielding two polypeptides with molecular masses of 38 kDa and 40 kDa. Immunohistochemical studies for determining the subcellular location of HtrA2 led to different results. Gray *et al.* (2000) showed a predominantly nuclear localisation whereas Faccio *et al.* (2000b) demonstrated an ER subcellular localisation. The latest study of Verhagen *et al.* (2002) showed that a significant proportion of HtrA2 is localised within the mitochondria. After UV irradiation, HtrA2 moves from the mitochondrial membrane to the cytosol where it might play a role in apoptosis because it interacts via its processed N-terminus with IAPs (inhibition of apoptosis proteins). Apoptosis is an important mechanism to remove excess, damaged or infected cells. Caspases represent the key effector proteases in this process. Members of the IAP family control the action of caspases. Binding of IAPs to caspases result in an inhibition of the protease. Mature HtrA2 has a proapoptotic activity because it

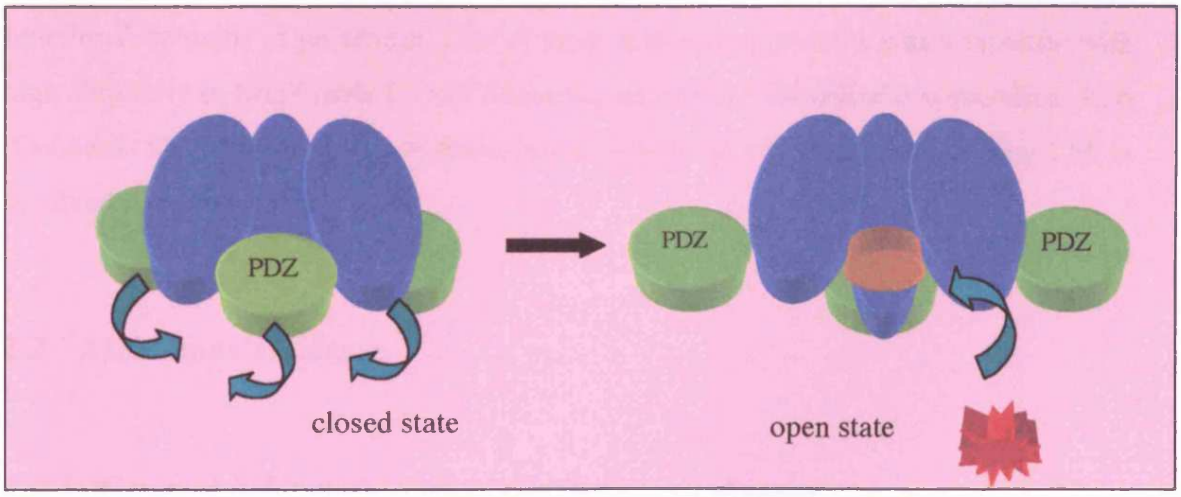

Fig. 2.8 A potential mechanism of activation of HtrA2.

The HtrA domains are coloured in blue, the PDZ domains in green and the active site in orange. Binding of a trimeric ligand to the N-termini of the HtrA core homotrimer leads to a conformational change. The PDZ domains rotate outwards and the active site (orange) is accessible for a misfolded substrate (red).

interacts through a tetrapeptide motif near the N-terminus with IAP and antagonizes IAP inhibition of active caspase-3 *in vitro* (Verhagen *et al.*, 2002).
In contrast to the DegP hexamer, the active form of mature HtrA2 is a homotrimer (Li *et al.*, 2002). The trimer contacts are made exclusively by the protease domains through a narrow region near the N-terminus giving rise to a hollow pyramid-shaped particle with the active sites facing inward. Interestingly, the entry to the active sites appears to be blocked by the position of the PDZ domains (Fig. 2.8). As a deletion of the PDZ domains leads to a constitutively active HtrA2, it was suggested that binding of a trimeric ligand such as a cell death receptor might displace the PDZ domains and make the active site accessible to substrates (Li *et al.*, 2002).

2.1.4 Involvement of L56 in Alzheimer's disease

Several proteolytic events are involved in the onset of Alzheimer's disease. Initial evidence for interaction of L56 and presenilin was obtained by using a bacterial two-hybrid system (Diplom thesis Cristian Behrends, 2002). Furthermore, a yeast-two hybrid screen was used to screen a brain cDNA library for interaction partners of functional domains of presenilin. One of these interacting proteins was a protease with high similarity to DegP from *E. coli*. Sequence alignments identified this protein as L56 (Genbank V04680). Because of these initial results, it might be possible that L56 is involved in Alzheimer's disease.

2.2 Alzheimer's disease

2.2.1 General information about Alzheimer's disease

Alzheimer's disease (AD) is the most common form of progressive dementia, currently affecting 17-25 million people worldwide. In western countries, it represents the fourth leading cause of death after heart disease, cancer and stroke. It is an irreversible, progressive brain disorder that occurs gradually and results in memory loss, unusual

behaviour, personality changes and a decline in thinking abilities. On average, AD patients live for 8 to 10 years after they are diagnosed; however, the disease can last for up to 20 years.

2.2.1.1 Structure and function of the brain

The brain integrates, regulates, initiates and controls functions in the whole body with the help of motor and sensory nerves outside of the brain and spinal cord. The brain governs thinking, personality, mood and the senses. We can speak, move and remember because of complex chemical processes that take place in our brains. The brain also regulates body functions that happen without our knowledge or direction, such as digestion of food.

The human brain is made up of billions of nerve cells, the neurones. Neurones communicate with each other and with sense organs by producing and releasing chemicals, the neurotransmitters. The loss or absence of any one of several chemical messengers or receptors disrupts cell-to-cell communication and interferes with normal brain function. Nerve cells need an efficient metabolism. They require adequate blood circulation to supply the cells with important nutrients, such as oxygen or glucose. Depriving the brain of oxygen or glucose causes nerve cells to die within minutes.

Another important process is the repair of injured nerve cells. Unlike most other body cells, neurones live a long time. Brain neurones have the capacity to last more than 100 years. In the adult, when neurones die (due to disease or injury) they are not replaced. Research shows that the damage seen in AD involves changes in all three of these processes, nerve cell communication, metabolism and repair.

2.2.1.2 The brain in Alzheimer's disease

In AD, the communication between the nerve cells breaks down. The destruction from AD ultimately causes these nerve cells to stop functioning, lose connection with other nerve cells and die. Death of many neurones in key parts of the brain harms memory, thinking and behaviour.

There are two abnormal structures found in the brain of AD patients. The amyloid plaques are dense deposits of an amyloid protein (called ß-amyloid), other associated proteins and non-nerve cells that gradually build up outside and around neurones (Fig. 2.9 and 2.10). The second abnormal structures are neurofibrillary tangles (Fig. 2.10), which are insoluble twisted fibres that build up inside neurones. The main component of these tangles is one form of the protein tau.

2.2.2 Genetic factors in AD

Two types of AD can be distinguished, sporadic and familial AD (FAD). Sporadic AD is the form we know from elderly persons. There is no obvious inheritance and the age of onset is 65 years or older. Several risk factors promote sporadic AD. One risk factor is a specific allele (ε4) encoding apolipoproteinE (ApoE) on chromosome 19 (Strittmatter *et al.,* 1993). ApoE is associated with cholesterol and helps carry blood cholesterol through the body. ApoEε4 is linked to an increased risk for AD. It is present in a high percentage in Aβ deposits in AD brain tissue (Namba *et al.,* 1991) and patients carrying the ε4 allele show a significantly higher Aβ plaque burden than patients lacking this allele. Why the ApoEε4 allele represents a risk factor is unknown but the best explanation is that this isoform somehow enhances the deposition or decreases the clearance of Aβ peptides (Selkoe, 2001).

FAD is found in families where AD follows a certain inheritance. The onset is early and affects people between the ages of 30 to 60 years. This early-onset form of AD progresses faster than the more common late forms. There are mutations in three different genes on three chromosomes that are linked to FAD. These genes are *presenilin1* (*ps1*) on chromosome 14, *presenilin2* (*ps2*) on chromosome 1 and amyloid precursor protein (*app*) on chromosome 21. The most common cause for autosomal dominant FAD is mutations in the *ps1* gene (Sherrington *et al.,* 1995). These account for 30-50% of all early-onset cases (Cruts *et al.,* 1996) and are the primary cause of AD with onset before the age of 55 years. There are more than 70 missense mutations of *ps1* known. In the *ps2* gene, mutations have been described in two families (Rogaev *et al.,* 1995). There are also several missense mutations identified in the *app* gene, which co-segregate with FAD. Mutations in *app* are very rare, affecting less than 25 families

worldwide but all these mutations are located either within or close to the Aß sequence (Czech *et al.*, 2000).

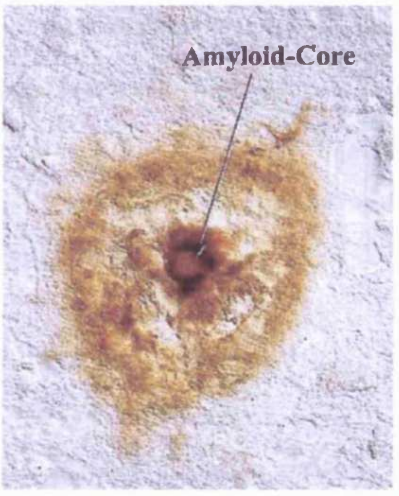

Fig. 2.9 Amyloid plaque.
Picture taken from www. Biozentrum.uni-frankfurt.de/Pharmakologie/Alzheimer.htm

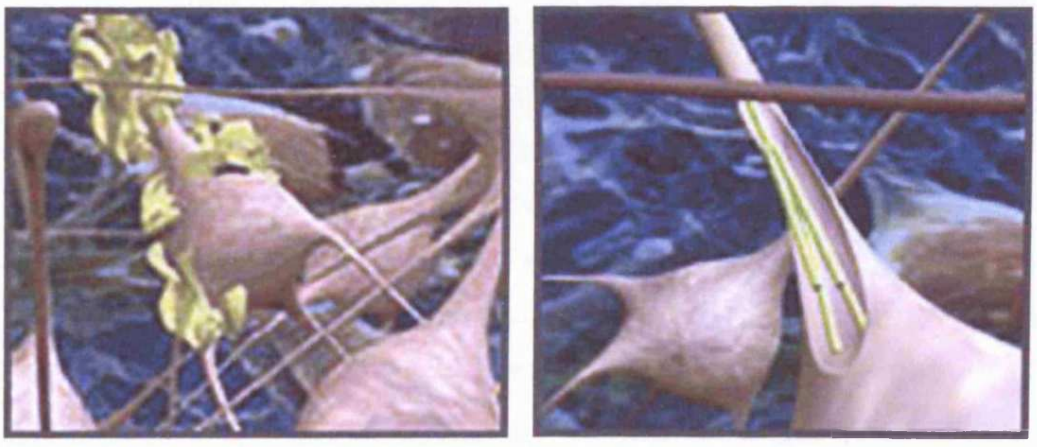

Fig. 2.10 Schematic picture of amyloid plaques and tangles.
Amyloid plaques (yellow) surrounding axons of a neuronal cell (left). Neurofibrillary tangles (yellow) within an axon of a neuronal cell (right). (Picture taken from www. Biozentrum.uni-frankfurt.de/Pharmakologie/Alzheimer.htm).

2.2.3 The amyloid precursor protein APP

APP comprises a family of type-I membrane spanning glycoproteins (Kang *et al.*, 1987; Tanzi *et al.*, 1987). These proteins contain the Aß segment that is important in the onset of AD. Alternative splicing of APP mRNA generates different isoforms of this protein ranging from 365 to 770 residues. The three major forms of APP are APP751, APP770 and APP695. Whereas the 751/770 forms are mainly expressed in non-neuronal cells (Selkoe, 1998), the 695 form is most highly expressed in neurones (Goedert, 1987; LeBlanc *et al.*, 1991). The difference between the 751/770 and the 695 forms is the presence of an exon encoding 56 residues in the longer APP forms that encodes a region homologous to the Kunitz-type serine protease inhibitor motif. Indeed the 751/770 residues form of APP, which is present in human platelets, inhibits the serine protease factor XIa in the coagulation cascade (Selkoe, 1998).

APP matures while being transported during secretion, becoming N- and O-glycosylated and tyrosyl-sulphated while moving through the trans-Golgi network (Weidemann *et al.*, 1989). Mature APP is cleaved by various proteases at several cleavage sites within and outside the membrane (Fig. 2.11). The function of APP remains to be fully understood but there is evidence that it is a neuronal receptor, which couples to an intracellular signalling pathway through the GTP binding protein G_0 (Mills and Reiner, 1999). Furthermore, APP binds to extracellular matrix components such as laminin and heparin and therefore cells which express APP, adhere more rapidly than cells lacking APP. A physiological implication of this process could be neurite outgrowth where cells have to adhere and be released from the ECM. Cavarec *et al.* (2002) identified the MOCA protein (molecule of cell adhesion), which is involved in the rapid degradation of APP by the proteasome and regulates cell adhesion via the APP pathway.

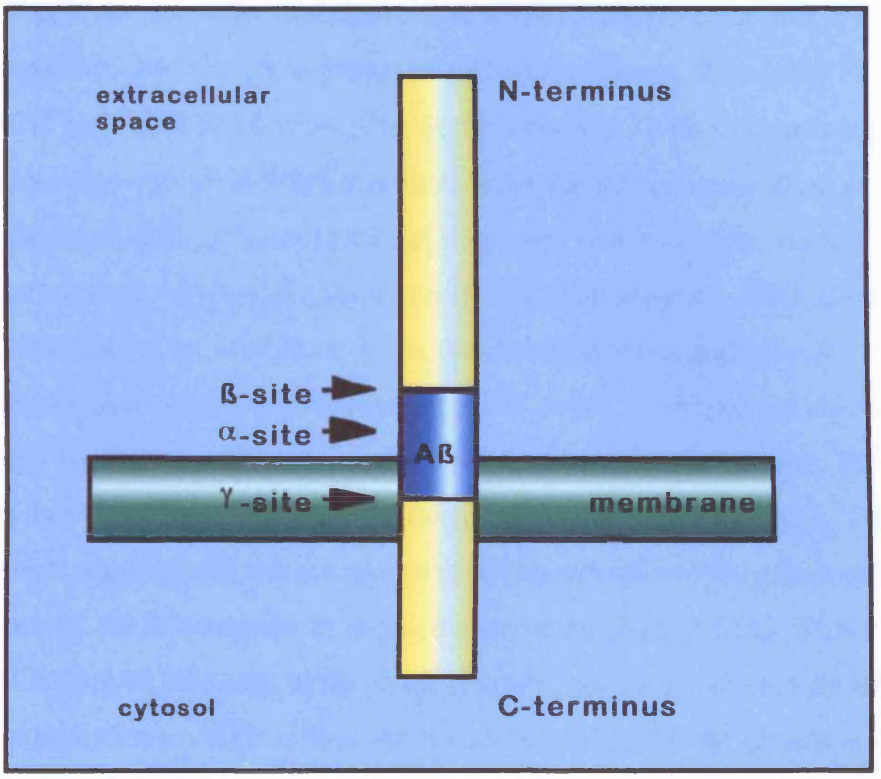

Fig. 2.11 Schematic representation of APP695, including the different secretase cleavage sites and the position of the Aß sequence.

2.2.4 APP cleavage events

2.2.4.1 The α- secretase pathway

Processing of APP by α-secretase was the first event in the processing pathway to be characterised in detail. Three metalloproteases ADAM 9, ADAM 10 and TACE (tumour necrosis factor-α-converting enzyme; ADAM 17) are involved in α-secretase cleavage. They belong to a family of membrane-anchored glycoproteins (ADAM) that are composed of several domains, a disintegrin domain, a cysteine-rich region and an epidermal growth factor repeat and a metalloprotease domain (Moss *et al.* 2001). TACE cleaves pro-tumour necrosis factor (TNF)-α, releasing the extracellular domain (TNF-α) in a similar manner to APP (Buxbaum *et al.*, 1998). The inhibition or knockout of TACE decreases the release of the α-cleavage product (Buxbaum *et al.*, 1998). Cells

that lack TACE do not show detectable α-secretase activity (Esler and Wolfe, 2001). Overexpression of ADAM 10 increases α-secretase cleavage (Lammich *et al.*, 1999). Thus, TACE and ADAM 10 may both be α-secretases. This α-secretase processing route involves cleavage of APP695 at residue 16 of the Aß sequence (Esch *et al.*, 1990). Although the exact cellular location of the cleavage event is unclear, evidence suggests that it may reside in a late Golgi compartment (Sambamurti *et al.*, 1992; De Strooper *et al.*, 1993; Kuentzel *et al.*, 1993) or at the plasma membrane (Ikezu *et al.*, 1998). The determinants of cleavage by α-secretase appear to be an α-helical conformation around the cleavage site and the distance of the hydrolysed peptide bond from the predicted membrane but are apparently independent of the sequence (Sisodia, 1992). This cleavage event results in the release of a soluble N-terminal APP fragment (sAPPα) and the retention of the C-terminus in the cell membrane (Fig. 2.12A). This C-terminal fragment (C83) of 10 kDa may undergo additional cleavage by an enzyme known as γ-secretase, which cleaves APP within the membrane (Fig. 2.12A) (Haass *et al.*, 1993). The resulting 3 kDa C-terminal fragment of APP is secreted to the ECM but its biological role remains unclear. Because this pathway does not produce intact Aß, it is nonamyloidogenic and does not lead to AD pathology.

2.2.4.2 The ß-secretase cleavage pathway

An alternative physiological processing pathway for APP results in the production of intact Aß (Haass *et al.*, 1993). The Aß segment begins on the extracellular side of APP (28 residues from the proposed membrane position) and extends 11-15 residues into the transmembrane domain (Fig. 2.11). Two cleavage events are required to produce Aß that are mediated by ß-secretase and γ-secretase. The ß-secretase cleavage occurs at the Met-Asp bond preceding the Aß N-terminus (Fig. 2.13). ß-secretase is a membrane-bound aspartic protease called BACE (ß-amyloid cleaving enzyme). It is an unusual member of the pepsin family, which has an N-terminal catalytic domain, containing two important aspartate residues (Asp93 and Asp289), linked to a 17-residue transmembrane domain and a short C-terminal cytoplasmic tail (Vassar *et al.*, 1999). It has its active site on the luminal side where ß-secretase cleavage occurs (Vassar *et al.*, 1999). BACE is expressed coordinately with APP in many regions of the brain, particularly in neurones

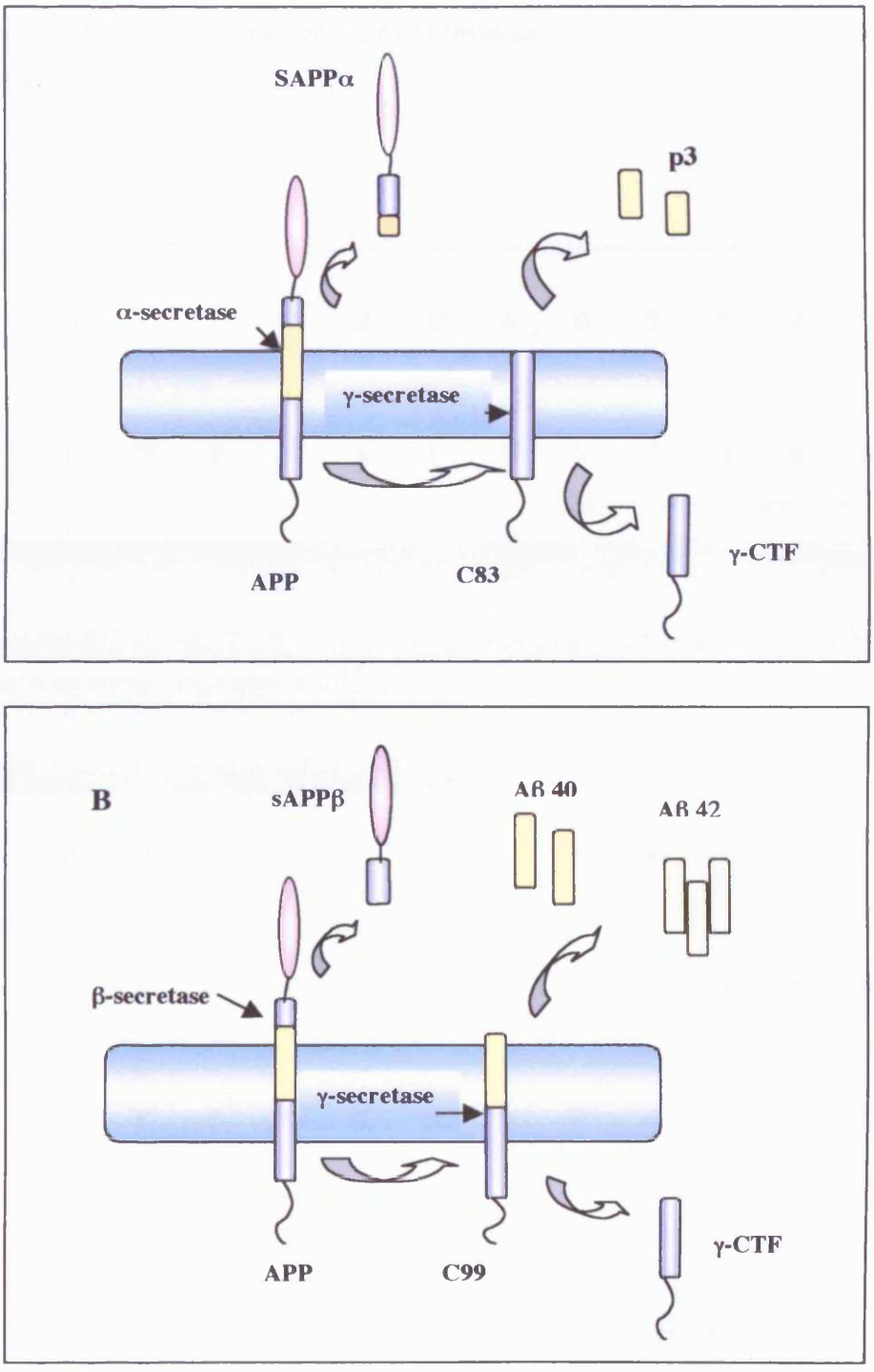

Fig 2.12 Schematic representation of the different APP cleavage pathways.

APP is the amyloid precursor protein that can be cleaved by α-secretases such as TACE, ADAM 9 or ADAM 10 (A), or in a different pathway by β-secretase BACE (β-amyloid cleaving enzyme) (B). Cleavage of APP by α-secretase produces SAPPα and C83 (A). Cleavage of APP by BACE produces sAPPβ and C99 (B). C99 and C83 are substrates for the γ secretase complex (the active component of which may be PS1). Cleavage of C83 by γ-secretase

produces soluble p3 (A) whereas cleavage of C99 produces either soluble Aβ40 or Aβ42 which aggregates (B).

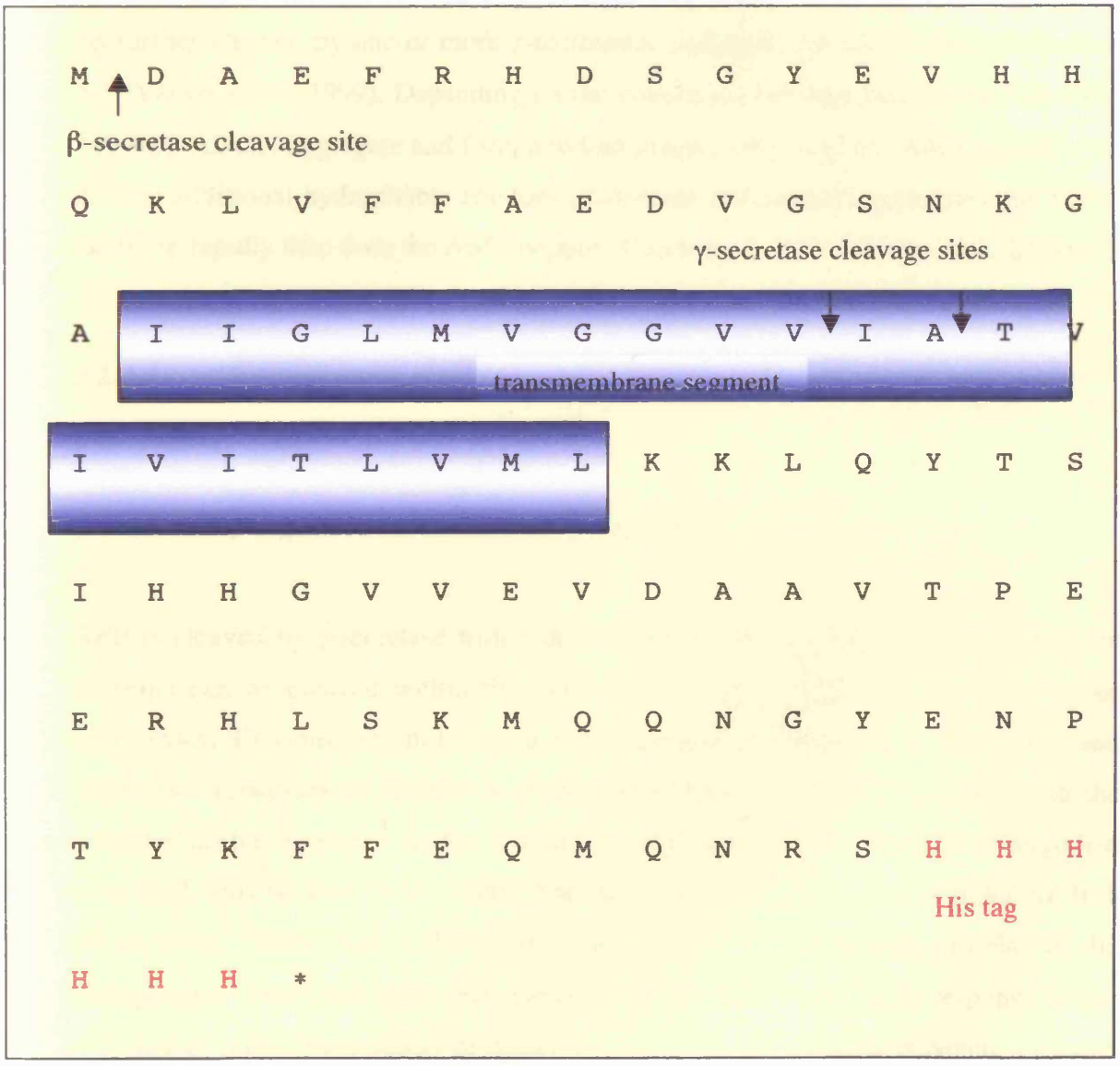

Fig. 2.13 Sequence of a recombinant form of C99 containing a C-terminal His Tag.
The postulated transmembrane domain is coloured in blue and the His Tag is in red. Cleavage by γ-secretase occurs after valine 40 or alanine 42.

(Vassar *et al.*, 1999). The subcellular distribution of BACE is primarily in Golgi and endosomes but it is also detectable at the plasma membrane (Esler and Wolfe, 2001).

Because BACE has its pH optimum in an acidic pH range, it is likely that it is active in acidic compartments such as endosomes (Vassar *et al.*, 1999). ß-secretase cleavage leads to the release of a soluble N-terminal fragment (sAPPβ ≈ 100 kDa) and a 12 kDa C-terminal fragment (C99) which remains membrane bound (Fig. 2.12 B). The N-terminal fragment might be a ligand for receptors of other cells (Selkoe, 2001). C99 can be further cleaved by one or more γ-secretases, leading to the release and secretion of Aß (Vassar *et al.*, 1999). Depending on the γ-secretase cleavage position (at Val-40 or Ala-42), Aß can aggregate and form amyloid plaques (Fig. 2.12 B). Aß42 peptide with its two additional hydrophobic residues (isoleucine and alanine) aggregates into fibrils far more rapidly than does the Aß40 peptide (Czech *et al.*, 2000; Clarke *et al.*, 2001).

2.2.4.3 The γ-secretase cleavage event

2.2.4.3.1 Rip-regulated intramembrane proteolysis

APP is cleaved by γ-secretase within the membrane. The fact that integral membrane proteins can be cleaved within the plane of the lipid bilayer is a new concept of proteolysis. This mechanism is called Rip (regulated intramembrane proteolysis) and influences processes as diverse as cellular differentiation, lipid metabolism and the unfolded protein response. So far, five proteins are known or postulated to undergo Rip in animal cells (Brown *et al.*, 2000). The most recently recognised examples are Ire1 (Niwa *et al.*, 1999) and ATF6 (Haze *et al.*, 1999), two membrane proteins in the endoplasmic reticulum (ER) that release their cytosolic domains in response to the presence of unfolded secretory proteins in the ER. Another example is Notch, a plasma membrane receptor whose cytosolic domain is released in response to Delta, a protein that dictates cell fate decisions (Annaert and De Strooper, 1999; Chan and Jan, 1999). The list also includes SREBPs (sterol regulatory element-binding proteins) that are membrane proteins of the ER whose cytosolic transcription factor domains are liberated when cells are deprived of sterols, thereby activating genes controlling lipid synthesis and uptake (Brown *et al.*, 2000). Another example is the C99 fragment of APP (see above).

In SREBP, Notch and APP, intramembrane cleavage does not occur until the bulk of the protein on the extracytosolic face has been removed by a primary processing event. This primary cleavage can occur in the lumen of the ER, in a post-ER compartment or at the cell surface (Brown *et al.*, 2000).

Three substrates are type-I membrane proteins (Ire1, Notch and APP) and have extracellular N-termini and cytosolic C-termini. One protein ATF6 is a type-II membrane protein with a cytosolic N-terminus. SREBP contains two membrane-spanning segments that are present in the bilayer as helical hairpins (Brown *et al.*, 2000). The three type-I membrane proteins require PS1 that is postulated to be an aspartic protease (Wolfe *et al.*, 1999). Proteolysis of ATF6 and SREBP is regulated by the polytopic Zn-dependent protease S2P (Brown *et al.*, 2000). Recently a unique serine protease, called Rhomboid, was identified. It is involved in the cleavage of the intramembrane domain of Spitz, a ligand for Drosophila epidermal growth factor (Urban *et al.*, 2001).

2.2.4.4 The presenilins

The *ps1* and *ps2* genes both contain 12 exons (Levy-Lahad *et al.*, 1996). PS1 and PS2 are both polytopic membrane proteins, consisting of 467 residues and 448 residues, respectively. It is proposed that PS1 has 8 transmembrane segments (TM) with its N-terminus and its C-terminus localised in the cytosol. Furthermore, PS1 contains a large cytosolic loop between TMs 6 and 7 and two conserved aspartate residues located within these TMs (Fig. 2.14). These aspartates could represent the active site of an aspartic protease. Presenilins are neither glycosylated nor modified by sulphation, acylation or addition of glycosaminoglycans (De Strooper *et al.*, 1997). The most prominent posttranslational modification of PS1 and PS2 is a proteolytic cleavage in the cytosolic loop between TMs 6 and 7 (Podlisny *et al.*, 1997) (Thinakaran *et al.*, 1996). So far, the precise cleavage site has not been determined and it is unclear if endoproteolysis of presenilin is an autoproteolytic cleavage event or performed by other proteases. Campbell *et al.* (2002) suggested that one potential "presenilinase" is an integral membrane protein. Inhibitor studies did not determine the protease class of the presenilinase but it is most likely that it represents an aspartic protease because

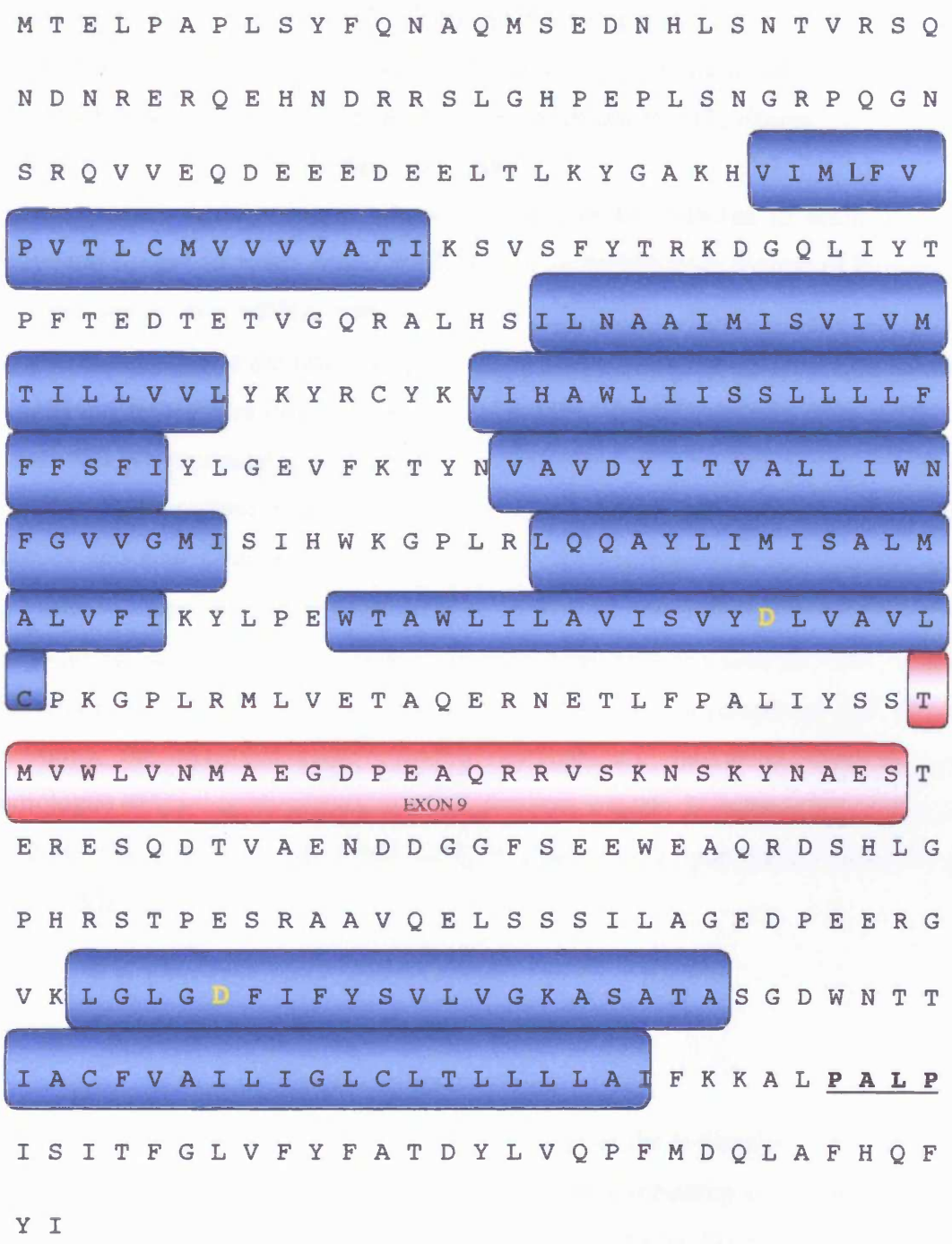

Fig. 2.14 Sequence of recombinant wild type PS1.

The transmembrane segments (TM) 1-8 are coloured in blue, the aspartates in TMs 6 and 7 in yellow, the exon 9 region in red and the PALP motif in bold face.

pepstatinA was the most potent inhibitor tested (Campbell *et al.*, 2002). The cleaved PS1 fragments remain associated and form a large heterooligomeric complex of 250

kDa (Capell *et al.*, 1998; Yu *et al.*, 1998) and it is thought that processed presenilins are active (Czech *et al.*, 2000). Furthermore, presenilins contain a highly conserved C-terminal PALP-motif, consisting of the amino acids proline (P), alanine (A) leucine (L) and proline (P) (Fig. 2.14) (Tomita *et al.*, 2001).

Presenilins are widely expressed; transcripts can be detected in brain and most peripheral tissues (Rogaev *et al.*, 1995). In the central nervous system of humans and rodents, presenilin mRNA and protein are essentially neuronal and are widely distributed throughout the brain (Kovacs *et al.*, 1996; Moussaoui *et al.*, 1996; Suzuki *et al.*, 1996). The regional distribution pattern of PS2 is almost identical to that of PS1.

Presenilins are produced at high levels in cerebral regions that are affected in AD (i.e. hippocampus, cerebral cortex and amygdala) and which are rich in senile amyloid plaques and neurofibrillary tangles. However, the expression of *ps1* and *ps2* is not restricted to these vulnerable regions. The functions of presenilin are unknown but they are required for cleavage of various transmembrane proteins such as APP, Notch1-4 (Saxena *et al.*, 2001) which is involved in embryonic development and cell fate decisions, the oncogene ErbB4 (avian erythroblastic leukaemia viral oncogene homologue 4) (Lee *et al.*, 2002), the cell adhesion protein E-cadherin (Marambaud *et al.*, 2002) (De Strooper *et al.*, 1999) and LDL (low density lipoprotein) receptor related protein (May *et al.*, 2002).

2.2.4.5 Is presenilin the unknown γ-secretase ?

Two models propose how PS1 could be involved in the γ-secretase cleavage event. First, presenilin participates directly in the γ-secretase mechanism as a cofactor or as the secretase itself (Xia *et al.*, 1997). Second, presenilin is involved in membrane trafficking of certain proteins including components of the γ-secretase reaction (Naruse *et al.*, 1998; Thinakaran *et al.*, 1998). Strong genetic and indirect biochemical evidence suggests that presenilin participates directly in the cleavage event. [1] Deletion of PS1 in mice dramatically reduces γ-secretase activity (DeStrooper *et al.*, 1998; DeStrooper *et al.*, 1999). [2] Knockout of both PS1 and PS2 resulted in a complete abolition of this APP processing event (Herreman *et al.*, 2000). [3] PS1 contains two highly conserved aspartate residues. They can also be aligned with the γ-secretase cleavage sites in APP

when considering the appropriate TMs (Esler and Wolfe, 2001). Mutations of these aspartates prevent endoproteolysis of PS1 as well as APP processing (Wolfe *et al.*, 1999) and lead to an accumulation of the substrates C99 and C83 (Xia *et al.*, 2000). [4] Mutations of the aspartates in a familial Alzheimer's disease (FAD) linked PS1 mutation PS1Δ9 (PS1 with deletion of the exon9 region), which is constitutively active, inhibited APP processing (Wolfe *et al.*, 1999). [5] Xia *et al.* (2000) showed that C99 and C83 that are substrates of γ-secretase could be co-immunoprecipitated with both PS1 and PS2. [6] Li *et al.* (2000) showed that the presenilin heterodimer copurifies with γ-secretase activity after solubilisation of isolated microsomes and size-exclusion chromatography. Furthermore, they demonstrated that photoactivatable derivatives of a peptidomimetic inhibitor that blocks γ-secretase activity bind covalently to presenilin subunits (Li *et al.*, 2000). Interestingly, introduction of the photoreactive group on one end of the inhibitor led to labelling of the N-terminal presenilin subunit while introduction on the other end resulted in the tagging of the C-terminal subunit. In addition, the inhibitors did not label the inactive wild type PS1 holoprotein but PS1Δ9 which is thought to be constitutively active (Li *et al.*, 2000). [7] Esler *et al.* (2000) developed peptidomimetic inhibitors based on the APP cleavage site that contain a difluoroalcohol group. These inhibitors bind presenilin heterodimers in cell lysates, isolated microsomes and whole cells. [8] The first approach to test γ-secretase inhibitors in mice was reported by Dovey *et al.* (2001). A small molecule inhibitor showed potent inhibition of Aβ production *in vitro*. Oral application of this inhibitor to mice led to a peak level in brain after 3 h accompanied by a 40% reduction in Aβ production. A 20% reduction could be maintained over 18 h whereas the levels of sAPPα and sAPPβ, the soluble products of α-and β-secretase cleavage remained relatively unaffected. However, specificity and toxicity of these compounds remains to be fully established.

Given these data, the predominant notion is that presenilin is indeed the active component of γ-secretase. However, there is one discrepancy termed the spatial paradox. The subcellular distribution of endogenous PS1 is primarily in the ER and Golgi compartment (Annaert *et al.*, 1999) but most of the Aβ production takes place at the cell surface (Perez *et al.*, 1999). A number of recent studies showed that PS1 could be detected in post-Golgi compartments (Zhang *et al.*, 1998) and recently Kaether *et al.* (2002) found a small but biologically active fraction of PS1 at the cell surface where γ-

secretase cleavage occurs. Also, *C. elegans* Spe-4 that is homologous to PS1 is involved in vesicle transport in spermatozoa (Arduengo et al., 1998). This relationship might suggest a role of PS1 in γ-secretase assembly. On the other hand, two homologous proteases, the bacterial type 4 prepilin protease family and signal peptidase which cleaves the signal peptide within the membrane and contains two aspartate residues in the membrane as active site have protease function (Weihofen *et al.*, 2002).
A new approach to identify transmembrane proteases was done by Grigorenko *et al.* (2002). A database search for proteins with two highly conserved aspartic residues and a conserved C-terminal PALP-motif (Fig. 2.14) identified several proteins of unknown function termed IMPAS which are represented in plants, yeast, vertebrates, invertebrates, and archaea. One protein found in *Dictyostelium discoideum* might be an ancient archetype of the presenilins. These proteins showed similarities in general structure as well as in the location of the conserved amino acids.

2.2.4.6 Interaction of presenilin with other proteins and mechanism of γ-secretase

At the subcellular level, presenilins are mainly localised in the ER (Cook *et al.* 1996; Kovacs *et al.*, 1996). A large fraction of APP is also present in this compartment. PS1 as well as PS2 can be co-immunoprecipitated with APP suggesting that these proteins interact. Mapping of the APP/PS2 interaction domains using truncated forms of PS2 revealed that the hydrophilic N-terminus (residues 1-87) was sufficient for binding to APP when targeted to the lumen of the ER (Pradier *et al.*, 1999). In addition, the region encompassing Aβ and the TM of APP interact with PS2 (Pradier *et al.*, 1999).
Yu *et al.* (2000) identified one member of the γ-secretase complex called nicastrin. The gene for nicastrin (*nicA*) is localised on chromosome 1 encoding a protein of 80 kDa. It contains a long N-terminal hydrophilic domain with several glycosylation sites, a 20 residue long hydrophobic putative transmembrane domain and a short (20 residues) hydrophilic C-terminus (Yu *et al.*, 2000). Nicastrin matures on the way to the cell surface while being N-glycosylated in the ER and Golgi compartments. There are several hints that nicastrin plays an important role in γ-secretase activity. (1) Nicastrin binds to APP and Notch, two substrates for the γ-secretase (Yu *et al.*, 2000). (2)

Mutations in nicastrin impair presenilin-dependent cleavage of Notch and APP (Chung and Struhl, 2001; Hu *et al.*, 2002). (3) A reduction of the *nicastrin* expression in *Drosophila* S2 cells led to a loss in presenilin fragment generation, suggesting that nicastrin might play a role in presenilin endoproteolysis (Hu *et al.*, 2002). (4) Inhibitor affinity matrix chromatography showed that nicastrin could be co-eluted with presenilin in an active complex (Esler *et al.*, 2002). (5) Immature unglycosylated nicastrin interacts with immature presenilin holoprotein in the ER and mature N-glycosylated nicastrin with mature endoproteolysed presenilin in Golgi enriched fractions (Yang *et al.* 2002; *Tomita et al.* 2002). Taken together, these data suggest that presenilin and nicastrin regulate each other's maturation and association into a stable complex. They may also influence the maturation and surface expression of other members of the complex and the cleavage event (Cupers *et al.*, 2001; Edbauer *et al.*, 2002).

Another member of the γ-secretase complex is PEN-2, a small 10 kDa protein of unknown function (Steiner *et al.*, 2002). Downregulation of PEN-2 leads to a reduction of presenilin levels as well as a loss in nicastrin maturation and γ-secretase complex formation. PEN-2 seems to be highly packed in the complex and is also important in Notch processing (Steiner *et al.*, 2002). So far, at least presenilin, nicastrin and PEN-2 are integral components of the γ-secretase complex. Removal of any of the three components results in a reduction of the amount of γ-secretase complexes and therefore in a loss of γ-secretase activity (Edbauer *et al.*, 2002; Francis *et al.*, 2002). One additional component of the complex is Aph-1. Aph-1a and 1b are the human homologues of *C. elegans* APH1 (Francis *et al.*, 2002). They were found to affect APH-2 that is the *C. elegans* homologue of nicastrin. Furthermore, Xu *et al.* (2002) identified a protein PSAP (presenilin associated protein) which interacts with the C-terminus of presenilin via its PDZ domain. PSAP contains several putative protein kinase C as well as tyrosine kinase phosphorylation sites. Interestingly, PSAP dos not interact with PS2 suggesting that PS1 and PS2 might be involved in different signal transduction pathways (Xu *et al.*, 2002).

All known proteases are hydrolases which require a water molecule for the cleavage of a peptide bond. If presenilin is the unknown γ-secretase and the active site lies within the membrane, how could the required water molecule enter the lipid bilayer to participate in the chemical reaction? First water could diffuse from outside the bilayer

into the active site as water freely diffuses through the lipid bilayer. A second possibility is that presenilin forms a pore or a channel in the membrane with polar residues facing inwards to allow the water molecule to enter.

2.2.4.7 Model of the cellular events leading to AD

Taken together, these data allow postulating a model for the cellular events leading to AD (Fig. 2.15). After translocation of presenilin and nicastrin into the ER, they both enter the secretory pathway and nicastrin is N-glycosylated and presenilin undergoes endoproteolysis. The two proteins associate and initiate formation of the γ-secretase complex. It is unclear if PEN-2 and perhaps other components of the complex are already associated at this point. The formed complex reaches the cell surface where it comes in contact with γ-secretase substrates such as C99, C83 or Notch.

APP is also glycosylated while being transported to the cell surface (Weidemann *et al.*, 1989). After arrival at the cell surface, APP is internalised by endocytosis together with BACE and, in the acidic environment of the endosomes, β-secretase cleavage occurs (Fig. 2.15). Interestingly, it seems that PS1 might play a role in APP endocytosis because inactivation of PS slows down APP endocytosis (Kaether *et al.*, 2002). This finding would implicate a role of presenilin in targeting of APP to the endosomal/lysosomal pathway. C99 and soluble sAPPβ (soluble fragment of APP after β-secretase cleavage) are brought back to the plasma membrane and sAPPβ is released into the ECM while C99 remains membrane-bound and can be cleaved by the γ-secretase. Subsequently, Aβ40 and Aβ42 are released into the ECM were they can aggregate and form senile plaques.

The C-terminal fragment γ-CTF forms a multimeric complex with the nuclear adaptor protein Fe65 and the histone acetyltransferase Tip60 (Fig. 2.15), which possess potential transcriptional activity (Cao and Sudhof, 2001). Therefore, it seems that γ-CTF is involved in signal transduction (Cao and Sudhof, 2001; Scheinfeld *et al.*, 2002). Furthermore, Roncarati *et al.* (2002) showed that APP and γ-CTF bind to Nbl/Numb, which are intracellular modulators of Notch. These findings suggested that released γ-CTF/Nbl/Numb complexes might physiologically regulate Notch activity. This complex might bind NICD (Notch intracellular domain) and antagonise the role of Notch in

generation, differentiation and cell fate decisions. One conclusion could be that γ-secretase has opposing effects on Notch signalling depending on the substrate cleaved. If Notch signalling is inhibited there might be an acceleration of neurodegenerative processes of AD by enhancing synapse loss, neurite dystrophy and neuronal degeneration (Roncarati *et al.*, 2002).

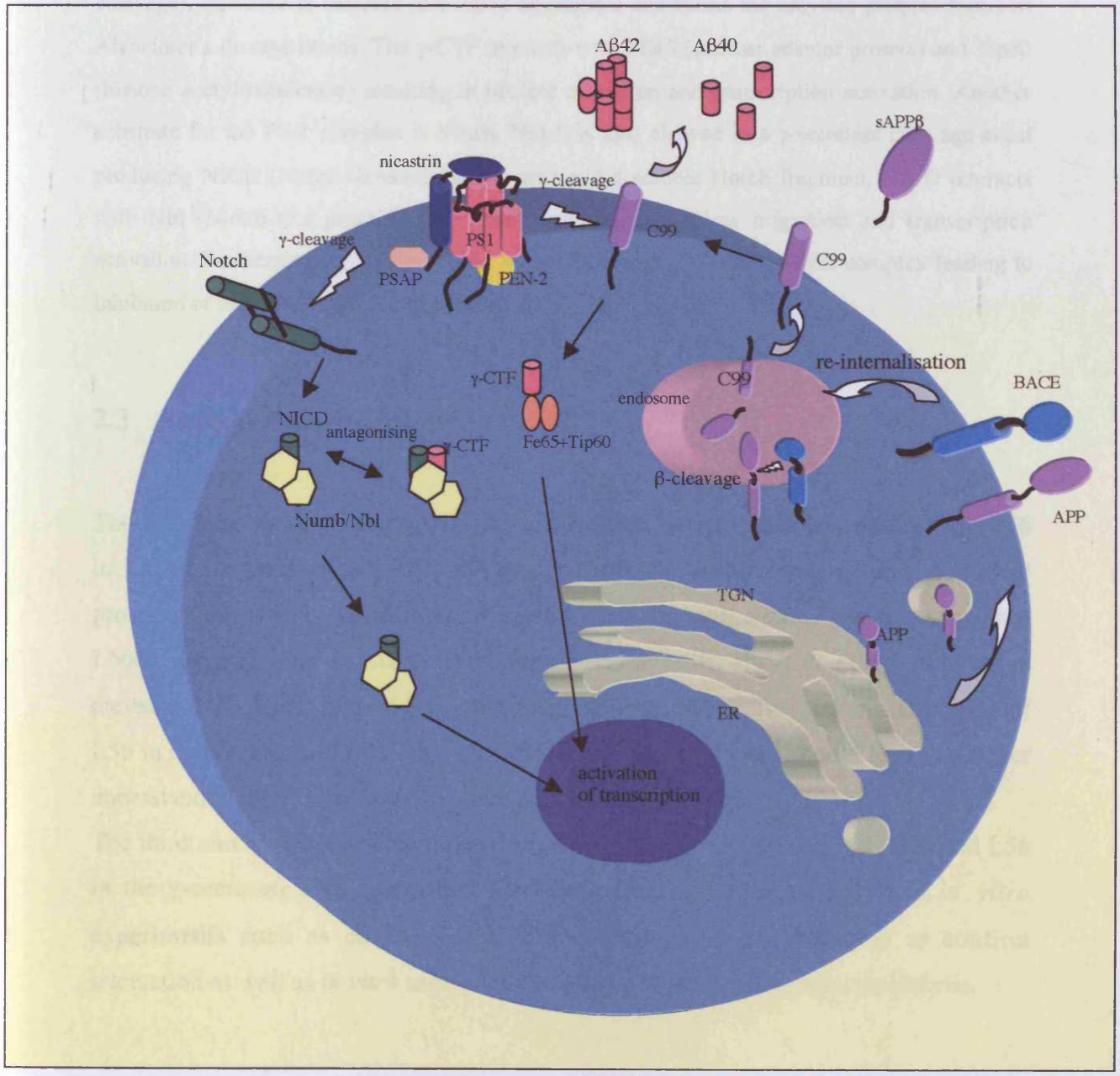

Fig. 2.15 Model of the cellular events leading to AD.

APP (amyloid precursor protein) is transported through the ER (endoplasmic reticulum) and TGN (Trans Golgi Network) to the cytoplasmic membrane. It is re-internalised together with

BACE (β-amyloid cleaving enzyme) and cleaved by BACE in the endosomes producing C99 and sAPPβ (soluble APP fragment: β-secretase cleavage product). Both products are then transported to the cytoplasmic membrane and C99 remains membrane bound. PS1 (presenilin 1) is also transported to the cytoplasmic membrane where it forms a complex with nicastrin, PEN-2 and PSAP (presenilin associated protein). This PS-1 complex cleaves C99 within the membrane producing Aβ40/42 and γ-CTF (C-terminal fragment of C99 after γ-secretase cleavage). Aβ40/42 is secreted and Aβ42 aggregates and forms the amyloid plaques found in Alzheimer's disease brains. The γ-CTF interacts with FE65 (nuclear adaptor protein) and Tip60 (histone acetyltransferase) resulting in nuclear migration and transcription activation. Another substrate for the PS-1 complex is Notch. Notch is also cleaved in a γ-secretase cleavage event producing NICD (Notch intracellular domain) and a soluble Notch fragment. NICD interacts with Nbl (Numb-like protein) and Numb resulting in nuclear migration and transcription activation. Furthermore, γ-CTF can also interact with the NICD/Numb/Nbl complex leading to inhibition of the Notch signalling pathway.

2.3 Aims of the project

The first aim of the project is the characterisation of the human serine protease L56 including its production in *E. coli*, purification and performance of chaperone and protease assays. The second aim of the project is the investigation of the involvement of L56 in diseases such as Alzheimer's disease and arthritis. Hu *et al.* (1998) showed an elevated mRNA and protein level of L56 in cartilage of arthritic patients. Detection of L56 in cells involved in the arthritic process and synovial fluid should lead to a better understanding of the role of L56 in this disease.

The third aim of the project is the investigation of the interaction of PS1, C99 and L56 in the γ-secretase cleavage event. The studies include *in vivo* as well as *in vitro* experiments such as co-expression of both proteins, co-purification to confirm interaction as well as *in vitro* assays with purified proteins to determine proteolysis.

3 Materials and Methods

3.1 Lab equipment, chemicals and enzymes

All chemicals and laboratory equipment which are not listed below (Table 3.1) were purchased from Boehringer Mannheim (Lewes, East Sussex, UK), Greiner Labortechnik (Darmstadt, Germany), Merck (Dorset, UK), Fisher Lifescience (Loughborough, Leicester, UK), Sigma (Poole, Dorset, UK), ICN (Basingstoke, Hampshire, UK), Peqlab (Erlangen, Germany), Amersham Pharmacia (Little Chalfont, Buckinghamshire, UK), or Roche (Lewes, East Sussex, UK). Restriction enzymes were ordered from New England Biolabs (Beverly, MA, USA). All other enzymes used were ordered from the suppliers listed in the table below (Table 3.2). The antibodies used were either from our collection or ordered from the suppliers listed in Table 3.3.

Table 3.1 Chemicals/Proteins

Chemicals/Proteins	Supplier
Sealkem agarose	FMC Bioproducts (Rockland, Maine, USA)
Acrylamide	ICN (Basingstoke, Hampshire, UK)
Ampicillin	AppliChem (Darmstadt, Germany)
Chloramphenicol	Sigma (Poole, Dorset, UK)
DMSO	AppliChem (Darmstadt, Germany)
DNA standard γ-DNA *BstEII* digested	New England Biolabs (Beverly, MA, USA)
DNA standard 100 bp or 1000 bp	New England Biolabs (Beverly, MA, USA)
NBT	AppliChem (Darmstadt, Germany)
Primer	MWG (Ebersberg, Germany)
Protein standards (LMW, broad range)	Biorad (Hertfordshire, UK),

	New England Biolabs (Beverly, MA, USA)
Gel filtration standard	Biorad (Hertfordshire, UK)
β-casein	ICN (Basingstoke, Hampshire, UK)
Aβ40/42 purified	Bachem AG (Bubendorf, CH)
Casein resorufin-labelled	Roche (Lewes, East Sussex, UK)
Qiagen maxi prep kit	QIAGEN (Crawley, West Sussex, UK)
Qiawell8 plasmid purification kit	QIAGEN (Crawley, West Sussex, UK)
Qiaquick gel extraction kit	QIAGEN (Crawley, West Sussex, UK)
Qiaquick PCR purification kit	QIAGEN (Crawley, West Sussex, UK)
XP	Sigma (Poole, Dorset, UK)

Table 3.2 Enzymes

Enzymes	**Supplier**
Calf intestine alkaline phosphatase (CIAP)	Boehringer Mannheim (Lewes, East Sussex, UK)
Klenow (large fragment)	New England Biolabs (Beverly, MA, USA)
Lysozyme	Sigma (Poole, Dorset, UK)
Shrimp alkaline phosphatase (SAP)	Roche (Lewes, East Sussex, UK)
T4 DNA ligase	Promega (Madison, WI, USA)
T4 DNA ligase (High concentrated)	Promega (Madison, WI, USA)
T4 polynucleotide kinase	New England Biolabs (Beverly, MA, USA)
Pfu polymerase	Stratagene (Cambridge, UK)
Vent polymerase	New England Biolabs (Beverly, MA, USA)

Table 3.3 Antibodies/antisera

Antibody/antisera	Poly-/monoclonal	Secondary antibody	Company
α-His	monoclonal	α-mouse IgG AP	QIAGEN (Crawley, West Sussex, UK
α-PhoA	monoclonal	α-mouse	laboratory collection
α-GroEL	polyclonal	α-rabbit	laboratory collection
α–MBP	polyclonal	α-rabbit	laboratory collection
α-PS1	polyclonal	α-rabbit	Santa Cruz (CA, USA)
α–C99	polyclonal	α-rabbit	Zymed Laboratories (San Francisco, CA, USA)
α-Aβ40 (1)	polyclonal	α-rabbit	Peptide (Scientific Marketing Associates, Barnet, UK)
α-Aβ40 (2)	polyclonal	α-rabbit	Santa Cruz (CA, USA)
α-Aβ42	polyclonal	α-rabbit	Oncogene (Cambridge, UK)
α-L56	polyclonal	α-rabbit	provided by Marco Paggi (Italy); affinity purified
α-L56	polyclonal	α-rabbit	laboratory collection

3.1.1 Specificity of the L56 antibodies

Immunising a rabbit with purified Δmac25L56 which also contained SlyD as a contaminant produced a polyclonal antiserum. The specificity of the antiserum was verified by Western

blotting of whole cell extracts producing or not producing L56. Our polyclonal antiserum was used for most of the Western blots. Affinity purified polyclonal α-L56 antibody was provided by Dr. Marco Paggi (Italy). The reason for using both, L56 antiserum and α-L56 antibody, was because a collaborator was trying immunostaining for which the affinity purified antibody is an advantage. In order to use the same antibody for addressing the role of L56 in arthritis, the affinity purified antibody was used throughout.

3.2 *E. coli* strains

Table 3.4 E. *coli* strains

Strain	Genotype	Reference
DHB4	F´*lacIQ pro/araD139 Δ(ara-leu)7697 ΔlacX74 ΔphoA-PvuII phoR ΔmalF3 galE galK thi rpsL*	Boyd *et al.*, 1987
CLC198	MC4100 *degP*::Tn*10*	laboratory collection
KU98	DHB4 *degP::kan treA::spec*	laboratory collection
FA113	DHB4 *gor522*..miniTn*10*Tet *trxB::kan* suppressor	laboratory collection (Bessette, 1999)
MH1	*ΔfhuA Δptr ΔdegP (htrA) ΔompT ΔhhoAB shhΔprc::kan*	laboratory collection
KU105	*treA::specΔtreRBC*.....ΔTn*10Δara714*.....Leu+ *degP::tet prlA...kan*	laboratory collection
RY3041	BL21 *slyD*::Tn*10*	laboratory collection

RY3080	BL21 *slyD::kan*	laboratory collection

3.3 Plasmids

Table 3.5 Plasmids

Plasmid	Genotype	Resistance	Reference
pTS1	puc19 *l56*	amp	Trueb *et al.*, 1996
pCS19	pQE-60 derivate with the *lacIQ* gene	amp	laboratory collection
C99pCIneo	*c99* in pCINeo	neo	laboratory collection
pSG4	pCS19 with the *ssl56* gene cloned into *NcoI/BglII*	amp	this work
pSG5	pCS19 with the *Δssl56* gene cloned into *NcoI/BglII*	amp	this work
pSG6	pCS19 with the *Δssc99* gene cloned into *NcoI/BglII*	amp	this work
pSG7	pCS19 with the *Δmac25l56* gene cloned into *NcoI/BglII*	amp	this work
pSG8	pSG5 with the *phoA* gene fused to the 3´end of the *l56* gene	amp	this work
pSG9	pSG5 with the *E. coli* DegPss cloned in front of the *Δssl56* gene into the *NcoI* site	amp	this work
pSG10	pSG7 with the *E. coli* DegPss cloned in	amp	this work

	front of the *Δmac25l56* gene into the *NcoI* site		
pSG11	pSG5 with the S321A exchange	amp	this work
pSG12	pSG6 with the chloramphenicol resistance and the *origin* of pACYC184; cloning sites *AvaI/SapI* (pSG6) and *HindIII/AvaI* (pACYC184)	cm	this work
pSG13	pSG7 with *Δmac25l56SA* from pSG11 cloned into *PstI/ BglII*	amp	this work
pSG14	pSG6 with *Δssc99* without the sequence for the C-terminal His Tag	amp	this work
pSG15	pSG4 with the chloramphenicol resistance and the *origin* of pACYC184; cloning sites *AvaI/SapI* (pSG4) and *HindIII/AvaI* (pACYC184)	cm	this work
pSG16	pSG7 with the chloramphenicol resistance and the *origin* of pACYC184; cloning sites *AvaI/SapI* (pSG7) and *HindIII/AvaI* (pACYC184)	cm	this work
pSG21	pSG14 with the chloramphenicol resistance and the *origin* of pACYC184; cloning sites *AvaI/SapI* (pSG14) and *HindIII/AvaI* (pACYC184)	cm	this work
pSG22	pSG6 with *Δssc99* encoding Gly25-Ser	amp	this work
pSG23	pSG6 with *Δssc99* encoding Gly29-Ser	amp	this work
pSG24	pSG6 with *Δssc99* encoding Gly33-Ser	amp	this work
pSG25	pSG6 with *Δssc99* encoding Gly37-Ser	amp	this work
pSG26	pSG6 with *Δssc99* encoding Gly38-Ser	amp	this work

pSG27	pSG6 with *Δssc99* encoding Ala42-Ser	amp	this work
pSG28	pSG6 with *Δssc99* encoding Gly29-Ser and Ala42-Ser	amp	this work
pSG31	pSG6 with *Δssc99* encoding Val45-Ile	amp	this work
pSG32	pSG6 with *Δssc99* encoding Gly29-Ser, Gly33-Ser and Ala42-Ser	amp	this work
pSG33	Enterotoxin plasmid Variant 3 with *l56*	amp	this work
pSG34	Enterotoxin plasmid Variant 6 with *l56*	amp	this work
pSG35	Enterotoxin plasmid Variant 8 with *l56*	amp	this work
Variant 3	Enterotoxin ss variant 3 in ssTIRPhoA	amp	Simmons, 1996
Variant 5	Enterotoxin ss variant 5 in ssTIRPhoA	amp	Simmons, 1996
Variant 6	Enterotoxin ss variant 6 in ssTIRPhoA	amp	Simmons, 1996
Variant 8	Enterotoxin ss variant 8 in ssTIRPhoA	amp	Simmons, 1996
pMH12	pGDR11 with *wtpsI*	amp	Thesis Mona Harnasch
pMH13	pGDR11 with *psIΔ9*	amp	Thesis Mona Harnasch
pHM14	pEDIE3 with *wtpsI* without His Tag under an arabinose promoter	amp	Thesis Mona Harnasch
pMH15	pEDIE3 with *psIΔ9* without His Tag under an arabinose promoter	amp	Thesis Mona Harnasch
pMH1	*wtpsI* in pCS19 (*NcoI/BglII* (PCR))	amp	Thesis Mona Harnasch
pMH2	*psI* fragment 1 cloned into pEDIE3 restriction sites *XmaI/XbaI*	amp	Thesis Mona Harnasch
pMH3	*psI* fragment 2 cloned into pEDIE3 restriction sites *XmaI/XbaI*	amp	Thesis Mona Harnasch
pMH4	*psI* fragment 3 cloned into pEDIE3	amp	Thesis

	restriction sites *XmaI/XbaI*		Mona Harnasch
pMH5	***psl* fragment 4 cloned into pEDIE3**	**amp**	**Thesis**
	restriction sites *XmaI/XbaI*		**Mona Harnasch**
pMH6	*psl* fragment 5 cloned into pEDIE3	amp	Thesis
	restriction sites *XmaI/XbaI*		Mona Harnasch
pMH7	***psl* fragment 6 cloned into pEDIE3**	**amp**	**Thesis**
	restriction sites *XmaI/XbaI*		**Mona Harnasch**
pMH8	*psl* fragment 7 cloned into pEDIE3	amp	Thesis
	restriction sites *XmaI/XbaI*		Mona Harnasch
pMH9	***psl* fragment 8 cloned into pEDIE3**	**amp**	**Thesis**
	restriction sites *XmaI/XbaI*		**Mona Harnasch**
pMH38	*wtpsl* without His Tag	amp	Thesis
			Mona Harnasch
pMH39	***psl*Δ9 without His Tag**	**amp**	**Thesis**
			Mona Harnasch
PMH10	*wtpsl* cloned into pEDIE3	amp	Thesis
	restriction sites *XmaI/XbaI*		Mona Harnasch

All generated plasmids were sequenced.

3.4 Media

The composition of media was as described by Miller (1972) and Silhavy *et al.*, (1984).

3.4.1 Liquid and solid media

All media were sterilised by autoclaving for 20 min. After cooling down to 50-60°C, the separately autoclaved or sterile filtered media supplements from Table 3.6 were added.

LB (Luria Bertani broth):

10 g/l Bacto-Tryptone

5 g/l Bacto-Yeast-Extract

7.5 g/l NaCl

(17 g/l Bacto-Agar for plates)

in distilled H_2O

NZA (NZ-AmineA):

10 g/l NZ-Amine

5 g/l Bacto-Yeast-Extract

7.5 g/l NaCl

(17 g/l Bacto-Agar for plates)

in distilled H_2O

G&L medium (Low phosphate medium < 1 mM Pi):

23,35 g/l NaCl

7,45 g/l KCl

72,5 g/l Tris

13,2 g/l $(NH_4)_2SO_4$

1,25 g/l $MgSO_4$

0,136 g/l KH_2PO_4

in distilled H_2O

adjust to pH 7.5 with HCl or use pre-made 600 mM Tris-HCl buffer pH 7.5

3.4.2 Supplements for media

All of the following substances were prepared as stock solutions and sterilised by filtration through a Millipore filter (diameter 0.45 μm)

Table 3.6 Media supplements

Supplement	Stock solution	Final concentration	Storage temperature
Ampicillin	100 mg/ml in distilled H_2O	200 µg/ml	4°C – 8°C
Chlor-amphenicol	30 mg/ml in 100% EtOH	15 µg/ml	4°C – 8°C
XP	30 mg/ml in 100% DMF	200 µg/ml	4°C – 8°C
IPTG	1 M in distilled H_2O	10 µM,100 µM, 1 mM	-20°C

3.5 Microbiological Methods

3.5.1 Sterilisation

Media, buffers and glassware were sterilised by autoclaving (20 min. 121°C, 1 bar). Solutions sensitive to heat were filter sterilised (0.2 µm pore size).

3.5.2 Growth conditions and storage of E. coli

The defined growth conditions are given in the protocols or results.
Liquid cultures (5 ml) were grown in 20 ml glass reaction tubes in a culture roller drum (ca. 50 rpm) at 37°C or 28°C. Liquid cultures over 5 ml were grown in Erlenmeyer flasks, with a volume 5 times bigger than the culture volume at 37°C or 28°C in incubator chests, shaking at 220 rpm.

Cultures on agar plates were grown at 37°C or 28°C for 10 to 15 hours. DMSO cultures were prepared for storage of bacterial strains at –80°C, where 1.7 ml of an overnight LB/NZA-culture was mixed with 126 µl DMSO (dimethyl sulphoxide) and quickly frozen.

3.5.3 Determination of the cell density

The density of a cell culture was determined by measurement of the optical density at a wavelength of 578 nm. Thereby an OD_{578} of 1 corresponds to 107 µg protein/ml and to a cell number of 10^9 cells.

3.6 Molecular biological methods

3.6.1 Preparation of double stranded plasmid DNA

The plasmid preparation kit from Qiagen was used for double-stranded DNA preparation. The Qiagen Maxi preparation kit was used for midi preparations from a culture volume of 100 ml.

3.6.2 Separation of DNA fragments on agarose gels

Following digestion with restriction enzymes, plasmid DNA was separated on 0.8% (w/v) agarose gels in TAE buffer (40 mM Tris, 1 µM EDTA (pH 8.0), 0.1% acetic acid) with a constant voltage of 80 or 110 V (depending on the size of the gel).
The DNA was stained in an ethidium bromide bath (1 µg/ml in TAE buffer) and visualised in UV light. The molecular weight of individual DNA fragments was determined using a variety of basepair standard markers (λ-DNA, *BstEII* digested, New England Biolabs).

3.6.3 Transformation

3.6.3.1 TSS transformation

For low yield transformations, the TSS (transformation and storage solution) method of transformation was used. LB/NZA cultures (5 ml), containing the appropriate antibiotics, were inoculated from a single colony and then grown at 37°C to an optical density at 578 nm of 0.5 (OD_{578} = 0.5). This culture was mixed with ice-cold 2 x TSS (20% (w/v) PEG-6000, 10% (v/v) DMSO, 100 mM $MgSO_4$ dissolved in LB/NZA medium). Plasmid DNA (1-3 µl) was added to 100 µl TSS culture and incubated on ice for 30 min. After this step, 1 ml of LB/NZA was added and a phenotypic expression for 1 h at 37°C was performed. This transformation reaction was then plated on LB/NZA agar plates with the appropriate antibiotics and incubated o/n at 37°C or 28°C.

3.6.3.2 Electrotransformation

For high yield transformations (ligation reactions), the electroporation method was used, according to the BioRad Electroporation Application Guide (Cat.No. 165-2100).

Preparation of competent cells

An overnight culture was diluted 1/100 in LB (+/- antibiotics) and was grown at 37°C to an OD_{578} of 0.5-1.0. The culture was chilled on ice for 15 min and centrifuged for 5 min at 5000 rpm in a GSA rotor. The supernatant was discarded and the pellets were resuspended in 1 volume of ice-cold sterile Millipore water. Subsequently, the cells were sedimented by centrifugation for 5 min at 5000 rpm in a GSA rotor and the pellets were resuspended in 1/2 volume of ice-cold and sterile Millipore water. A third centrifugation step, analogous to the steps before, was performed and the sedimented cells were resuspended in 1/50th volume of 20% ice-cold sterile glycerol. After sedimenting the cells in a SS34 rotor by

centrifugation for 5 min at 6000 rpm, the pellets were resuspended in 1/500th volume of 20% glycerol and aliquoted into 50 µl fractions. The aliquots were quickly frozen in liquid nitrogen and stored at -70°C

Electroporation

The competent cells were thawed on ice. Aliquots (1-3 µl) of the ligation reaction were added to a 50 µl cell aliquot and transferred into a 0.2 cm electroporation cuvette. An electric pulse of 2.5 kV (setting EC2 at the MicroPulser) was used and the cells were immediately transferred into 1 ml LB/NZA medium and incubated at 37°C for 1 h in an incubator. The cells were pelleted, resuspended in approximately 200 µl medium and plated on agar plates containing the required antibiotics.

3.6.4 DNA modifications

3.6.4.1 Dephosphorylation

To ligate DNA fragments carrying identical termini (blunt-end or generated by the action of one restriction enzyme), the termini were dephosphorylated to suppress self-ligation and circularisation of the plasmid DNA. This religation step can be minimised by removing the 5´-phosphates from both termini of the linear DNA with either shrimp alkaline phosphatase (SAP) or calf intestine alkaline phosphatase (CIAP). They both catalyse the removal of 5´phosphates from DNA. The advantage of SAP is that it can be completely and irreversible inactivated by heat treatment for 15 min at 65°C, unlike the CIAP, which must be separated from the DNA either by gel extraction or by using the PCR purification kit from Qiagen.

CIAP assay (for dephosphorylation of 20 µg DNA):

CIAP (3 µl of a 1 U/µl stock) and 1/10th volume of dephosphorylation buffer (10 x) were added to the restriction assay. The mixture was incubated for 30 min at 37°C for dephosphorylation of sticky ends and 60 min at 37°C for dephosphorylation of blunt ends and subsequently for 30 min at 56°C. After the dephosphorylation, 1/10th volume of 0.5 M EDTA pH 8.0 was added and the mixture was incubated for 20 min at 70°C. To achieve complete inactivation of the CIAP, an agarose gel was run and the required DNA fragment was cut out and the gel slice was extracted with the gel extraction kit from Qiagen.

SAP assay (for dephosphorylation of 20 µg DNA):

SAP (3 µl of a 1 U/µl stock solution) and 1/10th volume of dephosphorylation buffer (10 x) were added to the restriction assay. The mixture was incubated for 15 min at 37°C for dephosphorylation of sticky ends and for 60 min at 37°C for dephosphorylation of blunt ends. The SAP was then heat-inactivated for 15 min at 65°C and the mixture was used for ligation assays.

3.6.4.2 Phosphorylation of DNA fragments

The T4 polynucleotide kinase (New England Biolabs) was used for phosphorylation of primers or longer DNA fragments. It catalyses the transfer and exchange of Pi from the γ position of ATP to the 5'hydroxyl-terminus of polynucleotides (double-stranded and single-stranded DNA and RNA) and nucleoside-3'-monophosphates.

Assay:

50 µg oligonucleotides
10 µl kinase buffer 10 x
10 µl ATP (10 mM stock)
1 µl T4-Polynucleotide kinase (10,000 u/ml)

---

made up to 100 µl with sterile Millipore H_2O

The assay was incubated for 60 min at 37°C and the T4-polynucleotide kinase was heat-inactivated by incubation for 20 min at 65°C.

3.6.4.3 Filling of recessed 3 ′-termini (5 ′overhangs)

The large Klenow fragment was used for creation of blunt ends. The Klenow fragment is a proteolytic product of *E. coli* DNA Polymerase I, which retains polymerisation and 3'- 5' exonuclease activity, but has lost 5' – 3' exonuclease activity. Klenow retains the polymerisation fidelity of the holoenzyme without degrading 5'-termini.
To achieve blunt ends, the restriction assay (10 µl) was incubated with 3 µl of dNTP mix (stock 1 mM of each dNTP) and 3 µl of Klenow fragment (5 U/µl) for 15 min at 25°C. Following this reaction the Klenow fragment was heat-inactivated by incubation for 20 min at 75°C.
The Klenow fragment works well in most restriction buffers. If the DNA was in a special buffer or dissolved in water, the recommended 10 x Eco Pol reaction buffer was used in a volume of 1/10.

3.6.5 Polymerase Chain Reaction (PCR)

PCR was used for amplification of DNA fragments. A typical reaction is described below:

10 µl 10 x thermopolymerase buffer
2 µl 10 mM dNTP
1 µl DNA
1 µl 0.5 µg/ml coding strand (cs) oligonucleotide
1 µl 0.5 µg/ml non-coding strand (nc) oligonucleotide
1 µl 3 U/µl DNA-polymerase (*Vent*)
(10 µl DMSO)

made up to 100 µl with sterile Millipore H_2O

DMSO was used in every PCR reaction with the *l56* sequence as the GC-rich region of the *l56* gene had the potential to form secondary structures which could be relaxed by DMSO. It was not possible to get any PCR product without DMSO in these PCR reactions. The *c99* PCR reactions were performed without DMSO. The thermocycle protocol was adjusted to the melting temperature of the oligonucleotides and the efficiency of the DNA-polymerase used. A typical protocol is described below:

3 min at 94° C
followed by 40 cycles of
30 sec at 94°C
1 min at ca. 5°C below melting temperature of oligonucleotide
2 min/kb to amplify at 72°C
followed by
5 min at 72°C

The reactions were analysed by agarose gel electrophoresis (as described previously).

Table 3.7 PCR primer

cloning	**Sequence**	**Primer name**
pSG4	5'-TTCccatggcGATCCCGCGCGCCGCTCTTCTCC-3'	longdegPcs*NcoI*
pSG4, 5, 7	5'-gtcgaagatctTGGGTCAATTTCTTCGGGAATCactg-3'	longdegPncs*BglII*
pSG5	5'-catgccatggcaCAGCTGTCCCGGGCCGGCCGCTCG-3'	ΔssL56*NcoI*
pSG7	5'-CatgccatggcaGAGAGGCTGCACCGGCCGCCGGTCATC-3'	deltamac25L56
pSG6	5'-CATGCCatggatgcagaattccgacatgactcagg-3'	ΔssC99pCINeo*NcoI*
pSG6	5'-GAAGATCTgttctgcatctgctcaaagaacttgtaggttgg-3'	C99pCINeo*BglII*

3.6.5.1 *C*ross-over PCR

The cross-over PCR method was used instead of a site-directed oligomutagenesis to create the L56SA mutant. Two different PCR reactions were performed with the following primers:

Table 3.8 Cross-over PCR primer for pSG11 cloning.

Primer	Primer sequence	Primer name
1	5'-catgccatggcaCAGCTGTCCCGGGCCGGCCGCTCG-3'	ΔssL56*NcoI*
2	5'-GGTTTACTAACGGGCCgCCgGcGTTTCCatagttg-3'	L56SA*NaeI*ncs
3	5'-gtcgaagatctTGGGTCAATTTCTTCGGGAATCactg-3'	longdegPncs*BglII*
4	5'-caactatGGAAACgCcGGcGGCCCGTTAGTAAACC-3'	L56SA*NaeI*cs

Complementary L56SA oligonucleotides (primers 3 and 4) annealed within the *l56* gene and led to the exchange of the serine to an alanine while introducing a new *NaeI* site. The two different PCR products were separated on an agarose gel, removed and extracted with the gel extraction kit from Qiagen. Subsequently, fragments were annealed in the thermocycler at the complementary primer sequence and the overhangs were filled in with *Vent* polymerase.

Annealing reaction

10 µl PCR reaction 1

10 µl PCR reaction 2

5 µl thermopolymerase buffer 10 x

2 µl dNTP mix (stock 10 mM of each dNTP)

1 µl *Vent* polymerase (3 U/µl)

---

made up to 50 µl with sterile Millipore H_2O

The program for the annealing reaction and the fill in reaction was:

2 min 94°C
30 sec. 94°C
1 min 55°C | 10 cycles
3 min 74°C

Time of incubation at 74°C was chosen depending on the length of the overhangs (*Vent* polymerase requires 2 min per kb of DNA).
Subsequently, a third PCR reaction with the PCR primers 1 and 2 was performed after adding 50 µl of a PCR premix to the annealing reaction.

The premix contained:
5 µl thermopolymerase buffer 10 x
2 µl dNTP mix (stock 10 mM of each dNTP)
1 µl *Vent* polymerase
5 µl DMSO
---
made up to 50 µl with sterile Millipore H_2O

The resulting PCR product was *NcoI/BglII* digested and purified on an agarose gel with the gel extraction kit (Qiagen). The digested pure insert was used for cloning into pCS19.

3.6.6 Restriction digestions of plasmid DNA

The restriction digestions were mainly used for genotypic tests of created plasmids and for cloning. The enzymes were used in their recommended buffers to achieve an optimal result.

A typical restriction assay was:

x µl DNA (0.5-1µg for plasmid tests and 8-15 µg for cloning)

1/10 µl restriction buffer 10 x

x µl restriction enzyme (5-10 U/µg DNA)

---

made up to 20 µl for plasmid tests and 100 µl for cloning with sterile Millipore H_2O

Incubation times varied from 3 h to overnight depending on enzyme concentrations. Where possible enzymes were inactivated by incubation for 10 min at 65°C or by adding 1/10th volume of gel loading buffer (0.25% bromphenol blue, 0.25% xylene cyanol FF, 30% glycerol in H_2O).

3.6.7 Cloning

3.6.7.1 Isolation of DNA fragments from TAE-agarose gels

A clean scalpel was used to remove the DNA fragment from the agarose gel following ethidium bromide staining. Subsequently, the fragment was eluted with the help of the Qiaquick gel extraction kit (Qiagen). The elution was carried out by following the instructions of the supplier.

3.6.7.2 Ligation of compatible ends of vector and insert

After extraction and elution of the vector and insert fragments from the agarose gel, they were mixed in a ratio of 1:5, 5:1 and 5:5. T4-DNA ligase (1 µl) (Promega) and 10 x ligase buffer (2 µl) were added to each assay and made up with sterile Millipore water to a final volume of 20 µl. A sample with vector and without insert served as a control for religation.

For ligation of sticky ends, the assays were incubated overnight in a beaker filled with 2 l of tap water (14°C) in the cold room. The beaker was in a polystyrene box closed with a lid. For ligation of blunt-ends, the assays were incubated in the same way, but the water had a temperature of 24°C. Ligation was terminated following heat-inactivation at 65°C for 10 minutes. An aliquot (1-3 µl) of the ligation was transformed into competent cells by electroporation.

3.6.7.3 Cloning of the DegP signal sequence

The sequence for the DegP signal sequence (ss) was divided into two halves and oligonucleotides (100 µg) that had a complementary region of about 20 bp were phosphorylated by the T4 polynucleotide kinase for 1 h at 37°C. After phosphorylation, an annealing reaction of the two oligonucleotides was performed.

Annealing reaction

20 µg oligonucleotide 1
20 µg oligonucleotide 2
10 µl Eco Pol buffer 10 x
---
made up to 100 µl with sterile Millipore H_2O

PCR programme:

1 min 94°C
2 min 55°C | 10 cycles
2 min 37°C |
10 min 55°C

Then 5 µl of the Klenow fragment and 1µl dNTP mix (stock 10 mM of each dNTP) was added and incubated for 30 min at 25°C to fill-in the overhangs. The Klenow fragment was

heat-inactivated for 10 min at 75°C. The double strand oligonucleotide was cleaved with *NcoI*, the *NcoI* was heat-inactivated and the remaining ss oligonucleotide was ligated into the vector.

3.6.8 Site-directed oligomutagenesis with Pfu polymerase

Site-directed oligomutagenesis was used for the nucleotide exchange encoding for the different C99 Gly to Ser exchange mutants. Each oligonucleotide pair introduced a new restriction site into the plasmid for detection of the mutation.
First a PCR reaction mix was prepared as described below.

PCR reaction mix:

10 µl 10x Pfu buffer
2 µl 10 mM dNTP Mix
1 µl template DNA
1 µl 0.5 µg/ml coding strand (cs) oligonucleotide
1 µl 0.5 µg/ml non-coding strand (ncs) oligonucleotide
1 µl *Pfu* polymerase
---
made up to 100 µl with sterile Millipore water

Generally, a PCR reaction was performed with an extension time measured from the size of the plasmid. The *Pfu* polymerase has an efficiency of 1 nucleotide/min. The number of cycles was 16-20.
After the PCR reaction, the sample was incubated overnight at 37°C with the restriction enzyme *DpnI* to remove the methylated template DNA. *DpnI* was heat inactivated for 20 min at 65°C and an aliquot of 1-2 µl of the reaction was transformed into DHB4 by electroporation. After plasmid preparation, the transformants were tested for the introduced restriction sites.

Table 3.9 Oligomutagenesis primers

Cloning	Sequence	Primer name
pSG22	5'-ggtgttctttgcagaagaCgtCAgttcaaacaaagg-3'	*AatII1*Gly
pSG22	5'-cctttgtttgaacTGacGtcttctgcaaagaacacc-3'	*AatII1*Glyncs
pSG23	5'-gaagatgtgggAtcCaacaaaAgtgcaatcattgg-3'	*BamHI*2Gly
pSG23	5'-ccaatgattgcacTtttgttGgaTcccacatcttc-3'	*BamHI*2Glyncs
pSG24	5'-gggttcaaacaaaggCgcCatcattAgCctcatggtggg-3'	*KasI*3Gly
pSG24	5'-cccaccatgagGcTaatgatGgcGcctttgtttgaaccc-3'	*KasI*3Glyncs
pSG25	5'-gcaatcattggaTtAatggtgTCcggtgttgtcatag-3'	*AseI*4Gly
pSG25	5'-ctatgacaacaccgGAcaccatTaAtccaatgattgc-3'	AseI4Glyncs
pSG26	5'-ggactcatggtgggATCCgttgtcatagcgacag-3'	*BamHI*5Gly
pSG26	5'-ctgtcgctatgacaacGGATcccaccatgagtcc-3'	*BamHI*5Glyncs
pSG27	5'-cggtgttgtcataAGTacTgtgatcgtcatcacc-3'	*ScaI*6Ala
pSG27	5'-ggtgatgacgatcacAgtACTtatgacaacaccg-3'	*ScaI*6Alancs
pSG31	5'-gcgacagtgatcAtcatcacACtAgtgatgctgaag-3'	Londonmut.
pSG31	5'-cttcagcatcacTaGTgtgatgaTgatcactgtcgc-3'	Londonmut.ncs

3.7 Biochemical methods

3.7.1 SDS-PAGE

Gels were prepared using a Bio Rad system (Hemel Hempstead, Hertfordshire, UK) and 15 – 20 µl of samples were loaded carefully. The gel was run at 0.025 A for approximately 1 h in running buffer (33 mM Tris, 180 mM glycine, 10% SDS). Subsequently, the gel was either blotted or stained with Coomassie Blue (AppliChem, Darmstadt, Germany). Schaegger gels were used for separation of small proteins.

Table 3.10 Compositions of SDS-Minigels

Minigel:

	7%	10%	12%	15%	stacking gel
Buffer A (1.5 M Tris-HCl buffer pH 8.8, 0.4 % SDS)	**2.5 ml**	**2.5 ml**	**2.5 ml**	**2.5 ml**	*
Buffer B (0.5 M Tris-HCl buffer pH 6.8, 0.4% SDS)	*	*	*	*	2 ml
Acrylamide stock (30%)	**1.75 ml**	**2.5 ml**	**3 ml**	**3.75 ml**	**0.9 ml**
H_2O	5.75 ml	5 ml	4.5 ml	3.75 ml	5.1 ml
TEMED	**10 µl**	**10 µl**	**10 µl**	**25 µl**	**20 µl**
APS (stock 1%)	25 µl	25 µl	25 µl	25 µl	40 µl

Table 3.11 Composition of Schaegger gels.

	16.5% separation gel	**10% spacer gel**	**4% stacking gel**
Acrylamide (49.5% = 48 g / 100 ml acrylamide; 3% = 1.5 g / 100 ml bisacrylamide)	3.5 ml	1.5 ml	O.5 ml
Gel buffer (3 M Tris-HCl buffer pH 8.45; 0.3% SDS)	**3.5 ml**	**2.5 ml**	**1.55 ml**
H_2O	*	3.5 ml	4.2 ml
32% glycerol	**3.5 ml**	*	*
APS (10%)	32.5 µl	35 µl	25 µl
TEMED	**10 µl**	**10 µl**	**10 µl**

3.7.2 Immunoblot analysis (Western blot)

After separation of the sample proteins, the SDS-gel was placed into the prepared transfer-buffer (15 mM Tris, 120 mM glycine, 1/5th volume of methanol, 0.2% SDS). The blot membrane (FluoroTrans, Pall, Ireland) was activated in 100% methanol for a few seconds and the blotting-apparatus (Bio Rad Mini Trans-Blot® Cell) was constructed as recommended. The electrotransfer was performed for 1 h at 100 V. After transfer, the membrane can be stored between two Whatman papers (GB 003, Schleicher & Schuell, Germany) at –20°C.

Before detection of the protein band(s) with specific antibodies, the membrane was blocked for at least 1 h at RT on a table-shaker (or o/n) with 2% BSA (Sigma) in TBS-T (20 mM Tris-HCl buffer pH 7.5, 150 mM NaCl, 0.05% Tween-20) or 5% milk powder (Tesco) in TBS-T. After blocking, the membrane was incubated in 10 ml TBS-T with the appropriate concentration of primary antibody with shaking for 1 h. The following steps were performed at RT with shaking. After binding of the primary antibody, the membrane was washed three times for 5 min in 10 ml TBST-T. The washed membrane was incubated in 10 ml TBS-T with the recommended concentration of secondary antibody for 30-60 min. The described washing procedure was repeated and the membrane was incubated for 1 min in AP buffer (100 mM Tris-HCl buffer pH 9.5, 100 mM NaCl, 5 mM $MgCl_2$) before staining. About 10 ml of the prepared staining solution (10 ml AP buffer, 66 µl NBT (50 mg/ml in 70% DMF), 33 µl BCIP (40 mg/ml in 100% DMF)) was added. The staining reaction was terminated by gentle rinsing with tap water.

3.7.3 Coomassie staining

3.7.3.1 Rapid staining procedure with Coomassie Blue

This is a modification of a previously described technique (Fairbanks *et al.*, 1971) which involves heating the polyacrylamide gels in the staining solutions with a microwave. A total processing time of 20 min using the rapid Fairbanks method allows visualisation of as little as 5 μg of protein.

After SDS-gel-electrophoresis, the gel was heated for 30 sec in solution A (25% 2-propanol, 10% acetic acid, 0.05% Coomassie Blue) in a microwave and shaken for 5 min. Subsequently, solution B (10% 2-propanol, 10% acetic acid, 0.005% Coomassie Blue) was added, heated and discarded. The gel was treated in the same way with solution C (10% acetic acid, 0.002% Coomassie Blue). A complete destaining of the background was achieved by shaking the gel with destaining solution (10% acetic acid) for 1 h at RT.

3.7.4 Gel drying

After destaining, gels were dried using a special GelAir Drying Frame (Bio Rad). Gels were incubated in a gel-drying solution consisting of 5% ethanol and 10% glycerol in water for at least 30 min and placed between 2 sheets of cellophane. The gel was dried at 28°C overnight.

3.7.5 Preparation of spheroplasts

Spheroplasts were prepared to test if ssL56 was localised in the periplasm. Spheroplasts are *E. coli* cells with a permeabilised outer membrane and a digested murein layer. They can therefore be considered as vesicles mainly containing the inner membrane and the cytoplasm. An aliquot (2 ml) of cells overexpressing the gene of interest was centrifuged for 1 min at 10,000 rpm. Cells were washed once with TMK buffer (2 ml) (33 mM Tris-HCl buffer pH 8.0, 100 mM KCl, 5 mM $MgSO_4$) and the pellet was resuspended in 1 ml TMK buffer/40% sucrose. Spheroplasts were generated following the addition of EDTA (5 mM final concentration) and lysozyme (100 μg/ml final concentration) and incubation for

30 min on ice. Subsequently, spheroplasts were pelleted by centrifugation for 5 min at 6000 rpm. The pellet (spheroplasts) was resuspended in 100 µl 4 x SB/(DTT). The supernatant was precipitated with TCA and the precipitated proteins were resuspended in 100 µl 4 x SB/(DTT). An aliquot of 20 µl of each fraction was loaded on a SDS-gel.

3.7.6 TCA precipitation

TCA (340 µl of a 20% stock solution) was added to a sample volume of 1 ml. The samples were incubated on ice for 20 min. Subsequently a centrifugation step of 5 min was carried out (14000 rpm, table centrifuge). After removal of the supernatant, 1 ml of acetone (cold) was added to the pellet. Samples were then centrifuged for a further 5 min (14000 rpm) and the supernatants were discarded. Pellets were dried and then dissolved in sample buffer (4 x) before loading on a SDS-gel.

3.7.7 Zymogram

Ready gel zymogram was used to detect proteolytic activity of pre-purified L56. The gel contained casein which is a substrate for various proteases. The zymogram and the recommended buffers were from Biorad (Hertfordshire, UK). Samples were electrophoretically separated under reducing and non-reducing conditions, allowed to renature and consume the substrate. After gel electrophoresis the gel was incubated for 30 min in renaturing buffer (2.5% Triton X-100). Subsequently, the gel was incubated overnight at 37°C in developing buffer (50 mM Tris-HCl buffer pH 7.5, 200 mM NaCl, 5 mM $CaCl_2$, 0.02% Brij-35). The incubation was followed by Coomassie blue staining. Protease activity was detected as clear bands.

3.7.8 Purification by FPLC (Fast protein liquid chromatography)

3.7.9 Production of recombinant proteins

For production of recombinant proteins, plasmids encoding the different L56 or C99 constructs with a C-terminal His Tag were transformed into several *E. coli* strains. For expression, NZA (+ ampicillin) was inoculated with a single colony and cells were grown to saturation overnight. The overnight culture was diluted 1:50 in the same medium and growth was maintained at 28°C until the absorbance (578 nm) measured approximately 0.3 - 0.5. At this point, isopropyl-ß-D-thiogalactoside (IPTG) was added to a final concentration of 10 μM, 100 μM or 1 mM (see results). The culture was maintained for 4 h or overnight (see results) with shaking at 200 rpm. The cells were either used for purification or for SDS-PAGE.

3.7.10 Purification of L56 and C99

All steps were executed on ice or in a cold room at + 4°C to + 8°C. All buffers were chilled.

3.7.10.1 Preparation of soluble L56

The harvested cells from a 3-4 l culture, overproducing L56, were resuspended in approximately 10 ml/l cell lysis buffer, which consists of 50 mM sodium phosphate buffer pH 7.5 containing 300 mM NaCl (1 M urea for Δmac25L56 purifications). Cells were disrupted in a French press 3 x at 15000 psi. The French press extract was centrifuged for 30 min with 13000 rpm in a SS34 rotor (Beckman) at 4°C to separate the cell debris and the inclusion bodies from the soluble proteins. The supernatant fraction containing soluble L56 was used for purification.

3.7.10.2 Preparation of membranes

The harvested cells from a culture overproducing C99 or C99/PS1 were resuspended in lysis buffer (50 mM Tris-HCl buffer pH 8.5, 300 mM NaCl for purifications). Cells were disrupted by French pressing 3 x at 15000 psi. The cell debris and aggregates were removed by an initial centrifugation step at 13000 rpm for 20 min (GSA rotor, Beckman). The supernatant was ultracentrifuged for 45 min at 45000 rpm to sediment membranes (Ti 70 rotor, Beckman). The membranes were resuspended in 50 mM Tris-HCl buffer, pH 8.5 300 mM NaCl and collected again by ultracentrifugation as above. The membranes were stored at -70°C.

3.7.10.3 Solubilisation of membrane proteins

For the solubilisation of C99 or PS1/C99, the membrane suspension was adjusted to a protein concentration of 2-2.5 mg/ml (measured by a BCA (bicinchoninic acid) protein determination kit) with lysis buffer (50 mM Tris-HCl buffer pH 8.5, 300 mM NaCl for purifications and for solubilisation experiments) containing 1% detergent. Dodecylmaltoside (DDM), SDS, CHAPSO and Brij35 were used as detergents. The suspension was stirred for 1.5-2 h on ice or at room temperature for SDS and subsequently ultracentrifuged for 30 min at 45000 rpm. The supernatant containing the solubilised proteins was used for chromatography purification or solubilisation tests.

3.7.10.4 Spin NiNTA columns

Small NiNTA columns from Qiagen were used to determine the best purification conditions for L56. The procedure was carried out as recommended by the supplier. Different buffers were used, following a protocol in the supplier's manual. The only difference was that 2 x 600 μl of French press supernatant, derived from a 1 l culture, was loaded on each spin column.

3.7.10.5 Purification of L56 constructs with a NiNTA Superflow column

The column was equilibrated with five to ten CV (column volumes) equilibration buffer (50 mM sodium phosphate buffer pH 7.5, 300 mM NaCl) every time. The protein solution (soluble L56) was loaded on the column with a flow rate of 0.3 ml/min. After the protein was loaded on the column, it was washed with ten CV washing buffer 1 (50 mM sodium phosphate buffer pH 7.5, 300 mM NaCl, 10 mM or 20 mM imidazole for full-length L56 and Δmac25L56 purifications). An additional washing step with ten CV washing buffer 2 (50 mM sodium phosphate buffer pH 6.3, 300 mM NaCl for full-length L56 purifications) was added to remove contaminants. The protein was eluted with ten CV elution buffer (50 mM sodium phosphate buffer pH 7.5, 300 mM NaCl containing 500 mM imidazole). The flow rate for washing steps and elution was 2 ml/min.

3.7.10.6 C99 purification with a NiNTA Superflow column

The column was equilibrated with five to ten CV equilibration buffer (50 mM Tris-HCl buffer pH 8.5, 300 mM NaCl). The protein solution (solubilised C99) was loaded on the column with a flow rate of 0.3 ml/min. Subsequently the column was washed with ten CV washing buffer 1 (50 mM Tris-HCl buffer pH 8.5, 300 mM NaCl, 0.25% SDS). The detergent was exchanged by washing the column with ten CV washing buffer 2 (50 mM Tris-HCl buffer pH 8.5, 300 mM NaCl, 0.05% DDM). After washing the column with washing buffer 3 (50 mM Tris-HCl buffer pH 8.5, 300 mM NaCl, 30 mM imidazole, 0.05% DDM) the protein was eluted with elution buffer (50 mM Tris-HCl buffer pH 8.5, 300 mM NaCl, 500 mM imidazole, 0.05% DDM).

3.7.10.7 Co-purification of PS1ΔHis and C99+His with a POROS column loaded with copper

The POROS MC20 material was loaded with copper ions and prepared for purifications following the supplier's manual. The bed volume was 5 ml. The column was equilibrated with ten CV 50 mM Tris-HCl buffer pH 8.5, 300 mM NaCl, and 30 mM imidazole. The protein solution (solubilised PS1ΔHis/C99+His in 50 mM Tris-HCl buffer pH 8.5, 300 mM NaCl, 30 mM imidazole) was loaded on the column with a flow rate of 0.3 ml/min. Subsequently, the column was washed with ten CV washing buffer (50 mM Tris-HCl buffer pH 8.5, 300 mM NaCl, 30 mM imidazole). The elution was performed in three steps with 50 mM Tris-HCl buffer pH 8.5, 300 mM NaCl containing various imidazole concentrations (75 mM, 100 mM and 500 mM). Brij35 (0.1%) was added to all buffers used.

3.7.10.8 Anion exchange chromatography

The pre-packed POROS HQ column was equilibrated with ten CV 50 mM Tris-HCl buffer pH 7.5, 150 mM NaCl. The dialysed pre-purified Δmac25L56 was loaded on the POROS HQ column with a flow rate of 0.1 ml/min. The column was washed with 20 CV 50 mM Tris-HCl buffer pH 7.5, 150 mM NaCl and a step gradient with 50 mM Tris-HCl buffer pH 7.5 containing 250 mM, 500 mM or 1 M NaCl was performed. The flow rate for washing and elution was 0.2 ml/min.

3.7.10.9 Cation exchange chromatography

The cation exchange column was packed with SP Sepharose material up to a bed volume of 5 ml. The column was equilibrated with ten CV of 100 mM Hepes buffer pH 8.0, 100 mM ammonium sulphate. The pre-purified Δmac25L56SA protein was dialysed against 100 mM Hepes buffer pH 8.0, 100 mM ammonium sulphate and loaded on the SP Sepharose column with a flow rate of 1.0 ml/min. The protein was eluted with 20 CV 100 mM Hepes

buffer pH 8.0, 500 mM ammonium sulphate. The flow rate for the equilibration and the elution step was 2.0 ml/min.

3.7.10.10 Gel filtration chromatography

Gel filtration chromatography relies on the fact that molecules in solution are separated by size as they pass through a column packed with a chromatographic medium. Relatively small molecules can diffuse into the gel whereas large molecules will be prevented by their size from diffusing into the gel and are thus confined to the solution. Gel filtration chromatography was used to determine the oligomerisation state of Δmac25L56.
The gel filtration column was equilibrated with ten CV 50 mM Tris-HCl buffer pH 7.5, 150 mM NaCl at 0.1 ml/min. Purified Δmac25L56 (250 μg of a 1 μg/μl stock solution) was applied to the gel filtration column (Superdex 200, Pharmacia) by injection with a Superloop. The column was washed with one CV 50 mM Tris-HCl buffer pH 7.5, 150 mM NaCl. A gel filtration with a calibration protein kit (Biorad) consisting of thyroglobulin (bovine) 670 kDa, gamma globulin (bovine) 158 kDa, ovalbumnin (chicken) 44 kDa, myoglobulin (horse) 17 kDa and vitamin B-12 1.35 kDa served to calibrate the column. The molecular mass can be determined by using the following formula:

Kav=(Ve-V0)/(Vt-V0)
Ve= elution volume
V0= void volume of the column determined using Blue Dextran 2000 (10.8 ml for the Superdex 200 HR 10/30)
Vt= bed volume of the column (24 ml for the Superdex 200 HR 10/30)

Table 3.12: Kav in relation to the molecular mass

Molecular mass (Da)	Elution volume (Ve) (ml)	Kav
670000	11.9	0.083
158000	15.1	0.325
44000	17.7	0.522
17000	19.6	0.666
1350	23.1	0.931

3.7.11 Enzymatic assays

3.7.11.1 Determination of Δmac25L56 activity with resorufin-labelled casein

Casein is a non-specific substrate for proteases and is used to determine low protease activities. Resorufin is a bright red fluorescent dye that serves as the basis for enzyme substrates. Any effect of proteases on the non-specific substrate casein results in the release of resorufin-labelled peptides that cannot be precipitated by trichloroacetic acid. These peptides can be detected by spectrophotometry at 574 nm and serve as a reporter for proteolytic activity.

A volume of 15 µl of a resorufin-labelled casein stock solution (4 mg/ml in 50 mM Tris-HCl buffer pH 7.5 or other assay buffers as indicated) was mixed with 5 µg Δmac25L56 and made up with buffer to a final volume of 200 µl. If buffers of various pH values (Table 3.13) or additives such as NaCl or DTT were used, Δmac25L56 was pre-incubated for 30 min at 37°C in the appropriate buffer prior to adding the substrate. The reference (control incubation) which was subtracted from the values obtained consisted of 15 µl casein stock solutions made up with the same buffer and/or various additives (but no L56) to a final volume of 200 µl. For the determination of the temperature dependence such control incubations were performed for each temperature. The samples were incubated overnight in

the dark at the appropriate temperature. The reaction was terminated by the addition of stop reagent (6% TCA) and incubated for 10 min at room temperature in the dark. After centrifugation for 5 min at 13500 rpm (table centrifuge Eppendorf), 400 µl of the supernatants were mixed with 600 µl test buffer (50 mM Tris-HCl buffer pH 9.5) and the extinction of the sample was measured immediately at 574 nm.

The activity of DegP could be calculated as described below:

ε of casein = 66000 [l x mol^{-1} x cm^{-1}]

E = ε x c x d (Lambert-Beer)

c = E / 66000 x 1 = E / 66000 [mol x l^{-1}x mg^{-1}]

specific activity of DegP = c x V x V_F / t x amount of DegP = mol x min^{-1} x mg^{-1} DegP

ε = extinction coefficient of resorufin [l M^{-1} cm^{-1}]

d = light path [cm]

c = concentration [M]

E = extinction at a wavelength of 574 nm

V = incubation volume = 0.001 l

V_F = dilution factor = 5

t = time of reaction [min]

Table 3.13 Buffers for the determination of Δmac25L56 proteolytic activity at various pH values.

pH	buffer	ionic strength
5.5	50 mM Bis-Tris, 150 mM NaCl	196 mM
6.0	50 mM Bis-Tris, 150 mM NaCl	188 mM
6.5	50 mM Bis-Tris, 150 mM NaCl	175 mM
7.0	50 mM Bis-Tris, 150 mM NaCl	162 mM
7.5	50 mM Tris-HCl, 150 mM NaCl	190 mM
8.0	50 mM Tris-HCl, 150 mM NaCl	178 mM
8.5	50 mM Tris-HCl, 150 mM NaCl	164 mM
9.0	50 mM Tris-HCl, 150 mM NaCl	155 mM
9.5	50 mM Tris-HCl, 150 mM NaCl	151 mM
10.0	50 mM CAPS, 150 mM NaCl	162 mM
10.5	50 mM CAPS, 150 mM NaCl	176 mM
11.0	50 mM CAPS, 150 mM NaCl	189 mM

3.7.12 Casein, MalS, TreA, C99 and Aβ assays

Purified Δmac25L56 (10 μg) was incubated with 10 μg of one of the substrates (casein, C99, MalS or TreA) in 50 mM Tris-HCl buffer pH 8.5, 150 mM NaCl. When membranes were used in an assay, they were prepared and resuspended in 50 mM Tris-HCl buffer pH 8.5, 150 mM NaCl. The protein concentration was determined by using a BCA (bicinchoninic acid solution) protein determination kit (Sigma) following the supplier's manual. Lyophilised Aβ was resuspended in DMSO to a final concentration of 1 mg/ml and 0.5 or 1 μg was added to the assay. The standard assay had a final volume of 200 μl. Samples were incubated at 37°C or at the temperature indicated for various times. Subsequently, the samples were TCA precipitated, resuspended in 4 x sample buffer

containing 30 mM DTT and loaded on a SDS-gel or Schaegger gel. If the sample was loaded straight on a gel the final volume was 80 µl-100 µl.

3.7.13 γ-secretase assays

Purified C99London mutation (Val45Ile) (15 µg) was incubated with partially purified PS1 mutant (PS1Δ9) (10 µg) in either 150 mM sodium citrate buffer pH 6.8 or 50 mM Tris-HCl buffer pH 8.5, 150 mM NaCl for 1 h or overnight at 37°C. The final volume was 200 µl if TCA precipitation was carried out or 100 µl if the samples were loaded straight onto a Schaegger gel. Furthermore, DDM (10% stock solution in H_2O) was added to each assay in a final concentration of 0.05% to prevent aggregation of the membrane proteins.

3.7.14 Chaperone assays (MalS refolding)

For refolding assays, purified wtΔmac25L56 and Δmac25L56SA were added in two-fold molar excess to the substrate MalS. Purified unfolded MalS (in 50 mM Tris-HCl buffer pH 8.0, 8 M urea) was provided by Alexandra Beil, Cardiff University. MalS was diluted 1:50 in refolding buffer (100 mM Tris-HCl buffer pH 7.5, pH 8.0 or pH 8.5) to a final concentration of 0.065 mg/ml. The working stock solution of the various L56 proteins was 0.275 mg/ml with L56 being expected to have a trimeric oligomerisation state. As a control, BSA (NEB) was used in a two-fold molar excess of the concentration of the substrate.
Incubation buffer (338 µl of 100 mM Tris-HCl buffer pH 8.0) was incubated for 5 min at the appropriate temperature together with 5 µl of L56 working stock prior to adding the substrate MalS (7 µl). One sample containing equivalent amounts of buffer instead of L56 and MalS served as blank and one sample containing only MalS served as control for spontaneous refolding of MalS. The refolding reaction was incubated for 1 h at the appropriate temperature. Subsequently, 7 µl of 4-nitrophenyl-α-D-hexa(1-4)-glucopyranoside (NPG) (a substrate of MalS) was added and incubated for 1 h at 30°C to

perform the enzyme reaction. An aliquot of 100 μl was added to microwell plates and the absorbance at 420 nm was measured.

The refolding factor was determined by the following formula:

OD_{420} with chaperone / OD_{420} without chaperone

4 Results

4.1 L56

L56 (HtrA1) is a human serine protease of unknown function with high similarity to the stress-induced human protease HtrA2 and DegP from *E. coli* which functions as a chaperone and a protease. To characterise L56, *E. coli* was used as an expression system.

4.1.1 Cloning of full-length l56 in an expression vector

To investigate the characteristics of this human protease, it was important to find a suitable expression vector and *E. coli* strain. The *l56* cDNA was received as a gift from Dr. Beat Trueb (University of Bern, Switzerland) in a pUC19 vector. Since expression was not observed with this construct, the cDNA encoding full-length *l56* (containing the human signal sequence) was cloned into the expression vector pCS19. pCS19 is a pQE-60 derivative. pQE-60 vectors contain an optimal Shine-Dalgarno sequence for improved translation, a multiple cloning site, the sequence for a C-terminal His Tag and an ampicillin resistance gene. Expression is under control of the *tac* promoter that is IPTG inducible. pCS19 contains also the $lacI^{Q}$ gene, encoding the repressor for the *tac* promoter.

For cloning of the *l56* cDNA in pCS19, a PCR reaction was performed with two primers that flank the ends of the cDNA and introduce an *NcoI* site at the 5´ end of the cDNA and a *BglII* site at the 3´ end of the cDNA. The PCR reaction was only successful when DMSO was added, which could be explained by the possibility that the GC-rich 5´end of the *l56* cDNA may form secondary structures, preventing primer annealing. After digestion of the PCR product and the pCS19 vector with these enzymes, the PCR product was cloned as described in Materials and Methods (Fig. 4.1). The new plasmid was called pSG4.

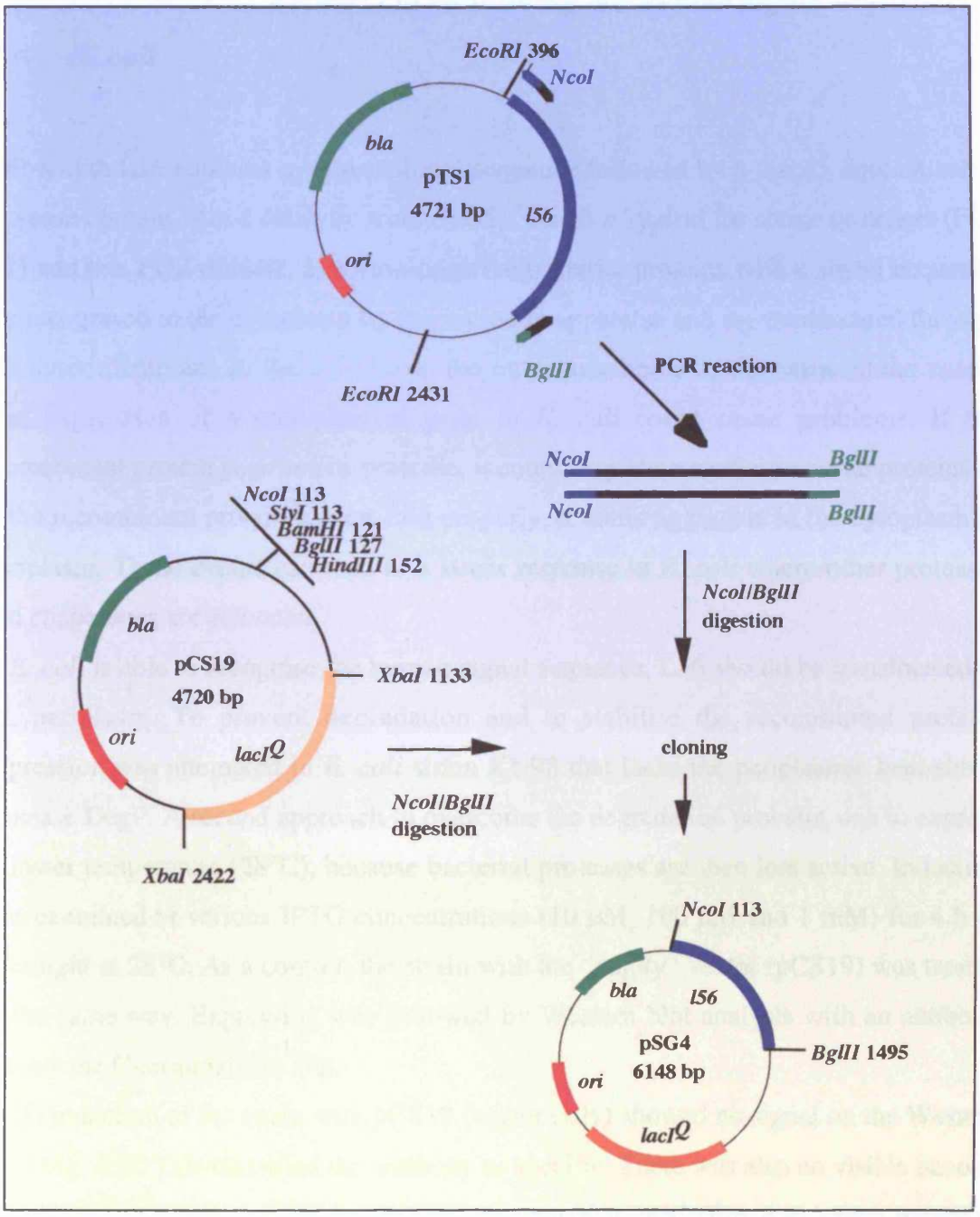

Fig. 4.1 Cloning of full-length *l56* into pCS19.

pTS1 served as template in the PCR reaction to amplify the *l56* cDNA with its human signal sequence. Restriction enzymes, cloning steps and vectors are shown.

4.1.2 Expression of human l56 containing the human signal sequence in E. coli

Full-length L56 contains a human signal sequence followed by a mac25 domain and a protease domain with a catalytic triad (HDS), which is typical for serine proteases (Fig. 4.2) and one PDZ domain. In Gram-negative bacteria, proteins with a signal sequence are recognised in the cytoplasm by the secretion apparatus and are translocated through the inner membrane to the periplasm, the outer membrane or the extracellular space. The expression of a recombinant gene in *E. coli* could cause problems. If the recombinant protein is an active protease, it could degrade essential bacterial proteins or if the recombinant protein cannot fold properly, it could aggregate in the cytoplasm or periplasm. These events can lead to a stress response in *E. coli* where other proteases and chaperones are activated.

If *E. coli* is able to recognise the human signal sequence, L56 should be translocated to the periplasm. To prevent degradation and to stabilise the recombinant protein, expression was attempted in *E. coli* strain KU98 that lacks the periplasmic heat-shock protease DegP. A second approach to overcome the degradation problem was to express at lower temperature (28°C), because bacterial proteases are then less active. Induction was examined at various IPTG concentrations (10 μM, 100 μM and 1 mM) for 4 h or overnight at 28°C. As a control, the strain with the "empty" vector (pCS19) was treated in the same way. Expression was followed by Western blot analysis with an antibody against the C-terminal His Tag.

IPTG induction of the strain with pCS19 (vector only) showed no signal on the Western blot (Fig. 4.3). This classified the antibody as specific. There was also no visible band in the uninduced strain, containing pSG4, after growth at 28°C (Fig. 4.4) which indicated that the promoter is tight under these growth conditions. Induction with 10 μM IPTG at 28°C for 4 h led to synthesis of L56 to the same amounts than with 100 μM or 1 mM IPTG (Fig. 4.4). Overnight induction at 28°C showed less intense bands for L56 and some degradation products were detectable (Fig. 4.4). Full-length L56 has a predicted molecular mass of 52 kDa. The set of lower molecular weight bands could represent degradation products resulting from either autoproteolysis or from degradation by

bacterial proteases. For this reason, induction at 28°C for 4 h was used for further expression experiments.

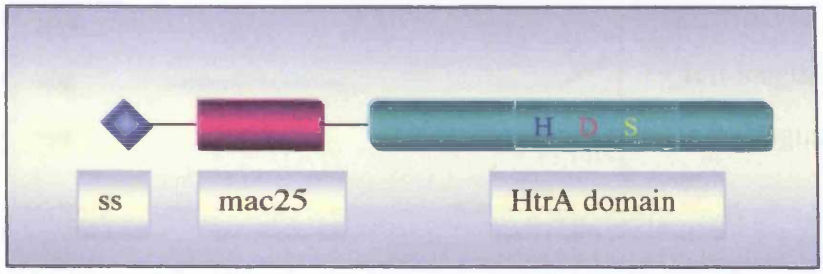

Fig. 4.2 Schematic representation of L56 with the human signal sequence.
The human signal sequence (ss) is coloured in blue; followed by the mac25 domain coloured in purple and the protease and PDZ domain core (HtrA domain) coloured in green. The three residues which represent the catalytic triad (HDS) are coloured in blue, red and yellow.

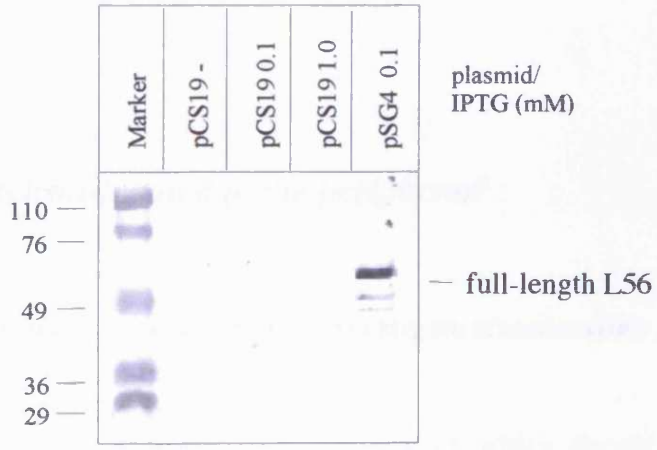

Fig. 4.3 Expression test with the "empty" vector.
A five millilitre culture of strain KU98 carrying the "empty" vector pCS19 was induced at $OD_{578} = 0.5$ with 100 µM or 1 mM IPTG. The cells were grown overnight at 28°C. The Western blot of the whole cell extracts was incubated with the α-His antibody. As control, cells overproducing L56 were loaded in the last lane. The molecular mass of the marker proteins is shown in kDa.

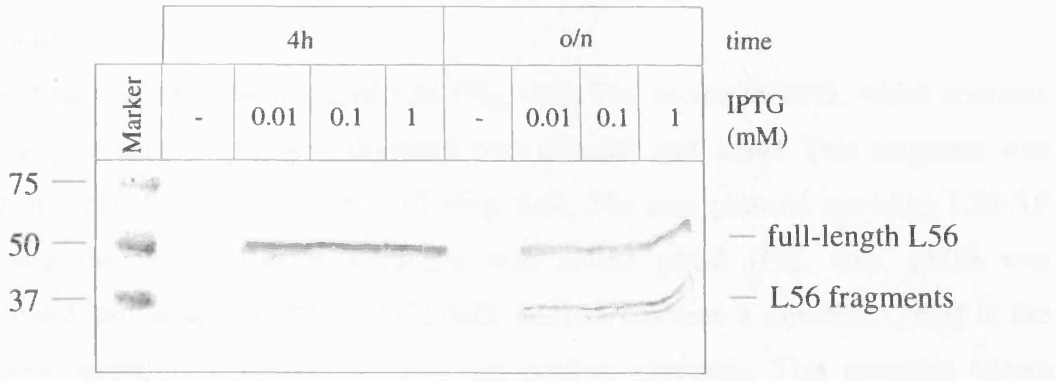

Fig. 4.4 Expression of *l56* containing the human signal sequence.

A five millilitre culture of strain KU98 carrying pSG4 (*l56* with the human signal sequence in pCS19) was induced at OD_{578} = 0.5 with 10 μM, 100 μM or 1 mM IPTG for 4 h or overnight at 28°C. The medium used was NZA. The Western blot of whole cell extract samples was incubated with the α-His antibody. o/n: overnight. The molecular mass of the marker proteins is shown in kDa.

4.1.3 Is the L56 translocated to the periplasm?

4.1.3.1 A *phoA* fusion as a method to investigate translocation

Full-length L56 contains a human signal sequence which should induce secretion. However, prokaryotic signal sequences differ from eukaryotic signal sequences in amino acid sequence in the different regions (the positively charged n-region, the hydrophobic h-region and the neutral but polar c-region) (Nielson *et al.*, 1997). Therefore, it is possible that *E. coli* is unable to recognise the human signal sequence as a translocation signal and does not secrete L56 to the periplasm.

One approach to test translocation of L56 to the periplasm is to use the *phoA* fusion technique (Boyd *et al.*, 1993). Alkaline phosphatase (AP) is only active in the periplasm. It has two disulphide bonds, which are important for proper folding and activity. In the cytoplasm, AP cannot fold properly and is not active. It is possible to

visualise AP activity by adding a substrate, XP, to agar plates. Blue colonies indicate AP activity.

AP was fused to the C-terminus of L56 (Fig. 4.5). The vector pSWFII, which contains signal sequenceless *phoA*, was digested with *HindIII* and *XmaI*. This fragment was cloned into pSG4, digested with *BglII* (Fig. 4.6). The new plasmid encoding L56-AP containing the human signal sequence was called pSG8 (Fig. 4.6). pSG8 was transformed into strains KU98 and KU105. KU105 contains a mutation (*prlA*) in the *secY* gene, encoding a protein of the translocation apparatus. This mutation allows translocation of proteins without or with defective signal sequences. Translocation was tested on plates, containing XP and various IPTG concentrations (10 μM or 100 μM). The plates were incubated overnight at 28°C or 37°C.

Fig. 4.5 Schematic representation of the L56-AP fusion protein containing the human signal sequence.

The human signal sequence (ss) is coloured in blue, the mac25 domain in purple and the protease core (HtrA domain) in green. The three residues which represent the catalytic triad (HDS) are coloured in blue, red and yellow. The fused AP is coloured in yellow/blue.

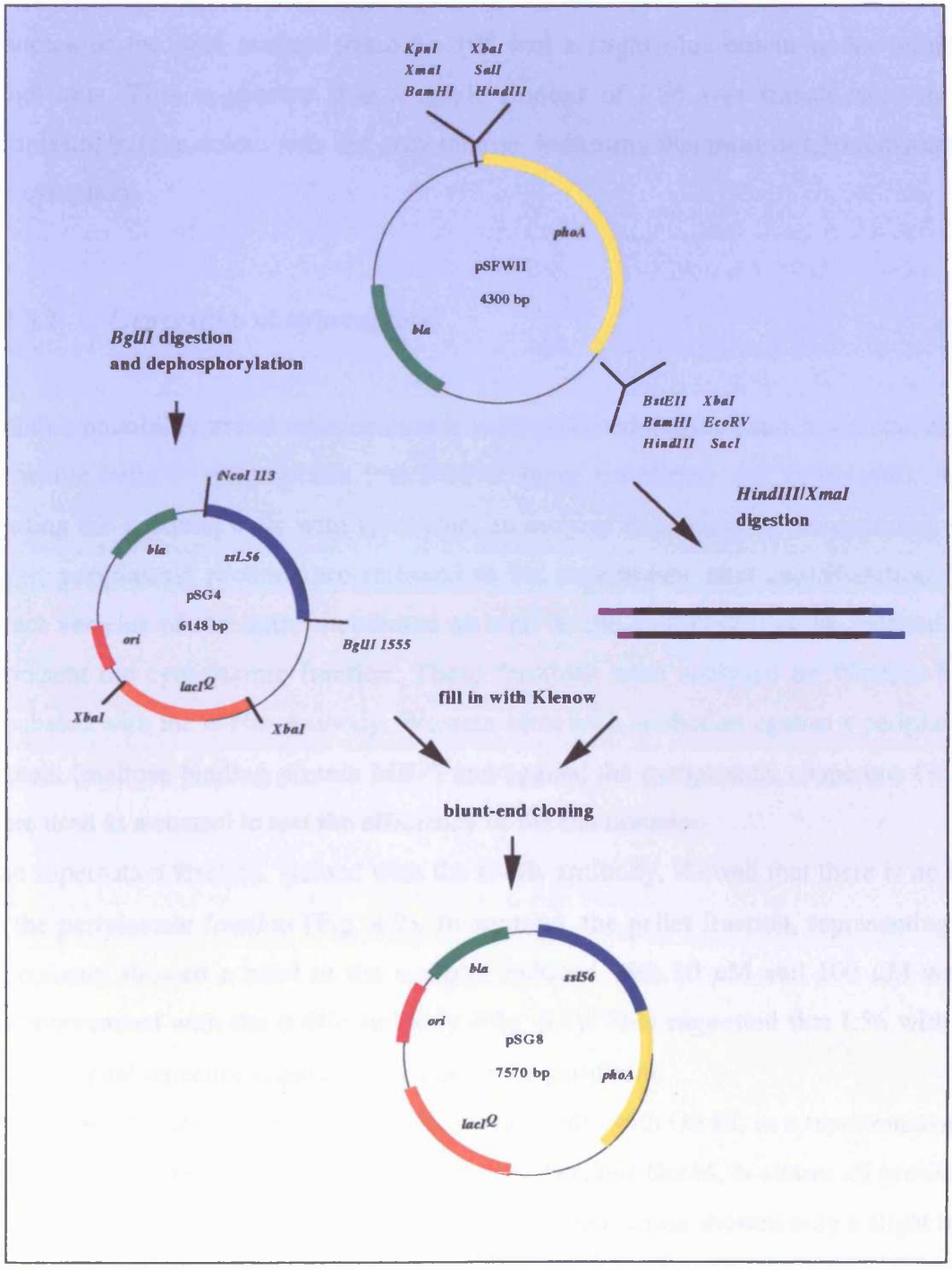

Fig. 4.6 Cloning of *l56-phoA* containing the human signal sequence.

The *phoA* gene (encoding AP) was from pSWFII and pSG4 served as vector. All cloning steps and the relevant restriction enzymes are shown.

The colonies of KU98, containing pSG8, remained white on indicator plates containing XP at both temperatures, even after induction with 100 μM IPTG. In contrast, the

colonies of the *prlA* mutant strain KU105 had a slight blue colour under inducing conditions. This suggested that a small amount of L56 was translocated to the periplasm, but the colour was not very intense, indicating that most of L56 remained in the cytoplasm.

4.1.3.2 Generation of spheroplasts

Another possibility to test translocation is to prepare periplasmic extracts via conversion of whole cells to spheroplasts (vesicles of inner membrane and cytoplasm). After treating the bacterial cells with lysozyme, an enzyme that degrades the peptidoglycan layer, periplasmic proteins are released to the supernatant after centrifugation. The intact vesicles of the inner membrane as well as the cytoplasm can be pelleted and represent the cytoplasmic fraction. These fractions were analysed on Western blots incubated with the α-His-antibody. Western blots with antibodies against a periplasmic protein (maltose binding protein MBP) and against the cytoplasmic chaperone GroEL were used as a control to test the efficiency of the fractionation.

The supernatant fraction, stained with the α-His antibody, showed that there is no L56 in the periplasmic fraction (Fig. 4.7). In contrast, the pellet fraction, representing the cytoplasm, showed a band in the samples induced with 10 μM and 100 μM which immunoreacted with the α-His antibody (Fig. 4.7). This suggested that L56 with the human signal sequence is not translocated to the periplasm.

The control Western blot with the α-GroEL antibody, with GroEL as a representative of the cytoplasmic fraction, confirmed the results, because GroEL is almost all present in the pellet fraction (Fig. 4.8), whereas the supernatant fraction showed only a slight band at about 60 kDa (Fig. 4.8).

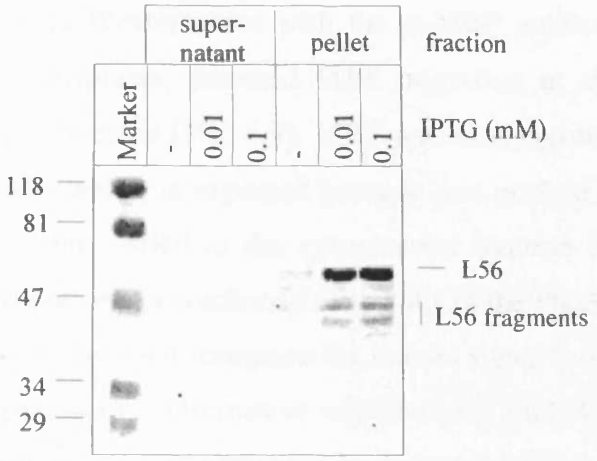

Fig. 4.7 Spheroplasts of strain KU98 expressing *l56* (α-His antibody).

A five millilitre culture was induced at OD_{578} = 0.5 with 10 µM or 100 µM IPTG. The cells were grown overnight in NZA medium at 28°C. Spheroplasts were prepared and the supernatant fraction (containing periplasmic proteins) as well as the pellet fraction (containing cytoplasmic proteins) were loaded on a 10% SDS-gel. The Western blot was incubated with the α-His antibody. The molecular mass of the marker proteins is shown in kDa.

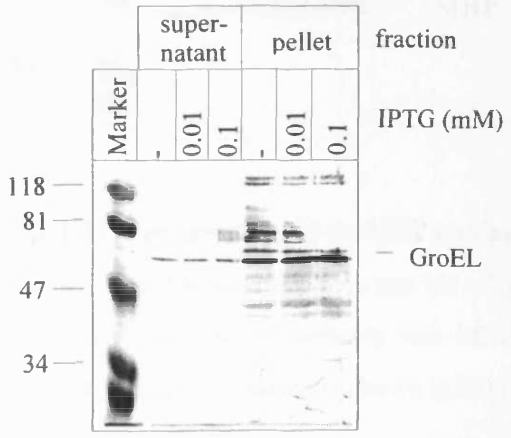

Fig. 4.8 Spheroplasts of strain KU98 expressing *l56* (α-GroEL antibody).

The same samples used in Fig. 4.7 were taken to test the efficiency of the fractionation. The Western blot was incubated with an α-GroEL antibody with GroEL as a representative of the cytoplasm. The molecular mass of the marker proteins is shown in kDa.

As expected, the control Western blot with the α-MBP antibody, with MBP as a representative of the periplasm, detected MBP migrating at about 40 kDa in the periplasmic supernatant fraction (Fig. 4.9). MBP was also present in the cytoplasmic pellet fraction (Fig. 4.9) which is expected because this method does not convert all cells to spheroplasts. Thus, MBP in the cytoplasmic fraction is the result of non-permeabilised cells. These results confirmed the results of the PhoA fusion experiments. They indicate that *E. coli* does not recognise the human signal sequence and L56 is not translocated to the periplasm. Alternative explanations include human L56 is not translocation competent or L56 was present as an inclusion body in the cytoplasm.

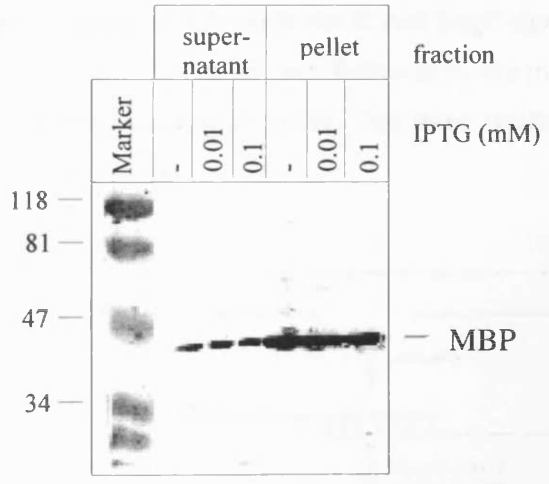

Fig. 4.9 Spheroplasts of strain KU98 expressing *l56* (α-MBP antibody).
The same samples used in Fig. 4.7 and 4.8 were taken to test the efficiency of the fractionation. The Western blot was incubated with an α-MBP antibody with MBP as a representative of the periplasm. The molecular mass of the marker proteins is shown in kDa.

4.1.4 Cloning the signal sequence of E. coli DegP in front of L56

A further attempt to translocate L56 into the periplasm was to use a bacterial signal sequence. L56 contains 16 cysteine residues in the mac25 domain that might form disulphide bonds. In the periplasm, the protein should be able to fold properly because of the oxidising environment. The signal sequence of the periplasmic *E. coli* protease

DegP was used (Fig. 4.10) because this protein shares homology to the HtrA domain of L56. The signal sequence was introduced by using two oligonucleotides with an overlapping region of 25 bp and flanking *NcoI* sites. The signal sequence was thus cloned via the *NcoI* site into pSG5. The new plasmid was called pSG9 (Fig. 4.11).

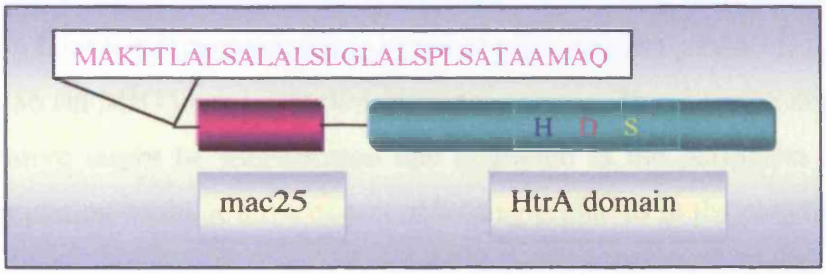

Fig. 4.10 Schematic representation of L56 with the *E. coli* DegP signal sequence.
The *E. coli* DegP signal sequence is shown in pink followed by the mac25 domain coloured in purple and the protease domain coloured in green. The three residues of the catalytic triad (HDS) are shown in blue, red and yellow.

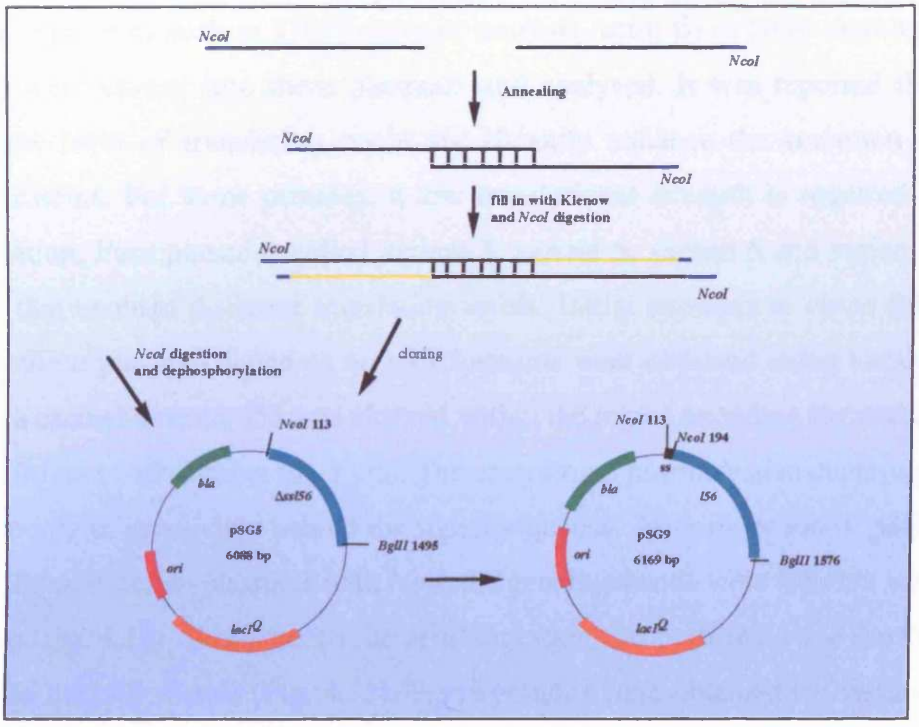

Fig. 4.11 Cloning of the *E. coli* DegP signal sequence in front of full-length *l56*.
All cloning steps and relevant restriction enzymes are shown.

4.1.5 Expression of cssl56

Various *E. coli* strains were tested for overproduction of cssL56 (L56 with the DegP signal sequence). A wt strain (DHB4), a strain which lacks the periplasmic protease DegP (KU98) and a strain lacking several periplasmic proteases (MH1) were tested for expression. Only faint bands corresponding to either a degradation product (in KU98) or to full-length L56 (in MH1) were detected (data not shown). These results suggest that this L56 derivative might be translocated and degraded in the periplasm. Potential reasons for degradation could be slow export or folding problems in the periplasm.

4.1.6 Cloning of an enterotoxin signal sequence in front of L56

Simmons and Yansura (1996) generated eight plasmids containing the signal sequence of the heat-stable enterotoxin II protein and altered translation initiation region (TIR) for translational efficiency. To quantify translation and translocation, *phoA* and a few other cDNAs encoding proteins such as TNFβ (tumour necrosis factor β) or NGF (neuronal growth factor) were cloned into these plasmids and analysed. It was reported that manipulating the level of translation could significantly enhance the secretion of heterologous proteins. For some proteins, a low translational strength is required to prevent aggregation. Four plasmids called variant 3, variant 5, variant 6 and variant 8 were obtained that enabled different translation levels. Initial attempts to clone full-length *l56* into these plasmids failed as no transformants were obtained using various host strains. In a second attempt, *l56* was cleaved within the region encoding the mac25 domain with *MluI* and with *NheI* at the 3´end. The enterotoxin plasmids also contain an *MluI* site for cloning of genes right behind the signal sequence. After digestion of pSG4 with *NheI* and the enterotoxin plasmids with *NotI,* the generated ends were filled in with Klenow enzyme (Fig. 4.12). Subsequently, an *MluI* digestion was performed and the *l56* insert was cloned into the vectors (Fig. 4.12). Transformants were obtained for variants 3, 6 and 8 but not for variant 5. The new plasmids were called pSG33 (variant 3-*l56*), pSG34 (variant 6-*l56*) and pSG35 (variant 8-*l56*) (Fig. 4.12).

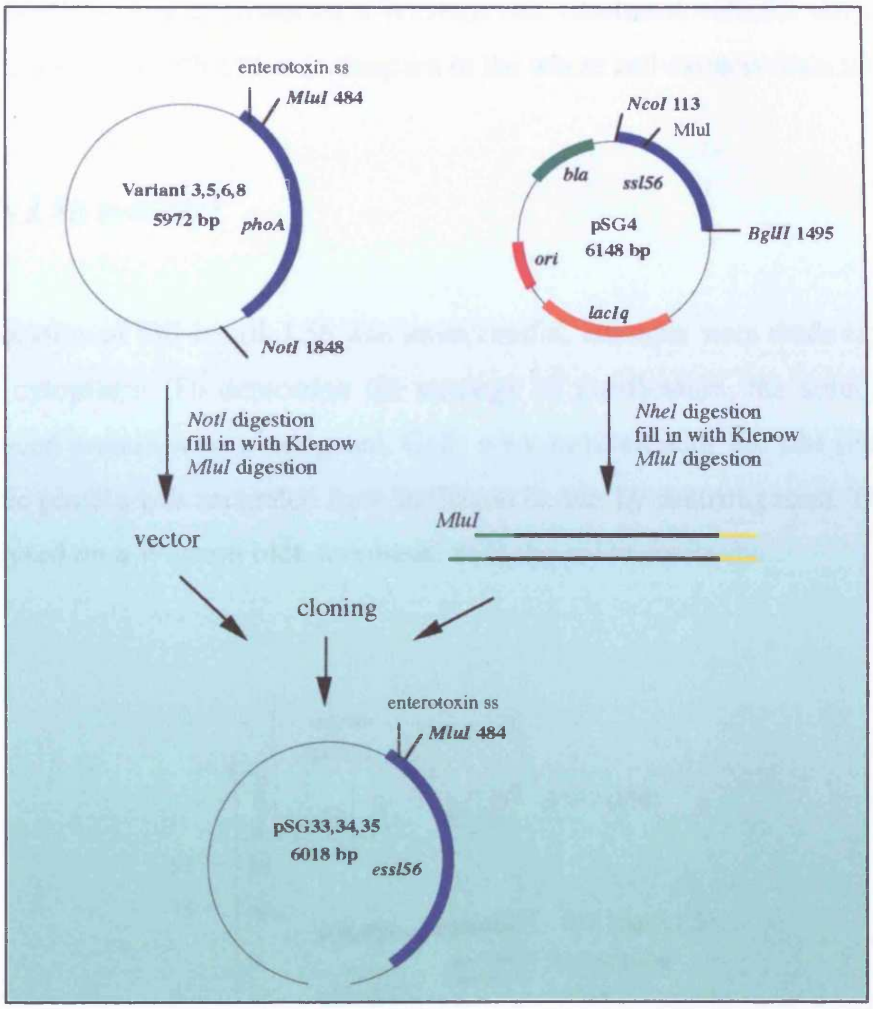

Fig. 4.12 Cloning of pSG33, pSG34 and pSG35.

Plasmid variants 3, 5, 6 and 8 contained the enterotoxin signal sequence with various translation initiation regions. All the cloning steps and relevant restriction enzymes are shown. ess = Enterotoxin signal sequence.

4.1.7 Expression of essl56 (L56 with Enterotoxin signal sequence)

All enterotoxin plasmids contain a *phoA* promoter which is induced at low phosphate concentrations. To test if the various essL56 constructs were produced, *E. coli* strain MH1 containing pSG33, 34 or 35 was grown overnight at 28°C in LB medium. LB is a rich medium with high phosphate concentration to prevent transcription of *essl56*. The overnight cultures were diluted 1:100 in low phosphate medium and grown for 20 h at

28°C. Expression was analysed on a Western blot incubated with the polyclonal L56 antiserum. No full-length L56 was detected in the whole cell extracts (data not shown).

4.1.8 Is L56 soluble?

As translocation of full-length L56 was unsuccessful, attempts were made to purify L56 from the cytoplasm. To determine the strategy of purification, the solubility of the overproduced protein was investigated. Cells were induced with 100 μM IPTG for 16 h and soluble protein was separated from inclusion bodies by centrifugation. The fractions were analysed on a Western blot, incubated with the α-His antibody.

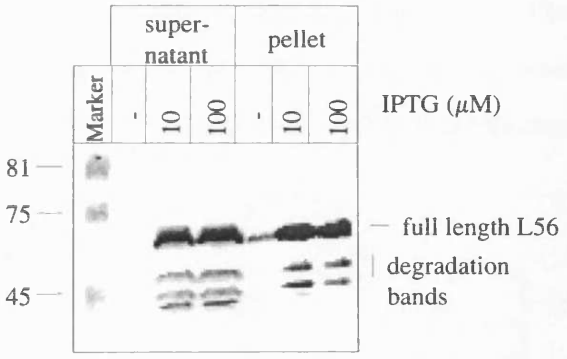

Fig. 4.13 Solubility test of L56.

A one litre culture of strain KU98 carrying pSG4 was induced at OD_{578} = 0.5 with 10 μM or 100 μM IPTG. The cells were grown overnight in NZA medium at 28°C. Fractions were prepared as described in Materials and Methods. An aliquot of 20 μl of the supernatant fraction containing soluble protein and 20 μl of the pellet fraction, containing cell debris and inclusion bodies, were loaded on a 10% reducing SDS-gel. The Western blot was incubated with the α-His antibody. The molecular mass of the marker proteins is shown in kDa.

L56 contains a cysteine-rich region (mac25 domain) and it is possible that these cysteine residues form disulphide bonds during preparation of cell extracts and lead to complex formations. The Western blot showed that the supernatant fraction as well as the pellet fraction contain L56 in a ratio of about 40% to 60% (Fig. 4.13). The Western blot indicated that almost half of the protein is soluble and can be used for purification.

4.1.9 Purification of L56 from the cytoplasm

4.1.9.1 NiNTA chromatography with NiNTA spin columns

In pCS19, L56 is produced with a C-terminal His tag (six His-residues), allowing purification via NiNTA chromatography. To establish optimal purification conditions, eight NiNTA spin columns were loaded with cell extract. After washing, each column was subjected to different elution conditions and samples were analysed for the presence of L56 by Western blotting. L56 was detected in the flow-through and washing fractions which might be due to overloading of the spin columns (Fig. 4.14). The presence of 100 mM imidazole led to elution of L56 that was also detected in samples eluted with 250 mM and 500 mM imidazole (Fig. 4.15). pH tests indicated that elution of the protein occurred only at pH 4.5 (Fig. 4.15). These results suggested a purification procedure using native conditions including two washing steps, one with 10 mM imidazole and one with pH 6.3. Elution could be performed with 300 or 500 mM imidazole.

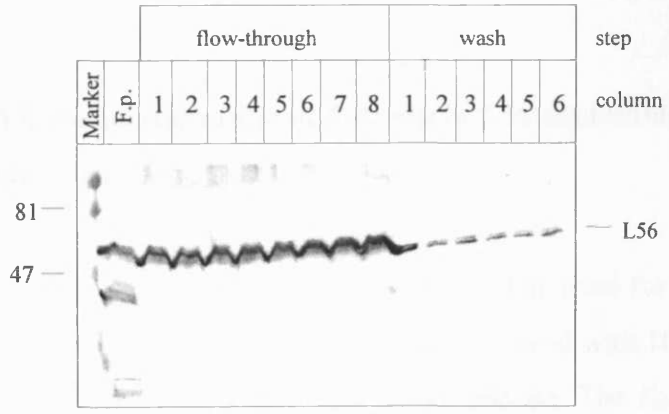

Fig. 4.14 NiNTA chromatography of full-length L56 with NiNTA spin columns
A one litre culture of strain KU98 carrying pSG4 was induced with 100 µM IPTG. Cells were grown overnight in NZA medium at 28°C. Soluble protein was prepared as described in Materials and Methods and 2 x 600 µl were loaded on each spin column (1-8 flow through). The columns (1-8) were washed 3 times with 50 mM sodium phosphate buffer pH 7.5, 300 mM NaCl. The Western blot was incubated with α-His antibody. F.p.= French press extract. The molecular mass of the marker proteins is shown in kDa.

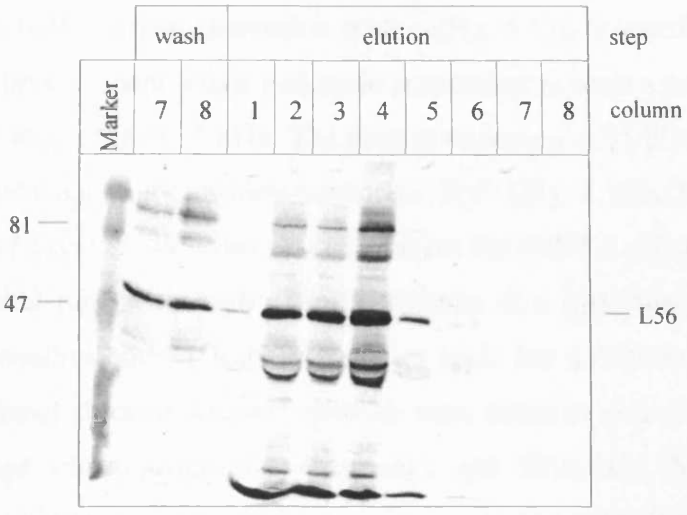

Fig. 4.15 NiNTA chromatography of full-length L56 with NiNTA spin columns

NiNTA spin columns (1-8) were loaded and washed as described in Fig. 4.14 and eluted with 50 mM sodium phosphate buffer pH 7.5, 300 mM NaCl, containing various imidazole concentrations (10 mM (1), 100 mM (2), 250 mM (3), 500 mM (4)) as well as with buffers of various pH values (pH 4.5 (5), pH 5.9 (6), pH 6.3 (7), pH 7.0 (8)). The Western blot was incubated with α-His antibody. The molecular mass of the marker proteins is shown in kDa.

4.1.9.2 NiNTA chromatography of full-length L56 containing the human signal sequence

Based on these results a NiNTA Superflow column was used for purification. A cell extract from a three litre culture grown at 28°C and induced with 100 μM IPTG for 4 h, was loaded on the column with a flow rate of 0.3 ml/min. The elution was performed with high imidazole concentrations (500 mM).

Purification steps were assessed on a Coomassie stained SDS-gel and on a Western blot. The Western blot showed that there is an overproduction of L56 and that almost all L56 was bound to the column (data not shown). Both washing steps (with 10 mM imidazole and with pH 6.3) led to a release of weakly bound proteins (Fig. 4.16). A clearly visible band of approximately 52 kDa was recovered in fractions after elution with buffer containing high imidazole (500 mM) (Fig. 4.16). This band immunoreacted with the α-

His antibody (data not shown). Two lower-molecular weight bands which were also immunoreactive in the earlier expression studies (Fig. 4.13), co-purified with L56 (Fig. 4.16). The two predominant bands and main contaminants were a protein migrating at 25 kDa and one migrating at 75 kDa. The protein migrating at 25 kDa was identified by N-terminal sequencing as the proline isomerase SlyD (Fig. 4.16). One explanation for the co-elution of SlyD in the same fractions from the NiNTA column is that it binds copper and nickel ions with high affinity because of a histidine-rich region in the protein (see SwissProt entry P30856). Because SlyD has a different isoelectric point than L56, additional chromatography methods were tested to remove this contaminant. Anion exchange chromatography (MonoQ), gel filtration (Superdex 200), a hydroxyapatite column and the use of centricon columns with different cut-off sizes (YM-30 with an cut-off of 30 kDa and YM-100 with an cut-off of 100 kDa) did not improve the purity of L56. These findings suggested that some of the contaminants interact directly with L56 possibly because it might be at least partially misfolded.

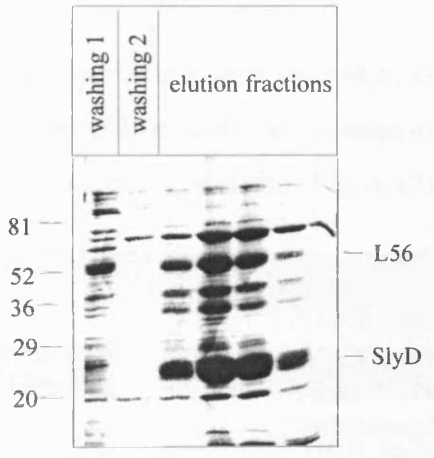

Fig. 4.16 NiNTA chromatography of full-length L56.

E. coli strain KU98 expressing *l56* (pSG4) was induced with 100 µM IPTG and grown overnight at 28°C in NZA medium. Soluble protein was prepared as described in Materials and Methods. The protein was loaded on a NiNTA Superflow column with a flow-rate of 0.3 ml/min. Washing steps with two buffers (50 mM sodium phosphate buffer pH 6.3, 300 mM NaCl (1) and 50 mM sodium phosphate buffer pH 7.5, 300 mM NaCl, 10 mM imidazole (2)) were performed. L56 was eluted with high imidazole (500 mM). The 10% SDS-gel was stained with Coomassie Blue. The molecular mass of the marker proteins is shown in kDa.

Therefore, *E. coli* strain FA113 was used in further experiments. Normally, the cytoplasm is a reducing environment that would interfere with disulphide bond formation in L56. FA113 contains mutations in the genes encoding thioredoxin reductase *trxB* and glutathione reductase *gor* which are both involved in the maintenance of the reducing environment. Due to the lack of *trxB* and *gor*, FA113 has a more oxidising cytoplasm allowing the formation of disulphide bonds (Bessette *et al.*, 1999). Thus, overproduction of L56 in this strain might allow disulphide bond formation and proper folding. NiNTA chromatography of L56 overproduced in strain FA113 was performed but no improvement in purity was detected (data not shown). The possibility that some of the 16 cysteine residues form incorrect disulphide bonds in the more oxidising cytoplasm of FA113 is a likely possibility. Therefore, L56 may be misfolded leading to tight interaction with for example chaperones.

4.1.10 Cloning of l56 without signal sequence

L56 with the human signal sequence is not translocated to the periplasm. To study the characteristics of this protein, it would be useful to produce also the mature protein, that is, the protein without its signal sequence (ΔssL56) (Fig. 4.17).

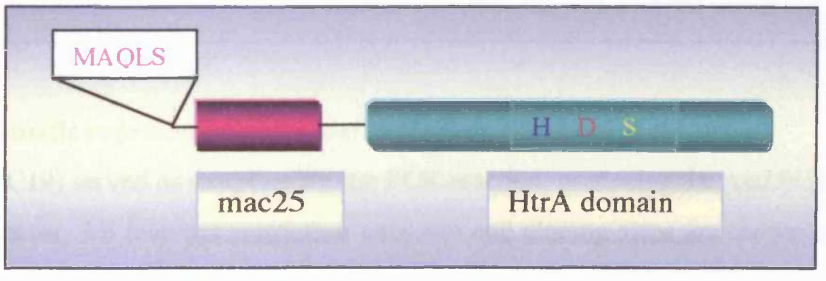

Fig. 4.17 Schematic representation of ΔssL56.

The N-terminal amino acids of the protein are shown in pink; followed by the mac25 domain coloured in purple and the protease core (HtrA domain) coloured in green. The three residues, which represent the catalytic triad (HDS) are coloured in blue, red and yellow.

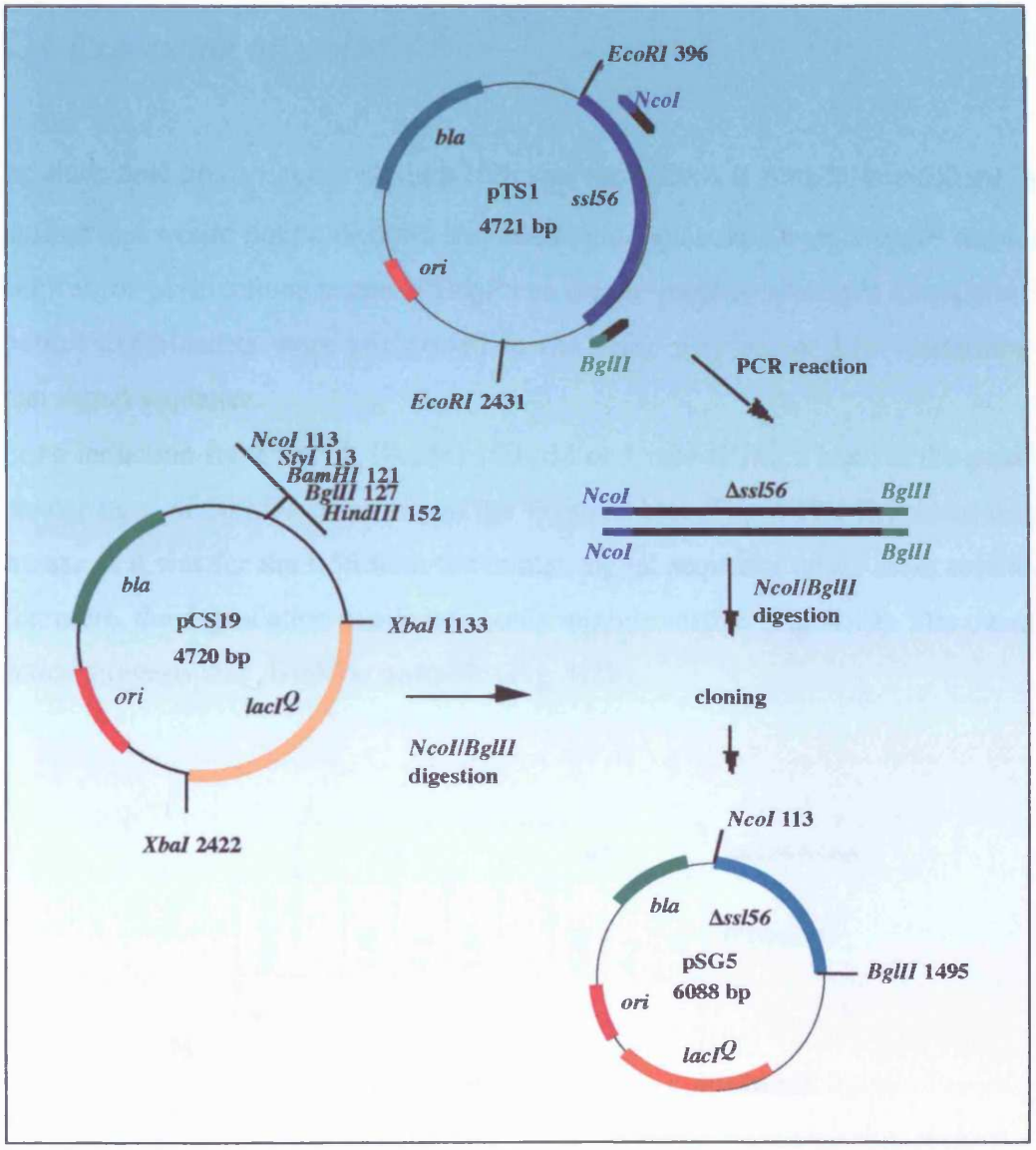

Fig. 4.18 Schematic representation of Δ*ssl56* cloning.

pTS1 (p*l56*pUC19) served as template for the PCR reaction, producing the Δ*ssl56* insert. pCS19 was used as vector. All relevant restriction enzymes and cloning steps are shown. Δss, without signal sequence.

Therefore, a PCR reaction, using pTS1 (p*l56*pUC19) as template, was performed with one primer that annealed after the signal sequence in the *l56* cDNA and introduced a *NcoI* site and the *BglII* primer for the 3´ end of the cDNA which was also used in the cloning of *l56* with the human signal sequence. The PCR product and the pCS19 vector were cleaved with the restriction enzymes *NcoI/BglII*. The new plasmid was called pSG5 (Fig. 4.18).

4.1.11 Expression of Δssl56

To produce ΔssL56 in *E. coli,* strain KU98 was used. Even if ΔssL56 is localised in the cytoplasm and would not be directly degraded by periplasmic DegP, a *degP*⁻ strain may be helpful for purifications because DegP can cleave proteins after cell disruption. The induction experiments were performed in the same way as for L56 containing the human signal sequence.

After an induction for 4 h with 10 μM, 100 μM or 1 mM IPTG, a band at the predicted molecular mass of 50 kDa occurred on the Western blot (Fig. 4.19). This band was not as intense as it was for the L56 with the human signal sequence under these conditions. Furthermore, the degradation bands were only slightly visible (Fig. 4.19). The overnight induction suggests that *Δssl56* is unstable (Fig. 4.19).

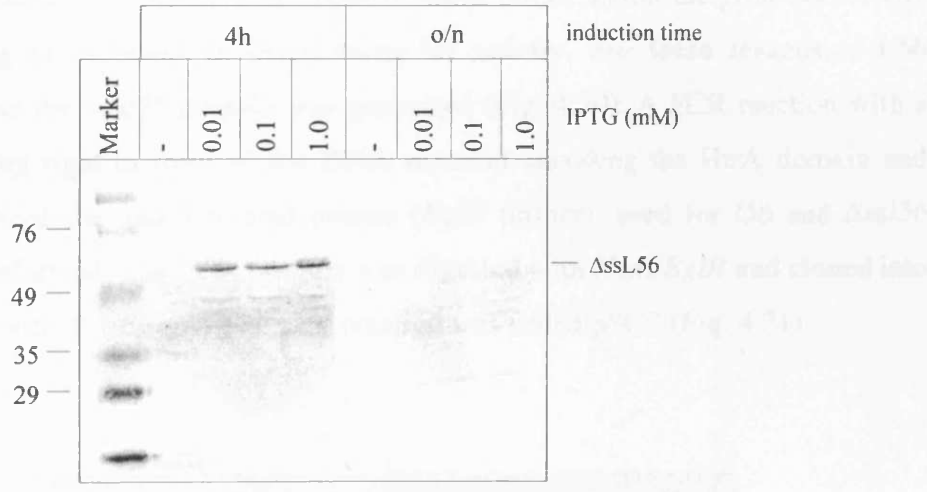

Fig. 4.19 Expression of *Δssl56* in strain KU98.

A five millilitre culture of strain KU98 carrying pSG5 was grown at 28°C in NZA medium and was induced at OD_{578} = 0.5 with 10 μM, 100 μM or 1 mM IPTG for 4 h or overnight. The Western blot of whole cell extracts was incubated with the α-His antibody. The molecular mass of the marker proteins is shown in kDa.

4.1.12 NiNTA chromatography of ΔssL56

An affinity chromatography was performed as for L56 (with the human signal sequence) but it was impossible to remove the contaminants observed in previous purifications (data not shown). Using 10 mM 2-mercaptoethanol during NiNTA chromatography or step-wise ammonium sulphate precipitation, using 10% steps, did not remove the contaminants (data not shown).

4.1.13 Cloning of l56 without the mac25 domain

The highly cysteine-rich region of the mac25 domain could be the cause of the purification problems. In case of folding problems of cytoplasmic L56, chaperones or other proteins will bind, and might thus co-purify as contaminants. Furthermore, if proper folding occurs, the Kazal-type-inhibitor motif might inhibit the protease activity of L56, leading to problems in determining its activity. For these reasons, a L56 construct without the mac25 domain was generated (Fig. 4.20). A PCR reaction with a primer, annealing right in front of the DNA segment encoding the HtrA domain and introducing a *NcoI* site and a second primer (*BglII* primer), used for *l56* and Δ*ssl56* cloning, was performed. The PCR product was digested with *NcoI/BglII* and cloned into pCS19 cleaved with *NcoI/BglII*. The new plasmid was called pSG7 (Fig. 4.21).

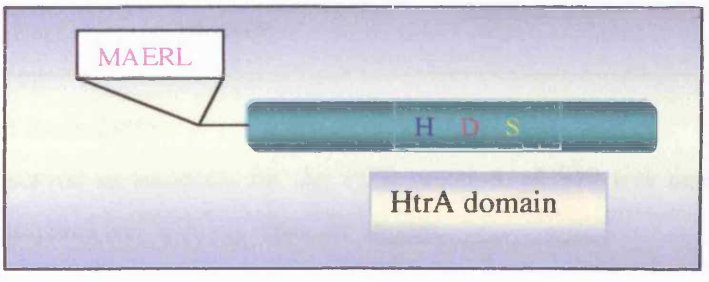

Fig. 4.20 Schematic representation of Δmac25L56.

The first amino acids of this construct are coloured in pink followed by the protease core (HtrA domain) coloured in green. The three amino acids which form the catalytic triad (HDS) are coloured in blue, red and yellow.

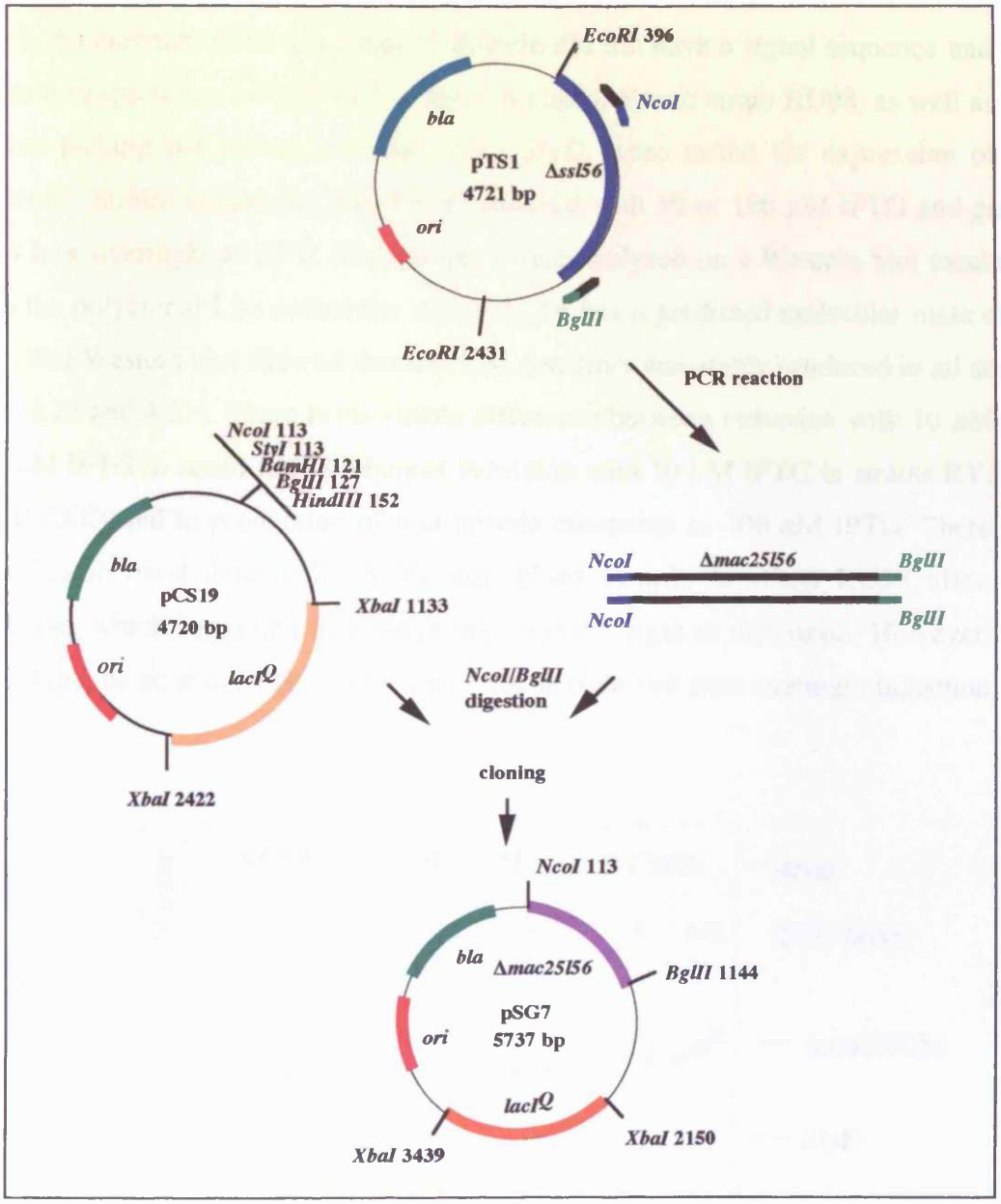

Fig. 4.21. Cloning of Δ*mac25l56*.

pTS1 (p*l56*pUC19) served as template for the PCR reaction. pCS19 was used as vector. All relevant restriction enzymes and cloning steps are shown.

4.1.14 Expression of Δmac25l56 in E. coli

The L56 construct without the mac25 domain did not have a signal sequence and was therefore expected to be localised in the cytoplasm. *E. coli* strain KU98, as well as two strains lacking the previous contaminant SlyD, were tested for expression of the construct. Strains containing pSG7 were induced with 10 or 100 μM IPTG and grown for 4 h or overnight at 28°C. The samples were analysed on a Western blot incubated with the polyclonal L56 antiserum. Δmac25L56 has a predicted molecular mass of 38 kDa. The Western blot showed that this L56 construct was stably produced in all strains (Fig. 4.22 and 4.23). There is no visible difference between induction with 10 μM and 100 μM IPTG in strain KU98 whereas induction with 10 μM IPTG in strains RY3041 and RY3080 led to production of less protein compared to 100 μM IPTG. There is a Δmac25L56 band detectable in the uninduced sample in strain KU98 after 4 h induction, which suggested that the promoter is not tight in this strain. However, this band might be an artefact because it could not be observed after overnight induction.

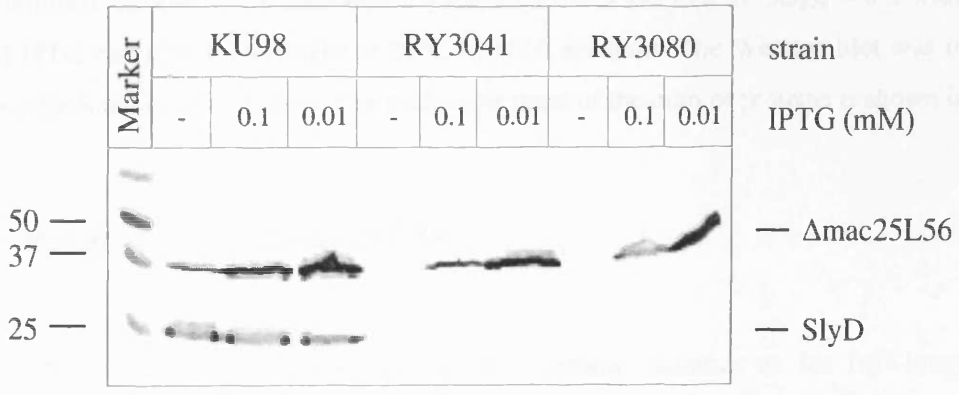

Fig. 4.22 Expression of *Δmac25l56* in various *E. coli* strains after 4 h induction.
A five millilitre culture of each strain (KU98, RY3041, RY3080) carrying pSG7 was induced at OD_{578} = 0.5 with 0.01 or 0.1 mM IPTG and grown for 4 h at 28°C in NZA medium. The Western blot was incubated with the polyclonal L56 antiserum which recognizes both L56 and SlyD. The molecular mass of the marker proteins is shown in kDa.

It seems that even Δmac25L56 is slightly degraded or autoproteolysed as was full-length L56 after overnight induction because an additional faint band appeared directly

below the Δmac25L56 band on the Western blot (Fig. 4.23). Furthermore, the polyclonal L56 antiserum recognises SlyD because it was present in the samples that were used to raise the antibody (*slyD* mutant strains were only available to us at a later time). SlyD is detectable in strain KU98 but as expected it is not detectable in strain RY3041 and RY3080 which do not produce this protein (Fig. 4.22 and 4.23). A SlyD minus strain was therefore used for purification.

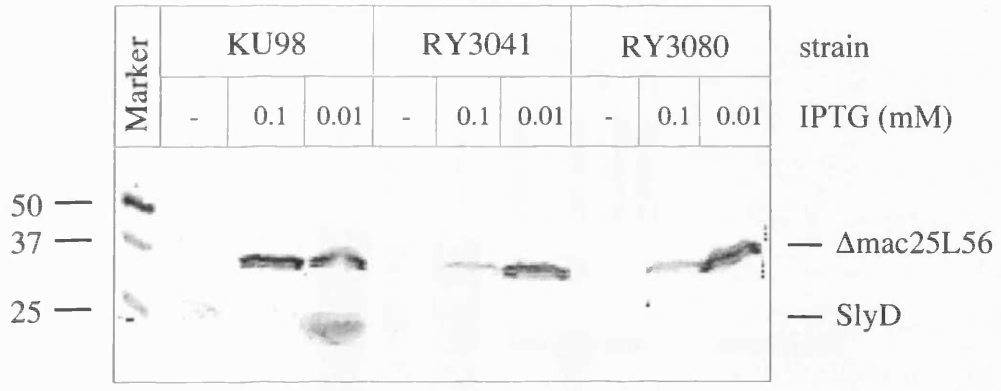

Fig. 4.23 Expression of *Δmac25l56* in various *E. coli* strains after overnight induction.
A five millilitre culture of each strain carrying pSG7 was induced at OD_{578} = 0.5 with 0.01 or 0.1 mM IPTG and grown overnight at 28°C in NZA medium. The Western blot was incubated with the polyclonal L56 antiserum. The molecular mass of the marker proteins is shown in kDa.

4.1.15 Purification of Δmac25L56

NiNTA chromatography was performed in a similar manner as for full-length L56. After loading the protein, one washing step with buffer containing 20 mM imidazole was carried out and the protein was eluted with high imidazole concentrations (500 mM). Subsequently, the pre-purified protein was loaded on an anion exchange column (POROS HQ) and eluted with a salt gradient. The isoelectric point of Δmac25L56 is 8.5. Therefore, it is positively charged at pH 7.5 and should not be able to bind to the positively charged column material. Purification steps were assessed on a Coomassie stained SDS-gel and on a Western blot incubated with the polyclonal L56 antiserum.

The Western blot showed overproduction and efficient binding to the NiNTA column (Fig. 4.25). The washing step with 20 mM imidazole led to an elution of several weakly bound proteins but also of some Δmac25L56 (Fig. 4.24 and 4.25). After elution from the NiNTA column, the protein was almost pure (Fig. 4.24). The yield was 1 mg protein per 1 l culture after dialysis and 250 μg/l after the POROS HQ chromatography. Unfortunately, 50 % of the protein precipitated during dialysis. In contrast to the contaminants, Δmac25L56 did not bind to the anion exchange column and could be detected in a pure form in the flow through fraction (Fig. 4.24).

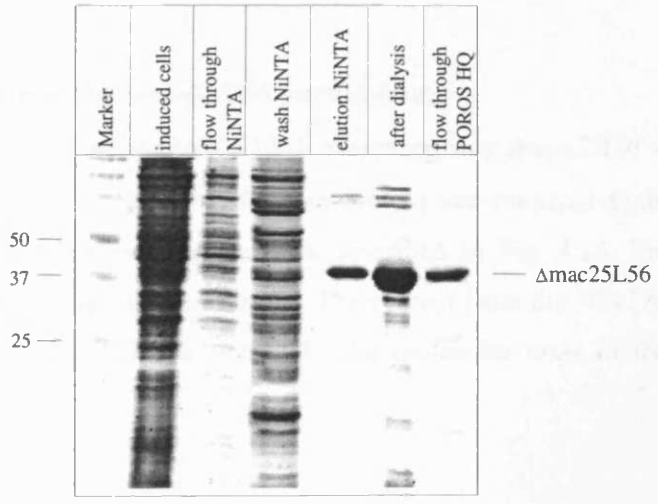

Fig. 4.24 Purification of Δmac25L56.

A three litre culture of *E. coli* strain RY3041 overexpressing *Δmac25l56* was induced with 100 μM IPTG for 4 h at 28°C. Soluble protein was prepared as described in Materials and Methods. Protein was loaded on a NiNTA Superflow column at 0.3 ml/min and one washing step with 50 mM sodium phosphate buffer pH 7.5, 300 mM NaCl containing 20 mM imidazole was performed. Protein was eluted with 50 mM sodium phosphate buffer pH 7.5, 300 mM NaCl containing 500 mM imidazole. Subsequently, the protein was dialysed against 50 mM Tris-HCl buffer pH 7.5, 150 mM NaCl and loaded on an anion exchange column (POROS HQ). Elution steps with various NaCl concentrations (250 mM, 500 mM, 1 M) were performed. The flow through fraction was loaded on a 12% SDS-gel. The protein from the NiNTA elution fraction was diluted 1:50 before loading on the SDS-gel. The gel was stained with Coomassie blue. The molecular mass of the marker proteins is shown in kDa.

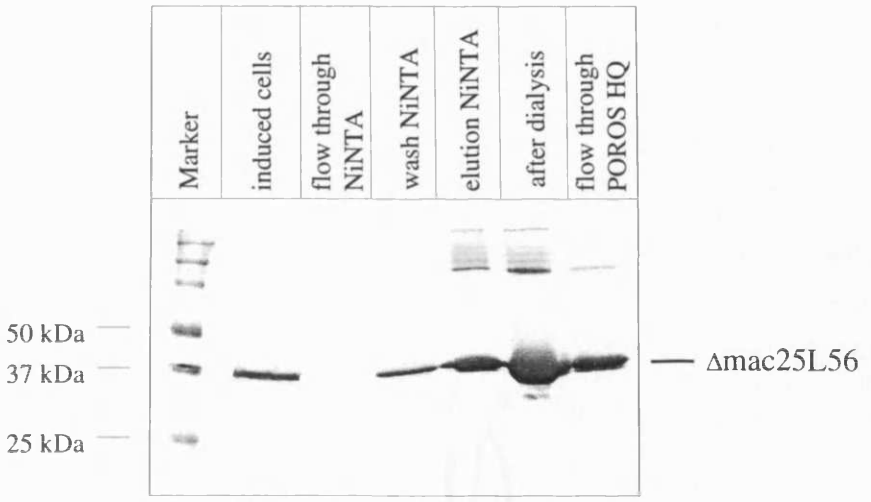

Fig. 4.25 Western blot of the Δmac25L56 purification.

A three litre culture of *E. coli* strain RY3041 overexpressing *Δmac25l56* was induced with 100 µM IPTG and grown for 4 h at 28°C. Soluble protein was prepared as described in Materials and Methods. The purification was done as described in Fig. 4.24. The Western blot was incubated with the polyclonal L56 antiserum. The protein from the NiNTA elution fraction was diluted 1:50 before loading on the SDS-gel. The molecular mass of the marker proteins is shown in kDa.

4.1.16 Does Δmac25L56 form oligomers?

The crystal structure of DegP indicated a hexamer composed of two trimers (Krojer *et al*, 2002). The connections between the two trimers are made of the LA loops of the protease domains (Krojer *et al*, 2002). In contrast, the crystal structure of the human homologue HtrA2 showed a trimeric conformation (Li *et al*, 2002). Sequence alignments demonstrated that HtrA2 as well as L56 (HtrA1) are lacking loop LA that is responsible for the hexamerisation in DegP. To examine the oligomeric state of Δmac25L56, a gel filtration chromatography with purified protein was performed. A gel filtration chromatography with a protein standard from Biorad served as a reference to determine the molecular masses of the peak fractions.

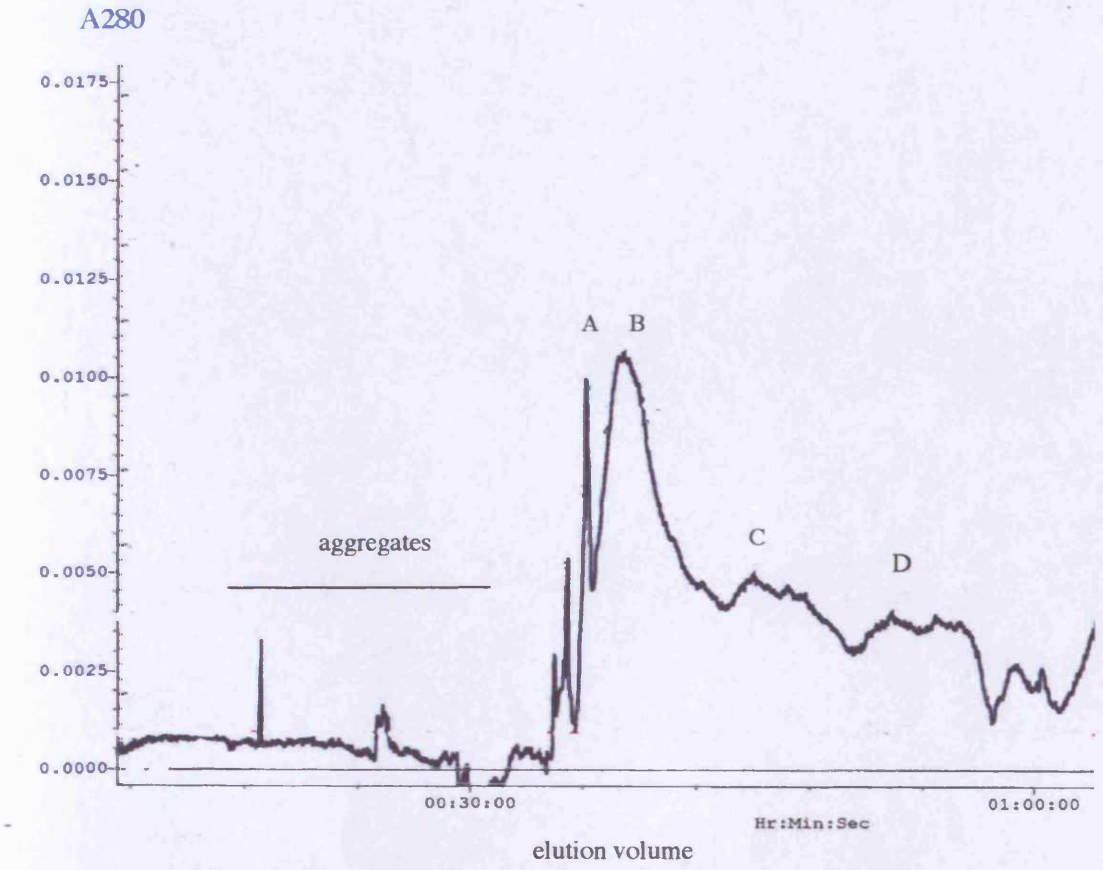

Fig. 4.26 Gel filtration chromatography of Δmac25L56.

Δmac25L56 (250 µg) was loaded on the gel filtration column (Sephadex 200) and eluted by washing the column with one column volume of 50 mM Tris-HCl buffer pH 7.5, 150 mM NaCl.

Table 4.1 Determination of the oligomeric state of Δmac25L56.

Peak	Molecular mass (kDa)	Elution volume (ml)	Suggested oligomeric state
A	**207**	**10.4**	**hexamer**
B	**135**	**11.3**	**trimer**
C	**37**	**14.0**	**monomer**
D	**9**	**16.5**	**degradation fragments**

The molecular mass of the peak fractions was determined as described in Materials and Methods.

The gel filtration experiment (Table 4.1 and Fig. 4.26) confirmed that Δmac25L56 forms a trimer because the main peak represented proteins with a molecular mass of 134.5 kDa (trimer). One minor peak was observed which represented a hexamer and a very small peak representing a monomer (Table 4.1 and Fig. 4.26). Although Δmac25L56 lacks its N-terminus, a trimeric conformation might still be suggested for full-length L56 because the authentic N-terminal domain of HtrA2 is not involved in trimerisation (Li *et al*, 2002).

It would have been interesting to investigate if the various multimers that were resolved by gel filtration are equally active. However, activity tests could not be carried out because the individual fractions did not contain sufficient material.

4.1.17 Is purified Δmac25L56 proteolytically active?

Several substrates are available to test proteolytic activity. Due to the fact that no natural substrates of L56 have been identified so far, a common substrate (casein) for serine proteases was used to test proteolytic activity. Casein serves as a non-specific substrate as it is rather unfolded.

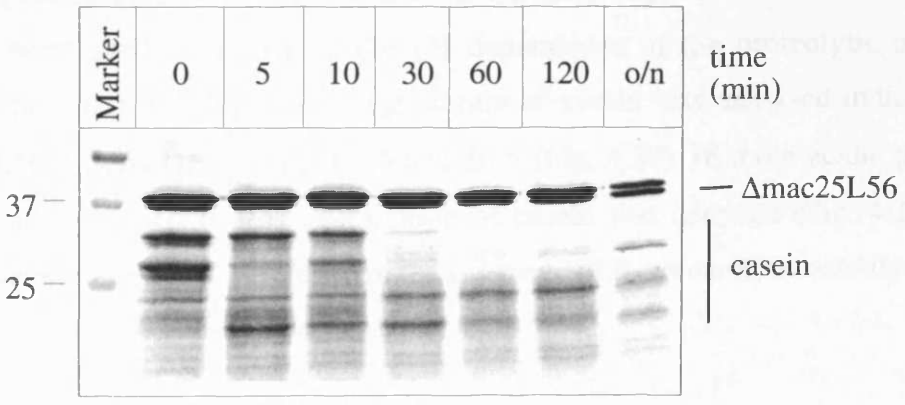

Fig. 4.27 Degradation of casein by Δmac25L56.

Casein (10 µg in assay buffer) was incubated with 10 µg purified Δmac25L56 in assay buffer (50 mM Tris-HCl buffer pH 8.5, 150 mM NaCl) for 0, 5, 10, 30, 60, 120 min or overnight at 37°C. The samples were TCA precipitated to stop the reaction and the pellets were resuspended in 20 µl sample buffer containing 30 mM DTT. The samples were loaded on a 12% SDS-gel and stained with Coomassie-Blue. The molecular mass of the marker proteins is shown in kDa.

Time-dependent degradation of casein by Δmac25L56 was observed. The Coomassie-stained SDS-gel showed that degradation of casein started after 5 min and was almost complete after 30 min (Fig. 4.27). Furthermore, it was possible to observe a slight degradation of Δmac25L56 in the overnight sample. The fact that pure L56 as well as pure commercially purchased casein was used suggested that this degradation is based on an autoproteolysis. Autoproteolysis was also observed for DegP and HtrA2 always leading to the removal of N-terminal extensions (Gray *et al.*, 2000).

4.1.18 The pH-dependence of Δmac25L56 activity

Cellular compartments of human cells vary in their pH values. For example, lysosomes and endosomes have an acidic pH value whereas the cytoplasm, the ER and Golgi compartment have a neutral pH value. L56 should be transported into the ER because of its signal sequence and might be secreted into the ECM. After transport to the ECM, it could be re-internalised and function in the lysosomal/endosomal pathway. Thus, the pH-dependence of a protease could represent a useful regulatory mechanism. *E. coli* DegP is active in a very broad pH range but the highest activity was detected in the physiological range between pH 7.0 and 7.5 (A. Beil, unpublished observations). Two methods were used to determine the pH dependence of the proteolytic activity of Δmac25L56. First, pH dependent degradation of casein was analysed indicating that Δmac25L56 is active between pH 7.5 and 10.5 (Fig. 4.28). In more acidic pH, that is between pH 5.5 and 7.0, less degradation of casein was detected (Fig. 4.28). These initial results suggested a difference in the pH range of the proteolytic activity of human L56 (HtrA1) and the bacterial homologue DegP.

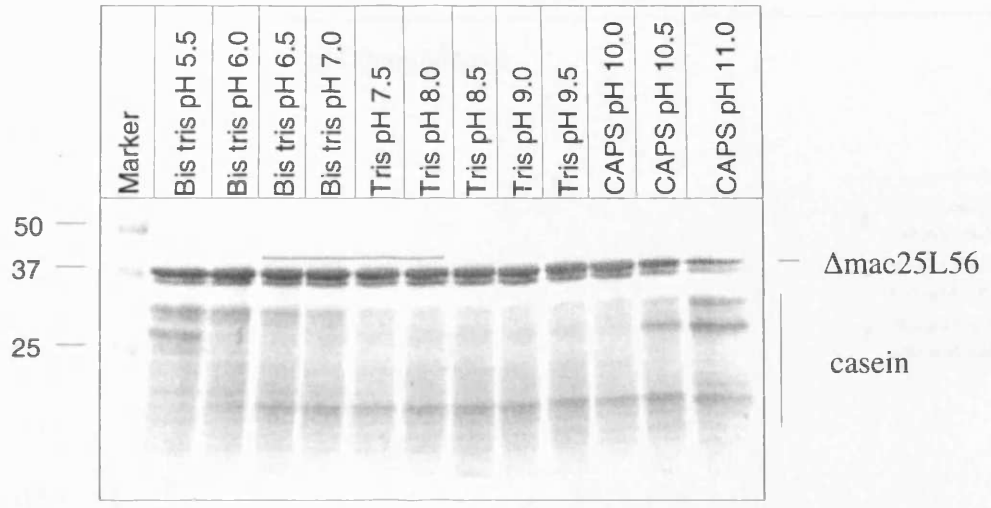

Fig. 4.28 pH dependent degradation of casein by Δmac25L56.

Δmac25L56 (10 µg) was pre-incubated in buffers of various pH values containing 150 mM NaCl for 20 min. Subsequently, casein (10 µg in assay buffer) was added and incubated for 30 min at 37°C. The samples were TCA precipitated to stop the reaction and resuspended in 20 µl sample buffer containing 30 mM DTT. The samples were loaded on a 12% SDS-gel and stained with Coomassie Blue. The molecular mass of the marker proteins is shown in kDa.

In a second approach, resorufin-labelled casein was used to determine the specific activity of Δmac25L56 at various pH values. The results indicated that Δmac25L56 had little activity between pH 5.5 and pH 7.0. The activity increased between pH 7.5 and 9.0 and a maximum was reached between pH 9.0 and 9.5 (Fig. 4.29) while a reduced, but significant, activity was detected between pH 10.0 and 10.5 (Fig. 4.29). Interestingly, Δmac25L56 seems to have its pH optimum in a non-physiological range (pH 9.5). Although the ionic strength in the buffers varied from 153 mM to 190 mM, this should not affect the proteolytic activity of Δmac25L56 because over the range of ionic strength from 150 mM up to 1 M NaCl little change in proteolytic activity was observed (see below, Fig. 4.30). The slightly elevated activity between pH 5.5 and 6.5 compared to pH 7 and 7.5 cannot be explained (Fig. 4.29). Further studies are required to establish if this result has any physiological significance.

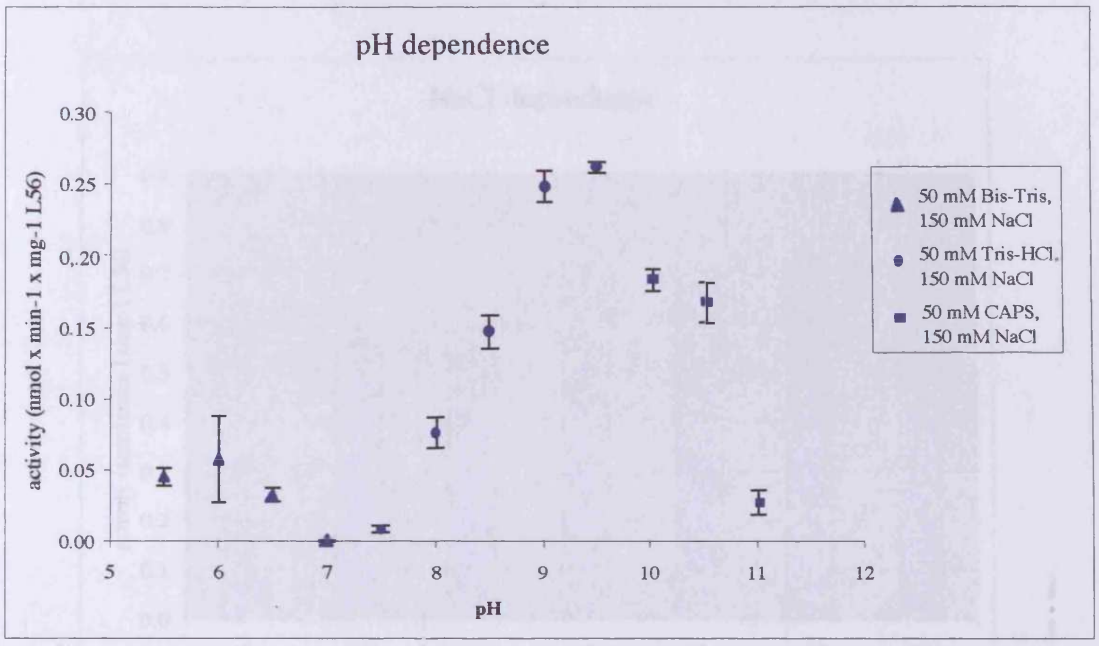

Fig. 4.29 Degradation of resorufin-labelled casein by Δmac25L56 at various pH values. Δmac25L56 (5 µg) was pre-incubated for 20 min in buffer of various pH values containing 150 mM NaCl. Subsequently, 60 µg of resorufin-labelled casein (in assay buffer) was added and samples were incubated overnight at 37°C. After TCA precipitation, the supernatants were mixed with buffer (50 mM Tris-HCl buffer pH 9.5) and the extinction was determined at 574 nm. The specific activity was calculated as described in Materials and Methods. The composition of the buffers is described in Materials and Methods (Table 3.13). Each individual assay was carried out three times and the relevant standard deviation is shown.

4.1.19 Effect of NaCl on Δmac25L56 proteolytic activity

The effect of NaCl on the proteolytic activity of Δmac25L56 was tested by analysing the degradation of resorufin-labelled casein in buffers containing various NaCl concentrations. These data indicated that a concentration of 20 mM NaCl is required for detectable proteolytic activity. There is a 6-fold increase in proteolytic activity between 0 mM and 20 mM NaCl (Fig. 4.30). The activity increases further from 20 mM to 60 mM but there is little difference in activity between 60 mM and 1 M NaCl (Fig. 4.30). The effect of NaCl could be due to a stabilisation of the active form of Δmac25L56 by supporting protein structure. Furthermore, it is known that hydrophobic substrates are more accessible to proteases when salt is added (Richards *et al.*, 1990).

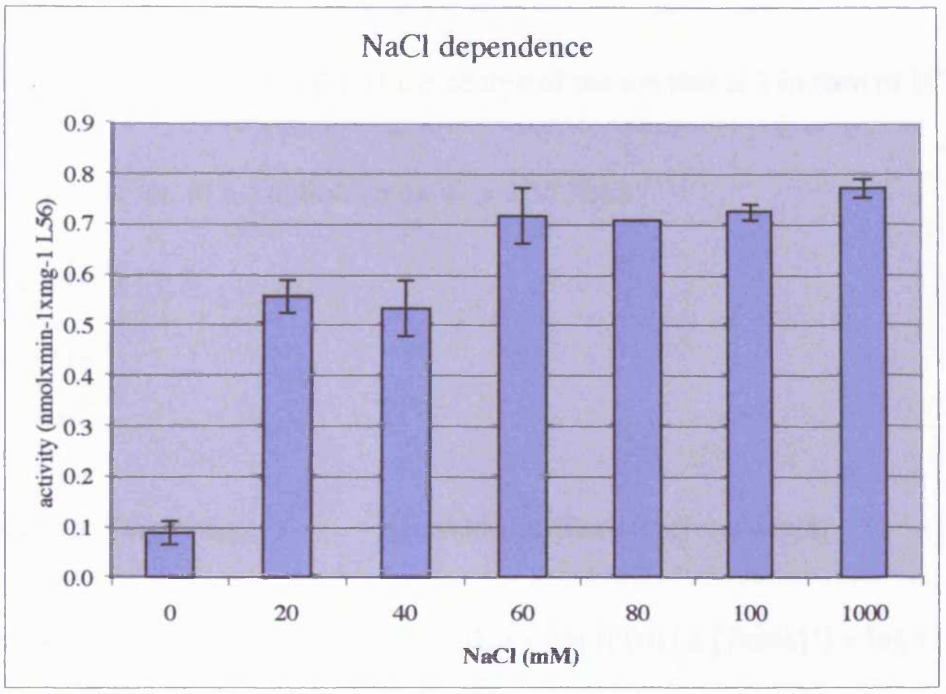

Fig. 4.30 NaCl-dependent degradation of resorufin-labelled casein by Δmac25L56.
Δmac25L56 (5 µg) was pre-incubated for 20 min at 37°C with 50 mM Tris-HCl buffer pH 8.5 and the various NaCl concentrations indicated. Resorufin-labelled casein (60 µg in assay buffer) was added and incubated overnight at 37°C. The samples were TCA precipitated, the supernatant was mixed with 50 mM Tris-HCl buffer pH 9.5 and the extinction was measured at 574 nm. One sample without Δmac25L56 served as reference. Each individual assay was carried out three times and the relevant standard deviation is shown.

The ionic strength of a solution can affect the pH. As L56 appears to exhibit pH-dependence (Fig. 4.29) it is required to consider the possible effects of NaCl on the pH of the buffer used. In dilute solutions (at low ionic strength), the activity of molecules (here for the individual components of Tris buffers $TrisH^+$, H^+ and Tris) correlates with their concentration. The activity is calculated as the activity coefficient multiplied by the concentration.

For ions at low ionic strength, the activity coefficient approaches 1 but at higher ionic strength it decreases. Debye and Huckel have generated a formula allowing to calculate the activity coefficient f_i of ion i in solutions of different ionic strength:

$f_i = 10^{-[0.5 \times z_i^2 \sqrt{I}]}$

(where I is the ionic strength and z_i is the charge of the ion that is 1 in case of H^+)

For a monovalent ion in a solution containing 1 M NaCl:

$f_i = 10^{-[0.5 \times 1^2 \sqrt{I}]}$

$= 10^{-0.5} = 0.316$

and log f = -0.5

$pH = pKa + \log (a_{Tris} \times a_{TrisH}^{-1})$ [Henderson-Hasselbach equation]

$pH = pKa + \log ([Tris] \times (f \times [TrisH])^{-1}) = pKa + \log ([Tris] \times [TrisH]^{-1}) - \log f$

at 1 M NaCl, $pH = pKa + \log ([Tris] \times [TrisH]^{-1}) + 0.5$

Therefore, the maximum correction needed (at 1 M NaCl) is an increase in pH of 0.5 units. This effect can cause quite a change in activity which increases by about 50% from pH 8.5 to pH 9 (Fig. 4.29). Therefore, high salt concentrations were avoided in future assays.

4.1.20 Temperature-dependence of the proteolytic activity of Δmac25L56

The activity of an enzyme is also dependent on the temperature. Commonly the activity of enzymes increases with temperature up to a certain temperature which is called the "optimum". A further increase in the temperature decreases the activity due to denaturation of the protein. This loss of activity may or may not be reversible on bringing the temperature back down to the optimum. The optimal temperature varies from enzyme to enzyme but is often in the range of 30°C-45°C for mammalian and microbial enzymes.

Spiess *et al.* (1999) showed that *E. coli* DegP has a temperature-dependent switch from chaperone to protease. DegP revealed chaperone activity at low temperature (28°C), whereas increasing the temperature from 37°C to 50°C led to elevated proteolytic activity. It would be interesting to examine if L56 has the same properties. Even though Zumbrunn and Trueb (1996) could not detect an induction or up-regulation of proteolytic activity of L56 by incubation of normal human fibroblasts at 42°C, purified Δmac25L56 was incubated with resorufin-labelled casein overnight at various temperatures and the extinction was determined at 574 nm.

The data in the present report confirmed that L56 activity increased with temperature. Only a slight proteolytic activity was observed at 18°C, 23°C, 28°C and 32°C (Fig. 4.31). Increasing the temperature from 37°C to 47°C led to a maximum of proteolytic activity (1.6 nmol resorufin-labelled casein x min^{-1} x mg^{-1} L56) at 47°C (Fig. 4.31). Incubation at 52°C and 57°C led to a decrease in activity (Fig. 4.31), which might be explained by a denaturing of the enzyme at these high temperatures. These data were confirmed by an incubation of Δmac25L56 with casein at the same temperatures for 0, 5 and 30 min. Incubation at 13°C, 18°C, 23°C and 28°C led to no or limited degradation after 30 min (Fig. 4.32 and 4.33) whereas raising the temperature to 47°C led to a total disappearance of the casein bands (Fig. 4.34 and 4.35).

Temperature and pH could influence the folded state of a substrate and therefore its accessibility and the rate of degradation. Given these considerations, the use of a short and thus unstructured peptide substrate would be advantageous. However, peptide substrates are not available for L56 and since its substrate specificity is unknown, our knowledge for designing a peptide substrate was insufficient.

It should also be noted that Tris buffers change the pH depending on the temperature. Therefore, the pH of the reaction buffer changed from pH 8.69 at 18 °C to 7.6 at 57 °C (Table 4.2). Because previous experiments indicated that the proteolytic activity of Δmac25L56 decreases at low pH, the decrease in proteolytic activity above 47°C could also be due to the decrease in pH.

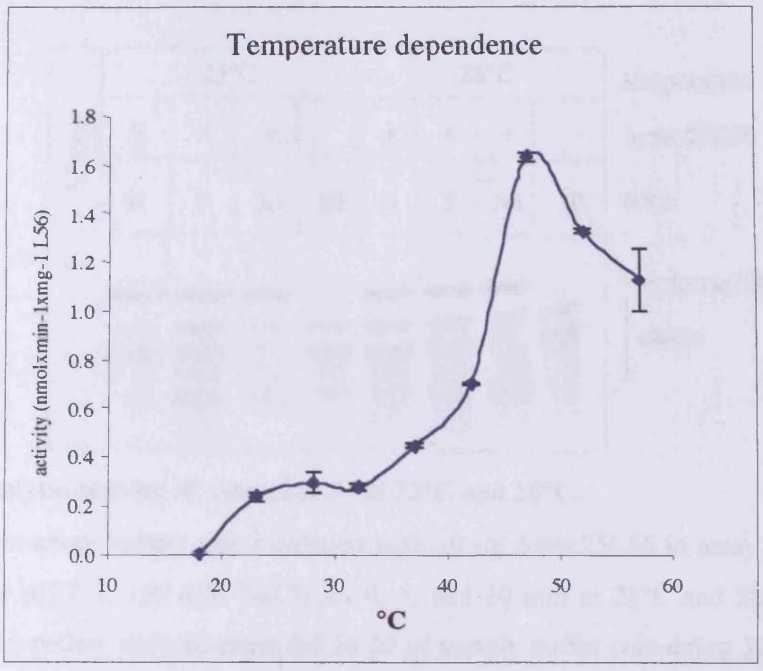

Fig. 4.31 Temperature dependent degradation of resorufin-labelled casein by Δmac25L56. Δmac25L56 (5 µg) was pre-incubated in 50 mM Tris-HCl buffer pH 8.5, 150 mM NaCl for 20 min at the various temperatures indicated. Resorufin-labelled casein (60 µg in assay buffer) was added and incubated overnight at the appropriate temperature. The samples were analysed by measuring the extinction at 574 nm. Each individual assay was carried out three times and the relevant standard deviation is shown.

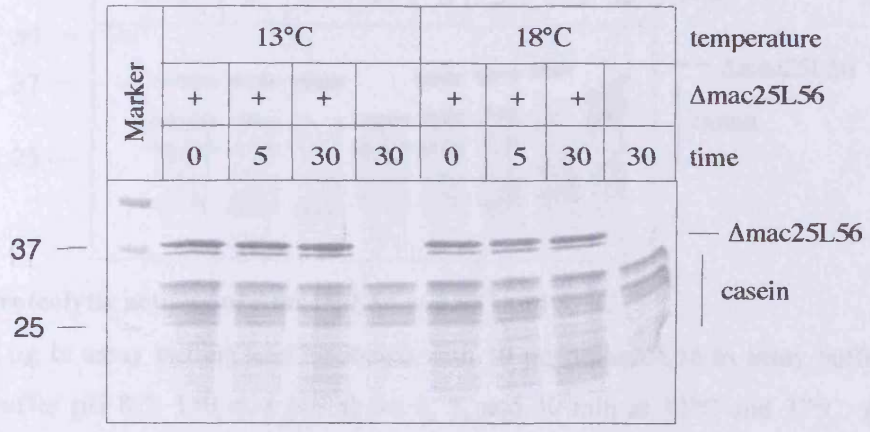

Fig. 4.32 Proteolytic activity of Δmac25L56 at 13°C and 18°C.
Casein (10 µg in assay buffer) was incubated with 10 µg Δmac25L56 in assay buffer (50 mM Tris-HCl buffer pH 8.5, 150 mM NaCl) for 0, 5, and 30 min at 13°C and 18°C. After TCA precipitation, the pellets were resuspended in 20 µl sample buffer containing 30 mM DTT and loaded on a 12% SDS-gel. The gel was stained with Coomassie Blue. The molecular mass of the marker proteins is shown in kDa.

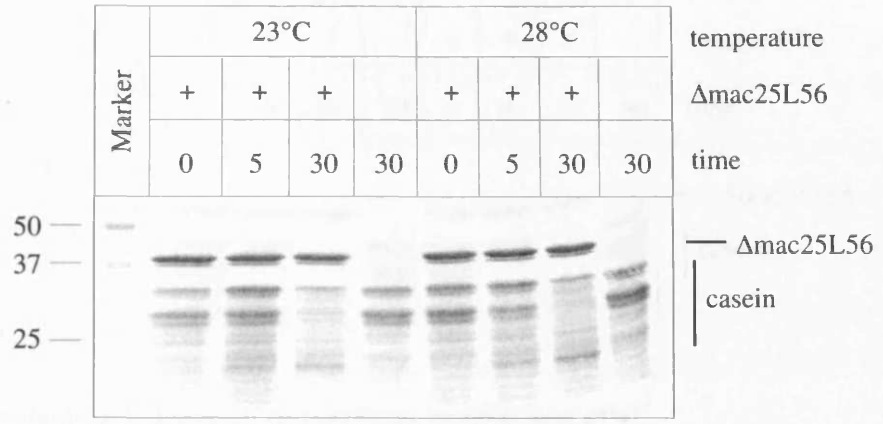

Fig. 4.33 Proteolytic activity of Δmac25L56 at 23°C and 28°C.

Casein (10 µg in assay buffer) was incubated with 10 µg Δmac25L56 in assay buffer (50 mM Tris-HCl buffer pH 8.5, 150 mM NaCl) for 0, 5, and 30 min at 23°C and 28°C. After TCA precipitation, the pellets were resuspended in 20 µl sample buffer containing 30 mM DTT and loaded on a 12% SDS-gel. The gel was stained with Coomassie Blue. The molecular mass of the marker proteins is shown in kDa.

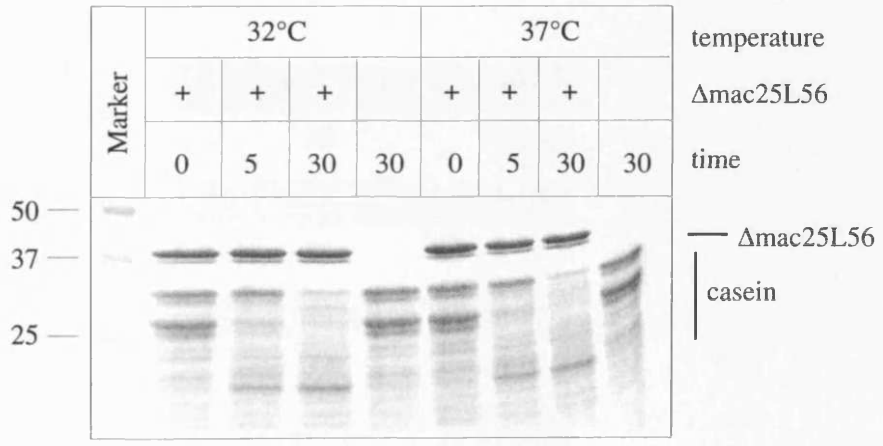

Fig. 4.34 Proteolytic activity of Δmac25L56 at 32°C and 37°C

Casein (10 µg in assay buffer) was incubated with 10 µg Δmac25L56 in assay buffer (50 mM Tris-HCl buffer pH 8.5, 150 mM NaCl) for 0, 5, and 30 min at 32°C and 37°C. After TCA precipitation, the pellets were resuspended in 20 µl sample buffer containing 30 mM DTT and loaded on a 12% SDS-gel. The gel was stained with Coomassie Blue. The molecular mass of the marker proteins is shown in kDa.

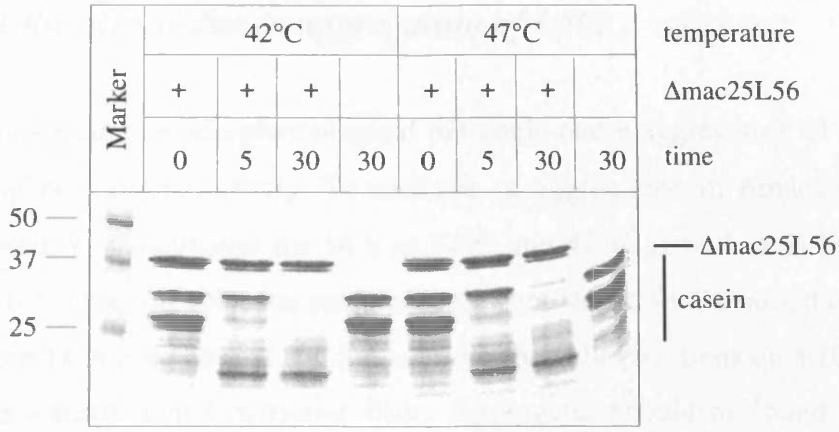

Fig. 4.35 Proteolytic activity of Δmac25L56 at 42°C and 47°C

Casein (10 µg in assay buffer) was incubated with 10 µg Δmac25L56 in assay buffer (50 mM Tris-HCl buffer pH 8.5, 150 mM NaCl) for 0, 5 and 30 min at 42°C and 47°C. After TCA precipitation, the pellets were resuspended in 20 µl sample buffer containing 30 mM DTT and loaded on a 12% SDS-gel. The gel was stained with Coomassie Blue. The molecular mass of the marker proteins is shown in kDa.

Table 4.2 The effect of the temperature on the pH value measured for 50 mM Tris-HCl buffer pH8.5 (adjusted at 23°C), 150 mM NaCl.

Temperature (°C)	pH
18	8.69
23	8.55
28	8.41
32	8.30
37	8.16
42	8.02
47	7.88
52	7.74
57	7.60

4.1.21 Are the effects due to aggregation of L56?

Elevated temperature or non-physiological pH could cause aggregation of Δmac25L56 and a loss of proteolytic activity. To exclude an aggregation of Δmac25L56, 10 μg purified protein was incubated for 16 h at 37°C and 47°C as well as in buffers of pH 7.0, 8.5 or 10.5. Subsequently, the samples were centrifuged for 30 min, the supernatant fractions were TCA precipitated and loaded with the pellet fractions on a 10% SDS-gel. The gel was stained with Coomassie Blue. Aggregates should be found in the pellet fractions and soluble protein in the supernatant fraction.

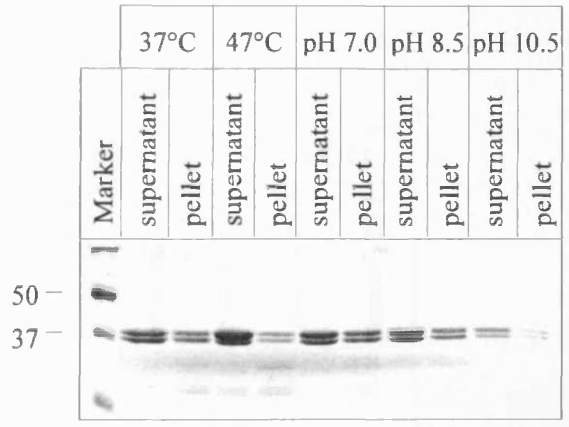

Fig. 4.36 Aggregation test of Δmac25L56.

Δmac25L56 (10 μg) was incubated overnight in 50 mM Tris-HCl buffer pH 8.5, 150 mM NaCl at 37°C or 47°C or in 50 mM Tris-HCl buffer pH 7.0, 150 mM NaCl; 50 mM Tris-HCl buffer pH 8.5, 150 mM NaCl and 50 mM CAPS buffer pH 10.5, 150 mM NaCl at 37°C. The samples were centrifuged for 30 min at 15000 rpm in an Eppendorf centrifuge. The supernatants were TCA precipitated, resuspended in sample buffer containing 30 mM DTT and loaded together with the pellet fractions on a 10% SDS-gel. The gel was stained with Coomassie Blue. The molecular mass of the marker proteins is shown in kDa.

The SDS-gel indicated that independent of the pH or the temperature, the ratio of soluble to aggregated protein was similar (Fig. 4.36). These results suggest that the observed temperature and pH effects cannot be explained by an aggregation of the purified protein. The diminished amount of protein in the samples incubated at pH 8.5 and 10.5 is unknown. However, one potential explanation is that during the long incubation period autolysis might have occurred.

4.1.22 Are disulphide bonds required for proteolytic activity of Δmac25L56?

Full-length L56 contains 16 cysteine residues which might be involved in intra- or intermolecular disulphide bond formation. Δmac25L56 still contains one cysteine residue. On a Coomassie-stained SDS-gel and a Western blot showing purified Δmac25L56, with or without 30 mM of the reducing agent DTT, a shift in migration from 37 kDa (monomer) to 76 kDa (dimer) without DTT was detectable (Fig. 4.37/4.38). This raises the possibility that an intermolecular disulphide bond is formed and this disulphide bond may therefore be affecting proteolytic activity.

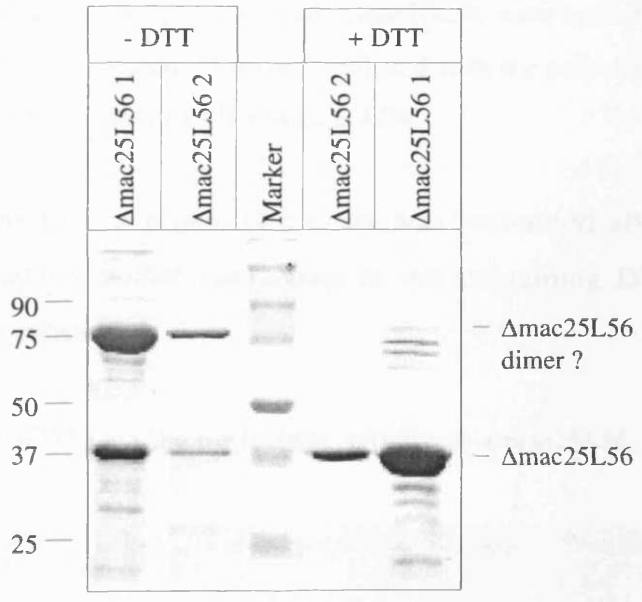

Fig. 4.37 DTT-dependent shift of Δmac25L56 analysed on a Coomassie-stained gel.
Various amounts (30 µg (1) or 10 µg (2)) of Δmac25L56 were loaded on a SDS-gel with or without 30 mM DTT. The gel was stained with Coomassie Blue. The molecular mass of the marker proteins is shown in kDa.

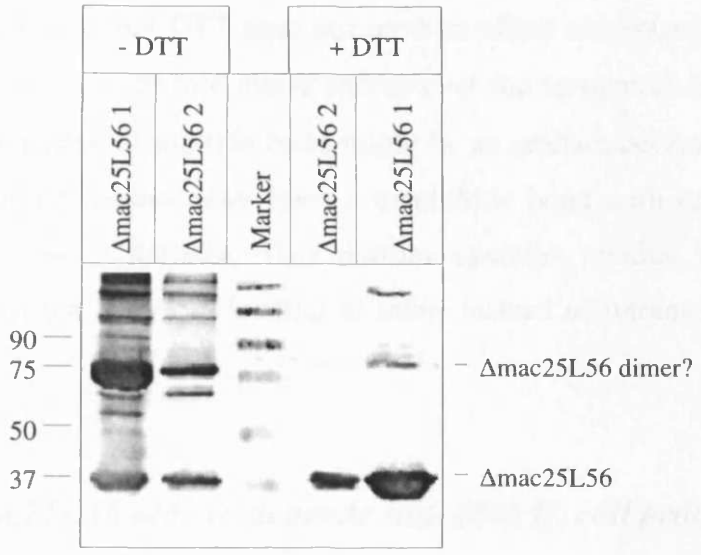

Fig. 4.38 DTT-dependent shift of Δmac25L56 analysed by Western blotting

Various amounts (30 µg (1) or 10 µg (2)) of Δmac25L56 were loaded on a SDS-gel with or without 30 mM DTT. The Western blot was incubated with the polyclonal L56 antiserum. The molecular mass of the marker proteins is shown in kDa.

To address this question, a proteolytic assay was performed after pre-incubation of Δmac25L56 in reaction buffer containing or not containing DTT using resorufin-labelled casein as a substrate.

Table 4.3 The effect of DTT on the proteolytic activity of Δmac25L56.

DTT concentration (mM)	Activity (nmol x min^{-1} x mg^{-1} L56)	Standard deviation
0	0.53	0.01
0.01	0.59	0.03

Δmac25L56 (5 µg) was pre-incubated in 50 mM Tris-HCl buffer pH 8.5, 150 mM NaCl with or without 0.01 mM DTT for 20 min at 37°C. Resorufin-labelled casein (60 µg in assay buffer) was added and incubated overnight at 37°C. After TCA precipitation, the extinction of the supernatant was measured in 50 mM Tris-HCl buffer pH 9.5 at 574 nm. Each individual assay was carried out three times and the relevant standard deviation is shown.

These results indicated that DTT does not have an effect on proteolytic activity when present in the assay in a 20-fold molar excess over the amount of Δmac25L56 (Table 4.3). Also, the potential disulphide bond might be an artefact because in the wild type protein this cysteine residue may form a disulphide bond with one of the cysteine residues in the mac25 domain. This partner cysteine residue is missing in the Δmac25L56 construct therefore leading to inter- instead of intramolecular disulphide bond formation.

4.1.23 Is Δmac25L56 able to degrade unfolded E. coli proteins?

L56 might degrade extracellular matrix proteins such as fibronectin, COMP and fibromodulin (46th and 47th Annual Meeting, Orthopaedic Research Society, March 2000, Orlando Florida and February 2001, San Francisco USA). However, the substrate specificity of L56 is not established. To address this question, two purified *E. coli* proteins, TreA and MalS were used in denatured form in proteolysis assays. Unfolded proteins were used because *E. coli* DegP has a strong preference for unfolded proteins (Clausen *et al.,* 2002). MalS is a periplasmic α-amylase, which is responsible for the degradation of long maltooligosaccharides. TreA is a trehalase hydrolysing trehalose into glucose.

The protease assays were performed in a similar manner to the casein assays. MalS degradation was already evident after 5 min and was almost complete after 60 min (Fig. 4.39A). Protease resistant MalS detectable after 3 h incubation (Fig. 4.39A) could represent folded MalS. Spontaneous refolding is possible because the denaturing agent urea is diluted in the assay. During control incubation of MalS in the absence of L56 for 180 min, MalS was not degraded (Fig. 4.39B) indicating that the MalS samples did not contain any relevant protease activity.

TreA degradation was also apparent after 5 min but it seems that after 30 min all of the degradable protein is removed and the remaining amount does not decrease even after o/n incubation (Fig. 4.40A). During control incubation of TreA in the absence of L56 for 180 min, no degradation was detected (Fig. 4.40B) indicating that the TreA samples

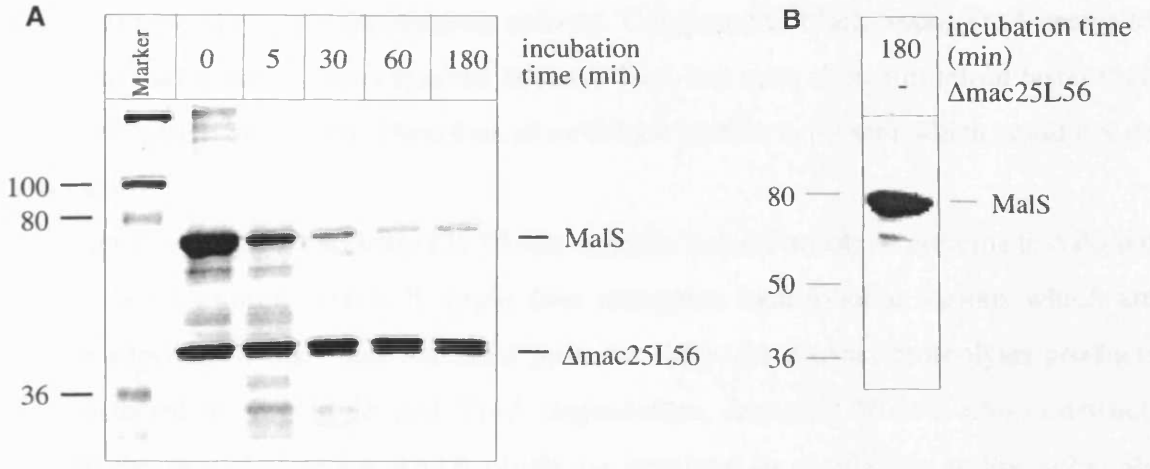

Fig. 4.39 MalS degradation by Δmac25L56.

A. MalS (10 µg) was incubated with 10 µg Δmac25L56 for 0, 5, 30, 60 and 180 min in 50 mM Tris-HCl buffer pH 8.5, 150 mM NaCl at 37°C. The samples were TCA precipitated, resuspended in sample buffer containing 30 mM DTT and analysed on a 10% SDS-gel. The gel was stained with Coomassie Blue. The molecular mass of the marker proteins is shown in kDa. B. Control incubation of MalS in the absence of L56.

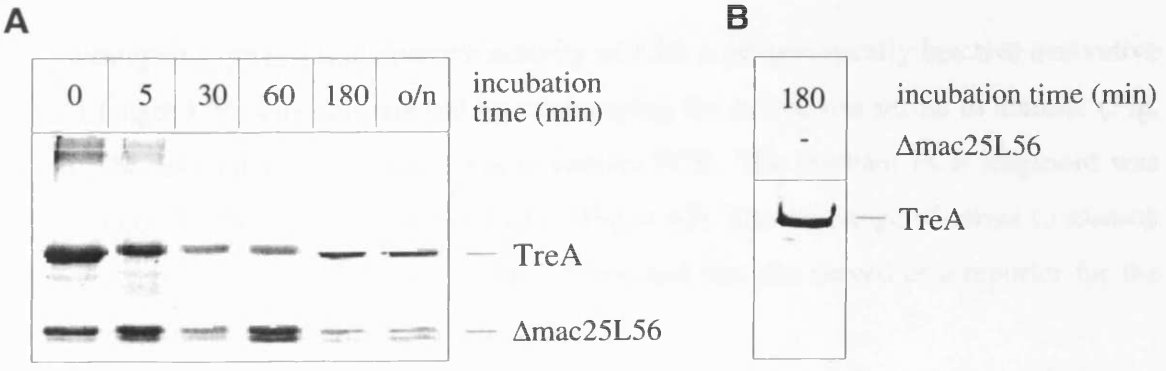

Fig. 4.40 TreA degradation by Δmac25L56.

A. TreA (10 µg) was incubated with 10 µg Δmac25L56 for 0, 5, 30, 60, 180 min and overnight (o/n) in 50 mM Tris-HCl buffer pH 8.5, 150 mM NaCl at 37°C. The samples were TCA precipitated, resuspended in sample buffer containing 30 mM DTT and analysed on a 10% SDS-gel. The gel was stained with Coomassie Blue. The molecular mass of the marker proteins is shown in kDa. B. Control incubation of TreA in the absence of L56.

did not contain any relevant protease activity. Compared to MalS, more TreA seems to be undegradable which was expected because TreA has been shown to refold faster than MalS (Uhland *et al.,* 2000). Therefore more folded protein is present which could not be degraded.

These results suggest that Δmac25L56 can degrade several unfolded proteins that do not need to be of human origin. It might thus recognize hydrophobic regions which are surface exposed in mis- and unfolded proteins. Also, no distinct proteolysis products were detected during MalS and TreA degradation. Δmac25L56 is a L56 construct, lacking the mac25 domain which might be involved in regulation and/or substrate recognition. However, autoproteolysis is observed in cultured human cells which produce protein fragments with the same molecular mass than Δmac25L56 (Hu *et al.,* 1998). These autoproteolytic fragments are active and can degrade proteins in human cells or the ECM similar to the Δmac25L56 construct and should thus have the same substrate specificity.

4.1.24 Generation of a L56SA and a Δmac25L56SA mutant

To investigate a potential chaperone activity of L56, a proteolytically inactive derivative of full-length L56 was constructed by exchanging the active site serine to alanine (Fig. 4.41). This mutant was generated via crossover PCR. The relevant PCR fragment was cloned into pCS19 via the *NcoI/BglII* sites (Fig. 4.42). The exchange of serine to alanine introduced an additional *NaeI* site in the cDNA and this site served as a reporter for the exchange. The new plasmid was called pSG11.

Subsequently, a Δmac25L56SA derivative was generated to produce a truncated version of the inactive protein. This construct could be useful for crystallisation and chaperone assays because purification of Δmac25L56 was successful whereas full-length L56 caused various problems. The *l56SA* fragment from pSG11 was cloned into pSG7 vector as a *PstI* and *BglII* fragment yielding pSG13 (Fig 4.43).

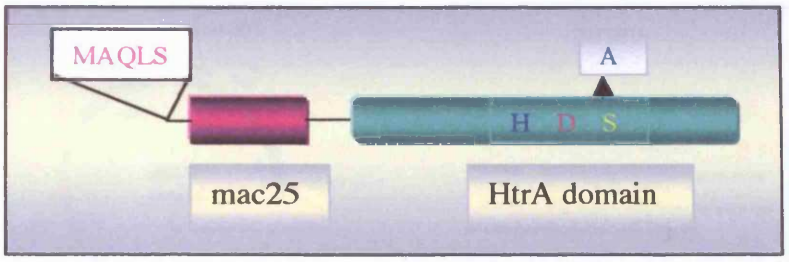

Fig. 4.41 Schematic picture of ΔssL56SA.

The N-terminal residues of signal sequenceless L56SA are shown in pink; followed by the mac25 domain coloured in purple and the protease core (HtrA domain) coloured in green. The catalytic serine is exchanged to alanine.

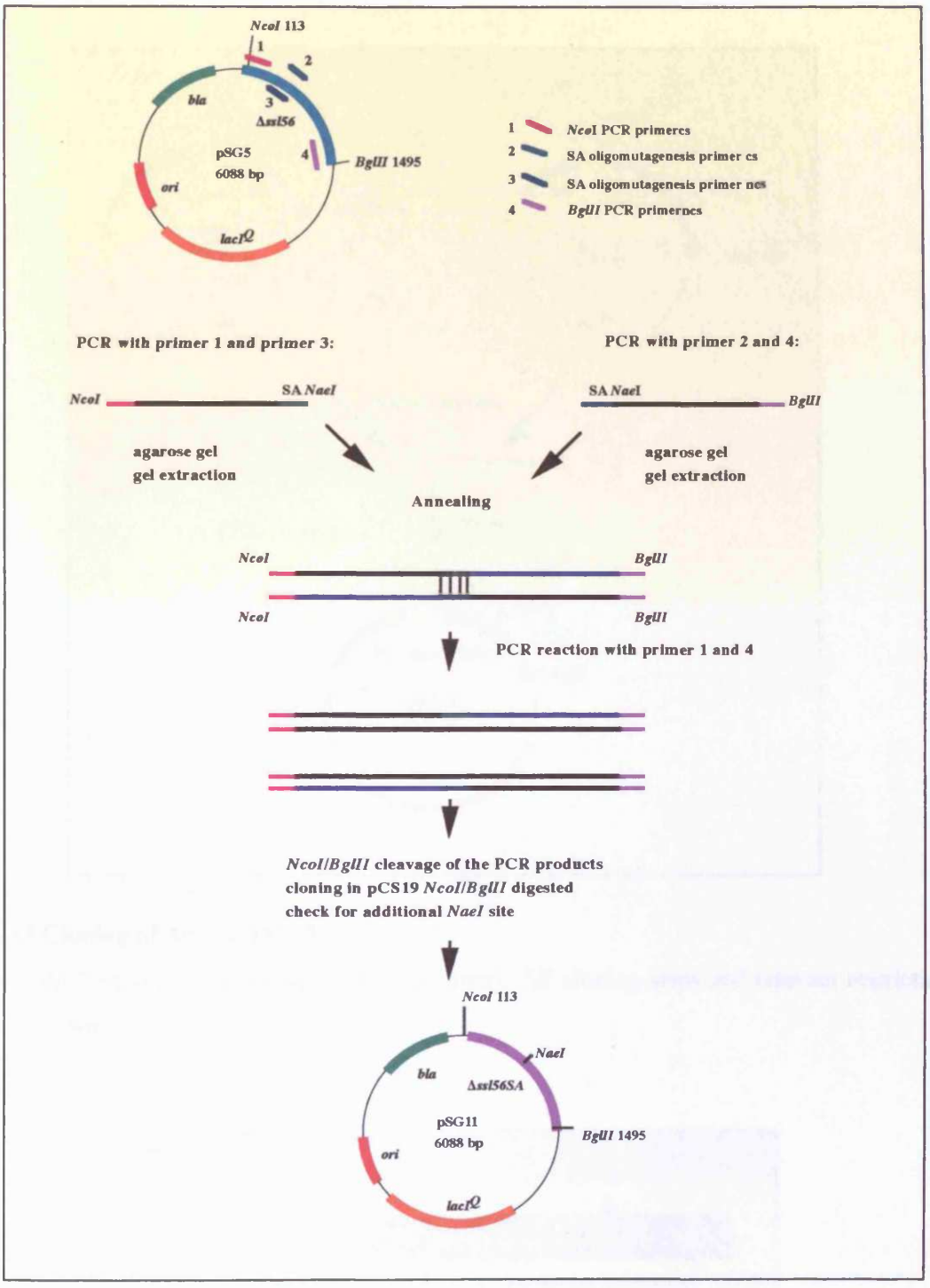

Fig. 4.42 Construction of full-length *l56SA* by cross-over PCR.

pSG5 served as template for the crossover PCR reactions. The oligomutagenesis primers introduced an additional *NaeI* site in the *l56* cDNA. All cloning steps and relevant restriction enzymes are shown.

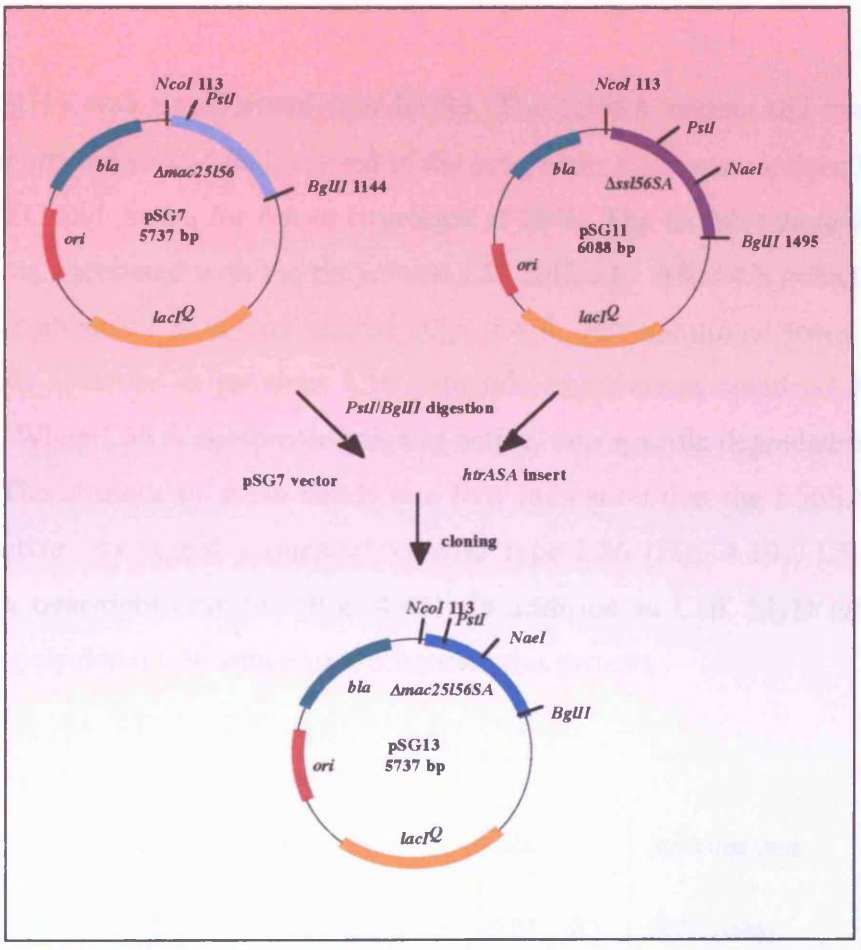

Fig. 4.43 Cloning of *Δmac25l56SA*.

Plasmid pSG7 served as vector and pSG11 as insert. All cloning steps and relevant restriction sites are shown.

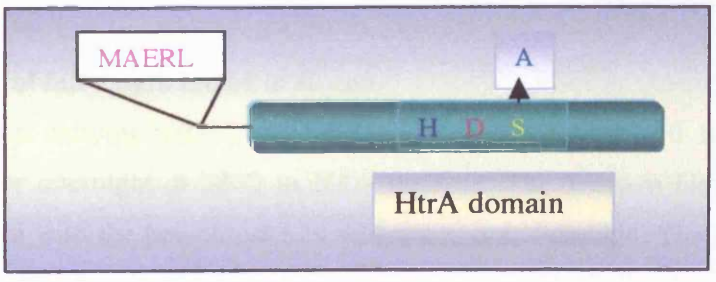

Fig. 4.44 Schematic picture of Δmac25L56SA.

The first amino acids of the protein are shown in pink; followed by the protease domain (HtrA core) coloured in green. The catalytic serine is exchanged to alanine.

4.1.25 Expression of the l56SA mutant in E. coli

Plasmid pSG11 was transformed into KU98. The L56SA mutant did not contain a signal sequence and should be localised in the cytoplasm. Cells were induced with 10 or 100 μM IPTG and grown for 4 h or overnight at 28°C. The samples were analysed on Western blots, incubated with the polyclonal L56 antibody. After 4 h induction, a band migrating at about 52 kDa was visible (Fig. 4.45). The additional lower molecular weight bands observed in previous L56 induction experiments could not be detected (Fig. 4.45). When L56 is autoproteolytically active, two specific degradation bands are produced. The absence of these bands is a first indication that the L56SA mutant is indeed inactive. As signal sequenceless wild type L56 (Fig. 4.19), L56SA is not produced in overnight cultures (Fig. 4.45). In addition to L56, SlyD was detected because the polyclonal L56 antiserum recognises this protein.

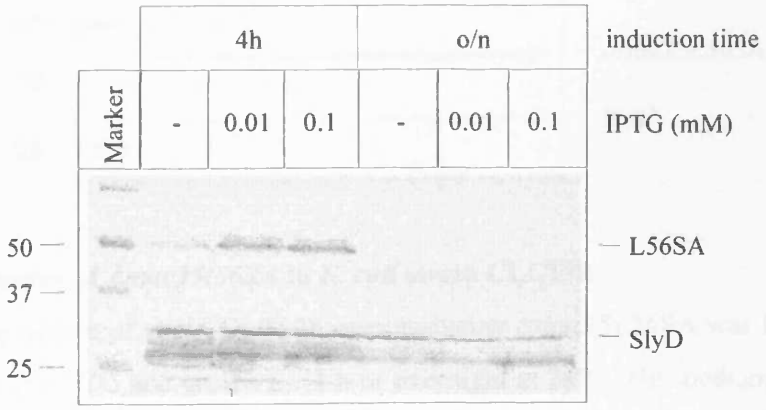

Fig. 4.45 Expression of full-length *l56SA* in *E. coli*.
A five millilitre culture carrying pSG11 was induced at OD_{578} = 0.5 with 10 or 100 μM IPTG and grown for 4 h or overnight at 28°C in NZA medium. The Western blot of whole cell extracts was incubated with the polyclonal L56 antiserum. o/n: overnight. The molecular mass of the marker proteins is shown in kDa.

4.1.26 Expression of Δmac25l56SA

E. coli strain KU98, overproducing Δmac25L56SA was induced with 10 or 100 μM IPTG and grown for 4 h or overnight at 28°C. The samples were analysed on a Western blot incubated with the polyclonal L56 antiserum. Δmac25L56SA was produced after 4 h and overnight induction and protein levels were comparable to Δmac25L56 (Fig. 4.25 and 4.46). Protein present in the uninduced samples suggests that the promoter of the expression vector is not tight in this strain (Fig. 4.46). Again, no degradation products could be detected indicating that the mutant is not proteolytically active.

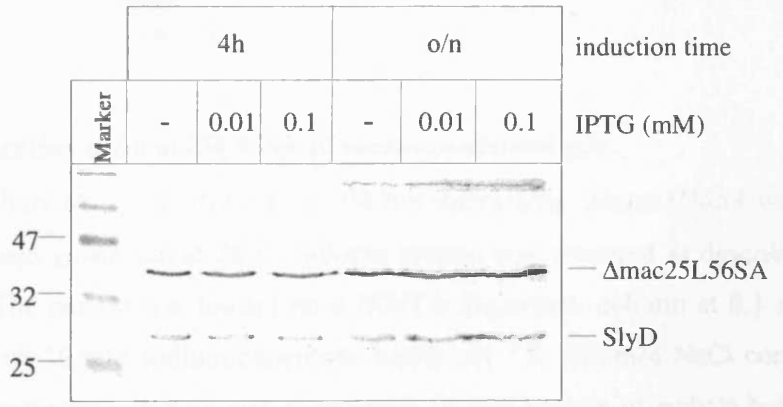

Fig. 4.46 Expression of *Δmac25l56SA* in *E. coli* strain CLC198.
A five millilitre culture of strain CLC198 overproducing Δmac25L56SA was induced at OD_{578} = 0.4 with 100 μM IPTG and grown for 4 h or overnight at 28°C. The medium used was NZA. The Western blot of whole cell extract was incubated with the polyclonal L56 antiserum. o/n =overnight. The molecular mass of the marker proteins is shown in kDa.

4.1.27 Purification of Δmac25L56SA

As purification of L56SA caused similar problems as L56 with several contaminants present in the elution fractions (data not shown), only Δmac25L56SA was purified following the procedure for the proteolytically active protein. The only difference was that a cation exchange column was used after NiNTA affinity chromatography.

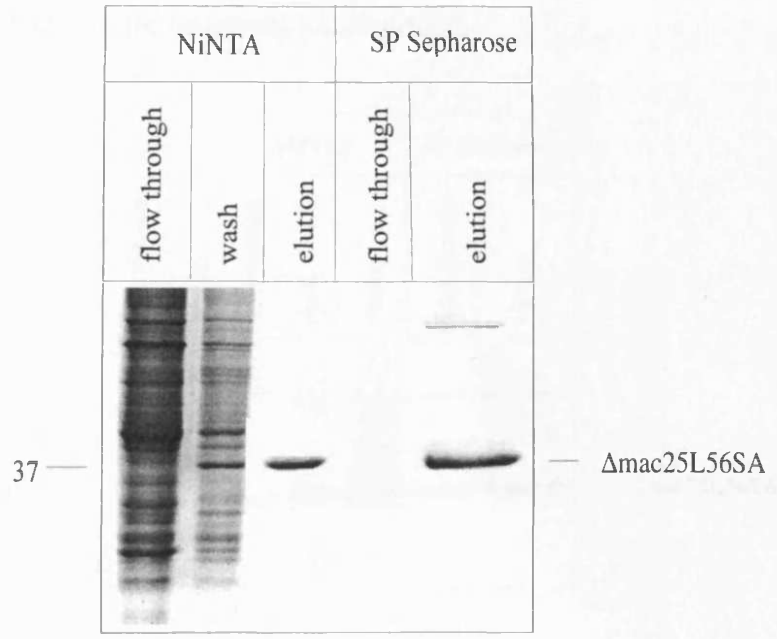

Fig. 4.47 Purification of Δmac25L56SA (Coomassie-stained gel).

A three litre culture of *E. coli* strain CLC198 overexpressing *Δmac25l56SA* was induced with 100 µM IPTG and grown o/n at 28°C. Soluble protein was prepared as described in Materials and Methods. The protein was loaded on a NiNTA Superflow column at 0.3 ml/min and one washing step with 50 mM sodium phosphate buffer pH 7.5, 300 mM NaCl containing 20 mM imidazole was performed. Protein was eluted with 50 mM sodium phosphate buffer pH 7.5, 300 mM NaCl containing 500 mM imidazole. Subsequently, the protein was dialysed against 100 mM Hepes buffer pH 8.0, 100 mM ammonium sulphate and loaded on a SP Sepharose column. Protein was eluted with 100 mM Hepes buffer pH 8.0, 500 mM ammonium sulphate and the peak fraction containing the protein of interest was loaded on a 12% SDS-gel. The molecular mass of one marker protein is shown in kDa.

The Western blot showed that Δmac25L56SA was overproduced (Fig. 4.48). Small amounts of Δmac25L56SA were detectable in the flow through as well as in the washing step during NiNTA chromatography (Fig. 4.48). Perhaps a re-used column material which might have a reduced binding capacity, is responsible for this effect. After elution, the protein seemed to be pure (Fig. 4.47) but a SP Sepharose step was included with half of the pre-purified protein to test the binding conditions for the SP Sepharose. Almost all protein bound to the column. Following elution, two bands were observed on a Coomassie- stained gel. However, the eluted protein was considered to be

pure due to the fact that both bands were recognised by the L56 antiserum (Fig. 4.48). The additional band might represent a L56 dimer.

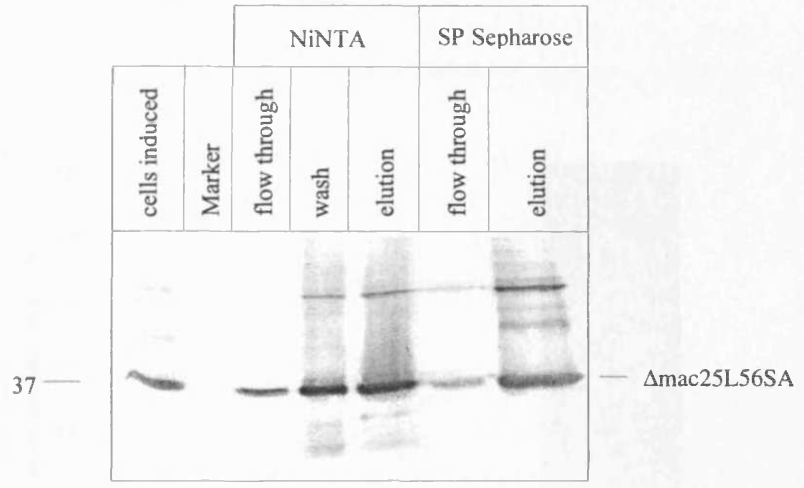

Fig. 4.48 Purification of Δmac25L56SA (Western blot).

A three litre culture of *E. coli* strain CLC198 overexpressing *Δmac25l56SA* was induced with 100 µM IPTG and grown o/n at 28°C. Soluble protein was prepared as described in Materials and Methods. The purification was done as described in Fig. 4.46. The Western blot was incubated with the polyclonal L56 antiserum. The molecular mass of one marker protein is shown in kDa.

The origin of the additional faint bands recognised by the L56 antiserum is unknown. However, it can be speculated that they might represent degradation products of a L56 dimer. Another explanation could be that the antiserum cross-reacts with other proteins as it is not affinity purified.

4.1.28 Is the purified Δmac25L56SA proteolytically active?

The proteolytic activity of purified Δmac25L56SA was determined by measuring degradation of resorufin-labelled casein. An assay with Δmac25L56 served as a reference.

The results indicated that Δmac25L56SA has almost no proteolytic activity (0.005 nmol resorufin-labelled casein x min^{-1} x mg^{-1} L56) (Fig. 4.49). Therefore, it could be used for refolding-assays to investigate the presence of a chaperone activity.

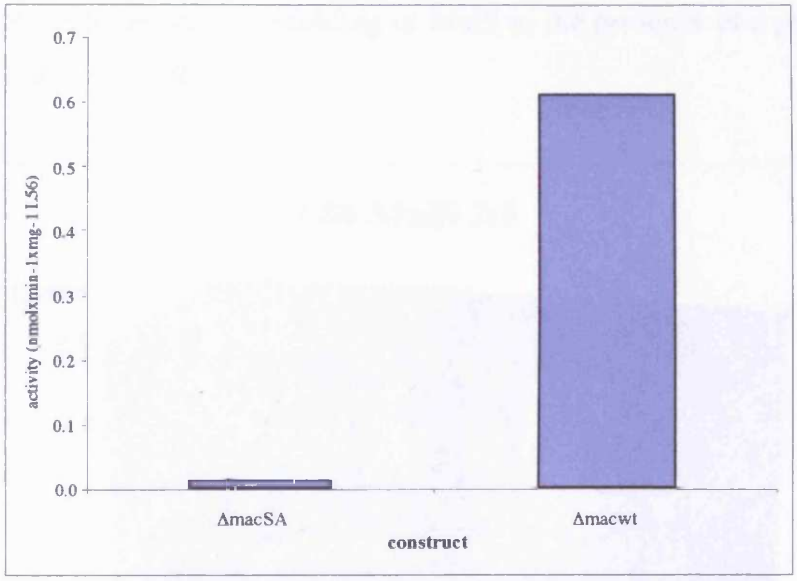

Fig. 4.49 Proteolytic activity of Δmac25L56SA.

Resorufin-labelled casein (60 µg in assay buffer) was incubated overnight with either Δmac25L56SA (10 µg) or Δmac25L56 (10 µg) in 50 mM Tris-HCl buffer pH 8.5, 150 mM NaCl at 37°C. The extinction of the supernatants was measured in 50 mM Tris-HCl buffer pH 9.5 at 574 nm.

4.1.29 Does Δmac25L56SA have chaperone activity?

Spiess *et al.* (1999) reported that *E. coli* DegP has a dual function as a chaperone at low temperatures (< 28°C) and as a protease at elevated temperatures. A proteolytically inactive mutant, DegPSA, in which the active site $serine_{210}$ is changed to alanine revealed temperature-independent chaperone activity (Spiess *et al.*, 1999). It would be interesting to examine if L56 has the same properties. Therefore, purified Δmac25L56 and Δmac25L56SA were used in a chaperone assay with unfolded MalS as substrate. Refolding of MalS was determined by assaying MalS activity via the hydrolysis of a specific substrate NPG. The enzymatic reaction leads to the generation of a yellow

product (nitrophenol) that absorbs light at 420 nm. Thus, the extinction at 420 nm served as a direct reporter for refolding of MalS.

The chaperone assays were performed in cooperation with Markus Eser in our laboratory as described in Materials and Methods. BSA (bovine serum albumin) served as negative control to determine refolding of MalS in the presence of a protein without chaperone activity (Fig. 4.50).

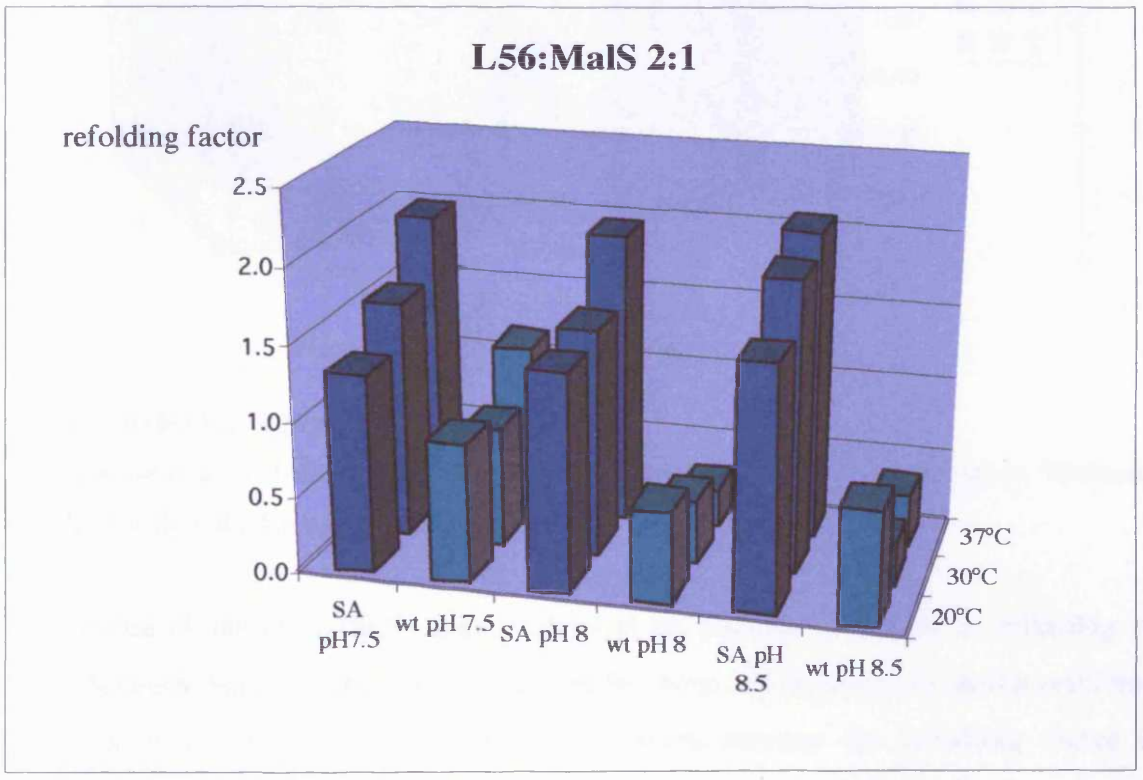

Fig. 4.50 Refolding of MalS by Δmac25L56 (wt/SA).

A chaperone assay with purified Δmac25L56 (wt) or Δmac25L56SA (SA) which was present in 2-fold excess to unfolded MalS, was performed as described in Materials and Methods. The assay was carried out at three different temperatures (20°C, 30°C and 37°C) as well as in three buffers of different pH values (pH 7.5, pH 8.0 and pH 8.5).

Refolding of MalS was not assisted in the presence of BSA at various pH values and temperatures as indicated by refolding factors between 0.9 and 1.2 (Fig. 4.51). BSA was therefore used as a control for a supplement that has no chaperone or protease activity.

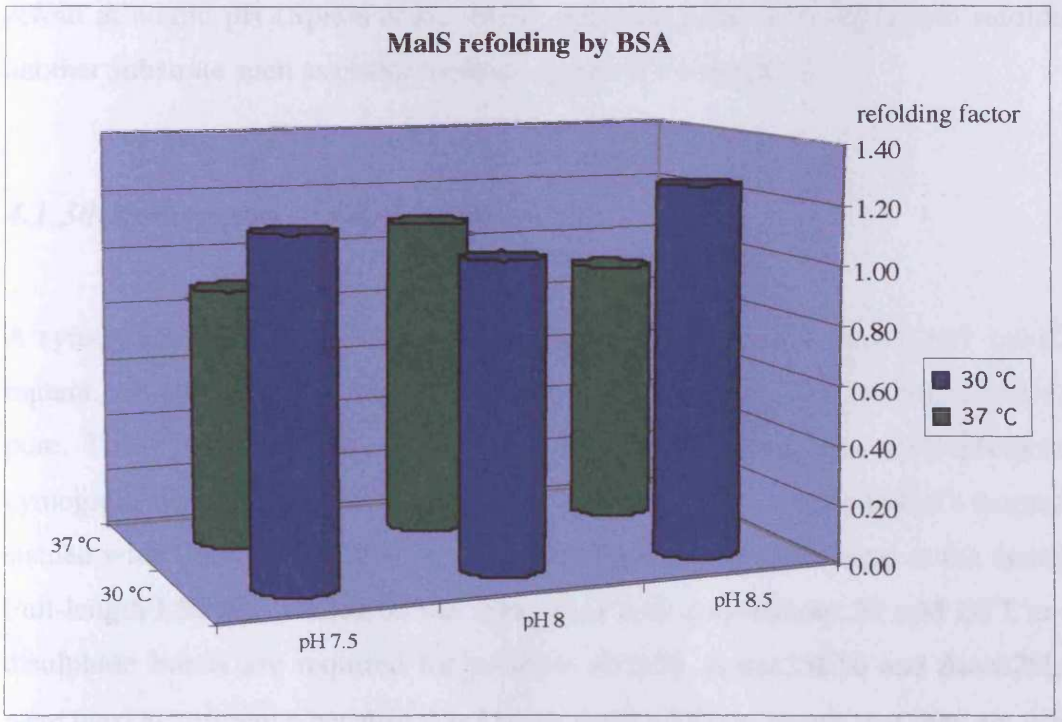

Fig. 4.51 Refolding of MalS by BSA.

A chaperone assay with a 2-fold excess of BSA was performed as a negative control. The assay was done as described in Materials and Methods.

The profile of the Δmac25L56 assays showed an obvious difference in refolding of MalS between Δmac25L56SA and Δmac25L56. Δmac25L56 seems to inhibit refolding of MalS at pH 8.0 and 8.5 at all temperatures because the refolding factor is significantly lower than for BSA (Fig. 4.50 and 4.51). Δmac25L56 has its pH optimum for proteolytic activity between pH 8.0 and 9.0. Therefore, it is likely that it can degrade unfolded MalS with increasing temperature and pH which leads to a decrease in refolding efficiency. Lowering the pH to 7.5 leads to a decrease in proteolytic activity and thus to a relative increase in refolding and MalS activity (Fig. 4.50 pH 7.5). However, this relative increase was never better than refolding in the presence of BSA (Figs. 4.50 and 4.51). In contrast, the refolding factors seem to increase in the presence of Δmac25L56SA when raising the temperature from 20°C to 37°C (Fig. 4.50) while there is little difference when using buffers of pH 7.5 and 8.5. These results suggest that Δmac25L56SA has chaperone activity that is comparable to DegPSA. It might be useful to perform additional chaperone assays at more acidic pH (pH 5-6) to test if Δmac25L56 has chaperone activity under these conditions. However, MalS cannot

refold at acidic pH (Spiess *et al.,* 1999) suggesting that L56-dependent refolding of another substrate such as citrate synthase might be investigated.

4.1.30 Zymogram of the L56 constructs

A zymogram was used to test the activity of pre-purified full-length L56 and L56SA mutant. An advantage of this method is that the protein of interest does not have to be pure. The zymogram contained casein as substrate. After gel electrophoresis, the zymogram was incubated in different buffers (according to the supplier's manual) and stained with Coomassie Blue. Depletion of casein causes clear areas in the zymogram. Full-length L56 was loaded on the zymogram with and without 30 mM DTT to test if disulphide bonds are required for protease activity. Δmac25L56 and Δmac25L56SA were used as reference because it is known from previous assays that they are active or inactive, respectively.

The zymogram indicated that full-length L56 as well as the three degradation bands were able to degrade casein even in the presence of 30 mM DTT (Fig. 4.52). These results implied that L56 does not require disulphide bonds for degradation of casein. Furthermore, they might suggest that L56 does not require autoproteolytic removal of its N-terminus for activation of proteolytic activity because full-length L56 degrades casein in the zymogram (Fig. 4.52). However, it should be noted that the N-terminus is not properly folded in the cytoplasm of *E. coli* and therefore the Kazal-type-inhibitor motif could not inhibit proteolytic activity. As expected, the SA mutants were unable to degrade casein. Furthermore, none of the contaminants showed proteolytic activity (Fig. 4.52). In all cases, it seemed that L56 forms enzymatically active oligomers which immunoreacted with the α-His antibody (data not shown). These oligomers were converted into monomers by adding DTT to the samples, suggesting that they were the consequence of disulphide bond formation.

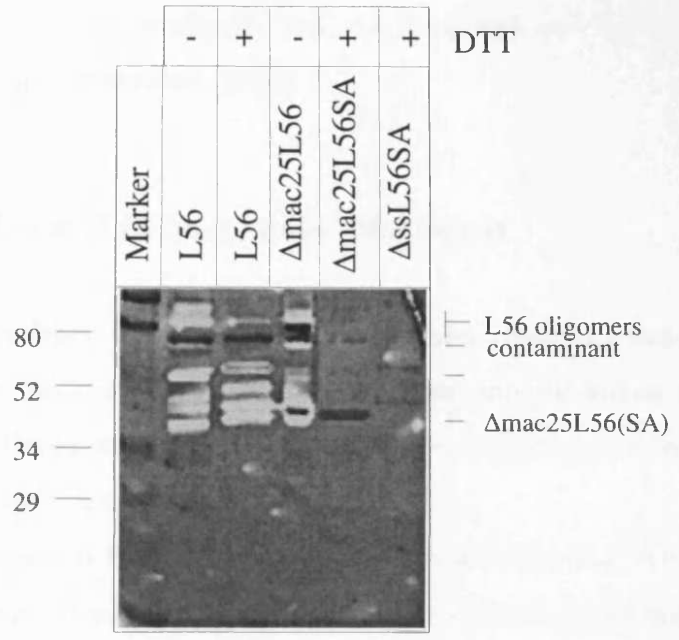

Fig. 4.52 Zymogram of various L56 constructs.

Pre-purified full-length L56 constructs (20-30 µg) and purified Δmac25L56 constructs (20-30 µg) were loaded with or without 30 mM DTT on a zymogram containing casein as substrate for proteases. After gel electrophoresis, the gel was treated as described in Materials and Methods and stained with Coomassie Blue. White bands indicate proteolytic activity. The molecular mass of the marker proteins is shown in kDa.

4.2 Is L56 involved in rheumatoid arthritis?

Hu *et al.* (2000) demonstrated that L56 mRNA and protein levels are increased 7-fold in cartilage of osteoarthritic patients. Osteoarthritis is the most prevalent form of degenerative joint disease. It involves chondrocyte loss and the breakdown of extracellular matrix components. These events lead to a degeneration of cartilage and the eventual deterioration of joint function (Hu *et al.* 1998). The role of L56 in this degenerative process has yet to be elucidated. It would be of interest to determine whether L56 is one of the proteins that instigates disease or alternatively, prevents disease through degradation of unfolded or aggregated proteins. Furthermore, it would be interesting to examine if it is also upregulated in rheumatoid arthritis. Rheumatoid arthritis is an inflammatory disorder that mainly affects the diarthrodial joint. It represents the most common form of inflammatory arthritis (Lee and Weinblatt, 2001).

It results in joint pain, stiffness and swelling and can lead to progressive joint destruction (Lee and Weinblatt, 2001).

4.2.1 Detection of L56 in synovial fibroblasts

Western blot analyses were performed using supernatants from synovial fibroblasts stimulated with various agents, rheumatoid synovial fibroblasts and also rheumatoid synovial fluid. These studies were carried out in collaboration with Dr. Simon Jones` laboratory (Cardiff University).

Unstimulated synovial fibroblasts were washed several times with PBS buffer before TCA precipitation. Western blots with affinity purified polyclonal α-L56 antibody of various amounts of whole cell extracts did not detect L56 (data not shown). As L56 contains a signal sequence, it might be secreted into the ECM. Therefore, supernatants of cultured synovial fibroblasts stimulated with different cytokines were loaded on a SDS- gel to examine whether L56 was secreted. Purified recombinant Δmac25L56 and partially purified recombinant full-length L56 served as controls. The Western blot was incubated with the affinity purified polyclonal α-L56 antibody. L56 was only detectable in the sample of the supernatant of synovial fibroblasts stimulated with normal human serum (NHS) (Fig. 4.53). In addition, the antibody recognised a protein migrating between 60 and 70 kDa in the samples containing NHS and foetal calf serum (FCS) (Fig. 4.53). This band could represent albumin. The Western blot was unable to confirm production of L56, as L56 might be already present in NHS.

To investigate whether L56 was present in NHS, serum from eight healthy volunteers was loaded on a SDS-gel. Again, partially purified recombinant full-length L56 and recombinant Δmac25L56 served as positive controls. The Western blot was incubated

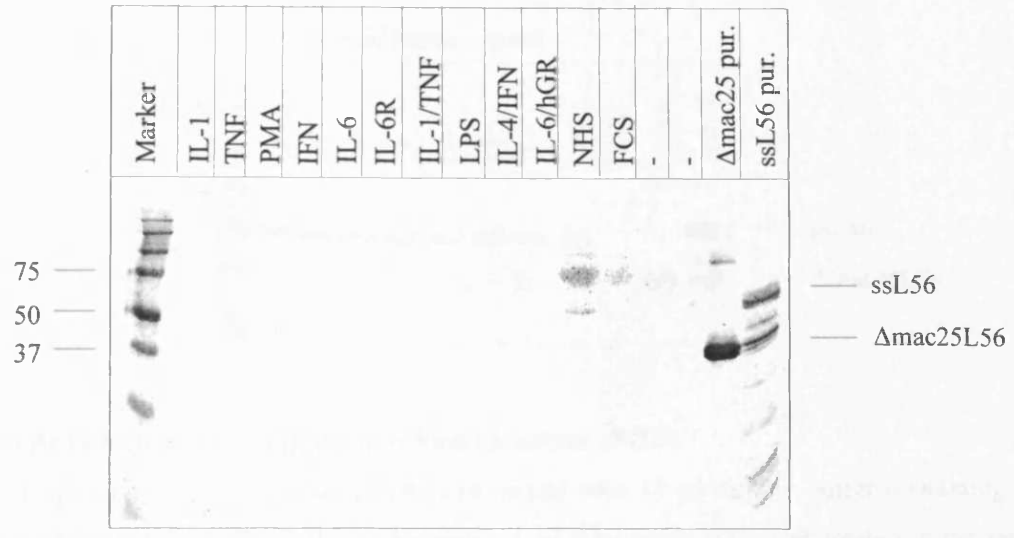

Fig. 4.53 Detection of L56 in the supernatants of stimulated synovial fibroblasts.
Synovial fibroblasts of rheumatoid arthritis patients were cultured and stimulated with different factors as indicated. IL-1 is interleukin 1, TNF is tumour necrosis factorβ, PMA is phorbol myristate acetate, IL-6 is interleukin-6, IL-6R is interleukin-6 receptor, LPS is lipopolysaccharide, NHS is normal human serum and FCS is foetal calf serum. An aliquot (1 µl) of the supernatant was mixed with 19 µl sample buffer containing 30 mM DTT and loaded on a SDS-gel. Partially purified full-length L56 and Δmac25L56 served as controls. The Western blot was incubated with affinity purified polyclonal α-L56 antibody. The molecular mass of relevant marker proteins is shown in kDa.

with the affinity purified polyclonal α-L56 antibody. These data indicated that L56 was present in NHS but not in FCS (Fig. 4.54). Because only 1 µl of the serum was loaded on the gel, the intensity of the L56 bands suggested that there were large amounts of L56 circulating in the blood. Furthermore, there was a faint band in all sera migrating at about 37 kDa that is the same position as Δmac25L56 (Fig. 4.54). This finding suggests that L56 undergoes autoproteolysis where the N-terminal extension is cleaved off because the same band is detectable in recombinant L56 samples as well as in samples after *in vitro* translation (Zumbrunn and Trueb, 1996).

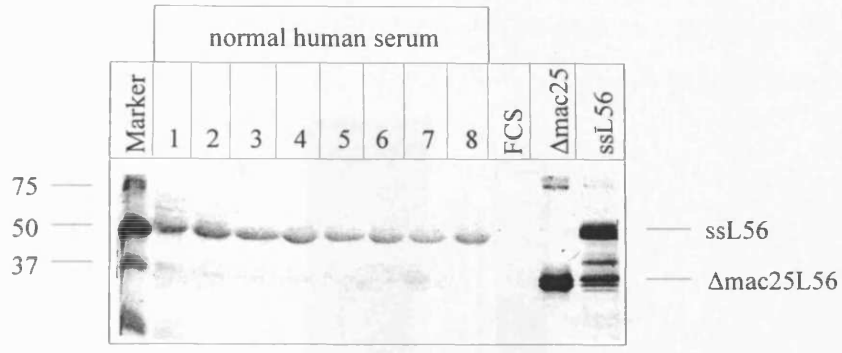

Fig. 4.54 Detection of L56 in normal human serum (NHS).

NHS (1 µl from different persons 1-8) was mixed with 19 µl sample buffer containing 30 mM DTT and loaded on a SDS-gel. Furthermore, 1 µl fetal calf serum was treated in the same way and loaded on the SDS-gel. Partially purified full-length L56 and purified Δmac25L56 served as positive controls. The Western blot was incubated with affinity purified polyclonal α-L56 antibody. The molecular mass of the marker proteins is shown in kDa.

4.2.2 Do white blood cells produce L56?

Blood consists of plasma (~ 50%) containing secreted proteins, white blood cells (< 1%) which are involved in the immune response, red blood cells (~ 45%) which are responsible for the transport of the oxygen and platelets (< 1%) which are involved in blood clotting. To investigate whether normal white blood cells produce L56, blood from healthy volunteers was separated (Fig. 4.55 A) and analysed on a Western blot incubated with the affinity purified polyclonal α-L56 antibody.

The Western blot suggested that white blood cells contain L56 (Fig. 4.55 B). Furthermore, there were some lower molecular weight bands in the white blood cell samples which might represent the autoproteolytic fragments (Fig. 4.55 B). Further experiments would have been required to determine which white blood cells produce L56.

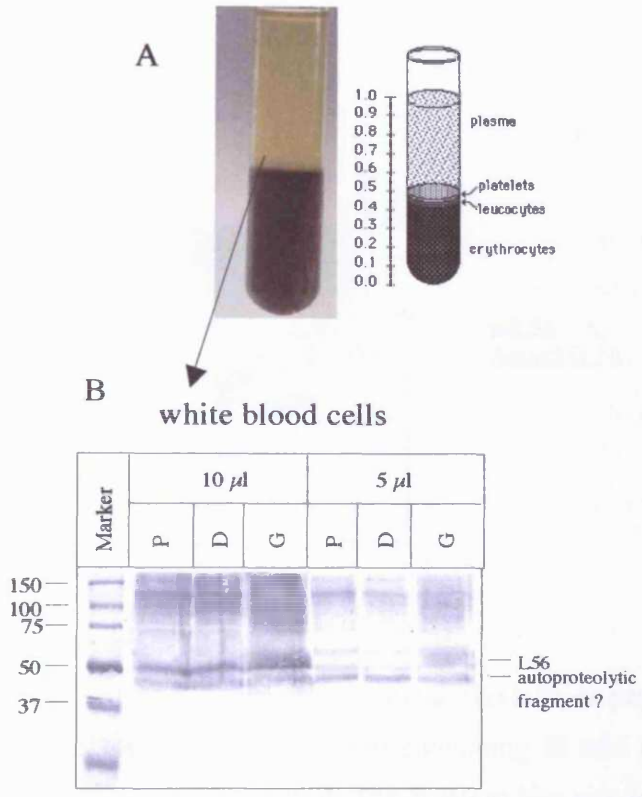

Fig. 4.55 Detection of L56 in white blood cells.

Blood of three volunteers (P, D and G) was separated (A) by Dr. Peter Richards (Dr. Simon Jones' laboratory). The white blood cell fraction was resuspended in TBS and 5 µl and 10 µl were loaded on a SDS-gel (B). The Western blot was incubated with affinity purified polyclonal α-L56 antibody. The molecular mass of the marker proteins is shown in kDa.

4.2.3 Is L56 present in synovial fluid?

A viscous substance known as synovial fluid lubricates normal articular joints. Levels of this fluid are elevated during joint inflammation as found in rheumatoid arthritis. It would be interesting to know whether L56 is present in this fluid. Rheumatoid synovial fluid of an arthritic patient was made available by Dr. Simon Jones (Cardiff University). Two different amounts of synovial fluid were loaded on a SDS-gel. Purified Δmac25L56 served as positive control. The Western blot showed that the gel was overloaded with 10 µl synovial fluid. In the diluted sample (1 µl) bands corresponding

to full-length L56 as well as to the autoproteolytic fragments were detected (Fig. 4.56). Interestingly, the amount of L56 in the synovial fluid appeared to be rather high.

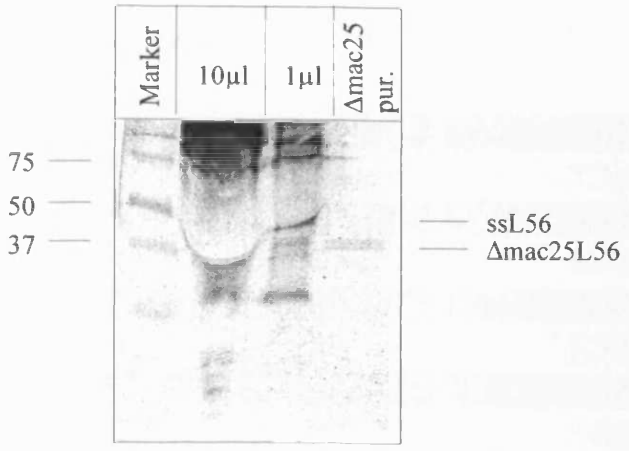

Fig. 4.56 Detection of L56 in synovial fluid.
Two different amounts (1 µl and 10 µl) of synovial fluid from patients suffering from rheumatoid arthritis were mixed with sample buffer containing 30 mM DTT and loaded on a SDS-gel. Purified Δmac25L56 served as control. The Western blot was incubated with affinity purified polyclonal α-L56 antibody. The molecular mass of the marker proteins is shown in kDa.

The rather poor quality of this Western blot was probably due to a very high protein concentration in the synovial fluids used as indicated by the extreme viscosity of the samples. Unfortunately, appropriate dilutions could not be performed because L56 detection required these amounts of material.

4.2.4 pH of osteoarthritic and rheumatoid arthritic fluid

Konttinen *et al.* (2002) reported that the pH in arthritic cartilage was 5.7 compared to 7.1 in cartilage of healthy people. As L56 is only active in a pH range between 7.5 and 9.5, it would be interesting to determine the pH of the synovial fluid because Western blot analysis indicated the presence of significant amounts of L56 in these samples. Therefore, the pH of various synovial fluids of osteoarthritic and rheumatoid arthritis

patients was estimated using pH indicator paper. All fluids had a pH in the range where L56 is active. It can thus be speculated that L56 might be proteolytically active in synovial fluid.

Table 4.4 pH of various synovial fluids.

Fluid number	Sex	OA/RA	pH
1	F	RA	7.7-8.0
2	F	OA	7.5-8.0
3	F	OA	8.0-8.5
4	F	RA	8.0-8.5
5	M	RA	7.5-8.0
6	F	RA	8.0-8.5
7	M	RA	8.0
8	F	RA	8.0-9.0
9	F	RA	7.5-8.0
10	F	OA	8.0-9.0
11	F	OA	8.0-9.0
12	F	OA	8.0
13	F	OA	8.0

Various synovial fluids from osteoarthritis (OA) or rheumatoid arthritis (RA) patients were analysed using pH paper. F = female and M = male.

4.2.5 Are there substrates for L56 in the synovial fluid?

Rheumatoid synovial fluid contains several proteins such as cytokines, matrix proteins and matrix metalloproteinases. It would be interesting to examine if there is a protein in the synovial fluid that can be degraded by L56. To address this question, purified Δmac25L56wt or Δmac25L56SA were incubated with rheumatoid synovial fluid and analysed on a SDS-gel stained with Coomassie Blue.

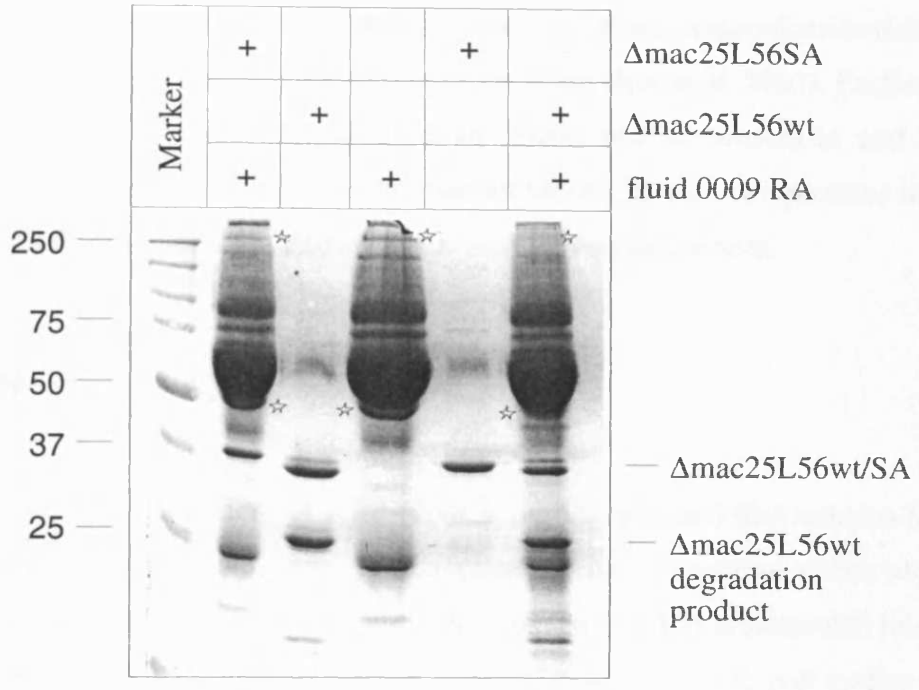

Fig. 4.57 Degradation of proteins in synovial fluid by Δmac25L56.

Synovial fluid of a rheumatoid arthritis patient (3.5 µl) was incubated with 20 µg purified Δmac25L56 or Δmac25L56SA for 3 h at 40°C in 50 mM Tris-HCl buffer pH 8.5, 150 mM NaCl. The final volume of the assay was 50 µl. Aliquots (10 µl) were loaded on a SDS-gel stained with Coomassie Blue. Purified protein and synovial fluid incubated under the same conditions served as controls. The asterisks indicated the proteins that were degraded by L56. The molecular mass of the marker proteins is shown in kDa.

The gel suggested that incubation of synovial fluid with Δmac25L56wt led to degradation of at least two proteins (Fig. 4.57), one that migrated at 50 kDa and a second at 250 kDa. Both proteins were still present in samples containing only the synovial fluid as control as well as samples containing synovial fluid plus inactive Δmac25L56SA. Future identification of these potential substrates might provide initial ideas about the possible role of L56 in this disease. Substrate identification could be achieved via 2-D gel electrophoresis and mass spectrometry or by N-terminal sequencing provided that sufficient quantities of these proteins could be obtained.

In addition to its potential role in arthritis, L56 might be involved in Alzheimer's disease. Gray *et al.* (2000) identified human HtrA2 as an interaction partner of PS1

using a yeast two-hybrid system and PS1 as bait. Also, tissue-distribution analysis showed that L56 is present in high levels in the brain (Nie *et al.* 2003). Furthermore, an in-house two-hybrid system suggested an interaction of presenilin and L56. We therefore explored the possibility of the interaction of L56 with two proteins involved in Alzheimer's disease, C99 and PS1, using *E. coli* as a model system.

4.3 C99

C99 is a C-terminal fragment of APP (containing 99 residues) that remains membrane bound after β-secretase cleavage. It is a substrate for γ-secretase which cleaves this fragment within the membrane. To study cleavage and to find proteins that interact with C99, *E. coli* was used as a model system. The advantage of the *E. coli* system is that no additional human proteins are present and could therefore represent a simple and well defined experimental system.

4.3.1 Cloning of c99 in an expression vector

To produce C99 in *E. coli*, the corresponding DNA fragment was cloned into pCS19. A PCR reaction using a *c99*pCINeo plasmid as template and two primers, one that annealed at the 5 ´end of the gene and introduced an *NcoI* site, and a second primer that annealed at the 3 ´end of the gene and introduced a *BglII* site was performed. The PCR product was cloned into pCS19 and the new plasmid was called pSG6 (Fig. 4.58).

4.3.2 Expression of c99 in E. coli

C99 production in *E. coli* was tested in strains DHB4 and KU98 which lacks the periplasmic DegP protease. Initially, induction was tested at 37°C with 10 μM IPTG for 4 h or overnight. As a control, the strains containing the "empty" vector (pCS19) were treated in the same way. Because C99 was engineered to contain a C-terminal His Tag, an α-His antibody was used for detection. Expression in DHB4 was almost undetectable

(Fig. 4.59). In contrast, after 4 h induction in KU98 a strong band migrating at about 21 kDa was detected (Fig. 4.59). This result indicated that C99 might be localised in the membrane because only then can it be degraded by the periplasmic protease DegP in DHB4.

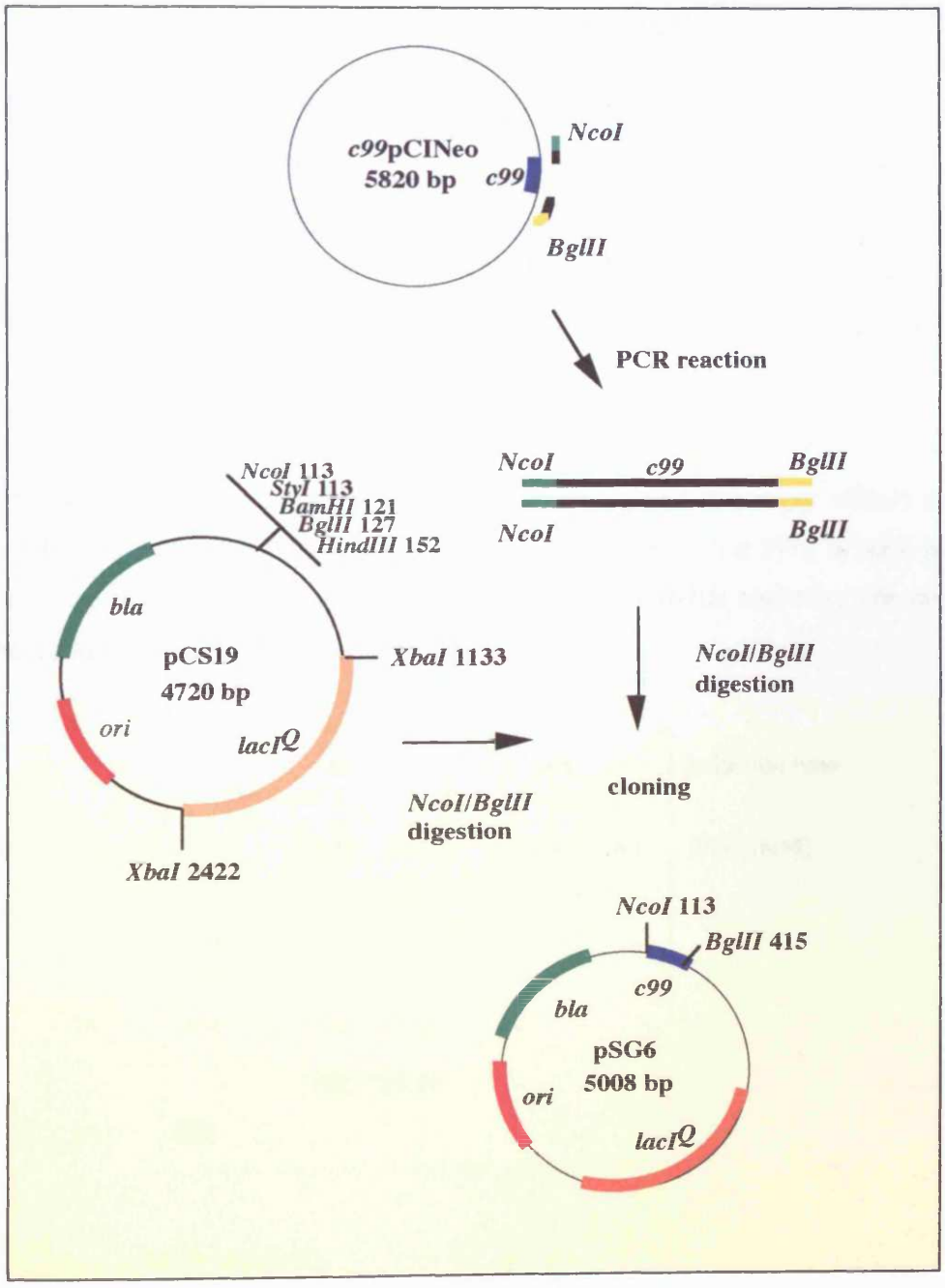

Fig. 4.58 Cloning of *c99* into an *E. coli* expression vector.

p*c99*pCINeo served as template. pCS19 was used as vector. All cloning steps and relevant restriction enzymes are shown.

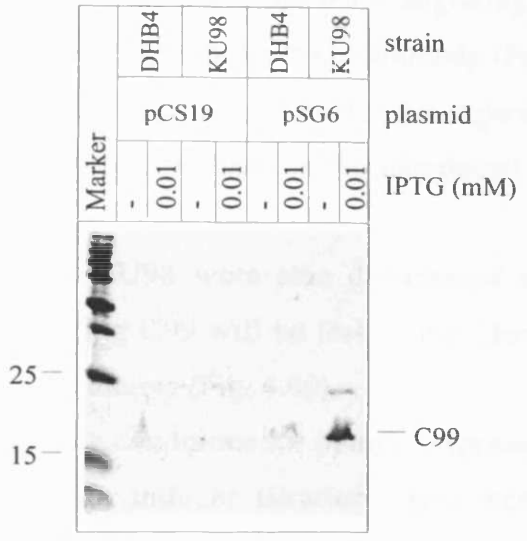

Fig. 4.59 Expression of *c99* in *E. coli* strains.

A five millilitre culture of strain KU98 and DHB4 carrying pCS19 (empty vector) or pSG6 (*c99*) was induced at OD_{578} = 0.5 with 10 µM IPTG and grown for 4 h at 37°C in NZA medium. The Western blot of whole cell extracts was incubated with the α-His antibody. The molecular mass of the marker proteins is shown in kDa.

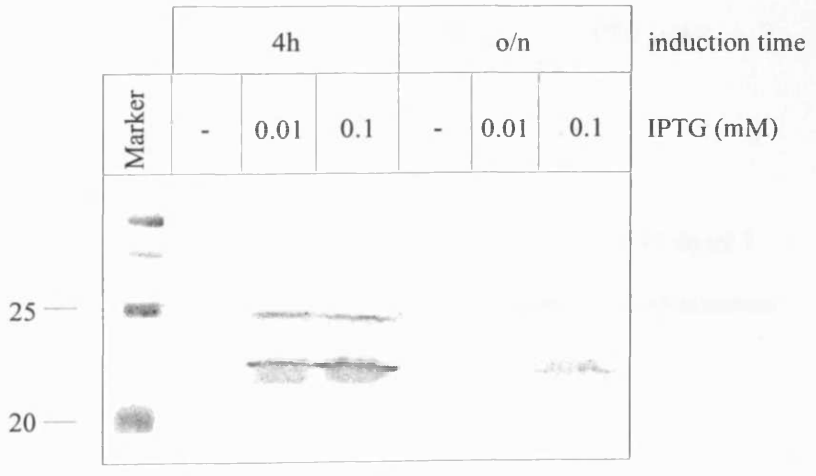

Fig. 4.60 Expression of *c99* at 28°C.

A five millilitre culture of strain KU98 carrying pSG6 was induced at OD_{578} = 0.4 with 10 or 100 µM IPTG and grown for 4 h or overnight at 28°C. The medium used was NZA. The Western blot of whole cell extracts was incubated with the α-C99 antibody. The molecular mass of the marker proteins is shown in kDa.

C99 was not detected in both strains after overnight induction (data not shown). Interestingly, C99 did not migrate at the expected molecular mass of 12 kDa in this gel system. Furthermore, there was an additional band migrating at about 24 kDa in the KU98 samples that immunoreacted with the α-His antibody (Fig. 4.59). An explanation for this band could be that C99 forms oligomers. As expected, strains carrying the "empty" vector showed no detectable band in the uninduced and induced lanes (Fig. 4.59).

Expression levels of *c99* in KU98 were also determined at 28°C because at low temperature, proteases degrading C99 will be less active. However, C99 was still not stably expressed in overnight cultures (Fig. 4.60).

Subsequently, the most suitable conditions for optimal expression in strain KU98 were determined by performing an inducer titration experiment using various IPTG concentrations (10, 20, 30, 40, 50, 70, 80, 100 μM) and low temperature (28°C). Based on Western blot analysis, it was concluded that induction with 10 μM IPTG is sufficient because no increase in protein level at higher IPTG concentrations was detected (Fig. 4.61). Again an additional higher molecular weight band is visible in all induced samples.

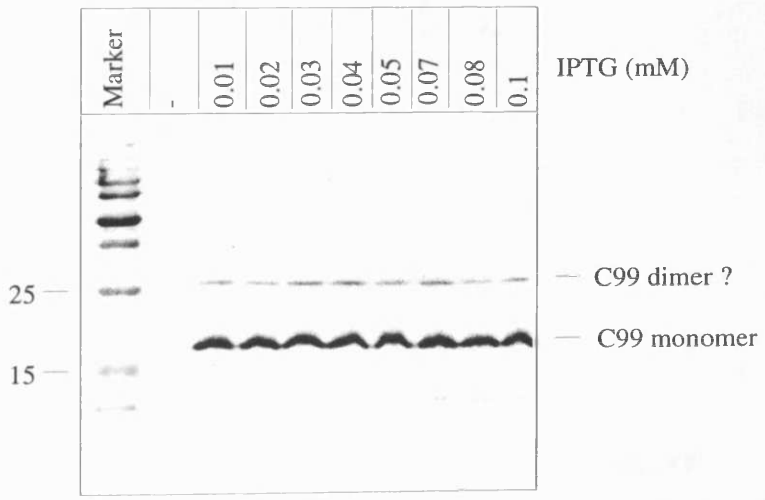

Fig. 4.61 Determination of the inducer concentration for *c99* expression in *E. coli*.

A five millilitre culture of strain KU98 carrying pSG6 was induced at OD_{578} = 0.5 with various IPTG concentrations (10, 20, 30, 40, 50, 70, 80, 100 μM). The cells were grown for 4 h at 28°C in NZA medium. The Western blot of whole cell extracts was incubated with the α-His antibody. The molecular mass of the marker proteins is shown in kDa.

4.3.3 Is C99 localised in the membrane?

To exclude the possibility that recombinant C99 is exclusively present in inclusion bodies, membrane fractions were prepared as described in Materials and Methods. To initially separate cell debris and aggregates from the membrane fraction, the lysed cell extract was subjected to centrifugation. The pellet contained the aggregates and the supernatant contained the membrane fraction. To sediment membranes, the supernatant was subsequently ultracentrifuged (described in section 3.7.10.2). Whole cell extracts, as well as the supernatant and pellet fractions of the ultracentrifugation, were analysed for the presence of C99 using Western blots. These data indicated that the majority of the overproduced protein was found in the membrane (pellet) fraction after ultracentrifugation of cleared cell lysate (Fig. 4.62). The higher molecular weight band which was initially detected in whole cell extracts, was also present in membrane fractions, suggesting that C99 might form oligomers in the cytoplasmic membrane (Fig. 4.62).

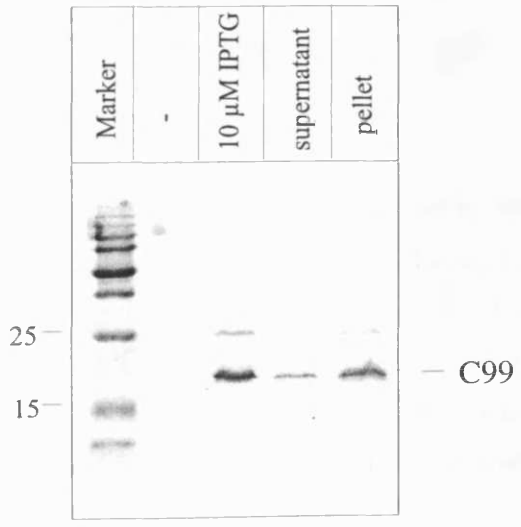

Fig. 4.62 Membrane preparation of *E. coli* strain KU98 expressing *c99*.
A one litre culture of strain KU98 carrying pSG6 was induced with 10 µM IPTG and grown for 4 h in NZA medium. Membranes were prepared as described in Materials and Methods. The Western blot was incubated with α-His antibody. The lanes following the marker proteins (shown in kDa) are whole cell extract uninduced (-) and induced (10µM IPTG) followed by supernatant after ultracentrifugation (soluble protein) and the relevant pellet fraction (membranes).

4.3.4 Solubilisation experiments with C99

The yield of a purified membrane protein is in part dependent on the efficiency of solubilisation. Therefore, various detergents were tested to determine the best conditions for solubilisation of C99. Cytoplasmic membrane fractions containing C99 were subjected to various detergents (DDM, Brij35, CHAPSO and SDS) in a final concentration of 1%. After ultracentrifugation, the supernatant (containing solubilised membrane proteins) was TCA precipitated and loaded on a 15% SDS-gel.

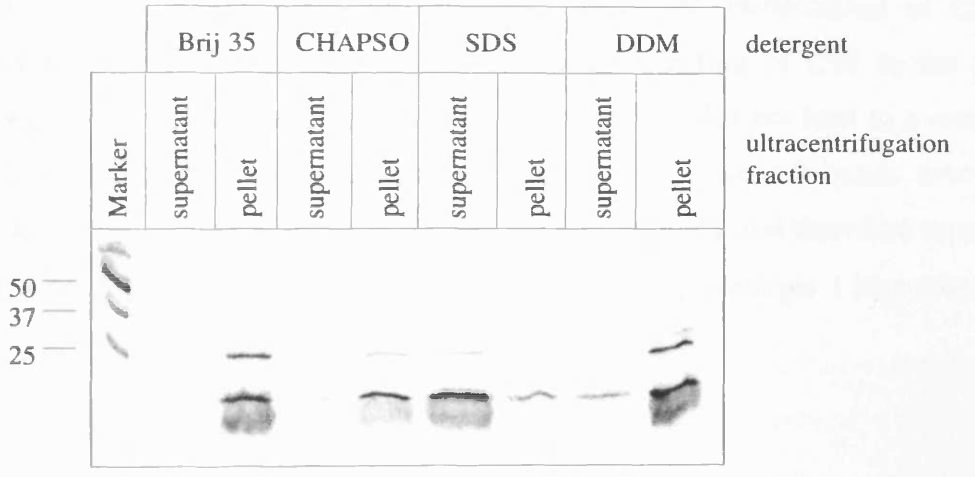

Fig. 4.63 Solubilisation of C99 by various detergents probed by Western blotting.
Membranes of a one litre culture of strain KU98 overproducing C99 were resuspended in 50 mM Tris-HCl buffer pH 8.0, 300 mM NaCl and solubilised for 2 h with SDS, DDM, CHAPSO or Brij35 on ice or at RT (SDS). All detergents were used in a final concentration of 1%. After an ultracentrifugation step at 40000 rpm for 30 min, the supernatants were TCA precipitated and loaded on a 15% SDS-gel. The Western blot was incubated with the α-C99 antibody. The molecular mass of the marker proteins is shown in kDa.

Western blotting with α-C99 antibody indicated that SDS is the most efficient detergent for solubilisation, yielding about 90% of soluble C99 (Fig. 4.63). Brij35 and CHAPSO showed no detectable C99 band in the solubilised (supernatant) fraction. A small amount of C99 was solubilised with DDM but the majority of the protein remained membrane-bound (Fig. 4.63). Interestingly, the higher molecular weight band was also

solubilised. Therefore, SDS was used for solubilisation followed by detergent exchange on the NiNTA column in the following purification experiments.

4.3.5 Purification of C99 with a NiNTA column

Purified C99 could be used in protease assays with purified L56 to test if it is a substrate. Also, C99 is a substrate of γ-secretase and cleavage of C99 produces Aβ peptides which aggregate and can form the senile plaques in brains of AD patients. As it has been suggested that PS1 contributes to γ-secretase activity, this hypothesis could be tested in protease assays using purified PS1 and C99. Purification of C99 was performed as described in Materials and Methods. Binding of C99 to the NiNTA column was efficient and washing with 30 mM imidazole did not lead to a removal of C99 (Fig. 4.64). After elution, the protein was pure because all bands detected by Coomassie staining immunoreacted with the α-C99 antibody and therefore represented C99 (Fig. 4.64 A and B). Average yields were 0.75 mg of protein per 1 litre culture.

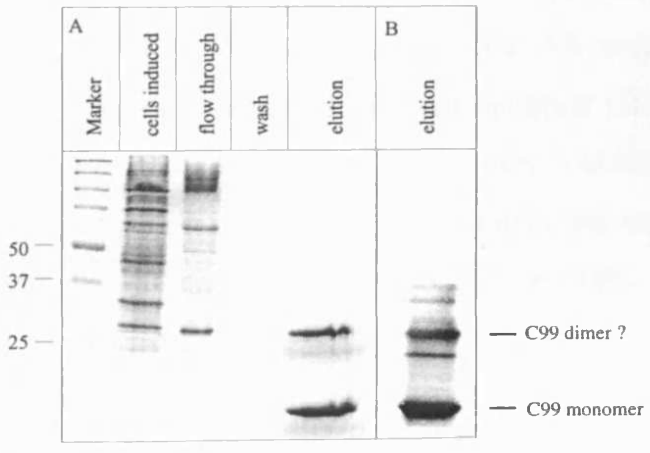

Fig. 4.64 NiNTA chromatography of C99.

Membranes from a 3 litre culture of strain KU98 overproducing C99 were solubilised for 2 h at RT with 1% SDS. Solubilised protein was loaded on a NiNTA column (flow rate of 0.3 ml/min). The column was washed with 50 mM Tris-HCl buffer pH 8.0, 300 mM NaCl, 0.25% SDS (wash), followed by further washing steps using 50 mM Tris-HCl buffer pH 8.0, 300 mM NaCl, 0.05% DDM to change the detergent and 50 mM Tris-HCl buffer pH 8.0, 300 mM NaCl, 0.05% DDM, 30 mM imidazole. Protein was eluted with 50 mM Tris-HCl buffer pH 8.0, 300 mM NaCl, 0.05% DDM, 500 mM imidazole. A) Coomassie stained SDS-gel. B) Western blot

of the elution fraction incubated with the α-C99 antibody. The molecular mass of the marker proteins is shown in kDa.

4.3.6 Glycine exchanges

C99 may form oligomers in *E. coli* membranes that are SDS and heat stable. Glycophorin A (GpA), a human transmembrane protein, shows similar SDS resistant dimers. In GpA, a Gly $(X)_3$ Gly motif is responsible for dimerisation in conjunction with a few surrounding residues (Lemmon *et al.*, 1992). C99 contains three Gly $(X)_3$ Gly motifs in the Aβ sequence plus one Gly $(X)_3$ Ala motif which can also be responsible for dimerisation (Orzaez *et al.*, 2000). Because these motifs occur in the Aβ sequence, there could be a connection between the oligomerisation of C99 observed in *E. coli* and aggregation of Aβ in human brains. To investigate if the Gly $(X)_3$ Gly motifs play a role in oligomerisation and aggregation of C99, some of the Gly residues were exchanged to remove the potential dimerisation motifs (Fig. 4.65). Serine was used for the exchange because it is an uncharged amino acid that is often found in transmembrane segments. Furthermore, a mutant form of APP was discovered in human brains that introduces a new Gly $(X)_3$ Gly motif in the Aβ sequence by exchanging $alanine_{42}$ to glycine. The mutation is called Flemish mutation (Hendricks *et al.*, 1992) and showed a higher aggregation rate of Aβ in early onset Alzheimer's disease patients (Demeester *et al.*, 2001). This mutation would be an interesting construct to investigate if faster aggregation is based on this additional dimerisation motif.

4.3.7 Generation of the C99 mutants

Site-directed oligomutagenesis was used to exchange the glycine residues and the alanine residue (Ala42). Primers annealing at the region of interest introduced new restriction sites to monitor the exchange using restriction digestion (Table 4.5).

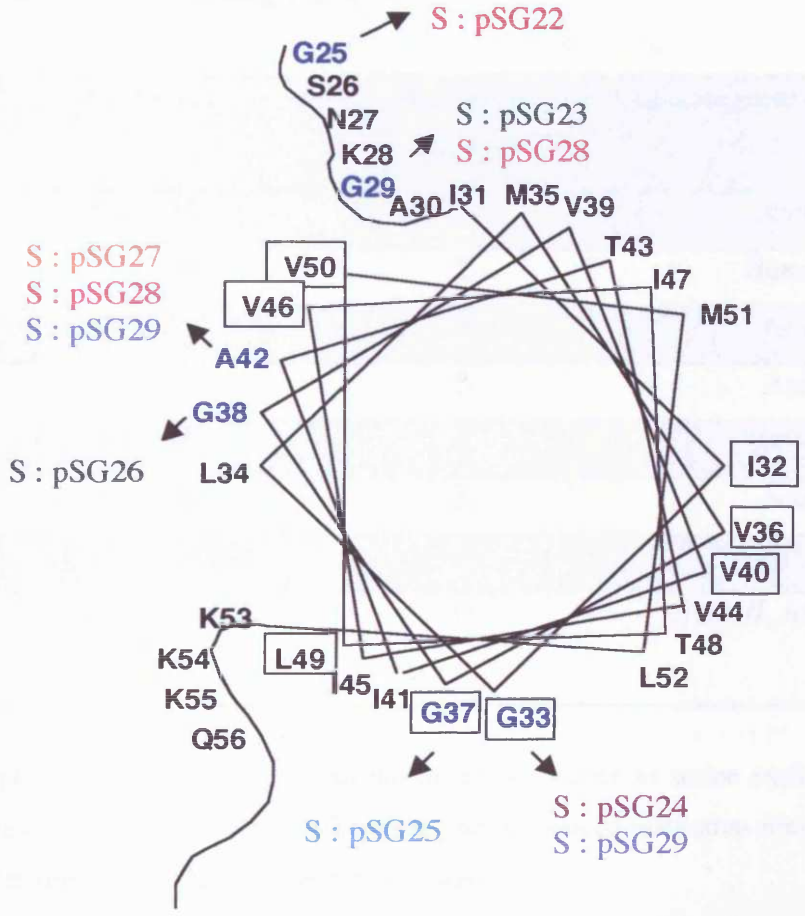

Fig. 4.65 Helical wheel of the putative transmembrane domain of C99.

A periodicity of 3.9 residues per turn was assumed and the glycine residues and one alanine residue, which may represent dimerisation motifs, are coloured blue. Residues that are localised at similar positions, as the residues sensitive for dimerisation in glycophorin A (GpA), are boxed. Names of the generated plasmids are shown.

4.3.8 Expression of the mutant C99 forms

The mutant C99 forms containing 0-4 dimerisation motifs were produced in *E. coli* strain KU98 to test if it is possible to detect a shift from dimer to monomer depending on the number of dimerisation motifs present.

Table 4.5 Glycine to serine exchanges in C99.

Plasmid	Exchange	Number of motifs	Introduced restriction site
pSG22	Gly25S	3	*AatII*
pSG23	Gly29S	2	*BamHI*
pSG24	Gly33S	2	*KasI*
pSG25	Gly37S	3	*AseI*
pSG26	Gly38S	3	*BamHI*
pSG27	Ala42S	3	*ScaI*
pSG28	Gly29S; Ala42S	1	*BamHI, ScaI*
pSG32	Gly29S; Gly37S; Ala42S	0	*BamHI, AseI, ScaI*

Names of the plasmids encoding C99 with the different glycine to serine exchanges and the alanine to serine exchange are shown. Furthermore, the introduced restriction sites as well as the number of the remaining Gly $(X)_3$ Gly motifs are listed.

All plasmids were transformed into strain KU98. Cells were induced at $OD_{578} = 0.4$ with 10 μM IPTG and grown further for 4 h at 28°C. To monitor expression, a Western blot analysis was carried out using α-C99 and α-Aβ40 (2) (see Table 3.3) antibodies. When compared to wtC99, each mutant protein showed the same ratio of monomer to dimer (Fig. 4.66). Initial interpretation of these data suggests that the proposed dimerisation motifs are not involved in oligomerisation of C99. However, in the triple mutant, Gly33 and Gly38 might represent a Gly $(X)_4$ Gly motif that might promote dimerisation. Also, mutants carrying the Ala42 to Ser exchange showed an additional band migrating right below the monomer band (Fig. 4.66). Because the α-Aβ40 antibody (2) used (see Table 3.3) recognizes the monomer at residue 40, it seems that these C99 derivatives are lacking the C-terminus because Western blotting with only the α-C99 antibody did not show this band (data not shown). It is thus possible that these mutants are more sensitive to degradation.

Further experiments with mutants lacking all dimerisation motifs and all glycine residues should be carried out. In addition, it could be helpful to purify the mutant

proteins and incubate them under various conditions in an attempt to detect C99 monomer formation corresponding to the number of dimerisation motifs.

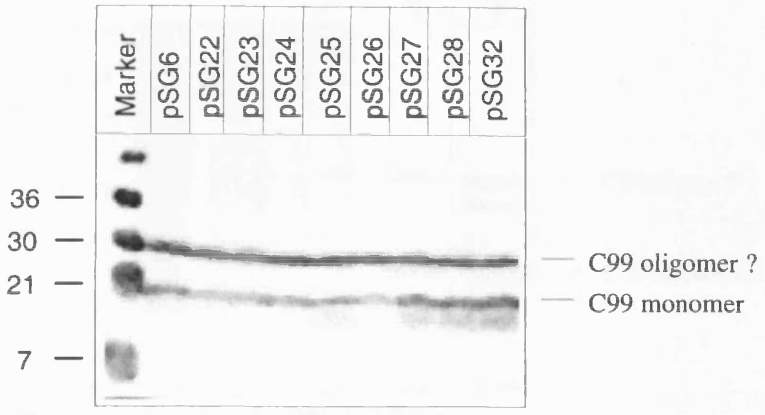

Fig. 4.66 Overproduction of the C99 mutants.

A five millilitre culture of strain KU98 overproducing one of the mutant C99 proteins was induced with 50 µM IPTG and grown for 4 h at 28°C. The Western blot was incubated with the α-C99 antibody and α-Aβ40 antibody (2) (described in Table 3.3). The molecular mass of the marker proteins is shown in kDa.

4.3.9 Purification of C99Gly37Ser and C99Gly29Ser Gly37Ser Ala42Ser.

As discussed above, purification of the C99 glycine exchange mutants would be useful for determining the contribution of the glycine residues in oligomerisation of C99. Therefore, two of the mutants, one with one glycine residue exchanged to serine and another one with two glycine residues and the alanine residue exchanged to serine, were purified following the procedure established for wtC99.

The Coomassie-stained gels showed that the C99 mutant proteins are pure after NiNTA chromatography and no visible difference in the ratio of monomer to oligomers was detected in the elution fractions (Fig. 4.67 and Fig. 4.68).

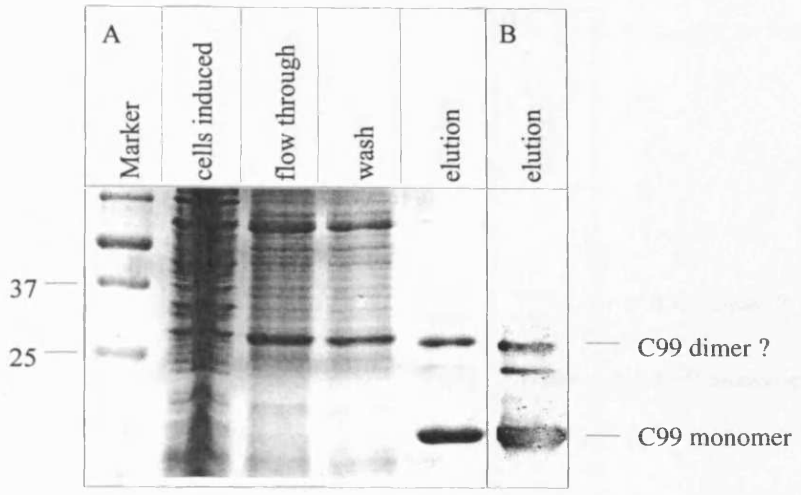

Fig. 4.67 NiNTA chromatography of C99Gly37Ser.

Membranes were prepared from a 3 litre culture of strain KU98 overproducing C99Gly37Ser and solubilised for 2 h at RT with 1% SDS. Solubilised protein was loaded on a NiNTA column with a flow rate of 0.3 ml/min. The column was washed with three buffers. Initially, with 50 mM Tris-HCl buffer pH 8.0, 300 mM NaCl, 0.25% SDS (wash), followed by 50 mM Tris-HCl buffer pH 8.0, 300 mM NaCl, 0.05% DDM to change the detergent and finally with 50 mM Tris-HCl buffer pH 8.0, 300 mM NaCl, 0.05% DDM, 30 mM imidazole to remove weakly bound proteins. Protein was eluted with 50 mM Tris-HCl buffer pH 8.0, 300 mM NaCl, 0.05% DDM, 500 mM imidazole. A) Coomassie stained SDS-gel. B) Western blot of the elution fraction incubated with the α-C99 antibody. The molecular mass of the marker proteins is shown in kDa.

There is evidence that wtC99 oligomerisation increases at acidic pH (pH4.5) (data not shown). If the Gly $(X)_3$ Gly motifs were involved in oligomerisation, the mutant proteins should not oligomerise to the same extend as wtC99. However, incubation of the C99 mutant proteins at acidic pH led to the same pattern of bands as wtC99, suggesting that the introduced mutations did not affect oligomerisation (data not shown). Furthermore, gel filtration experiments with wtC99 and C99Gly29Ser Gly37Ser Gly42Ser did not show any difference in peak pattern (data not shown). Further experiments have to be carried out to investigate if the Gly $(X)_3$ Gly motif is involved in the oligomerisation of C99.

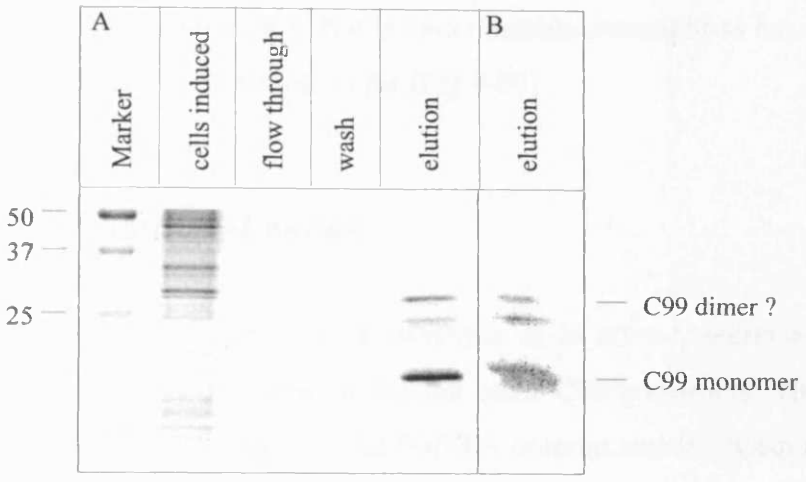

Fig. 4.68 NiNTA chromatography of C99Gly29Ser Gly37Ser Gly42Ser.
Purification was carried out as described in Fig. 4.67. A) Coomassie stained SDS-gel. B) Western blot of the elution fraction incubated with the α-C99 antibody. The molecular mass of the marker proteins is shown in kDa.

4.3.10 Generation of a mutant form of C99 (London mutation) involved in AD

About 90 % of the FAD linked mutations were found in the genes encoding PS1 and PS2. In addition, there are several missense mutations identified in the *app* gene which co-segregate with FAD. Although these mutations are very rare, they all lead to an increase in Aβ42 production. One of these FAD linked mutations (Val717 to Ile) is called the London mutation. This mutant APP is often used for γ-secretase assays because it increases production of Aβ42 and simplifies detection of this fragment. Purified C99London would be a useful substrate for γ-secretase assays to test if purified PS1Δ9, the constitutively active mutant form of PS1, is able to cleave C99. Site-directed oligomutagenesis was used to generate this mutant (pSG31).

4.3.11 Expression of c99London in strain KU98

E. coli strain KU98 carrying pSG31 was induced with 10 μM IPTG and grown further for 4 h or overnight at 28°C. Samples were taken and analysed on a Western blot incubated with the α-C99 antibody. The Western blot indicated that C99London is

produced after 4 h induction at 28°C but is also unstable overnight as has been detected for the other C99 constructs analysed so far (Fig 4.69).

4.3.12 Purification of C99London

C99London was purified to serve as a substrate in *in vitro* γ-secretase assays. The purification procedure was the same as for the other C99 constructs. The Coomassie-stained gel showed that C99 bound to the NiNTA column and the washing step eluted weakly bound proteins (Fig. 4.70). After elution, the protein was pure (Fig. 4.70) and could thus be used in γ-secretase assays.

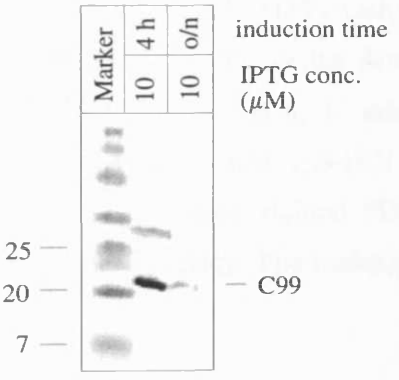

Fig. 4.69 Expression of *c99London*.
A five millilitre culture of strain KU98 overproducing C99London was induced with 10 μM IPTG and grown for 4 h or overnight at 28°C. The Western blot of whole cell extracts was incubated with the α-C99 antibody. The molecular mass of the marker proteins is shown in kDa.

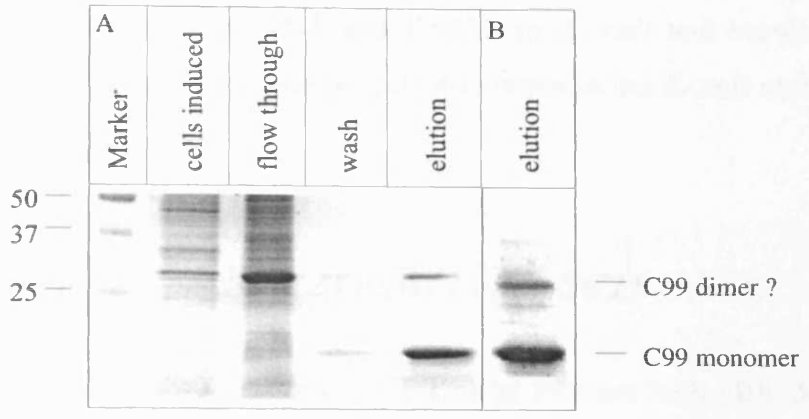

Fig. 4.70 NiNTA chromatography of C99London (Val45Ile)

Membranes were prepared from a 3 litre culture of strain KU98 overproducing C99London and solubilised for 2 h at RT with 1% SDS. The solubilised protein was loaded on a NiNTA column with a flow rate of 0.3 ml/min. The column was washed with three buffers. Initially, with 50 mM Tris-HCl buffer pH 8.0, 300 mM NaCl, 0.25% SDS (wash), followed by 50 mM Tris-HCl buffer pH 8.0, 300 mM NaCl, 0.05% DDM to change the detergent and finally with 50 mM Tris-HCl buffer pH 8.0, 300 mM NaCl, 0.05% DDM, 30 mM imidazole to remove weakly bound proteins. The protein was eluted with 50 mM Tris-HCl buffer pH 8.0, 300 mM NaCl, 0.05% DDM, 500 mM imidazole. A) Coomassie stained SDS-gel. B) Western blot of the elution fraction incubated with the α-C99 antibody. The molecular mass of the marker proteins is shown in kDa.

4.4 C99 and PS1

Presenilin is another important protein involved in the onset of Alzheimer's disease. It has eight transmembrane domains and two highly conserved aspartates in transmembrane segments 6 and 7. There is strong genetic and indirect biochemical evidence that presenilin could be the unknown γ-secretase cleaving C99. PS1Δ9 is one of the mutant forms identified in FAD. It lacks a part of the loop region between transmembrane domain 6 and 7 and is thought to be constitutively active. Co-overproduction of PS1 together with C99 would be an initial experiment to investigate an interaction of these proteins or cleavage of C99.

Mona Harnasch overproduced PS1 and PS1Δ9 in *E. coli* and topological studies confirmed that they should have the proper orientation in the *E. coli* membrane (thesis Mona Harnasch, 2003).

4.4.1 Cloning and expression of pSG12 and pSG21

The plasmids encoding C99 and the two forms of PS1 are both pBR derivatives and have the same origin of replication and are thus incompatible for co-expression experiments. Therefore, pSG6 and pSG14, another plasmid encoding C99 without a His Tag, were cleaved to remove the pBR origin and the ampicillin resistance. Subsequently, the origin of pACYC184 and the gene conferring chloramphenicol resistance were cloned into these vectors. The new plasmids were called pSG12 and pSG21 (Fig. 4.71).

Production of C99 from the newly generated plasmids was tested before using for co-expression studies. The Western blot indicated that each plasmid produced C99 in approximately the same amount and were thus suitable for co-expression studies (data not shown).

4.4.2 Co-overproduction of C99 and PS1

For co-expression experiments, KU98 overproducing *c99* and *ps1* or *ps1Δ9* was grown for 4 h or overnight at 28°C. Samples were loaded on a SDS-gel and Western blots were performed with either α-C99 and α-Aβ40 (1) or α-PS1 antibodies (see Table 3.3). Presenilin constructs had exactly the same amino acid composition as human PS1. This might be important because PS1 is very sensitive to changes in the C-terminal amino acid sequence. Changing only one amino acid in the C-terminus prevents formation of the γ-secretase complex in eukaryotes (Tomita *et al.*, 2001).

The Western blot showed that C99 is stabilised during overnight expression by co-expression of *ps1* and *ps1Δ9* (Fig. 4.72). This result suggested that the proteins interact and PS1 protects C99 from degradation in *E. coli*. However, Aβ40 formation was not detected. Perhaps the lipid composition of *E. coli* membranes interferes with γ-secretase

activity. Another possibility is that PS1 alone does not confer γ-secretase activity. Recent studies suggested that three other proteins (nicastrin, APH1 and PEN-2) are required for γ-secretase cleavage (Francis *et al.*, 2002).

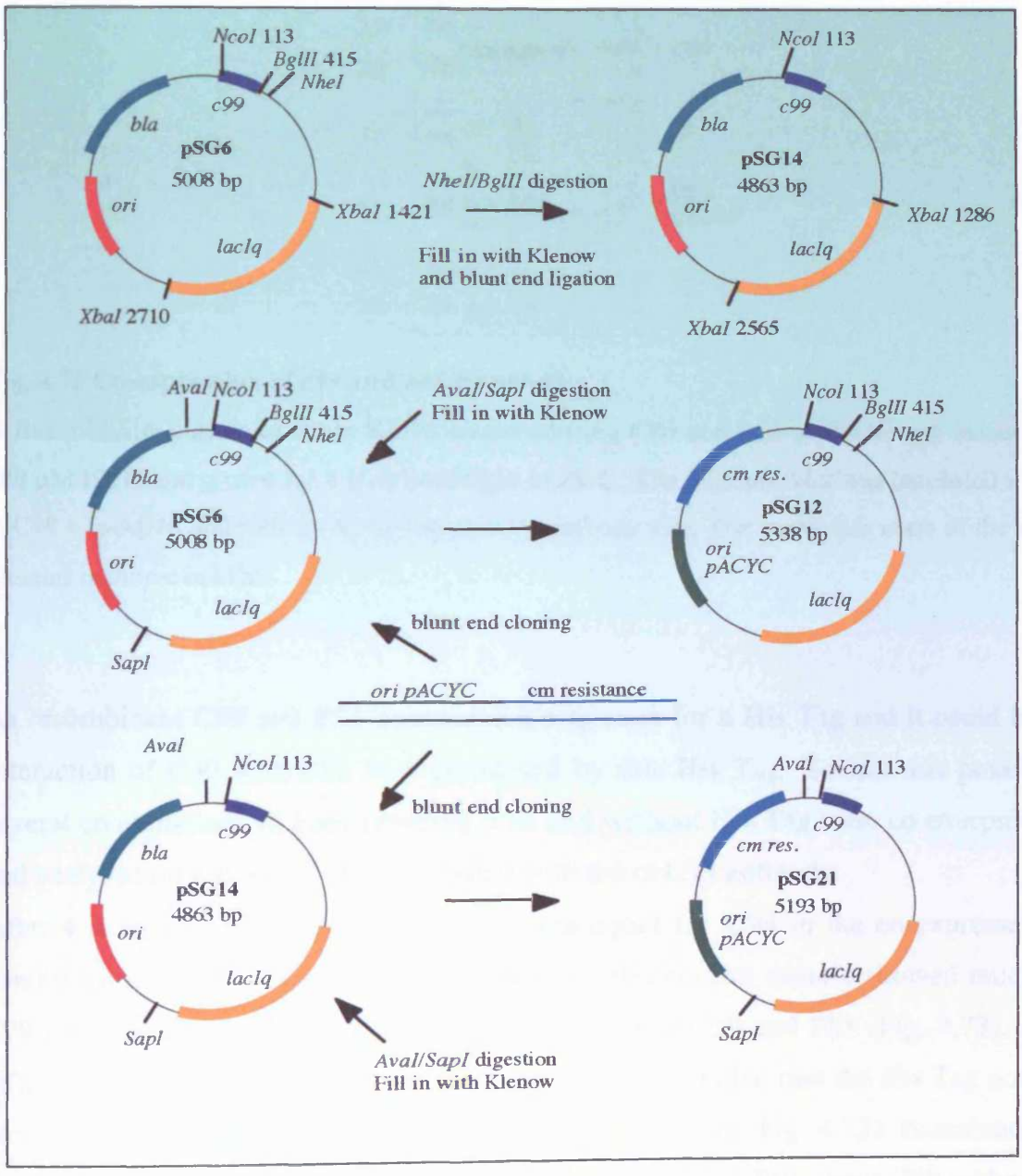

Fig. 4.71 Cloning of pSG12, pSG14 and pSG21.

pSG14 encodes *c99* without a His Tag. Plasmids pSG12 and pSG21 contain the chloramphenicol resistance and the origin of replication from pACYC184. *ori* = origin of replication; cm = chloramphenicol; bla = gene encoding for the ampicillin resistance protein. All cloning steps and relevant restriction enzymes are shown.

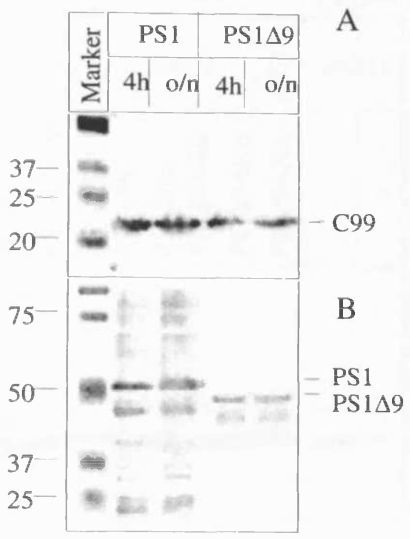

Fig. 4.72 Co-expression of *c99* and *ps1* or *ps1Δ9*.

A five millilitre culture of strain KU98 overproducing C99 and PS1 or PSIΔ9 was induced with 100 µM IPTG and grown for 4 h or overnight at 28°C. The Western blot was incubated with the α-C99 + α-Aβ40 antibodies (A) or the α-PS1 antibody (B). The molecular mass of the marker proteins is shown in kDa.

As recombinant C99 and PS1 contained a sequence for a His Tag and it could be that interaction of C99 with PS1 was promoted by this His Tag. To test this possibility, several combinations of both proteins with and without His Tag were co-overproduced and analysed on a Western blot incubated with the α-C99 antibody.

After 4 h induction, the protein levels were equal for C99 in the co-expressed and control samples but, after overnight induction, the control sample showed much less C99 compared to samples from strains co-producing C99 and PS1 (Fig. 4.73). As no difference in C99 levels was detected, it could be concluded that the His Tag does not promote stabilisation and thus protein-protein interaction (Fig. 4.73). Examination of the C99 bands indicated that C99 with His Tag migrates slightly above C99 without His Tag (Fig. 4.73).

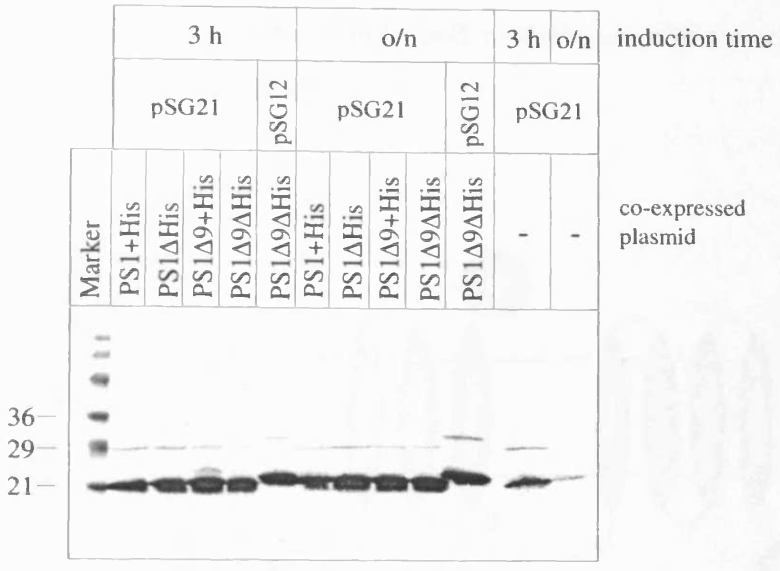

Fig. 4.73 Co-overproduction of C99 and PS1 or PS1Δ9 with and without His Tag.

A five millilitre culture of *E. coli* strain KU98 overexpressing pSG12 (*c99* with His Tag) or pSG21 (*c99* without His Tag) together with pMH12 (*ps1* with His Tag), pMH14 (*ps1* without His Tag) or pMH13 (*ps1Δ9* with His Tag), pMH15 (*ps1Δ9* without His Tag). The cells were induced with 100 µM IPTG and grown for 3 h or overnight at 28°C. Whole cell extracts were subjected to Western blotting using the α-C99 antibody. The molecular mass of the marker proteins is shown in kDa.

4.4.3 Co-expression of c99 and ps1 fragments

As C99 and PS1 seem to interact during recombinant production in *E. coli*, it would be interesting to use this system to determine the binding site for C99. Therefore, C99 was co-overproduced with various C-terminal truncations of PS1 fused to alkaline phosphatase. Mona Harnasch generated these PS1 constructs for topological studies (thesis Mona Harnasch, 2003). The constructs contained increasing numbers of transmembrane segments of PS1 (Fig. 4.74). The rationale for this experiment was that recombinant C99 is not produced during overnight incubation. Coexpression of PS1 constructs was expected to increase C99 levels when these PS1 fragments were large enough to contain an interaction site for C99.

Plasmids encoding the various PS1 fragments were transformed separately into KU98 containing pSG12 (*c99* with His tag). Cells were grown under inducing conditions for 3

h (C99 without PS1) and overnight. Whole cell extracts were analysed on a Western blot incubated with an α-C99 antibody.

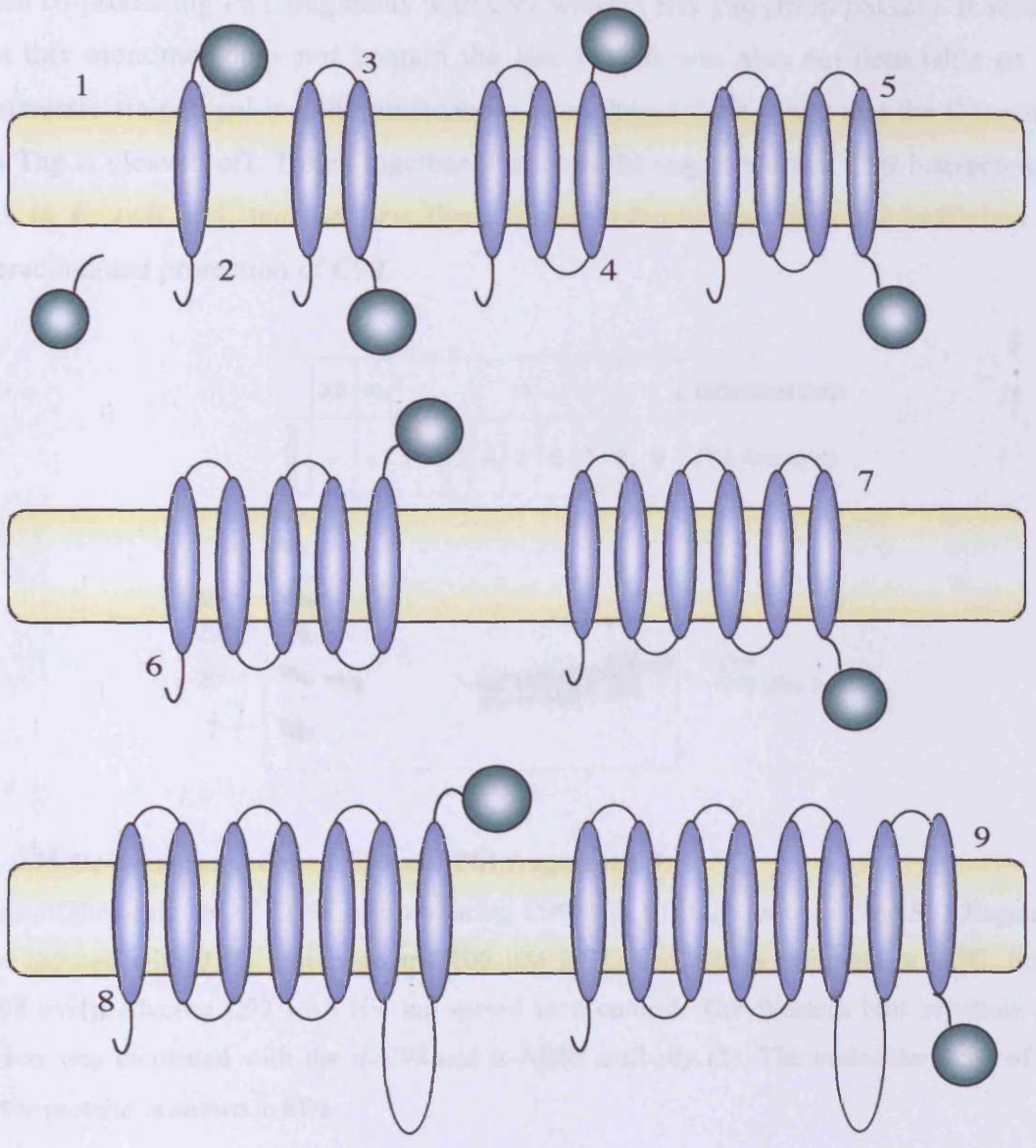

Fig. 4.74 Schematic representation of the C-terminal truncations of PS1 fused to alkaline phosphatase (AP). Alkaline phosphatase (coloured in green) was fused to PS1 after each transmembrane domain (thesis Mona Harnasch, 2003). The constructs were called 1-9.

Stabilisation during overnight induction occurred with fragment 4 that contained the first three transmembrane segments of PS1, suggesting a binding site for C99 in this fragment of PS1 (Fig. 4.75). All larger constructs were stabilising C99 as well (Fig. 4.75). Interestingly, an additional C99 band could be detected which is not observed when co-producing PS1 fragments with C99 without His Tag (from pSG21). It seemed that this monomer does not contain the His Tag. It was also not detectable on the Coomassie-stained gel in C99 purifications providing a further hint that the C-terminal His Tag is cleaved off. Taken together, these results suggested that C99 interacts with PS1 in *E. coli* and that the first three transmembrane segments are sufficient for interaction and protection of C99.

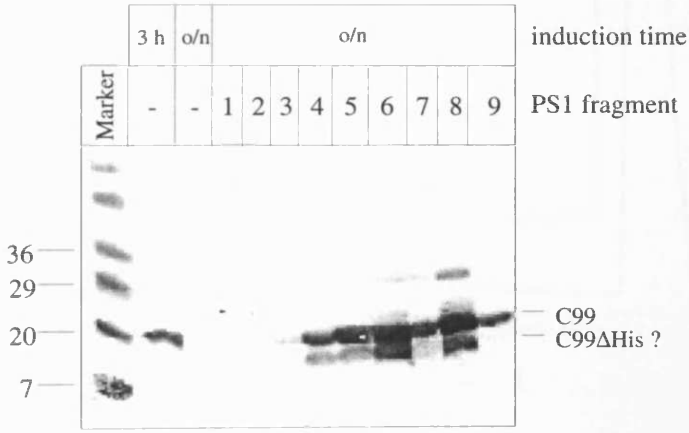

Fig. 4.75 Co-overproduction of C99 and PS1 fragment 1-9.
Five millilitre cultures of KU98 overproducing C99 with His tag and one of the PS1 fragments were induced with 0.1% arabinose and 100 µM IPTG and grown overnight at 28°C. Strain KU98 overproducing C99 with His tag served as a control. The Western blot of whole cell extracts was incubated with the α-C99 and α-Aβ40 antibody (2). The molecular mass of the marker proteins is shown in kDa.

4.4.4 Co-purification of C99 and PS1

The *in vivo* stabilisation assay described above provided initial evidence that recombinant PS1 and C99 interact. For further confirmation, a co-purification experiment of His tagged C99 and PS1 without His Tag was carried out on a copper

loaded POROS column. The chromatogram showed one main peak corresponding to the elution step with 500 mM imidazole and a smaller peak corresponding to the elution with 100 mM imidazole (Fig. 4.76).

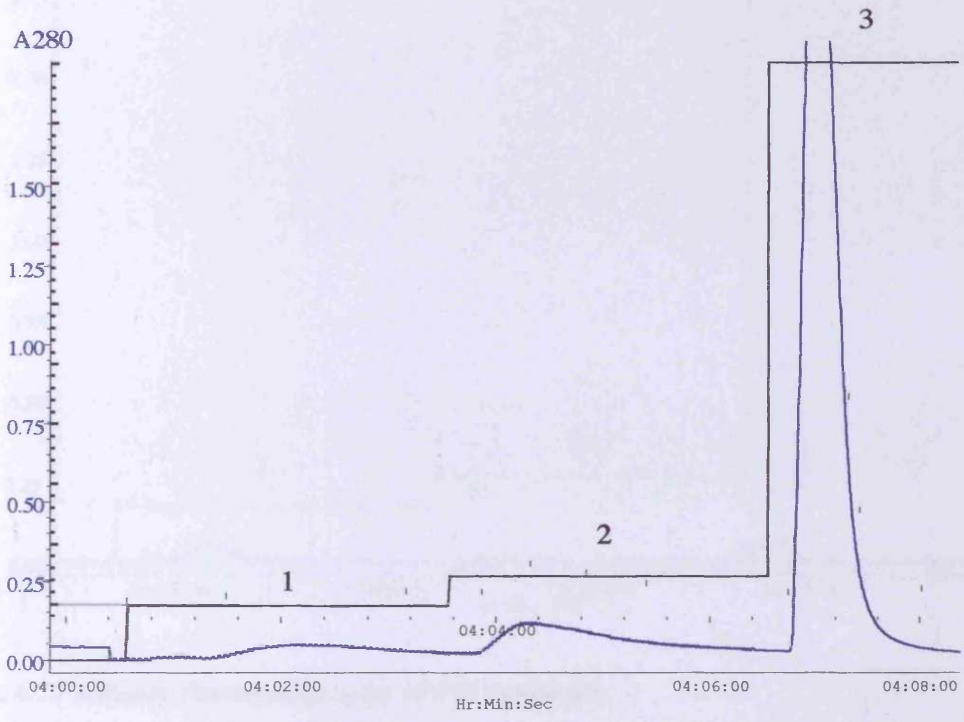

Fig. 4.76 Affinity chromatography of PS1ΔHis and C99+His.
Membranes from a 2 litre culture of strain KU98 overproducing PS1ΔHis/C99+His were prepared and solubilised with 50 mM Tris-HCl buffer pH 8.5, 300 mM NaCl, 30 mM imidazole containing 2% Brij35. The protein was loaded on a POROS column loaded with copper and three elution steps with buffer (50 mM Tris-HCl buffer pH 8.5, 300 mM NaCl, 0.2% Brij35) containing 75 mM (1), 100 mM (2) or 500 mM (3) imidazole were performed. The elution profile shows the absorbance at 280 nm.

In order to demonstrate that the co-elution of PS1ΔHis and C99+His Tag was not based on an interaction of PS1 with the POROS column, membranes of KU98 overproducing PS1ΔHis were prepared in the same way and loaded on a copper loaded POROS column using the same washing and elution conditions. The chromatogram suggested that in the absence of C99 PS1 binds only weakly to the column as only small amounts of protein were eluted by treatment with 75 mM and 500 mM imidazole (Fig. 4.77).

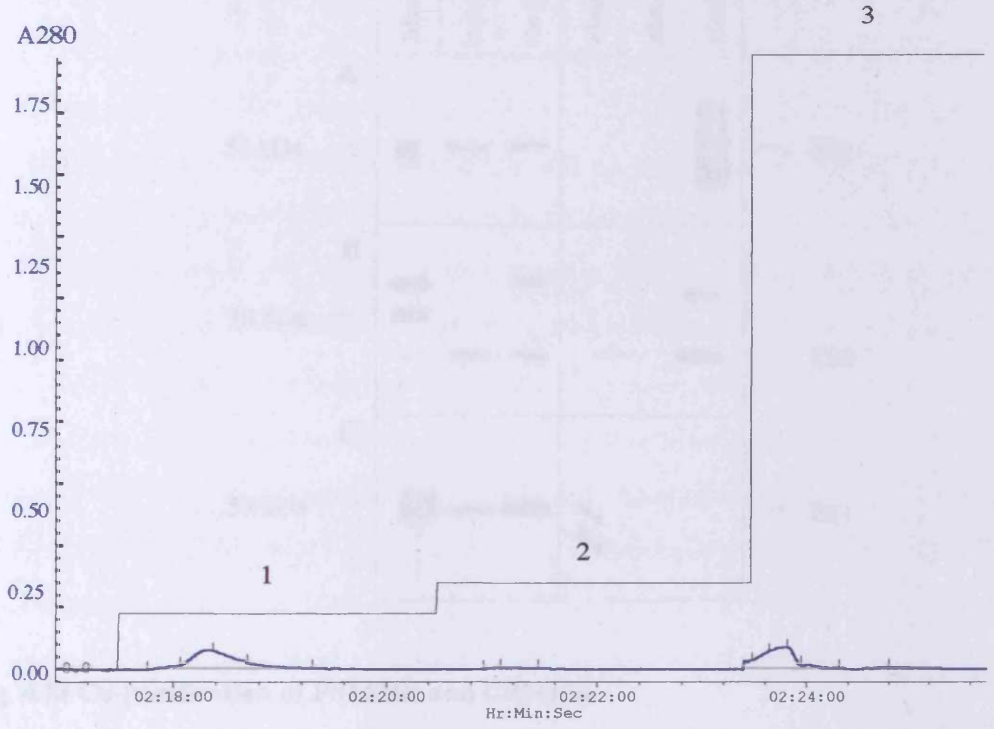

Fig. 4.77 Affinity chromatography of PS1 (control).

Membranes from a 2 litres culture of strain KU98 overproducing PS1ΔHis were prepared and solubilised with 50 mM Tris-HCl buffer pH 8.5, 300 mM NaCl, 30 mM imidazole containing 2% Brij35. The protein was loaded on a POROS column loaded with copper and three elution steps with buffer (50 mM Tris-HCl buffer pH 8.5, 300 mM NaCl, 0.2% Brij35) containing 75 mM (1), 100 mM (2) or 500 mM (3) imidazole were performed. The elution profile shows the absorbance at 280 nm.

To further analyse these results, a Western blot was carried out using relevant fractions. A 1:50 dilution of all the elution fractions was loaded on a SDS-gel and the Western blot was either incubated with α-C99 (B) or α-PS1 antibodies (A and C) (Fig. 4.78).

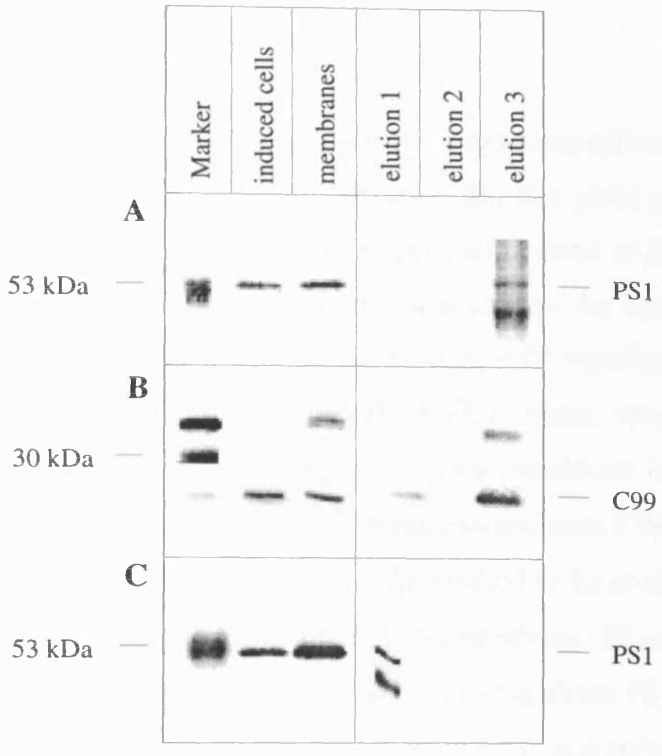

Fig. 4.78 Co-purification of PS1ΔHis and C99+His.

Purification was carried out as described in Fig. 4.76 and Fig. 4.77. A 1:50 dilution of the elution fractions was loaded on a SDS-gel followed by Western blotting using either α-C99 antibody (B) or α-PS1 antibody (A and C). A and B represent the elution fraction of the co-purification whereas C represents the elution fractions of the control purification. Elution 1 = 75 mM imidazole, elution 2 = 100 mM imidazole, elution 3 = 500 mM imidazole. The molecular mass of the marker proteins is shown in kDa.

The Western blot indicated that all proteins were present in roughly equal amounts in the induced cells and after membrane preparation (Fig. 4.78). PS1 and C99 bound together to the copper loaded POROS column and were co-eluted in the 500 mM imidazole elution step (Fig 4.78 A+B). The control chromatography indicated that PS1 binds only weakly to the column as it eluted already in the 75 mM imidazole elution step (Fig. 4.78 C). Therefore, it can be concluded that co-elution of PS1ΔHis and C99+His was based on an interaction of both proteins.

4.4.5 γ-secretase assay

Several attempts to purify PS1 (with or without His Tag) using affinity chromatography, anion exchange chromatography and gel filtration did not yield pure protein (thesis Mona Harnasch, 2003). Mass spectrometry experiments done at Hoffmann LaRoche (Basel, Switzerland) identified several contaminants such as the DnaK chaperone, Lon protease as well as OmpA, 16 kDa heat shock protein, ATP synthase beta chain ATPB and phosphate transport ATP-binding protein PSTB. Since several reports in the literature described γ-secretase assays using solubilised membrane fractions or partially purified PS1 complex, partially purified PS1Δ9 protein and pure C99London (Val45Ile) were used in a γ-secretase assay. According to the method of Li *et al.* (2000), the buffer used was 150 mM sodium citrate buffer pH 6.8. Alternatively, 50 mM Tris-HCl buffer pH 8.0, 150 mM NaCl was also used. A sample containing either PS1Δ9 or C99London was incubated under the same conditions overnight at 37°C and served as control. Also, 1 μg of pure Aβ40 incubated overnight at 37°C in each buffer served as a control.

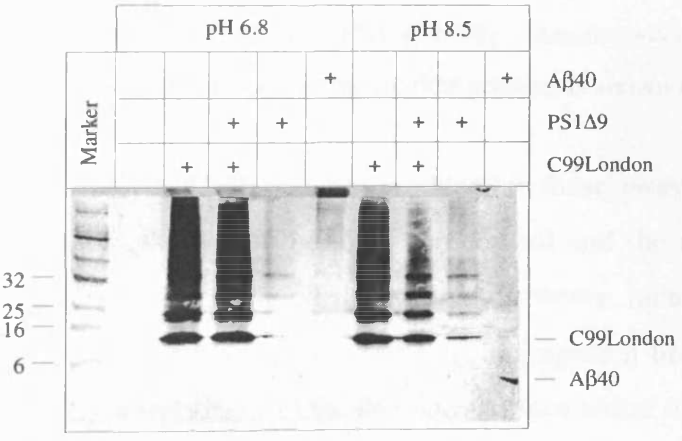

Fig. 4.79 Western blot of the γ-secretase assay.

Partially purified PS1Δ9 (10 μg) was incubated overnight with purified C99London (15 μg) in either 150 mM sodium citrate buffer pH 6.8 or 50 mM Tris-HCl buffer pH 8.5, 150 mM NaCl at 37°C. In addition, 1 μg Aβ40 or 15 μg C99London were incubated overnight in either 150 mM sodium citrate buffer pH 6.8 or 50 mM Tris-HCl buffer pH 8.5, 150 mM NaCl at 37°C to serve as controls. The samples were TCA precipitated, resuspended in sample buffer containing 30 mM DTT and loaded on a Schaegger gel. The Western blot was incubated with the α-C99 and α-Aβ40 (2)/α-Aβ42 antibodies. The molecular mass of the marker proteins is shown in kDa.

All samples contained DDM in a final concentration of 0.05% to prevent aggregation of the membrane proteins. The samples were TCA precipitated and analysed on a Schaegger gel. A Schaegger gel was used because it was impossible to detect Aβ in our SDS-PAGE system. On conventional SDS-PAGE, Aβ remained in the stacking gel, which might be explained by the acidic pH of the stacking gel. The Western blot was incubated with the α-C99 and α-Aβ40 (1)/α-Aβ42 antibody.

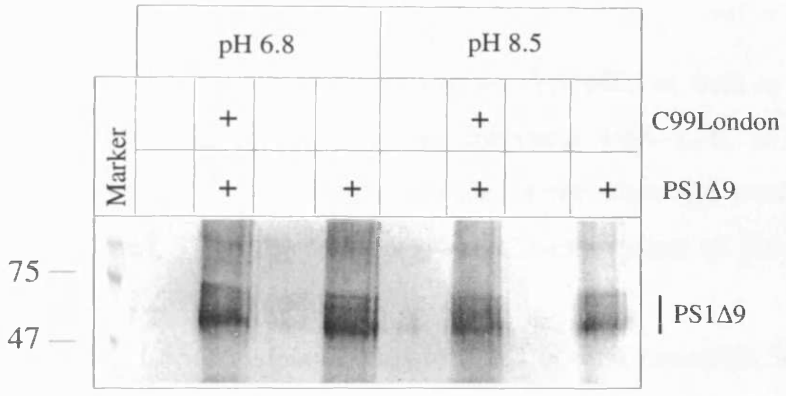

Fig. 4.80 Control Western blot of the γ-secretase assay.

To confirm the presence of PS1, relevant samples described in Fig. 4.79 were loaded on a 10 % SDS-gel followed by Western blotting using α-PS1 antibody. Samples were diluted 1:50 before loading on the SDS-gel. The molecular mass of the marker proteins is shown in kDa.

Independent of the buffer used, Aβ40 was not produced in these assays. Also, no visible difference in the intensity of the C99 band of the control and the assay sample was detected on the Western blot (Fig. 4.79). Interestingly, however, incubation of Aβ40 in 150 mM sodium citrate buffer pH 6.8 may lead to aggregation because the peptide accumulated in the stacking gel (Fig. 4.79). In contrast, incubation of Aβ40 in 50 mM Tris-HCl buffer pH 8.5, 150 mM NaCl did not lead to an aggregation because only the monomer band was detectable (Fig. 4.79). This finding should be taken into account for future γ-secretase assays.

There are two explanations for these results. Firstly, Aβ is produced but remains undetectable by the current method. This explanation is possible because 1 μg pure Aβ is hardly recognised by the antibody. Using a different antibody against Aβ might improve detection of small amounts of Aβ via ELISA. Secondly, PS1 is unable to cleave C99 because other members of the γ-secretase complex such as nicastrin, PEN-2

and APH-1 are not present. Therefore recombinant expression of the entire γ-secretase complex might be an interesting way forward.

4.5 C99, PS1 and L56

4.5.1 Presenilin and L56

A yeast two-hybrid system (GenBank accession no. V04680) as well as an in-house *E. coli* two-hybrid system suggested that PS1 interacts with L56. It was therefore interesting to examine if L56 is involved in one of the cleavage events (γ-secretase cleavage or cleavage of PS1 in the loop region). Co-expression of *l56* and *ps1* could give a first indication if L56 can process PS1.
The plasmids encoding L56 constructs (full-length L56 and Δmac25L56) and PS1 are pBR derivatives and have the same origin of replication. Therefore, the origin and the chloramphenicol resistance of pACYC184 were cloned into pSG5 and pSG7. The new plasmids were called pSG15 and pSG16 (Fig. 4.81).

4.5.2 Co-expression of l56 and ps1

Initially cleavage of PS1 by L56 or Δmac25L56 was assayed via co-overproduction in *E. coli* strain KU98 followed by Western blot analysis. Using various induction and incubation conditions (induction for 4 h followed by incubation overnight in media of various pH values such as pH 4.5, pH 6.8 and pH 8.5 at 28°C or 37°C), no changes of PS1 levels or any processed forms of PS1 were observed suggesting that L56 does not cleave PS1 under these conditions (data not shown). As expected, full-length L56 was unstable after overnight incubation but Δmac25L56 was still detectable and should have been able to degrade PS1 (data not shown). An explanation for these results could either be that L56 is not involved in PS1 processing or that improper assay conditions were chosen.

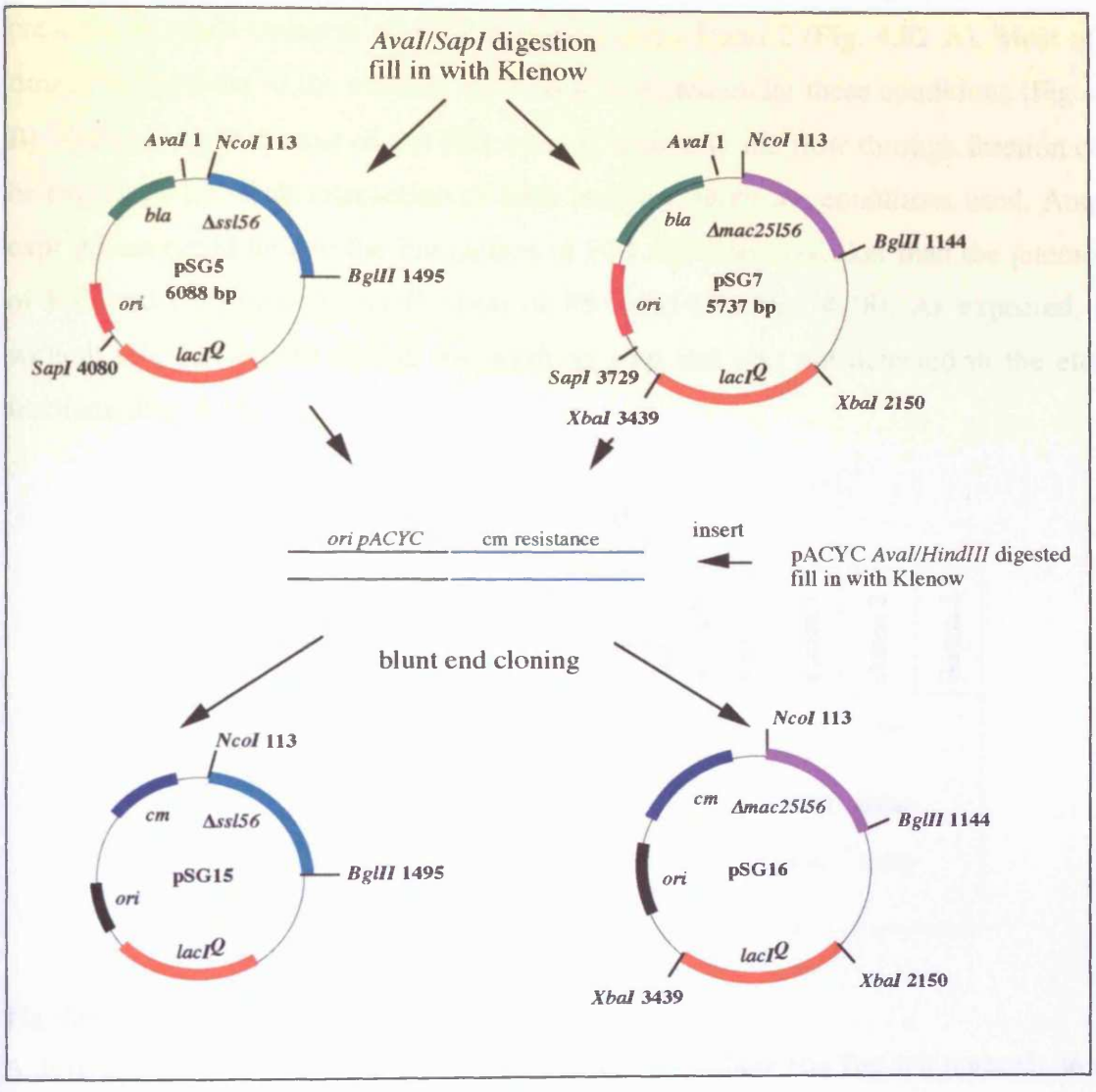

Fig. 4.81 Cloning of pSG15 and pSG16.

The amp resistance gene and the ColE1 *ori* of pSG5 and pSG7 were exchanged for the chloramphenicol resistance gene and the *ori* of pACYC184. All cloning steps and relevant restriction enzymes are shown.

4.5.3 Co-purification of L56 and PS1

Two-hybrid systems could give false positive results and it is therefore important to use additional methods to show that PS1 interacts with L56. Therefore, a co-purification experiment with His tagged L56 and non-His tagged PS1 was carried out.

Western blot analysis of relevant fractions after NiNTA chromatography indicated the presence of small amounts of PS1 in elution steps 1 and 2 (Fig. 4.82 A). Most of the Δmac25L56 bound to the column and was also eluted under these conditions (Fig. 4.82 B). The finding that most of the PS1 was detectable in the flow through fraction could be explained by weak interaction of both proteins under the conditions used. Another explanation could be that the interaction of PS1 and L56 is weaker than the interaction of PS1 and C99 (see co-purification of PS1 and C99 Fig. 4.78). As expected, PS1 without His Tag eluted during the washing step and was not detected in the elution fractions (Fig. 4.83).

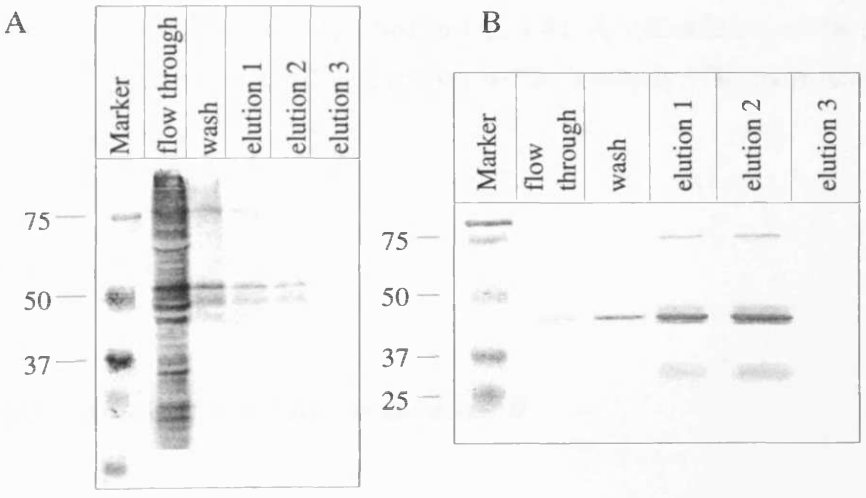

Fig. 4.82 Co-purification of PS1 and Δmac25L56.

A three litre culture of strain KU98 overproducing PS1 without His Tag and Δmac25L56 with His Tag was induced with 100 µM IPTG for 4 h at 28°C. Cells were lysed and solubilised with 2% Brij35 for 2 h on ice. Solubilised proteins were loaded on a NiNTA Superflow column and washed with 50 mM Tris-HCl buffer pH 8.0, 300 mM NaCl, 0.2% Brij35 containing 30 mM imidazole (wash). A step gradient with 50 mM Tris-HCl buffer pH 8.0, 300 mM NaCl, 0.2% Brij35 containing 75 mM (elution 1), 100 mM (elution 2) or 500 mM imidazole (elution 3) was performed to elute protein. A 1:20 dilution of the peak fractions was analysed on Western blots incubated with α-PS1 antibody (A) or polyclonal L56 antiserum (B). The molecular mass of the marker proteins is shown in kDa.

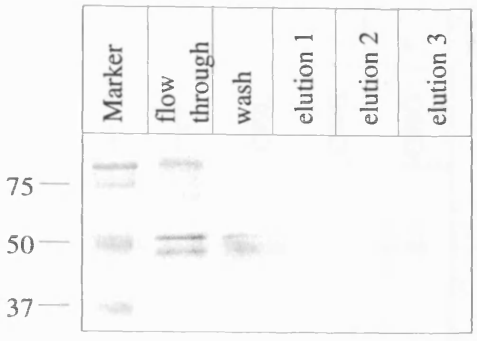

Fig. 4.83 Affinity chromatography of PS1 (control).
A three litre culture of strain KU98 overproducing PS1ΔHis was induced with 100 µM IPTG for 4 h at 28°C. The cells were lysed and solubilised with 2% Brij35 for 2 h on ice. The chromatography was performed as described in Fig. 4.82. A 1:20 dilution of the peak fractions was analysed on a Western blot incubated with α-PS1 antibody. The molecular mass of the marker proteins is shown in kDa.

4.6 L56 and C99

4.6.1 Degradation of C99 by Δmac25L56

Although L56 does not seem to be involved in PS1 cleavage, it could play a role in the cleavage of another interaction partner of PS1, for example C99. Initially, co-expression experiments of *c99* and *l56* were performed to examine a possible cleavage event. Strain KU98 overproducing C99 from pSG12 and either ΔssL56 or Δmac25L56 was induced with 100 μM IPTG and grown for 4 h or o/n at 28°C or 37°C. Western blots indicated that C99 is not degraded after 4 h induction and, as expected, there is no stabilisation of C99 overnight (data not shown). Because C99 is unstable during overnight induction, it is problematic to distinguish between degradation mediated by *E. coli* proteases or L56.

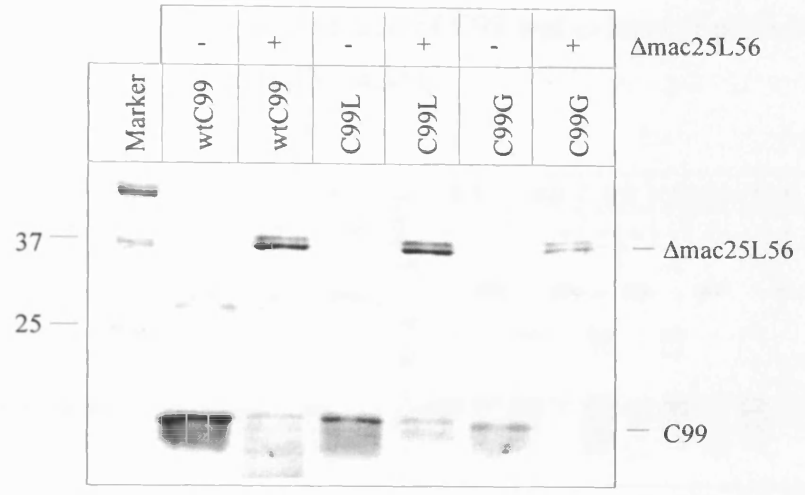

Fig. 4.84 C99 degradation by Δmac25L56.

Purified Δmac25L56 (10 µg) was incubated overnight with either 10 µg wtC99, C99London (C99L) or C99Gly29Ser Gly37Ser Ala42Ser (C99G) in 50 mM Tris-HCl buffer pH 8.5, 150 mM NaCl at 37 °C. The samples were TCA precipitated, resuspended in sample buffer containing 30 mM DTT and loaded on a 12% SDS-gel. The gel was stained with Coomassie Blue. Each C99 construct (10µg) incubated in the same buffer overnight at 37°C served as control. The molecular mass of the marker proteins is shown in kDa.

Therefore, an assay with purified protein was carried out. DDM was not added to the assay because 0.05% DDM inhibits proteolytic activity of Δmac25L56. The samples were analysed on a 12% SDS-gel stained with Coomassie Blue. Purified C99 incubated without protease served as control.

The Coomassie stained gel showed that Δmac25L56 is able to degrade C99 and there is no visible difference between the three C99 constructs examined (Fig. 4.84). Although degradation of C99 by L56 did not lead to a specific degradation product, it would be interesting to test whether Aβ is produced.

4.6.2 Is C99 degradation also pH dependent?

Previous experiments indicated that casein degradation by Δmac25L56 is pH dependent. Incubation of purified C99 with purified Δmac25L56 in buffers of various pH values was used to determine if C99 degradation is also pH dependent. Samples were incubated overnight at 37°C, TCA precipitated and analysed on a 12% SDS-gel stained

with Coomassie Blue. A slight degradation of C99 was evident at pH 5.5 but was more efficient between pH 7.5 and 10.0 (Fig. 4.85).

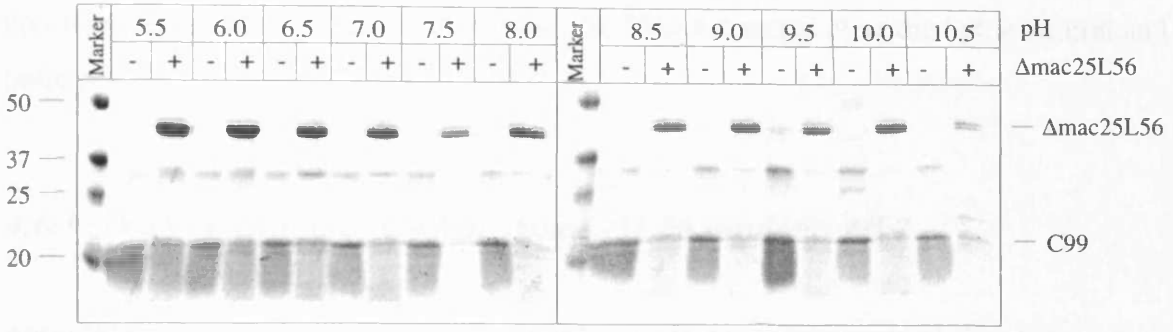

Fig. 4.85 C99 degradation by Δmac25L56 in the pH range from pH 5.5 to pH 10.5.
Δmac25L56 (10 µg) was pre-incubated for 30 min at 37°C in buffers of various pH values prior to adding the substrate (10 µg C99). Samples were incubated overnight at 37°C, TCA precipitated and loaded on a 12% SDS-gel. The gel was stained with Coomassie Blue. The molecular mass of the marker proteins is shown in kDa.

The assay was repeated with 10 µg C99 and 10 µg Δmac25L56 to compare C99 degradation at more acidic (pH 5.5) and basic pH (pH 8.5). After TCA precipitation, proteins were loaded on a 12% SDS-gel and stained with Coomassie Blue.

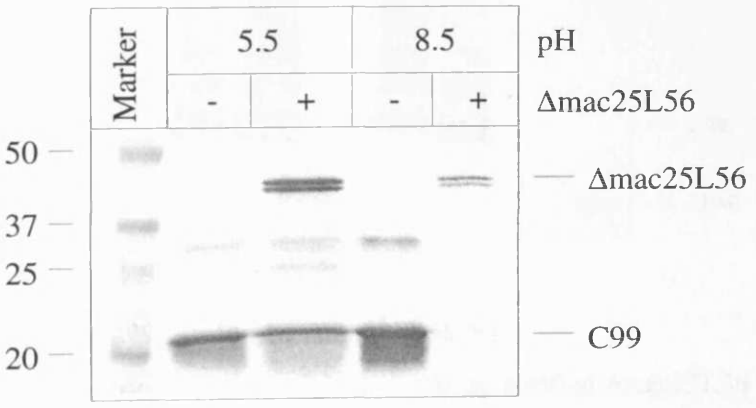

Fig. 4.86 Comparison of the C99 degradation at pH 5.5 and pH 8.5
Δmac25L56 (10 µg) was pre-incubated for 30 min at 37°C in buffers of either pH 5.5 or pH 8.5 prior to adding the substrate (10 µg C99). The samples were incubated overnight at 37°C, TCA precipitated and loaded on a 12% SDS-gel. The gel was stained with Coomassie Blue. The molecular mass of the marker proteins is shown in kDa.

Degradation of C99 was not detected at pH 5.5 (Fig. 4.86). In contrast, C99 was completely degraded at pH 8.5 (Fig. 4.86). Degradation should be due to the proteolytic activity of Δmac25L56 because the C99 controls did not show any degradation and previous experiments indicated that Δmac25L56 is not active at acidic but at neutral and basic pH.

4.6.3 Does cleavage of C99 by Δmac25L56 produce Aβ ?

Δmac25L56 seems to degrade purified C99 in a pH-dependent manner. The Coomassie-stained gels did not show any specific degradation band suggesting that C99 is completely degraded by Δmac25L56. However, it would be interesting to test if Aβ is produced as one of the cleavage products. Detection of Aβ in γ-secretase assays can be problematic because only small amounts (ng range) are produced.

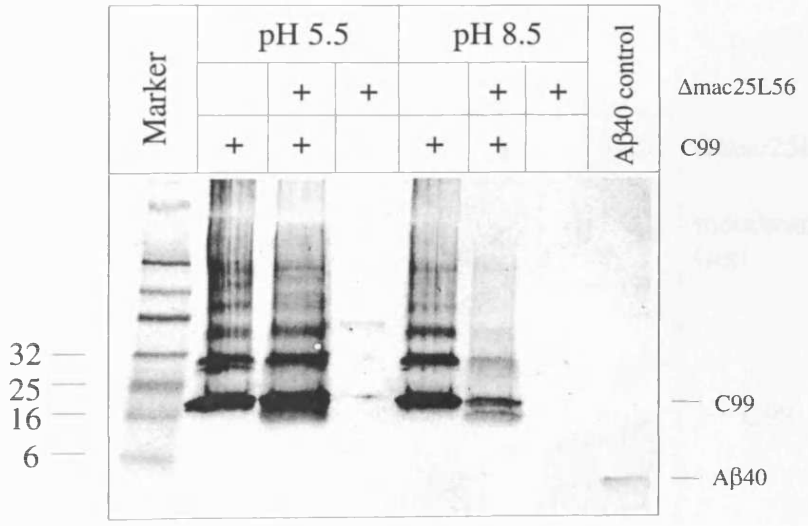

Fig. 4.87 Degradation of C99London by Δmac25L56.

C99London (15 µg) was incubated overnight with 10 µg purified Δmac25L56 in either 50 mM Bis-Tris buffer pH 5.5, 150 mM NaCl or 50 mM Tris-HCl buffer pH 8.5, 150 mM NaCl at 37°C. Each protein incubated under the same conditions and Aβ40 (1 µg) served as controls. Samples were TCA precipitated and loaded on a Schaegger gel. The Western blot was incubated with α-C99 and α-Aβ40 antibodies (1). The molecular mass of marker proteins is shown in kDa.

The degradation assay of C99 using purified Δmac25L56 was performed in buffers of pH 5.5 and 8.5 and analysed on a Schaegger gel. Purified Aβ40 (1 μg) was used as a positive control and α-C99 and α-Aβ40 (1) antibodies were used for detection. The α-Aβ40 antibody recognises 1 μg Aβ40 but only a faint band is produced (Fig. 4.87). At pH 8.5, C99 partially disappeared but no Aβ40 was detectable, while, at pH 5.5, no degradation of C99 was observed (Fig. 4.87).

4.6.4 Is L56 able to degrade membrane-bound C99?

Degradation of membrane-bound C99 would indicate that the hydrophobic areas which might be exposed when using detergent-solubilised and purified C99 are not the initial signal for substrate recognition. To test if Δmac25L56 is able to degrade membrane-bound C99, purified Δmac25L56 was mixed with various amounts of membranes from strain KU98 overproducing C99. Membranes incubated without Δmac25L56 served as control.

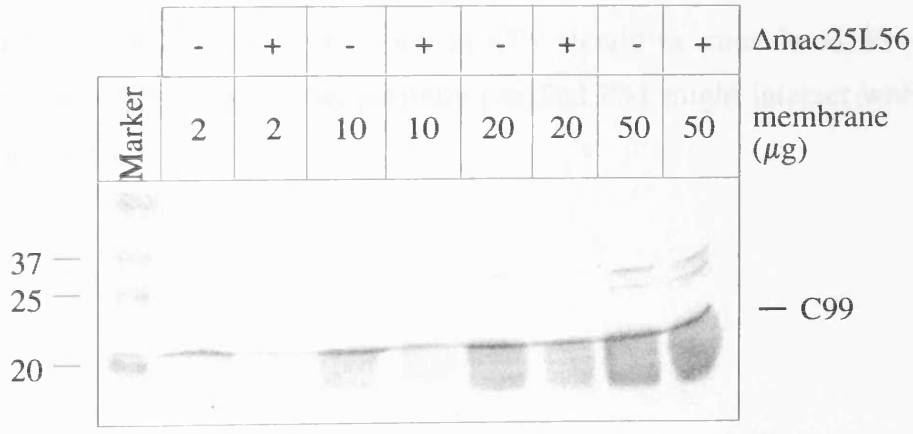

Fig. 4.88 Degradation of membrane-bound C99 by Δmac25L56.

Membrane fractions of strain KU98 overproducing C99 were prepared and resuspended in 50 mM Tris-HCl buffer pH 8.5, 150 mM NaCl. BCA protein determination was carried out and membranes in the amounts indicated were incubated with or without 10 μg purified Δmac25L56 for 16 h at 37°C. Samples were mixed with sample buffer containing 30 mM DTT and loaded on a 12% SDS-gel. The Western blot was incubated with α-C99 antibody. The molecular mass of the marker proteins is shown in kDa.

Interestingly, the Western blot showed that membrane-bound C99 could also be degraded by Δmac25L56 (Fig. 4.88). The samples containing 2 and 10 μg membranes showed degradation of C99 by Δmac25L56 whereas the sample containing 20 μg membranes showed only a slight difference in the assay and control sample (Fig. 4.88). There is no difference in band intensity detectable with 50 μg membranes.

4.6.5 Does PS1 protect C99 from being degraded by L56?

As C99 interacts with PS1, it would be interesting to examine if partially purified PS1Δ9 could prevent degradation of C99 by Δmac25L56. PS1Δ9 prevents degradation of purified C99 suggesting that their interaction renders C99 inaccessible to L56 (Fig. 4.89 A). As expected, Δmac25L56 degrades C99 (Fig. 4.89 A) and the controls showed that PS1Δ9 as well as Δmac25L56 are present in the samples (Fig. 4.89 B and C).
C99 is not abundant in human cells because of its short half-life. C99 might thus be rapidly degraded in human cells. It is attractive to speculate that degradation of C99 by L56 could compete with processing of C99 by γ-secretase. However, alternative explanations for the detected protection of C99 should be considered. For example, chaperones that are present in the partially purified PS1 might interact with C99 and cause stabilisation.

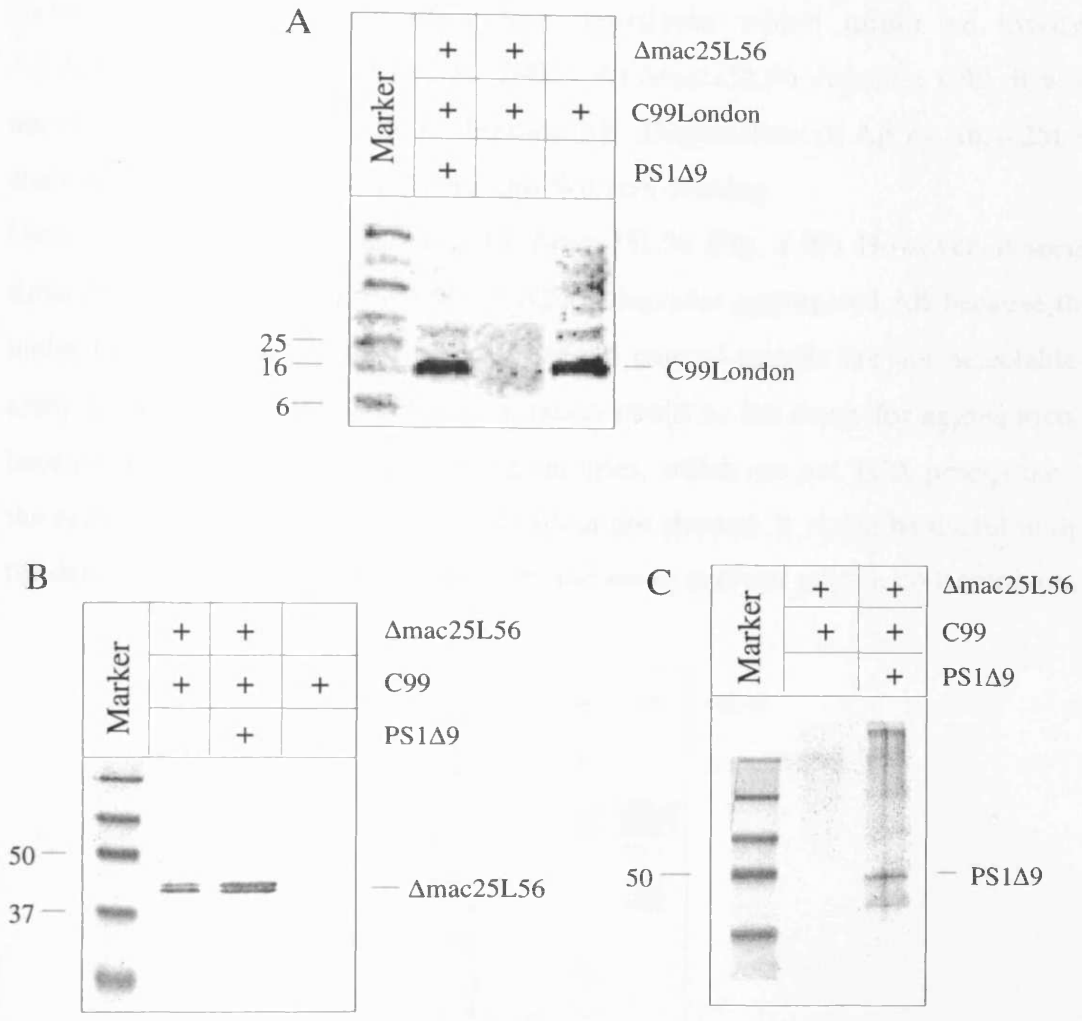

Fig. 4.89 Protection of C99 by Δmac25L56.

Purified C99London (10 µg) was incubated with or without partially purified PS1Δ9 (10 µg) and 10 µg Δmac25L56 in 50 mM Tris-HCl buffer pH 8.5, 150 mM NaCl at 37°C. Samples were separated on a Schaegger gel. The Western blot was incubated with the α-C99 antibody (A), the polyclonal L56 antiserum (B) or an α-PS1 antibody (C). The molecular mass of the marker proteins is shown in kDa.

4.6.6 Is Δmac25L56 able to degrade Aβ?

Qiu *et al.* (1998) showed that insulin-degrading enzyme is able to degrade monomeric but not dimeric or aggregated Aβ. There are a few other proteases such as cathepsin D and cathepsin E, gelatinase A and gelatinase B, trypsin- or chymotrypsin-like

endopeptidases, aminopeptidase and neprilysin which might be involved in Aβ degradation (Suh and Checler, 2002). As Δmac25L56 degrades C99, it would be interesting to test if it is able to degrade Aβ. Degradation of Aβ by Δmac25L56 was analysed using purified components and Western blotting.

Monomeric Aβ40 is not degraded by Δmac25L56 (Fig. 4.90). However, it seems that Δmac25L56 prevents aggregation of Aβ or degrades aggregated Aβ because the high molecular weight bands appearing in the Aβ control sample are not detectable in the assay sample (Fig. 4.90). TCA precipitation could be the cause for aggregation of Aβ because it aggregates at acidic pH but samples, which are not TCA precipitated, show the same high molecular weight bands (data not shown). It might be useful to optimise the detection of Aβ to be able to perform the assay at lower protein concentration.

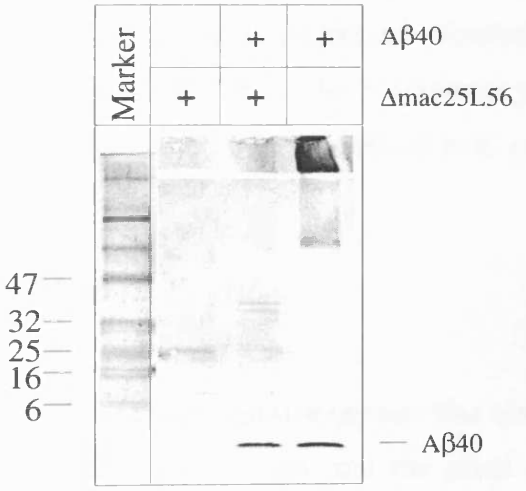

Fig. 4.90 Degradation of Aβ by Δmac25L56.

Purified Δmac25L56 (10 µg) was incubated overnight with 1 µg Aβ40 in 50 mM Tris-HCl buffer pH 8.5, 150 mM NaCl at 37°C. Samples were TCA precipitated and loaded on a Schaegger gel. The Western blot was incubated with α-Aβ40 antibody (1). The molecular mass of the marker proteins is shown in kDa.

5 Discussion

5.1 L56

5.1.1 Expression of l56

Stable expression of *l56* was observed in strain KU98, even after overnight induction. Interestingly, GST (glutathione-S-transferase)-HtrA2 fusions were stably produced in baculovirus/Sf9 cells while N-terminal truncations were observed when HtrA2 was not fused to GST (Savopoulos *et al.*, 2000). It is therefore possible that an exposed N-terminus may be required for autoproteolytic events in baculovirus/Sf9 cells. In *E. coli*, only the HtrA domain of HtrA2 was stably expressed. Similarly, Δmac25L56 is more stably expressed than full-length L56. Thus, the N-terminal parts of L56 and HtrA2 seem to present problems during recombinant expression in *E. coli*.

5.1.2 Translocation of L56 in E. coli

Full-length L56, containing the human signal sequence was not translocated in *E. coli*, as shown by experiments with spheroplasts and the *phoA* fusion technique. One explanation could be that L56 is not translocation competent or that *E. coli* is unable to recognize the human signal sequence.

Signal sequences from different organisms differ in amino acid composition of the positively charged n-region, the hydrophobic h-region and the neutral but polar c-region. The prokaryotic h-regions for example are dominated by leucine (L) and alanine (A) residues in approximately equal proportions and, in eukaryotes, they are dominated by leucine residues with some occurrence of valine (V), alanine (A), phenylalanine (F) and isoleucine (I) (Nielsen, 1997). The h-region of the L56 signal sequence contains eight leucines as well as some alanines and should be acceptable for *E. coli* as a translocation signal. Close to the cleavage site at residue -3 and -1, prokaryotes accept alanine residues exclusively (Nielsen, 1997), which are presented in L56, allowing

processing by leader peptidase. One explanation for inefficient translocation could be that the human L56 signal sequence has more positively charged residues in the early mature region compared to the n-region. It was shown by Prinz (1996) that charge distribution is critical for export. After introduction of the *E. coli* DegP signal sequence at the N-terminus of ΔssL56, the protein appears to be translocated. This is supported by the fact that expression of this protein is not detectable in strain KU98 and DHB4 whereas cytoplasmically localised L56 is stably overproduced after 4 h and overnight in KU98. Production in a strain lacking several periplasmic proteases led to detectable amounts of protein after 4 h, indicating that either the protein is less stable with the DegP signal sequence or it is translocated to the periplasm and remains partially stable because of the lack of some periplasmic proteases.

Table 5.1 Signal sequences of L56, DegP and Enterotoxin.

Signal sequence	Sequence
L56	M A I P R A A L L P L L L L L L A A P A S A|Q L S R A A G R
DegP	M A K T T L A L S A L A L S L G L A L S P L S A T A|A M A
Enterotoxin	M K K N I A F L L A S M F V F S I A T N A Y A|

Leucine residues are coloured in red and the positively charged arginine residues in blue.
The cleavage site for the signal peptidase is indicated as a line.

Examination of export of L56 in this *E. coli* strain was not successful because the strain grew poorly and could not be used for purification or spheroplast generation. Cloning of an enterotoxin signal sequence, which was successfully used in the translocation of several proteins such as NGF (neuronal growth factor), TNF (tumour necrosis factor) and alkaline phosphatase (Simmons and Yansura, 1996), did not lead to detectable amounts of L56 in the periplasm but further studies should be carried out to improve the

expression conditions. In this context, the *l56-phoA* fusion could be used as a screening system for mutants that are able to export L56. The actual selection would be growth on minimal β-glycerol-P plates.

5.1.3 Oligomeric state of L56

E. coli DegP forms an active hexamer by dimerisation of two trimers. The two trimers, which are stabilised exclusively by the protease domain, form a funnel-shaped structure with the protease domains located on top and the mobile PDZ domains on the outside (Krojer, 2002). The two trimers are connected by the long loops LA of opposing trimers wound around each other and forming the corner pillars of the internal chamber (Krojer, 2002) (Clausen *et al.*, 2002).

The human homologue HtrA2 forms a trimer, which is also exclusively mediated by the protease domain particularly by N-terminal sequences (Clausen *et al.*, 2002; Maurizi, 2002). Three residues (Tyr 147, Phe 149, Phe 256) from each monomer stack against one another to form an aromatic cylinder lined with aromatic rings (Maurizi, 2002). Hexamerisation does not take place because the long loop LA, which mediates hexamerisation in DegP, is lacking in human HtrA proteins. L56 showed a trimeric oligomerisation state similar to HtrA2 as judged from gel filtration experiments. Sequence alignments of HtrA2, L56 and DegP suggested that the homotrimerisation domain found in HtrA2 is conserved in L56 and that loop LA is also lacking. Furthermore, an HtrA homologue in *Thermotoga maritima*, which has a shortened loop LA, forms a trimer similar to the human homologues. However, it should be noted that only the protease domain was crystallized (Kim *et al.*, 2002). This evidence suggests that the oligomerisation state depends on the existence and length of loop LA.

5.2 Proteolytic activity of L56

5.2.1 Autoproteolytic activity of L56

Full-length L56 appeared as three or four distinct bands on Western blots, one that migrates at the size of full-length L56 and two or three lower molecular weight bands migrating between 40 and 45 kDa. The intensity of these bands increased after overnight induction and at elevated temperatures. L56 is either degraded by *E. coli* proteases or by autoproteolytic activity. Published evidence supports the latter model. *In vitro* transcription/translation of L56 led to a band pattern that was comparable to the pattern observed after overproduction in baculovirus transfected Sf9 cells (Hu *et al.*, 1998). The observed bands were eliminated following the exchange of the active site serine to an alanine suggesting that these bands were produced by autoproteolysis. The recombinant full-length L56SA mutant, produced in strain KU98, also lacks these lower molecular weight bands and the zymogram showed that this mutant is proteolytically inactive. The lower molecular weight bands in L56 seem to be N-terminal truncations because the C-terminal His-Tag remained detectable.

Autoproteolytic activity is also observed for *E. coli* DegP (Skorko-Glonek *et al.*, 1995). Furthermore, HtrA2 shows autoproteolytic activity where the first 133 N-terminal residues are removed and the proteolytically inactive SA mutant prevents this truncation (Savopoulos *et al.*, 2000). Autoproteolysis could represent a regulatory mechanism because processed HtrA2 exposes an IAP (inhibitor of apoptosis proteins) binding motif at its N-terminus. IAPs are caspase inhibitors and their HtrA2-dependent inactivation induces apoptosis (Clausen *et al.* 2002). Other human HtrAs such as L56 contain different N-terminal extensions, which might be involved in regulation or substrate recognition (Zumbrunn and Trueb, 1996) (Clausen *et al.* 2002). The N-terminal domain of L56 shows high similarity to insulin-like growth factor binding proteins (IGFBP) suggesting a role in IGFBP cleavage. Furthermore, it contains four of the six conserved cysteine residues and the conserved tyrosine residue found in the Kazal-type-inhibitor motif also present in trypsin inhibitor (Zumbrunn and Trueb, 1996) suggesting a possible autoinhibition of L56. Recent studies showed that L56 forms stable complexes with α1-antitrypsin in serum of different cell lines, which might represent an additional

inhibitory mechanism (Hu *et al.,* 1998). Even though full-length and truncated L56 were proteolytically active in zymograms, it cannot be concluded that the Kazal-type inhibitor motif in the mac25 domain acts as a regulator of L56 activity because it is not properly folded when produced in the reducing environment of the cytoplasm.

5.2.2 Biochemical characterisation of L56

Enzymes commonly show a temperature-dependent bell shaped curve of activity. The activity increases up to a maximum (highest activity) and decreases afterwards. The decrease in activity at elevated temperatures can be explained by denaturation of the enzyme above certain temperatures.

E. coli DegP is a heat shock protein that is upregulated in response to several stress stimuli (Spiess *et al.,* 1999). Spiess *et al.* (1999) reported that DegP is proteolytically inactive between 4°C and 22°C while its activity increases 8-fold between 28°C and 42°C. HtrA2 activity increases 3-fold between 37°C and 45°C (Verhagen *et al.,* 2002). Although Zumbrunn and Trueb, (1998) could not detect a change in the mRNA level of L56 in normal human fibroblasts when shifting the temperature from 37°C to 41°C for 4 hours, we could demonstrate a 5-fold increase of proteolytic activity of L56 when

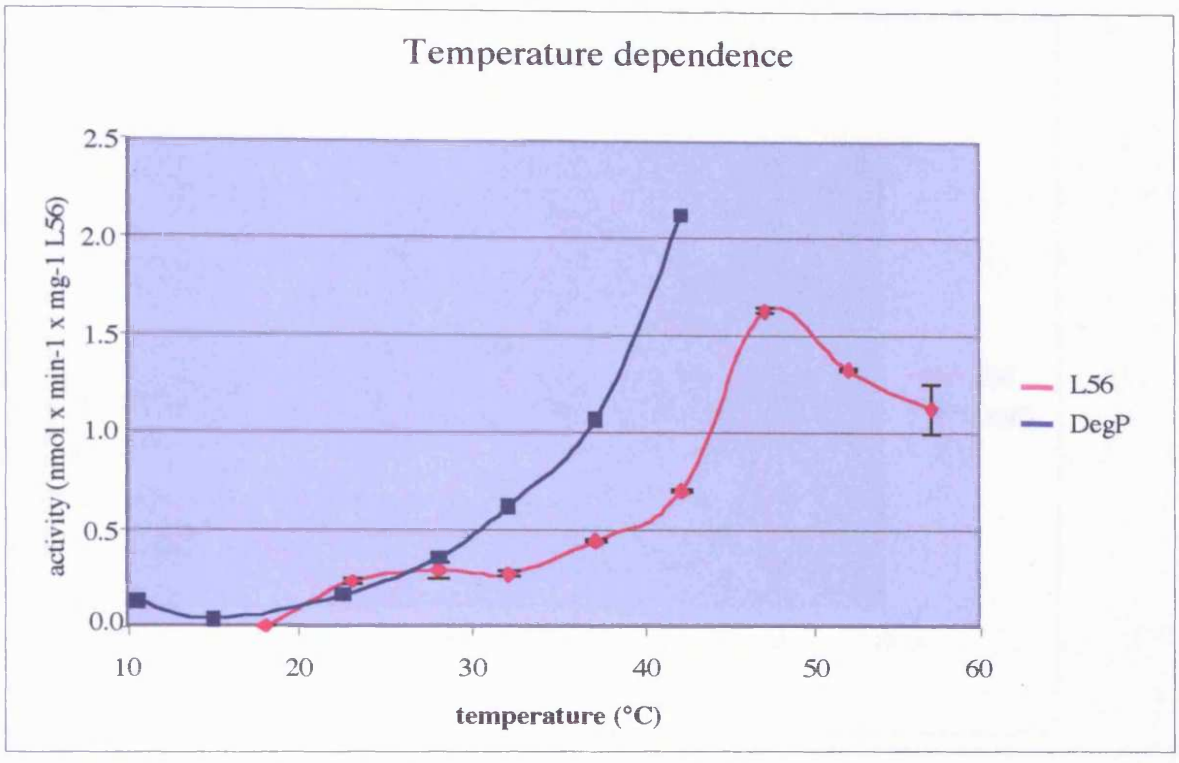

Fig. 5.2 Temperature dependence of the proteolytic activities of L56 and DegP.
Purified DegP or Δmac25L56 was incubated overnight with resorufin-labelled casein in 50 mM Tris-HCl buffer pH 7.5 and 50 mM Tris-HCl buffer pH 8.5, 150 mM NaCl respectively. The specific activity was determined as described in Materials and Methods. DegP proteolytic activity was determined by Alexandra Beil (Ehrmann laboratory).

raising the temperature from 28°C to 45°C (Fig. 5.2). While the increase in proteolytic activity is not as strong as in DegP (Fig. 5.2), the observed temperature-dependent activation could suggest that L56 might be involved in the degradation of unfolded proteins that are generated for example during inflammatory processes in which the temperature in the affected area is often increased.

In addition to temperature, pH may also be involved in the regulation of L56 activity. While *E. coli* DegP has a broad pH spectrum with an maximum for proteolytic activity at pH 7.5, L56 exhibited proteolytic activity mainly between pH 7.5 and 10.0 (Fig. 5.3). The slight activity of L56 between pH 5.5 and 6.5 compared to pH 7 and 7.5 cannot be explained and the physiological implications are not clear. However, L56 is thought to be secreted due to its signal sequence, but it could also be re-internalised by binding to a

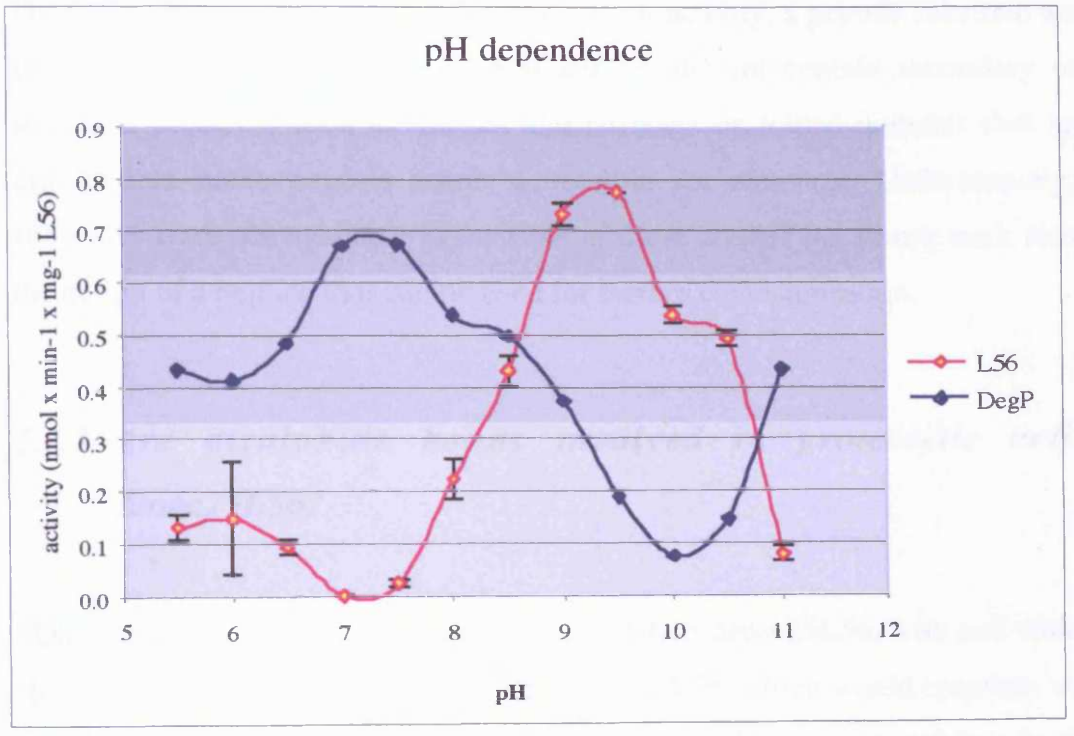

Fig. 5.3 pH dependence of the proteolytic activities of DegP and L56.
Purified DegP or Δmac25L56 were incubated overnight with resorufin-labelled casein in buffers of various pH (Table 3.13 Materials and Methods). Specific activity was determined as described in Materials and Methods. DegP proteolytic activity was determined by Alexandra Beil (Ehrmann laboratory).

receptor at the cell surface and act in the lysosomal pathway where the pH is between 5.0 and 6.0. If this were the case, it could be speculated that pH mediates a compartment-specific regulation of L56 activity. Effects of the pH in the proteolytic activity of other human HtrAs have not yet been reported.

Unlike other heat shock proteases, DegP activity is largely independent of cofactors such as ATP, the pH, reducing agents or divalent cations (Swamy *et al.*, 1983). However, 20 mM salt is required to achieve detectable amounts of L56 activity. Increasing the salt concentration to 150 mM NaCl leads to a further increase in activity. This salt effect could be explained by either a stabilisation of the protein by salt ions or by facilitating the accessibility of hydrophobic areas of the substrate (resorufin-labelled casein). The latter model is supported by the finding that addition of salt increases the accessibility of an oligopeptide substrate for HIV-1 protease (Richards *et al.*, 1990).

For proper biochemical characterisation of L56 activity, a peptide substrate would have been advantageous. Short peptide substrates do not contain secondary or tertiary structural elements such as helices and β-sheets or folded domains that have to be unfolded to make peptide bonds accessible for cleavage. Unfortunately, peptide substrates were not available at the time of these studies but future work must include the design of a peptide that can be used for further characterisation.

5.2.3 Are disulphide bonds involved in proteolytic activity of Δmac25L56?

SDS-PAGE and Western blot analyses of purified Δmac25L56, with and without DTT, showed a change in the migration behaviour of L56, which would correlate with a shift from monomer to dimer. Full-length L56 contains 16 cysteine residues in the mac25 domain that are expected to form disulphide bonds. Furthermore, the last 40 residues of the IGF binding domain and the first 20 residues of the protease domain show similarity to the Kazal-type inhibitor motif found in Trypsin inhibitor (Zumbrunn and Trueb, 1996). This inhibitor motif consists of a conserved tyrosine and six cysteine residues that form 3 disulphide bonds. The conserved tyrosine residue as well as four of the six cysteine residues are present in L56 suggesting the presence of two disulphide bonds (Zumbrunn and Trueb, 1996). The truncated Δmac25L56 construct still contains one of these cysteine residues, which may be highly reactive and form an intermolecular disulphide bond because the intramolecular partner is lacking. Although *E. coli* DegP has two cysteine residues, it does not appear to have disulphide bonds as indicated by the crystal structure (Krojer *et al.*, 2002). In addition, a DegP deletion mutant containing only one of the cysteine residues, showed the same shift in SDS-PAGE (Thesis Alexandra Beil, 2003). These findings suggest that the observed shift in migration might be an artefact. Also, a 20-fold molar excess of DTT did not have any effect on the proteolytic activity of Δmac25L56 suggesting that the potential intermolecular disulphide bond does not influence proteolytic activity.

5.2.4 Substrate specificity of L56

DegP is a general protease. Its substrates include hybrid proteins (Strauch and Beckwith, 1988) recombinant proteins (Baneyx *et al.*, 1991) misfolded periplasmic proteins (Betton *et al.*, 1998) PhoA or MalS and largely unstructured proteins such as casein. All substrates are expected to be at least partially unfolded.

Although HtrA2 degrades β-casein, no natural substrates have been identified so far. L56 degrades casein and unfolded *E. coli* proteins such as MalS and TreA suggesting little sequence specificity. Furthermore, L56 is able to degrade purified as well as membrane-bound C99, and might thus play a role in the onset of Alzheimer's disease. However, as truncated L56 lacking its mac25 domain was used in these tests, no final conclusion can be drawn.

While DegP forms a cage such as ClpAP (an ATP dependent cytoplasmic protease in *E. coli*) and the proteasome with its proteolytic sites located in the inner wall of the cavity (Krojer *et al.*, 2002), HtrA2 has a trimeric structure where access to the active sites seems restricted by its PDZ domains (Maurizi, 2002). It has been proposed that binding of a trimeric ligand to the PDZ domains initiates a conformational change and the active sites become accessible to the substrate (Maurizi, 2002). Truncated L56 has a trimeric structure and shows high homology to the protease domain of HtrA2. Therefore, a similar mechanism of activation might be proposed. However, a crystal structure or additional biochemical characterisations are required to answer this question.

5.2.5 Does L56 reveal chaperone activity?

DegP has a dual function as a chaperone at low temperature and a protease at high temperature (Spiess *et al.*, 1999). A proteolytically inactive SA mutant reveals chaperone activity independent of the temperature (Spiess *et al.*, 1999). The combination of chaperone and protease activity in one protein provides a direct and rapid response to protein folding problems. Additional proteins have already been identified which demonstrate the same dual function such as FtsH (transmembrane protease which degrades sigma factor RpoH) (Suzuki *et al.*, 1997). No chaperone activity tests have been reported for HtrA2 but L56 might have chaperone activity under

certain conditions because the proteolytically inactive L56SA mutant showed an increase in refolding of MalS. Proteolytically active L56 did not exhibit chaperone activity which could be explained by the fact that it degrades unfolded MalS under these conditions. Further experiments must be performed to find conditions in which proteolytically active L56 displays chaperone activity.

5.2.6 Involvement of HtrA in arthritis

Although the function of L56 is still unclear, published evidence suggests its involvement in tumour suppression as L56 mRNA is absent or significantly downregulated in ovarian cancer (Shridhar *et al.*, 2002) and melanomas (Baldi *et al.*, 2002). Furthermore, overproduction of L56 inhibits proliferation *in vitro* and tumour growth *in vivo* (Baldi *et al.*, 2002). In addition, Hu *et al.* (1998) showed that L56 mRNA and protein level is increased 7-fold in osteoarthritic cartilage. High levels of L56 were present in synovial fluid of rheumatoid arthritis and osteoarthritis patients. The pH of such fluids was in the range where L56 is proteolytically active. L56 could not be detected in supernatants of stimulated synovial fibroblasts, which would suggest that other cells produce the L56 and secrete it into the synovial fluid. In addition, L56 was identified in normal human serum.

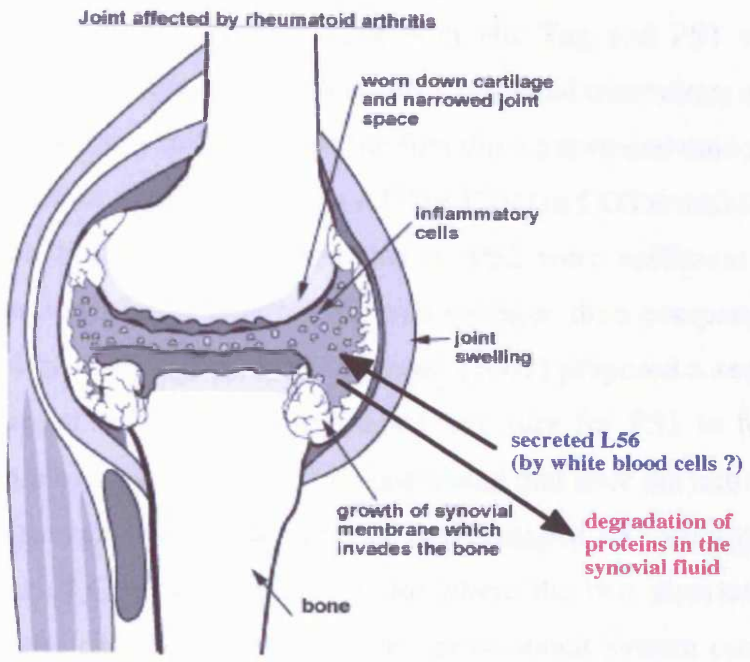

Fig. 5.4 Knee in rheumatoid arthritis.

Two proteins in synovial fluid could be identified which were degraded by Δmac25L56 after 3 h incubation at 42°C. Further investigations into the identity of these proteins may lead to a greater understanding of the role played by L56 in arthritis. (Picture taken from www.cchs.net…./health-info/docs/0700/0739.asp?index=4924).

These findings suggest that leukocytes may be one potential source of L56 and that these cells may be responsible for the production of L56 in inflammatory disease. Further investigations including separation of leukocyte populations are required to determine the exact source of L56.

5.3 PS1, C99 and L56

5.3.1 Interaction of C99 with presenilin

Overproduction of C99 and PS1 or PS1Δ9 in *E. coli* showed a stabilising effect on C99 after overnight induction. This stabilisation was the first indication that both proteins interact and PS1 protects C99 from being degraded by *E. coli* proteases. Xia *et al.*

(1997) demonstrated that APP co-immunoprecipitates with PS1 in extracts of transfected cells. Co-purification of C99 with His Tag and PS1 without His Tag confirmed that these proteins interact. Various C-terminal truncations of PS1 were used to map one interaction site of C99 to the the first three transmembrane segments of PS1. Mapping of interaction sites of PS2 with APP or C100 in COS transfected cells showed that the first two transmembrane domains of PS2 were sufficient for interaction. However, interaction of full-length PS2 was stronger than compared to C-terminal truncations (Pradier *et al.*, 1999). Annaert *et al.* (2001) proposed a second binding site at the C-terminus of PS1 and a ring-shaped structure for PS1 to form the binding pocket. Based on these results, it might be postulated that after the initial binding of C99 to the first three transmembrane domains of a ring-shaped PS1, conformational change promotes transfer of C99 into the active site where the two aspartates are localised. Taken together, the data obtained from the recombinant system correlate well with results from eukaryotic cells, indicating that *E. coli* might be a useful model to study APP processing.

5.3.2 γ-secretase assays

Strong evidence suggests that presenilin is the active component of γ-secretase which produces Aβ peptides. As yet, it has not been possible to purify PS1 from eukaryotic cells. Therefore, all assays to detect Aβ production were carried out with solubilised complex or membrane fractions (Li *et al.*, 2000; Shizuka-Ikeda *et al.*, 2002). To establish whether PS1 is able to produce Aβ, partially purified recombinant PS1 was incubated with purified recombinant C99 under the conditions used by Li *et al.* (2000). However, no Aβ production was detected. One explanation could be that the detection system used was not sensitive enough as the antibody used detects pure Aβ only at amounts > 1 μg and the amounts obtained from human cells appear to be at a considerably lower concentration. Therefore it might be helpful to use ELISA, which is more sensitive. Furthermore, Yu *et al.* (2000) identified nicastrin as an essential member of the γ-secretase complex as it co-elutes with presenilin in an active complex (Esler *et al.*, 2002). Nicastrin matures on the way to the cell surface, being N-

glycosylated and associated with presenilin as well as Notch and APP, two substrates of γ-secretase (Yu *et al.*, 2000). Another member of the complex is PEN-2, a small 10 kDa protein of unknown function, which has already been identified (Steiner *et al.*, 2002). Downregulation of this protein leads to reduction of presenilin levels and nicastrin maturation and therefore to a decrease in the amounts of active complex at the cell surface (Steiner *et al.*, 2002). A third protein is APH-1, a polytopic membrane protein, which is also detected in the γ-secretase complex (Francis *et al.*, 2002). Because removal of any of the components results in a reduction of the amount of γ-secretase complex and therefore in the loss of γ-secretase activity, it seems likely that this might be the reason why γ-secretase activity remained undetectable in the present study. It would therefore be useful to co-express the other members of the complex in *E. coli* and to identify which proteins are required for cleavage of C99.

5.3.3 Oligomerisation of C99

Expression of *c99* in *E. coli* yielded a protein that does not migrate at the predicted size of 12 kDa but at approximately 20 kDa. This was dependent on the gel system used as demonstrated by the fact that monomeric C99 migrated at 20 kDa in the SDS-PAGE system and at 12 kDa in the Schaegger gel. This behaviour could be due to pH variations in the stacking and separation gels.

Additional bands migrating at about 26 kDa and above were observed in both gel systems in whole cell extracts as well as after purification of C99. These findings suggested that C99 might form oligomers (dimers and trimers) in the *E. coli* membrane. Chong *et al.* (1994) expressed *CT105* in *E. coli* and this protein migrated at 18 kDa, which is also higher than the predicted size of 10.5 kDa. It was reported that overproduction of C100 in COS transfected cells showed a similar band pattern as observed for C99 in *E. coli* (Pradier *et al.*, 1999), suggesting that the oligomerisation is not an artefact of the *E. coli* system.

A more detailed examination of the C99 sequence could offer an explanation as to why oligomers are formed. The human erythrocyte sialoglycoprotein glycophorin GpA is a single transmembrane spanning protein that forms SDS stable non-covalent homodimers by interaction of two α-helices (Orzaez *et al.*, 2000). Glycophorin contains

a seven-residue motif (L75 I76 X X G79 V80 X X G83 V84 X X T87), which plays a key role in dimerisation. C99 contains three Gly $(X)_3$ Gly motifs within its transmembrane region (Fig. 5.5), which could be responsible for a dimerisation. Mutagenesis of residues 73-95 of GpA, involving the Gly $(X)_3$ Gly motif, showed that every 3.9 residues in the α-helix is more or less critical in dimerisation (Lemmon *et al.* 1992). The largest effects were detectable for the two glycine residues Gly79 and Gly83. Substitution of Gly83 with two nonpolar amino acids (alanine, leucine, isoleucine or methionine) led to a dimer disruption. Gly79 substituted to valine or leucine prevented dimerisation whereas exchanging to alanine had no significant effect. Exchange of one of the glycines to a polar amino acid such as serine, threonine, or tyrosine disrupted dimerisation completely (Lemmon *et al.*, 1992). A helical wheel projection of Cα positions assuming a periodicity of 3.9 residues per turn demonstrated that the residues sensitive in mutational analysis are clustered on one side of the helix interface (Lemmon *et al.*, 1992) (Fig. 5.6). Repeating this analysis with C99, according to the GpA helical wheel, revealed a clustering of almost the same residues on one interface of the helix. One cluster showed two glycine residues and one leucine residue but the threonine residue found in the same cluster in GpA is not present (Fig. 5.5). There are two possibilities in C99 for the second cluster, either the site of the helical wheel with three valines and one isoleucine residue or if Gly38 and Ala42 play a role in dimerisation the site with two valines and the glycine and alanine residues may be involved in dimerisation. Furthermore, several glycine residues, which align on one face of a putative α-helix were shown to be important in the dimerisation of class II MHC-α (major histocompatibility complex) and β chains (Cosson and Bonifacino, 1992). These findings support the model that the glycine residues and possibly two of the valine residues (Val46 and Val50) as well as Ile32 and Leu49, are involved in dimerisation similar to that observed in GpA. In addition, it was shown for GpA that the residues located at the putative extramembrane end of the reported GpA helix have an essential and specific role for dimer stability. Therefore, the distance of the charged residues that are usually present at the flanking regions of the TM segments and the orientation from the core of the dimerisation motif might be important (Orzaez *et al.*, 2000). It could be hypothesised that the prokaryotic membrane composition or its thickness promotes dimerisation. In addition, the potential Gly $(X)_3$ Gly motif could serve as a possible

explanation as to why Aβ42 is more amyloidogenic than Aβ40. Cleavage by γ-secretase at residue 42 generates an additional dimerisation motif, Gly $(X)_3$ Ala. Thus, Aβ42 might aggregate more readily than Aβ40, which lacks the additional motif. It has been reported for GpA that in some cases one of the glycine residues in a dimerisation motif can be exchanged by alanine, without interfering with dimerisation (Lemmon *et al.*, 1992).

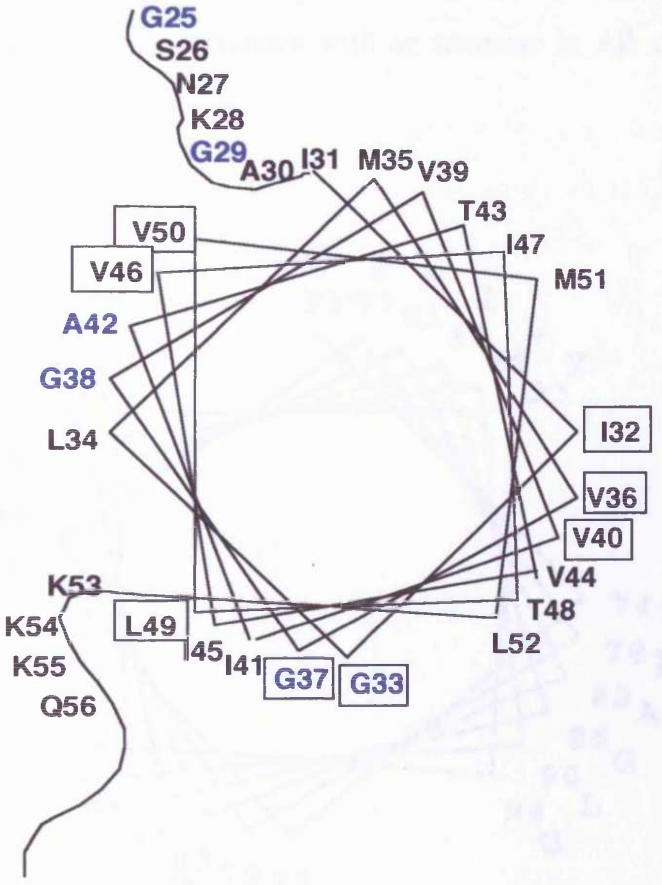

Fig. 5.5 Helical wheel of the putative transmembrane domain of C99.
A periodicity of 3.9 residues per turn was assumed and the glycine residues and one alanine residue, which may represent dimerisation motifs, are coloured blue. Residues that are localised at similar positions to the residues sensitive for dimerisation in glycophorin A are boxed.

The presence of one Gly $(X)_3$ Gly motif and various other residues might be sufficient for dimerisation in C99 and may therefore explain why the generated Gly exchange mutants produced monomers and dimers. Additional residues will have to be exchanged

and tested to understand the molecular basis of C99 oligomerisation and ultimately of Aβ42 aggregation.

The purified C99 mutants containing two or less dimerisation motifs still showed the same band pattern as C99 (wt) on SDS-PAGE. The C99 Gly29Ser Gly37Ser Ala42Ser mutant does not contain a true Gly $(X)_3$ Gly motif but Gly37 and Gly38 are located at the same interface of the backbone and might act as a dimerisation motif. Furthermore, some valine residues (Val46 and Val50) could play an additional role in oligomerisation. Interestingly, incubation of the purified C99 constructs at acidic pH led to an increase in oligomers, which correlates with an increase in Aβ aggregation at acidic pH.

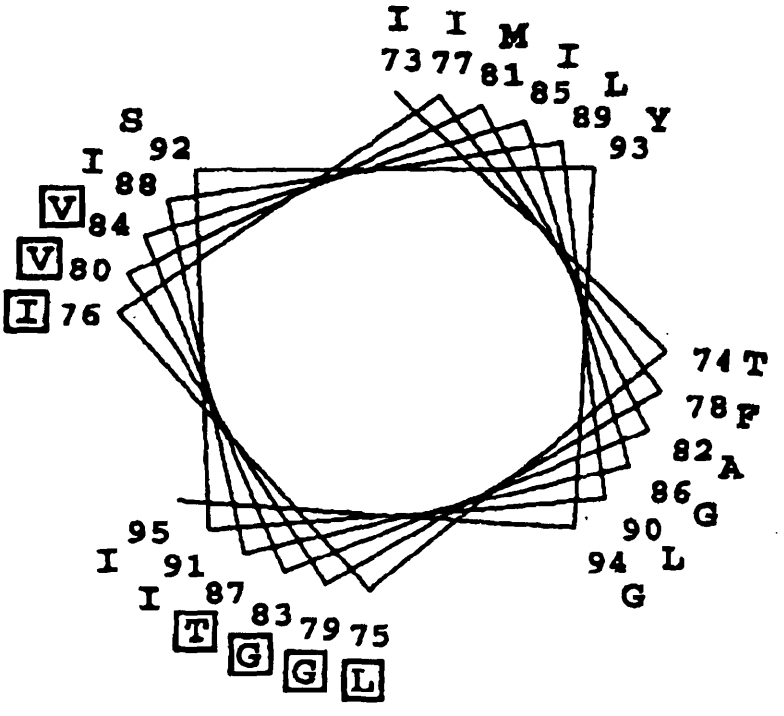

Fig. 5.6 Helical wheel projection of Cαpositions for the transmembrane helix of glycophorin A assuming a periodicity of 3.9 residues per turn.

Positions determined to be sensitive in the mutational analysis and therefore likely to be at the dimer interface, are boxed and are seen to cluster at one face of the helix. (picture taken from Lemmon *et al.*, (1992)).

5.3.4 Involvement of L56 in Alzheimer's disease/Degradation of C99 and Aβ by Δmac25L56

C99 has a high turnover rate in eukaryotic cells (Weidemann *et al.*, 1989). In the present report, Δmac25L56 degraded purified as well as membrane-bound recombinant C99. Although monomeric Aβ40 was not degraded by L56 *in vitro*, aggregated Aβ was removed. L56 is expressed in brain tissues (Nie *et al.*, 2003) and, as it is expected to be secreted into the extracellular space, it might co-localise with the N-terminus of C99 and with oligomers of secreted Aβ40. Therefore, binding and cleavage of C99 and aggregated Aβ40 might also occur *in vivo*. Future experiments in a native system are required to prove and characterise the potential involvement of L56 in the APP pathway. If L56-dependent processing of APP fragments could be verified *in vivo*, induction of L56 might have beneficial effects in the context of AD. For example, investigating levels and aggregation of Aβ40 in brains of a transgenic mouse model of AD could be explored if ways to manipulate L56 levels or L56 activity could be identified.

5.4 Conclusions

E. coli might represent an efficient and simple biological system to produce active L56 and human membrane proteins as demonstrated by cloning of relevant cDNAs into a His Tag vector containing an improved Shine-Dalgarno sequence and a tightly controlled promoter. Furthermore, *E. coli* was used to study protein-protein interactions of soluble and integral membrane proteins such as PS1, C99 and L56. A potential advantage of the recombinant system might be that only proteins of interest are present while close homologues and derivatives produced in the native background such as splice forms are excluded, simplifying the interpretation of data. Potential limitations of the system include the fact that not all posttranslational modifications such as glycosylation or phosphorylation are occurring in *E. coli*. However, functional expression of eukaryotic protein kinases and phosphatases was recently successful (Yue

et al., 2000; Shaywitz *et al.*, 2000; Hoffmann *et al.*, 1994) and future developments may lead to further improvements.

The initial characterisation of purified L56 sets a platform for future studies with the intention to further understand L56 using peptide substrates and inhibitors. Additional biochemical characterisation and future *in vivo* studies will improve our understanding of the physiological role of this protease in healthy human cells and in the context of various diseases. The presence of L56 and at least two substrates in synovial fluids from arthritic patients suggests a functional role for L56 in this chronic condition. A positive correlation between L56 levels and disease severity may prove useful in monitoring the effects of various disease modifying drugs or for the design of novel treatments. In addition, our data suggest that L56 might have a role in the APP pathway and thus in the onset of Alzheimer's disease. Determining the precise cleavage sites in C99 and Aβ, verifying the involvement of L56 in the APP pathway and determining the L56 levels in relevant AD brain tissues represent exciting opportunities for future research.

6 References

Annaert, W. and B. De Strooper (1999). "Presenilins: molecular switches between proteolysis and signal transduction." Trends Neurosci **22**: 439-43.

Annaert, W. G., L. Levesque, K. Craessaerts, I. Dierinck, G. Snellings, D. Westaway, P. S. George-Hyslop, B. Cordell, P. Fraser and B. De Strooper (1999). "Presenilin 1 controls gamma-secretase processing of amyloid precursor protein in pre-golgi compartments of hippocampal neurons." J Cell Biol **147**: 277-94.

Arduengo, M.P., O. K. Appleberry, P. Chuang and L´Hernault S.W. (1998) „The presenilin protein family member spe-4 localizes tp an ER/Golgi derived organelle and is required for proper cytoplasmic partitioning during *C. elegans* spermatogenesis." J. Cell Sci. **111**: 3645-54

Bahl, H., H. Echols, D. B. Straus, D. Court, R. Crowl and C. P. Georgopoulos (1987). "Induction of the heat shock response of *E. coli* through stabilization of sigma 32 by the phage lambda cIII protein." Genes Dev **1**: 57-64.

Baldi, A., A. De Luca, M. Morini, T. Battista, A. Felsani, F. Baldi, C. Catricala, A. Amantea, D. M. Noonan, A. Albini, P. G. Natali, D. Lombardi and M. G. Paggi (2002). "The HtrA1 serine protease is down-regulated during human melanoma progression and represses growth of metastatic melanoma cells." Oncogene **21**: 6684-8.

Baneyx, F., A. Ayling, T. Palumbo, D. Thomas and G. Georgiou (1991). "Optimization of growth conditions for the production of proteolytically-sensitive proteins in the periplasmic space of *Escherichia coli*." Appl Microbiol Biotechnol **36**: 14-20.

Barrett, A. J. (1994). "Classification of peptidases." Methods Enzymol **244**: 1-15.

Baxter, R. C. (2000). "Insulin-like growth factor (IGF)-binding proteins: interactions with IGFs and intrinsic bioactivities." Am J Physiol Endocrinol Metab **278**: 967-76

Behrends C. (2002). "Charakterisierung von Protein-Protein Interaktionen in Escherichia coli." Diplom thesis. Fachbereich Biologie. University of Konstanz.

Bessette, P. H., F. Aslund, J. Beckwith and G. Georgiou (1999). "Efficient folding of proteins with multiple disulfide bonds in the Escherichia coli cytoplasm." Proc Natl Acad Sci U S A **96**: 13703-8.

Betton, J. M., N. Sassoon, M. Hofnung and M. Laurent (1998). "Degradation versus aggregation of misfolded maltose-binding protein in the periplasm of *Escherichia coli*." J Biol Chem **273**: 8897-902.

Blow, D.M. (1997). "The tortuous story of Asp ... His ... Ser: structural analysis of alpha-chymotrypsin." Trends Biochem Sci **22**: 405-8

Bode, W., E. Meyer, Jr. & J. C. Powers. (1989). "Human leukocyte and porcine pancreatic elastase: X-ray crystal structures, mechanism, substrate specificity, and mechanism- based inhibitors". Biochemistry **28**: 1951-63.

Bode, W., P. J. Barbosa Pereira, A. Bergner, S. Macedo-Ribeiro, R. Huber, G. Matschiner, H. Fritz and C. P. Sommerhoff (1998). " Human β-tryptase is a ring-like tetramer with active sites facing a central pore." Nature **392**: 306-11.

Bode, W., U. Marquardt, F. Zettl, R. Huber and C. P. Sommerhoff (2002). " The crystal structure of human α1-tryptase reveals a blocked substrate-binding region." J Mol Biol **321**: 491-502.

Boyd, D., B. Traxler, and J. Beckwith (1993). "Analysis of the topology of a membrane protein using a minimum number of alkaline phosphatase fusions." J Bacteriol **175**: 553-6.

Brown, M. S., J. Ye, R. B. Rawson and J. L. Goldstein (2000). "Regulated intramembrane proteolysis: a control mechanism conserved from bacteria to humans." Cell **100**: 391-8.

Burgess, R. R. (1996). "Purification of overproduced Escherichia coli RNA polymerase sigma factors by solubilizing inclusion bodies and refolding from Sarkosyl." Methods Enzymol **273**: 145-9.

Buxbaum, J. D., K. N. Liu, Y. Luo, J. L. Slack, K. L. Stocking, J. J. Peschon, R. S. Johnson, B. J. Castner, D. P. Cerretti and R. A. Black (1998). "Evidence that tumor necrosis factor alpha converting enzyme is involved in regulated alpha-secretase cleavage of the Alzheimer amyloid protein precursor." J Biol Chem **273**: 27765-7.

Campbell, W. A., M. K. Iskandar, M. L. Reed and W. Xia (2002). "Endoproteolysis of presenilin in vitro: inhibition by gamma-secretase inhibitors." Biochemistry **41**: 3372-9.

Cao, X. and T. C. Sudhof (2001). "A transcriptionally [correction of transcriptively] active complex of APP with Fe65 and histone acetyltransferase Tip60." Science **293**: 115-20.

Capell, A., J. Grunberg, B. Pesold, A. Diehlmann, M. Citron, R. Nixon, K. Beyreuther, D. J. Selkoe and C. Haass (1998). "The proteolytic fragments of the Alzheimer's disease-associated presenilin-1 form heterodimers and occur as a 100-150-kDa molecular mass complex." J Biol Chem **273**: 3205-11.

Cavarec, L., T. Kamphausen, B. Dubourg, I. Callebaut, F. Lemeunier, D. Metivier, J. Feunteun, G. Fischer and N. Modjtahedi (2002). "Identification and characterization of Moca-cyp. A Drosophila melanogaster nuclear cyclophilin." J Biol Chem **277**: 41171-82.

Chan, Y. M. and Y. N. Jan (1999). "Presenilins, processing of beta-amyloid precursor protein, and notch signaling." Neuron **23**: 201-4.

Cho, K. O., C. A. Hunt and M. B. Kennedy (1992). "The rat brain postsynaptic density fraction contains a homolog of the *Drosophila* discs-large tumor suppressor protein." Neuron **9**: 929-42.

Chong, Y. H., J. M. Jung, W. Choi, C. W. Park, K. S. Choi, Y. H. Suh (1994). "Bacterial expression, purification of full-length and carboxyl terminal fragment of Alzeimer amyloid precursor protein and their proteolytic processing." Life Sci. **54:** 1259-68.

Christman, M. F., R. W. Morgan, F. S. Jacobson and B. N. Ames (1985). "Positive control of a regulon for defenses against oxidative stress and some heat-shock proteins in *Salmonella typhimurium*." Cell **41**: 753-62.

Chung, H. M. and G. Struhl (2001). "Nicastrin is required for presenilin-mediated transmembrane cleavage in *Drosophila*." Nat Cell Biol **3**: 1129-32.

Clark, N. J., W. F. Crow, S. Younkin and S. Naylor (2001). "Analysis of in vivo-derived amyloid-β polypeptides by on-line two-dimensional chromatography-mass spectrometry." Analytical Biochemistry **298**: 32-9.

Claussen, M., B. Kubler, M. Wendland, K. Neifer, B. Schmidt, J. Zapf and T. Braukle (1997). "Proteolysis of insulin-like growth factors (IGF) and IGF binding proteins by cathepsin D." Endocrinology **138**: 3797-803

Clausen, T., C. Southan and M. Ehrmann (2002). "The HtrA family of proteases. Implications for protein composition and cell fate." Mol Cell **10**: 443-55.

Clemmons, D. R. (1998). "Role of insulin-like growth factor binding proteins in controlling IGF actions." Mol. Cell. Endocrinol. **140**: 19-24

Cook, D. G., J. C. Sung, T. E. Golde, K. M. Felsenstein, B. S. Wojczyk, R. E. Tanzi, J. Q. Trojanowski, V. M. Lee and R. W. Doms (1996). "Expression and analysis of presenilin 1 in a human neuronal system: localisation in cell bodies and dendrites." Natl Acad Sci **93**: 9223-28.

Cosson, P. and J. S. Bonifacino (1992). "Role of transmembrane domain interactions in the assembly of class II MHC molecules." Science **258**: 659-62.

Cruts, M., L. Hendriks and C. Van Broeckhoven (1996). "The presenilin genes: a new gene family involved in Alzheimer disease pathology." Hum Mol Genet **5**: 1449-55.

Cupers, P., M. Bentahir, K. Craessaerts, I. Orlans, H. Vanderstichele, P. Saftig, B. De Strooper and W. Annaert (2001). "The discrepancy between presenilin subcellular localization and gamma-secretase processing of amyloid precursor protein." J Cell Biol **154**: 731-40.

Czapinska, H. and J. Otlewski (1999). "Structural and energetic determinants of the S1-site specificity in serine proteases." Eur J Biochem **260**: 571-95.

Czech, C., G. Tremp and L. Pradier (2000). "Presenilins and Alzheimer's disease: biological functions and pathogenic mechanisms." Prog Neurobiol **60**: 363-84.

Demeester, N., C. Mertens, H. Caster, M. Goethals, J. Vandekerckhove, M. Rosseneu and C. Labeur (2001). "Comparison of the aggregation properties, secondary structure and apoptotic effects of wild-type, Flemish and Dutch N-terminally truncated amyloid beta peptides." Eur J Neurosci **13**: 2015-24.

De Strooper, B., L. Umans, F. Van Leuven and H. Van Den Berghe (1993). "Study of the synthesis and secretion of normal and artificial mutants of murine amyloid precursor protein (APP): cleavage of APP occurs in a late compartment of the default secretion pathway." J Cell Biol **121**: 295-304.

De Strooper, B., M. Beullens, B. Contreras, L. Levesque, K. Craessaerts, B. Cordell, D. Moechars, M. Bollen, P. Fraser, P. S. George-Hyslop and F. Van Leuven (1997). "Phosphorylation, subcellular localization, and membrane orientation of the Alzheimer's disease-associated presenilins." J Biol Chem **272**: 3590-8.

DeStrooper, B., P. Saftig, K. Craessaerts, H. Vanderstichele, G. Guhde, W. Annaert, K. von Figura and F. van Leuven (1998). "Deficiency of presenilin-1 inhibits the normal cleavage of amyloid precursor protein." Nature **391**: 387

De Strooper, B., W. Annaert, P. Cupers, P. Saftig, K. Craessaerts, J. S. Mumm, E. H. Schroeter, V. Schrijvers, M. S. Wolfe, W. J. Ray, A. Goate and R. Kopan (1999). "A presenilin-1-dependent gamma-secretase-like protease mediates release of Notch intracellular domain." Nature **398**: 518-22.

DiCera, E. and M. M. Krem (2003). "Serine proteases." Encyclopedia of the human genome 1-9.

Dovey, H. F., V. John, J. P. Anderson, L. Z. Chen, P. de Saint Andrieu, L. Y. Fang, S. B. Freedman, B. Folmer, E. Goldbach, E. J. Holsztynska, K. L. Hu, K. L. Johnson-Wood, S. L. Kennedy, D. Kholodenko, J. E. Knops, L. H. Latimer, M. Lee, Z. Liao, I. M. Lieberburg, R. N. Motter, L. C. Mutter, J. Nietz, K. P. Quinn, K. L. Sacchi, P. A. Seubert, G. M. Shopp, E. D. Thorsett, J. S. Tung, J. Wu, S. Yang, C. T. Yin, D. B. Schenk, P. C. May, L. D. Altstiel, M. H. Bender, L. N. Boggs, T. C. Britton, J. C. Clemens, D. L. Czilli, D. K. Dieckman-McGinty, J. J. Droste, K. S. Fuson, B. D. Gitter, P. A. Hyslop, E. M. Johnstone, W. Y. Li, S. P. Little, T. E. Mabry, F. D. Miller and J. E. Audia (2001). "Functional gamma-secretase inhibitors reduce beta-amyloid peptide levels in brain." J Neurochem **76**: 173-81.

Edbauer, D., E. Winkler, C. Haass and H. Steiner (2002). "Presenilin and nicastrin regulate each other and determine amyloid beta-peptide production via complex formation." Proc Natl Acad Sci U S A **99**: 8666-71.

Ellison, D., J. Hinton, S. J. Hubbard and R. J. Beynon (1995). "Limited proteolysis of native proteins: the interaction between avidin and proteinase K." Protein Sci. **4**: 1337-45.

Esch, F. S., P. S. Keim, E. C. Beattie, R. W. Blacher, A. R. Culwell, T. Oltersdorf, D. McClure and P. J. Ward (1990). "Cleavage of amyloid beta peptide during constitutive processing of its precursor." Science **248**: 1122-4.

Esler, W. P., W. T. Kimberly, B. L. Ostaszewski, T. S. Diehl, C. L. Moore, J. Y. Tsai, T. Rahmati, W. Xia, D. J. Selkoe and M. S. Wolfe (2000). "Transition-state analogue inhibitors of gamma-secretase bind directly to presenilin-1." Nat Cell Biol **2**: 428-34.

Esler, W. P. and M. S. Wolfe (2001). "A portrait of Alzheimer secretases--new features and familiar faces." Science **293**(5534): 1449-54.

Esler, W. P., W. T. Kimberly, B. L. Ostaszewski, W. Ye, T. S. Diehl, D. J. Selkoe and M. S. Wolfe (2002). "Activity-dependent isolation of the presenilin- gamma -secretase complex reveals nicastrin and a gamma substrate." Proc Natl Acad Sci U S A **99**: 2720-5.

Faccio, L., A. Chen, C. Fusco, S. Martinotti, J. V. Bonventre and A. S. Zervos (2000a). "Mxi2, a splice variant of p38 stress-activated kinase, is a distal nephron protein regulated with kidney ischemia." Am J Physiol Cell Physiol **278**: C781-90.

Faccio, L., C. Fusco, A. Chen, S. Martinotti, J. V. Bonventre and A. S. Zervos (2000b). "Characterization of a novel human serine protease that has extensive homology to bacterial heat shock endoprotease HtrA and is regulated by kidney ischemia." J Biol Chem **275**: 2581-8.

Faccio, L., C. Fusco, A. Viel and A. S. Zervos (2000c). "Tissue-specific splicing of Omi stress-regulated endoprotease leads to an inactive protease with a modified PDZ motif." Genomics **68**: 343-7.

Fanning, A. S. and J. M. Anderson (1998). "PDZ domains and the formation of protein networks at the plasma membrane." Curr Top Microbiol Immunol **228**: 209-33.

Fowlkes, J. and M. Freemark (1992). "Evidence for a novel insulin-like growth factor (IGF)-dependent protease regulating IGF-binding protein-4 in dermal fibroblasts." Endocrinology **131**: 2071-6.

Fowlkes, J. L., J.J Enghild, K. Suzuki and H. Nagase (1994). "Matrix metalloproteinases degrade insulin-like growth factor-binding protein-3 in dermal fibroblast cultures." J Biol Chem **269**: 25742-46.

Fairbanks, G., T. L. Steck (1971). "Electrophoretic analysis of the major polypeptides of the human erythrocyte membrane." Biochemistry **10**: 2606-2617.

Francis, R., G. McGrath, J. Zhang, D. A. Ruddy, M. Sym, J. Apfeld, M. Nicoll, M. Maxwell, B. Hai, M. C. Ellis, A. L. Parks, W. Xu, J. Li, M. Gurney, R. L. Myers, C. S. Himes, R. Hiebsch, C. Ruble, J. S. Nye and D. Curtis (2002). "aph-1 and pen-2 are required for Notch pathway signaling, gamma-secretase cleavage of betaAPP, and presenilin protein accumulation." Dev Cell **3**: 85-97.

Goedert, M. (1987). "Neuronal localization of amyloid beta protein precursor mRNA in normal human brain and in Alzheimer's disease." Embo J **6**: 3627-32.

Gottesman, S. (1989). "Genetics of proteolysis in Escherichia coli." Annu Rev Genet **23**: 163-98.

Gray, C. W., R. V. Ward, E. Karran, S. Turconi, A. Rowles, D. Viglienghi, C. Southan, A. Barton, K. G. Fantom, A. West, J. Savopoulos, N. J. Hassan, H. Clinkenbeard, C. Hanning, B. Amegadzie, J. B. Davis, C. Dingwall, G. P. Livi and C. L. Creasy (2000). "Characterization of human HtrA2, a novel serine protease involved in the mammalian cellular stress response." Eur J Biochem **267**: 5699-710.

Grigorenko, A. P., Y. K. Moliaka, G. I. Korovaitseva and E. I. Rogaev (2002). "Novel class of polytopic proteins with domains associated with putative protease activity." Biochemistry (Mosc) **67**: 826-35.

Haass, C., A. Y. Hung, M. G. Schlossmacher, D. B. Teplow and D. J. Selkoe (1993). "beta-Amyloid peptide and a 3-kDa fragment are derived by distinct cellular mechanisms." J Biol Chem **268**: 3021-4.

Harnasch, M. D. (2003). "Structure and function studies of the human Presenilin-1 by using an expression system in E. coli." PhD thesis, Cardiff University.

Haze, K., H. Yoshida, H. Yanagi, T. Yura and K. Mori (1999). "Mammalian transcription factor ATF6 is synthesized as a transmembrane protein and activated by proteolysis in response to endoplasmic reticulum stress." Mol Biol Cell **10**: 3787-99.

Hedstrom, L (2002). "Serine protease mechanism and specifity." Chem Rev **102**: 4501-23.

Hendricks, L., C. M. van Duijn, P. Cras, M. Cruts, W. van Hul, F. van Harskamp, A. Warren, M. G. McInnis, S. E. Antonarakis, and J. J. Martin (1992). "Presenile dementia and cerebral haemorrhage linked to a mutation at codon 692 of the beta-amyloid precursor protein gene." Nature Genet **1**: 218-21.

Herreman, A., L. Serneels, W. Annaert, D. Collen, L. Schoonjans and B. De Strooper (2000). "Total inactivation of gamma-secretase activity in presenilin-deficient embryonic stem cells." Nat Cell Biol **2**: 461-2.

Hoffmann, R., S. Jung, M. Ehrmann and H. W. Hofer (1994). "The *Saccharomyces cerevisiae* gene PPH3 encodes a protein phosphatase with properties different from PPX, PP1 and PP2A." Yeast **10:** 567-78.

Horii, A., T. Kobayashi, N. Tomita, T. Yamamoto, S. Fukushige, T. Murotsu, M. Ogawa, T. Mori and K. Matsubara (1987). "Primary structure of human pancreatic secretory trypsin inhibitor (PSTI) gene." Biochem Biophys Res Commun **149**: 635-41.

Hu, S. I., M. Carozza, M. Klein, P. Nantermet, D. Luk and R. M. Crowl (1998). "Human HtrA, an evolutionarily conserved serine protease identified as a differentially expressed gene product in osteoarthritic cartilage." J Biol Chem **273**: 34406-12.

Hu, Y., Y. Ye and M. E. Fortini (2002). "Nicastrin is required for gamma-secretase cleavage of the *Drosophila* Notch receptor." Dev Cell **2**: 69-78.

Hubbard, S. J., S. F. Campbell and J.M. Thornton (1991). "Molecular recognition. Conformational analysis of limited proteolytic sites and serine proteinase protein inhibitors." J Mol Biol **220**: 507-30.

Hubbard, S. J. (1998). "The structural aspects of limited proteolysis of native proteins." Biochim Biophys Acta **1382**: 191-206.

Huber, R., D. Kukla, W. Bode , P. Schwager, K. Bartels, J. Deisenhofer and W. Steigemann (1974). "Structure of the complex formed by bovine trypsin and bovine pancreatic trypsin inhibitor. II. Crystallographic refinement at 1.9 A resolution." J Mol Biol **89**: 73-101.

Ikezu, T., B. D. Trapp, K. S. Song, A. Schlegel, M. P. Lisanti and T. Okamoto (1998). "Caveolae, plasma membrane microdomains for alpha-secretase-mediated processing of the amyloid precursor protein." J Biol Chem **273**: 10485-95.

Itoh, M., A. Nagafuchi, S. Yonemura, T. Kitani-Yasuda and S. Tsukita (1993). "The 220-kD protein colocalizing with cadherins in non-epithelial cells is identical to ZO-1, a tight junction-associated protein in epithelial cells: cDNA cloning and immunoelectron microscopy." J Cell Biol **121**: 491-502.

Iwata, N., S. Tsubuki, Y. Takaki, K. Watanabe, M. Sekiguchi, E. Hosoki, M. Kawashima-Morishima, H. J. Lee, E. Hama, Y. Sekine-Aizawa and T. C. Saido (2000). "Identification of the major Abeta1-42-degrading catabolic pathway in brain parenchyma: suppression leads to biochemical and pathological deposition." Nat Med **6**): 143-50.

Kaether, C., S. Lammich, D. Edbauer, M. Ertl, J. Rietdorf, A. Capell, H. Steiner and C. Haass (2002). "Presenilin-1 affects trafficking and processing of betaAPP and is targeted in a complex with nicastrin to the plasma membrane." J Cell Biol **158**: 551-61.

Kang, J., H. G. Lemaire, A. Unterbeck, J. M. Salbaum, C. L. Masters, K. H. Grzeschik, G. Multhaup, K. Beyreuther and B. Muller-Hill (1987). "The precursor of Alzheimer's disease amyloid A4 protein resembles a cell-surface receptor." Nature **325**: 733-6.

Kardos, J., A. Bodi, P. Zavodszky, I. Venekei and L. Graf (1999). "Disulfide-linked propeptides stabilize the structure of zymogen and mature pancreatic serine proteases." Biochemistry **38**: 12248-57.

Kato, M. V., H. Sato, T. Tsukada, Y. Ikawa, S. Aizawa and M. Nagayoshi (1996). "A follistatin-like gene, mac25, may act as a growth suppressor of osteosarcoma cells." Oncogene **12**: 1361-4.

Khan, A. R. and M. N. G. James (1998). "Molecular mechanism for the conversion of zymogens to active proteolytic enzymes." Prot Sci **7**: 815-36.

Kim, D. Y., D. R. Kim, S. C. Ha, N. K. Lokanath, C. J. Lee, H. Y. Hwang and K. K. Kim (2002). "Crystal structure of the protease domain of a heat-shock protein HtrA from *Thermotoga maritima*." J Biol Chem 278:6543-5.

Kolmar, H., P. R. Waller and R. T. Sauer (1996). "The DegP and DegQ periplasmic endoproteases of *Escherichia coli*: specificity for cleavage sites and substrate conformation." J Bacteriol **178**: 5925-9.

Konttinen, Y. T., J. Mandelin, T. F. Li, J. Salo, J. Lassus, M. Liljestrom, M. Hukkanen, M. Takagi, I. Virtanen and S. Santavirta (2002). "Acidic cysteine endoproteinase cathepsin K in the degeneration of the superficial articular hyaline cartilage in osteoarthritis." Arthritis Rheum **46**: 953-60.

Kopito, R R. (2000). "Aggresomes, inclusion bodies and protein aggregation." Trends Cell Biol. **10**: 524-30.

Kovasc, D. M., H. J. Fausett, K. J. Page, T. W. Kin, R. D. Moir, D. E. Merriam, R. D. Hollister, O. G. Hallmark, R. Mancini, K. M. Felsenstein, B. T. Hyman, R. E. Tanzi and W. Wasco (1996). "Alzheimer-associated presenilins 1 and 2: neuronal expression in brain and localisation to intracellular membranes in mammalian cells." Nat. Med. **2**: 224-9.

Krojer, T., M. Garrido-Franco, R. Huber, M. Ehrmann and T. Clausen (2002). "Crystal structure of DegP (HtrA) reveals a new protease-chaperone machine." Nature **416**: 455-9.

Kuentzel, S. L., S. M. Ali, R. A. Altman, B. D. Greenberg and T. J. Raub (1993). "The Alzheimer beta-amyloid protein precursor/protease nexin-II is cleaved by secretase in a trans-Golgi secretory compartment in human neuroglioma cells." Biochem J **295**: 367-78.

Lah, J. J. and A. I. Levey (2000). "Endogenous presenilin-1 targets to endocytic rather than biosynthetic compartments." Mol Cell Neurosci **16**: 111-26.

Lammich, S., E. Kojro, R. Postina, S. Gilbert, R. Pfeiffer, M. Jasionowski, C. Haass and F. Fahrenholz (1999). "Constitutive and regulated alpha-secretase cleavage of Alzheimer's amyloid precursor protein by a disintegrin metalloprotease." Proc Natl Acad Sci U S A **96**: 3922-7.

Lazure, C. (2002). "The peptidase zymogen proregions: nature's way of preventing undesired activation and proteolysis." Cur. Pharm. Design **8**: 125-33.

LeBlanc, A. C., H. Y. Chen, L. Autilio-Gambetti and P. Gambetti (1991). "Differential APP gene expression in rat cerebral cortex, meninges, and primary astroglial, microglial and neuronal cultures." FEBS Lett **292**: 171-8.

Lee, D. M. and M. E. Weinblatt (2001). "Rheumatoid arthritis." Lancet **358**: 903-11.

Lee, H. J., K. M. Jung, Y. Z. Huang, L. B. Bennett, J. S. Lee, L. Mei and T. W. Kim (2002). "Presenilin-dependent gamma-secretase-like intramembrane cleavage of ErbB4." J Biol Chem **277**: 6318-23.

Lemmon, M. A., J. M. Flanagan, R. T. Herbert, J. Zhang and D. M. Engelman (1992). "Sequence specifity in the dimerisation of transmembrane a-helices." Biochemistry **31**: 12719-25.

Levy-Lahad, E., P. Poorkaj, K. Wang, Y. H. Fu, J. Oshima, J. Mulligan and G. D. Schellenberg (1996). "Genomic structure and expression of STM2, the chromosome 1 familial Alzheimer disease gene." Genomics **34**: 198-204.

Li, W., S. M. Srinivasula, J. Chai, P. Li, J. W. Wu, Z. Zhang, E. S. Alnemri and Y. Shi (2002). "Structural insights into the pro-apoptotic function of mitochondrial serine protease HtrA2/Omi." Nat Struct Biol **9**: 436-41.

Li, Y. M., M. Xu, M. T. Lai, Q. Huang, J. L. Castro, J. DiMuzio-Mower, T. Harrison, C. Lellis, A. Nadin, J. G. Neduvelil, R. B. Register, M. K. Sardana, M. S. Shearman, A. L. Smith, X. P. Shi, K. C. Yin, J. A. Shafer and S. J. Gardell (2000). "Photoactivated gamma-secretase inhibitors directed to the active site covalently label presenilin 1." Nature **405**: 689-94.

Lipinska, B., S. Sharma and C. Georgopoulos (1988). "Sequence analysis and regulation of the *htrA* gene of *Escherichia coli*: a sigma 32-independent mechanism of heat-inducible transcription." Nucleic Acids Res **16**: 10053-67.

Lipinska, B., M. Zylicz and C. Georgopoulos (1990). "The HtrA (DegP) protein, essential for *Escherichia coli* survival at high temperatures, is an endopeptidase." J Bacteriol **172**: 1791-7.

Ly, L. P. and D. J. Handelsman (2002). "Muscle strength and ageing: methodological aspects of isokinetic dynamometry and androgen administration." Clin Exp Pharmacol Physiol **29**: 37-47.

Marambaud, P., J. Shioi, G. Serban, A. Georgakopoulos, S. Sarner, V. Nagy, L. Baki, P. Wen, S. Efthimiopoulos, Z. Shao, T. Wisniewski and N. K. Robakis (2002). "A presenilin-1/gamma-secretase cleavage releases the E-cadherin intracellular domain and regulates disassembly of adherens junctions." Embo J **21**: 1948-56.

Marquardt, U., F. Zettl, R. Huber, W. Bode and C. P. Sommerhoff (2002). "The crystal structure of human α1-tryptase reveals a blocked substrate-binding region." J Mol Biol **321**: 491-502.

Maurizi, M. R. (1992). "Proteases and protein degradation in *Escherichia coli*." Experientia **48**: 178-201.

Maurizi, M. R. (2002). "Love it or cleave it: tough choices in protein quality control." Nat Struct Biol **9**: 410-2.

May, P., Y. K. Reddy and J. Herz (2002). "Proteolytic processing of low density lipoprotein receptor-related protein mediates regulated release of its intracellular domain." J Biol Chem **277**: 18736-43.

Miller, C. G. (1987). "Protein degradation and proteolytic modification." *In E. C. Neidhardt, J.L. Ingraham, K. B. Low, B. Magasanik, M. Schaechter and H. E. Umbarger. Escherichia coli and Salmonella typhimurium: Cellular and Molecular Biology. American Society for Microbiology. Washington. D. C.,* 680-91.

Miller J. (1972). "Experiments in molecular genetics." Cold Spring Harbour, NY, Cold Spring Harbour Laboratory.

Mills, J. and P. B. Reiner (1999). "Regulation of amyloid precursor protein cleavage." J Neurochem **72**: 443-60.

Moss, M. L., J. M. White, M. H. Lambert and R. C. Andrews (2001). "TACE and other ADAM proteases as targets for drug discovery." Drug Discov. Today **6**: 417-26.

Moussaoui, S., C. Czech, L. Pradier, V. Blanchard, B. Bonici, M. Gohin, A. Imperato and F. Revah (1996). "Immunohistochemical analysis of presenilin-1 expression in the mouse brain." FEBS Lett **383**: 219-22.

Mueller, H. T., J. P. Borg, B. Margolis and R. S. Turner (2000). "Modulation of amyloid precursor protein metabolism by X11alpha /Mint-1. A deletion analysis of protein-protein interaction domains." J Biol Chem **275**: 39302-6.

Namba, Y., M. Tomonaga, H. Kawasaki, E. Otomo and K. Ikeda (1991). "Apolipoprotein E immunoreactivity in cerebral amyloid deposits and neurofibrillary tangles in Alzheimer's disease and kuru plaque amyloid in Creutzfeldt-Jakob disease." Brain Res **541**: 163-6.

Naruse, S., G. Thinakaran, J. J. Luo, J. W. Kusiak, T. Tomita, T. Iwatsubo, X. Qian, D. D. Ginty, D. L. Price, D. R. Borchelt, P. C. Wong and S. S. Sisodia (1998). "Effects of PS1 deficiency on membrane protein trafficking in neurons." Neuron **21**: 1213-21.

Neidhardt, F.C., R. A. Van Bogelen, V. Vaughn (1984). "The genetics and regulation of heat-shock proteins." Annu. Rev. Genet. **18**: 295-329.

Nie, G. Y., A. Hampton, Y. Li, J. K. Findlay and L. A. Salamonsen (2003). "Identification and cloning of two isoforms of human HtrA3, characterisation of its genomic structure and comparison of its tissue distribution with HtrA1 and HtrA2." Biochem J **371**: 39-48.

Nielsen H., J. Engelbrecht, S. Brunak and G. von Heijne (1997). "Identification of prokaryotic and eukaryotic signal peptides and prediction of their cleavage sites." Protein Eng **10**: 1-6.

Niwa, M., C. Sidrauski, R. J. Kaufman and P. Walter (1999). "A role for presenilin-1 in nuclear accumulation of Ire1 fragments and induction of the mammalian unfolded protein response." Cell **99**: 691-702.

Orzaez, M., E. Perez-Paya and I. Mingarro (2000). "Influence of the C-terminus of the glycophorin A transmembrane fragment on the dimerisation process." Protein Science **9**: 9998-9.

Pereira, P. J. B., A. Bergner, S. Macedo-Ribeiro, R. Huber, G. Matschiner, H. Fritz, C. P. Sommerhoff and W. Bode (1998). "Human β-tryptase is a ring-like tetramer with active sites facing a central pore." Nature **392**: 306-11.

Perez, R. G., S. Soriano, J. D. Hayes, B. Ostaszewski, W. Xia, D. J. Selkoe, X. Chen, G. B. Stokin and E. H. Koo (1999). "Mutagenesis identifies new signals for beta-amyloid precursor protein endocytosis, turnover, and the generation of secreted fragments, including Abeta42." J Biol Chem **274**: 18851-6.

Perona, J. J. and C. S. Craik (1995). "Structural basis of substrate specificity in the serine proteases." Protein Sci **4**: 337-60.

Podlisny, M. B., M. Citron, P. Amarante, R. Sherrington, W. Xia, J. Zhang, T. Diehl, G. Levesque, P. Fraser, C. Haass, E. H. Koo, P. Seubert, P. St George-Hyslop, D. B. Teplow and D. J. Selkoe (1997). "Presenilin proteins undergo heterogeneous endoproteolysis between Thr291 and Ala299 and occur as stable N- and C-terminal fragments in normal and Alzheimer brain tissue." Neurobiol Dis **3**: 325-37.

Polverino de Laureto, P., E. Scaramella, M. Frigo, F. G. Wondrich, V. De Filippis, M. Zambonin and A. Fontana (1999). "Limited proteolysis of bovine alpha-lactalbumin: isolation and characterization of protein domains." Protein Sci. **8**: 2290-303.

Polverino de Laureto, P., D. Vinante, E. Scaramella, E. Frare and A. Fontana (2001). "Stepwise proteolytic removal of the beta subdomain in alpha-lactalbumin. The protein remains folded and can form the molten globule in acid solution." Eur J Biochem. **268**: 4324-33.

Polverino de Laureto, P., E. Frare, R Gottardo., H. Van Dael and A. Fontana (2002). "Partly folded states of members of the lysozyme/lactalbumin superfamily: a comparative study by circular dichroism spectroscopy and limited proteolysis." Protein Sci. **11**: 2932-46.

Ponting, C. P. (1997). "Evidence for PDZ domains in bacteria, yeast, and plants." Protein Sci **6**: 464-8.

Pradier, L., N. Carpentier, L. Delalonde, N. Clavel, M.-D. Bock, L. Buee, L. Mercken, B. Tocque and C. Czech (1999). "Mapping the APP/Presenilin (PS) binding domains: the hydrophilic N-terminus of PS2 is sufficient for interaction with APP and can displace APP/PS1 interaction." Neurobiology of disease **6**: 43-55.

Prinz, W. A., C. Spiess, M. Ehrmann, C. Schierle and J. Beckwith (1996). "Targeting the signal sequenceless proteins for export in *Escherichia coli* with altered protein translocase." Embo J **15**: 5209-17.

Qiu, W. Q., D. M. Walsh, Z. Ye, K. Vekrellis, J. Zhang, M. B. Podlisny, M. R. Rosner, A. Safavi, L. B. Hersh and D. J. Selkoe (1998). "Insulin-degrading enzyme regulates extracellular levels of amyloid beta-protein by degradation." J Biol Chem **273**: 32730-8.

Rawlings, N. D. and A. J. Barrett (1994). "Families of serine peptidases." Methods Enzymol **244**: 19-61.

Richards, A. D., L. H. Phylip, W. G. Farmerie, P. E. Scarborough, A. Alvarez, B. M. Dunn, P. H. Hirel, J. Konvalinka, P. Strop, L. Pavlickova, V. Kostka and J. Kay (1990). "Sensitive, soluble chromogenic substrates for HIV-1 proteinase." J Biol Chem **265**: 7733-6.

Rogaev, E. I., R. Sherrington, E. A. Rogaeva, G. Levesque, M. Ikeda, Y. Liang, H. Chi, C. Lin, K. Holman and T. Tsuda (1995). "Familial Alzheimer's disease in kindreds with missense mutations in a gene on chromosome 1 related to the Alzheimer's disease type 3 gene." Nature **376**: 775-8.

Roncarati, R., N. Sestan, M. H. Scheinfeld, B. E. Berechid, P. A. Lopez, O. Meucci, J. C. McGlade, P. Rakic and L. D'Adamio (2002). "The gamma-secretase-generated intracellular domain of beta-amyloid precursor protein binds Numb and inhibits Notch signaling." Proc Natl Acad Sci U S A **99**: 7102-7.

Sambamurti, K., J. Shioi, J. P. Anderson, M. A. Pappolla and N. K. Robakis (1992). "Evidence for intracellular cleavage of the Alzheimer's amyloid precursor in PC12 cells." J Neurosci Res **33**: 319-29.

Savopoulos, J. W., P. S. Carter, S. Turconi, G. R. Pettman, E. H. Karran, C. W. Gray, R. V. Ward, O. Jenkins and C. L. Creasy (2000). "Expression, purification, and functional analysis of the human serine protease HtrA2." Protein Expr Purif **19**: 227-34.

Saxena, M. T., E. H. Schroeter, J. S. Mumm and R. Kopan (2001). "Murine notch homologs (N1-4) undergo presenilin-dependent proteolysis." J Biol Chem **276**: 40268-73.

Schechter, I. and A. Berger (1967) "On the size of the active site in proteases" Biochem. Biophys Res Com 27: 157-62.

Scheinfeld, M. H., E. Ghersi, K. Laky, B. J. Fowlkes and L. D'Adamio (2002). "Processing of beta-amyloid precursor-like protein-1 and -2 by gamma-secretase regulates transcription." J Biol Chem **277**: 44195-201.

Selkoe, D. J. (1998). "The cell biology of beta-amyloid precursor protein and presenilin in Alzheimer's disease." Trends Cell Biol **8**: 447-53.

Selkoe, D. J. (2001). "Alzheimer's disease: genes, proteins and therapy." Physiological Reviews **81**: 741-65

Seol, J. H., S. K. Woo, E. M. Jung, S. J. Yoo, C. S. Lee, K. J. Kim, K. Tanaka, A. Ichihara, D. B. Ha and C. H. Chung (1991). "Protease Do is essential for survival of *Escherichia coli* at high temperatures: its identity with the *htrA* gene product." Biochem Biophys Res Commun **176**: 730-6.

Shaywitz, A. J., Dove, S. L., Kornhauser, J. M., Hochschild, A. & Greenberg, M. E. (2000). "Magnitude of the CREB-dependent transcriptional response is determined by the strength of the interaction between the kinase-inducible domain of CREB and the KIX domain of CREB-binding protein." Mol Cell Biol **20:** 9409-22.

Sherrington, R., E. I. Rogaev, Y. Liang, E. A. Rogaeva, G. Levesque, M. Ikeda, H. Chi, C. Lin, G. Li, K. Holman et al. (1995). "Cloning of a gene bearing missense mutations in early-onset familial Alzheimer's disease." Nature **375**: 754-60.

Shimasaki, S., M. Koga, F. Esch, K. Cooksey, M. Mercado, A. Koba, N. Ueno, S. Y. Ying, N. Ling and R. Guillemin (1988). "Primary structure of the human follistatin precursor and its genomic organization." Proc Natl Acad Sci U S A **85**: 4218-22.

Shizuka-Ikeda, M., E. Matsubara, M. Ikeda, M. Kanai, Y. Tomidokoro, Y. Ikeda, M. Watanabe, T. Kawarabayashi, Y. Harigaya, K. Okamoto, K. Maruyama, E. M. Castano, P. St George-Hyslop and M. Shoji (2002). "Generation of amyloid beta protein from a presenilin-1 and betaAPP complex." Biochem Biophys Res Commun **292**: 571-8.

Shridhar, V., A. Sen, J. Chien, J. Staub, R. Avula, S. Kovats, J. Lee, J. Lillie and D. I. Smith (2002). "Identification of underexpressed genes in early- and late-stage primary ovarian tumors by suppression subtraction hybridization." Cancer Res **62**: 262-70.

Shotton, D. M. and H. C. Watson. (1970). "Three-dimensional structure of tosyl-elastase." Nature **25**: 811-16

Silhavy, T. J., Berman, M. L. and L. W. Enquist (1984). "Experiments with gene fusions." *Cold Spring Harbor Press. Cold Spring Harbor, New York.* pp 303.

Simmons, L. C. and D. G. Yansura (1996). "Translational level is a critical factor for the secretion of heterologous proteins in *Escherichia coli.*" Nat Biotechnol **14**: 629-34.

Sisodia, S. S. (1992). "Beta-amyloid precursor protein cleavage by a membrane-bound protease." Proc Natl Acad Sci U S A **89**: 6075-9.

Skorko-Glonek, J., K. Krzewski, B. Lipinska, E. Bertoli and F. Tanfani (1995). "Comparison of the structure of wild-type HtrA heat shock protease and mutant HtrA proteins. A Fourier transform infrared spectroscopic study." J Biol Chem **270**: 11140-6.

Skorko-Glonek, J., A. Wawrzynow, K. Krzewski, K. Kurpierz and B. Lipinska (1995). "Site-directed mutagenesis of the HtrA (DegP) serine protease, whose proteolytic

activity is indispensable for *Escherichia coli* survival at elevated temperatures." Gene **163**: 47-52.

Songyang, Z., A. S. Fanning, C. Fu, J. Xu, S. M. Marfatia, A. H. Chishti, A. Crompton, A. C. Chan, J. M. Anderson and L. C. Cantley (1997). "Recognition of unique carboxyl-terminal motifs by distinct PDZ domains." Science **275**: 73-7.

Spiess, C., A. Beil and M. Ehrmann (1999). "A temperature-dependent switch from chaperone to protease in a widely conserved heat shock protein." Cell **97**: 339-47.

Stadtman, E. R. (1990). "Covalent modification reactions are marking steps in protein turnover." Biochemistry **29**: 6323-31.

Stein, R.L., A. M. Strimpler, H. Hori and J. C Powers (1987). "Catalysis by human leukocyte elastase: mechanistic insights into specificity requirements". Biochemistry. **26**: 1301-5.

Steiner, H., E. Winkler, D. Edbauer, S. Prokop, G. Basset, A. Yamasaki, M. Kostka and C. Haass (2002). "PEN-2 is an integral component of the gamma-secretase complex required for coordinated expression of presenilin and nicastrin." J Biol Chem **277**: 39062-5.

Strauch, K. L. and J. Beckwith (1988). "An *Escherichia coli* mutation preventing degradation of abnormal periplasmic proteins." Proc Natl Acad Sci U S A **85**: 1576-80.

Strittmatter, W. J., A. M. Saunders, D. Schmechel, M. Pericak-Vance, J. Enghild, G. S. Salvesen and A. D. Roses (1993). "Apolipoprotein E: high-avidity binding to beta-amyloid and increased frequency of type 4 allele in late-onset familial Alzheimer disease." Proc Natl Acad Sci U S A **90**: 1977-81.

Suh, Y. H. and F. Checler (2002). "Amyloid precursor protein, presenilins, and alpha-synuclein: molecular pathogenesis and pharmacological applications in Alzheimer's disease." Pharmacol Rev **54**: 469-525.

Suzuki, C. K., M. Rep, J. M. van Digl, K. Sud, L. A. Grivell, G. Schatz (1997). "ATP-deüendent proteases that also chaperone protein biogenesis." Trends Biochem. Sci. **22**: 118-23.

Suzuki, T., K. Nishiyama, S. Murayama, A. Yamamoto, S. Sato, I. Kanazawa and Y. Sakaki (1996). "Regional and cellular presenilin 1 gene expression in human and rat tissues." Biochem Biophys Res Commun **219**: 708-13.

Swamy, K. H., C. H. Chung and A. L. Goldberg (1983). "Isolation and characterization of protease do from Escherichia coli, a large serine protease containing multiple subunits." Arch Biochem Biophys **224**: 543-54.

Tanzi, R. E., J. F. Gusella, P. C. Watkins, G. A. Bruns, P. St George-Hyslop, M. L. Van Keuren, D. Patterson, S. Pagan, D. M. Kurnit and R. L. Neve (1987). "Amyloid beta

protein gene: cDNA, mRNA distribution, and genetic linkage near the Alzheimer locus." Science **235**: 880-4.

Thinakaran, G., D. R. Borchelt, M. K. Lee, H. H. Slunt, L. Spitzer, G. Kim, T. Ratovitsky, F. Davenport, C. Nordstedt, M. Seeger, J. Hardy, A. I. Levey, S. E. Gandy, N. A. Jenkins, N. G. Copeland, D. L. Price and S. S. Sisodia (1996). "Endoproteolysis of presenilin 1 and accumulation of processed derivatives in vivo." Neuron **17**: 181-90.

Thinakaran, G., J. B. Regard, C. M. Bouton, C. L. Harris, D. L. Price, D. R. Borchelt and S. S. Sisodia (1998). "Stable association of presenilin derivatives and absence of presenilin interactions with APP." Neurobiol Dis **4**: 438-53.

Tomita, T., T. Watabiki, R. Takikawa, Y. Morohashi, N. Takasugi, R. Kopan, B. De Strooper and T. Iwatsubo (2001). "The first proline of PALP motif at the C terminus of presenilins is obligatory for stabilization, complex formation, and gamma-secretase activities of presenilins." J Biol Chem **276**: 33273-81.

Tomita, T., R. Katayama, R. Takikawa and T. Iwatsubo (2002). "Complex N-glycosylated form of nicastrin is stabilized and selectively bound to presenilin fragments." FEBS Lett **520**:117-21.

Tsai, C. J., P. Polverino de Laureto, A. Fontana and R. Nussinov (2002). "Comparison of protein fragments identified by limited proteolysis and by computational cutting of proteins." Protein Sci. **11**: 1753-70.

Uhland, K., M. Mondigler, C. Spiess, W. Prinz and M. Ehrmann (2000). "Determinants of translocation and folding of TreF, a trehalase of *Escherichia coli*." J Biol Chem **275**: 23439-45.

Urban, S., J. R. Lee and M. Freeman (2001). "*Drosophila* rhomboid-1 defines a family of putative intramembrane serine proteases." Cell **107**: 173-82.

Vassar, R., B. D. Bennett, S. Babu-Khan, S. Kahn, E. A. Mendiaz, P. Denis, D. B. Teplow, S. Ross, P. Amarante, R. Loeloff, Y. Luo, S. Fisher, J. Fuller, S. Edenson, J. Lile, M. A. Jarosinski, A. L. Biere, E. Curran, T. Burgess, J. C. Louis, F. Collins, J. Treanor, G. Rogers and M. Citron (1999). "Beta-secretase cleavage of Alzheimer's amyloid precursor protein by the transmembrane aspartic protease BACE." Science **286**: 735-41.

Verhagen, A. M., J. Silke, P. G. Ekert, M. Pakusch, H. Kaufmann, L. M. Connolly, C. L. Day, A. Tikoo, R. Burke, C. Wrobel, R. L. Moritz, R. J. Simpson and D. L. Vaux (2002). "HtrA2 promotes cell death through its serine protease activity and its ability to antagonize inhibitor of apoptosis proteins." J Biol Chem **277**: 445-54.

Walker, G. C. (1987). "The SOS response of Escherichia coli. *In E. C. Neidhardt, J. L. Ingraham, K. B. Low, Magasanik, M. Schaechter, M. and H. E. Umbarger. Escherichia coli and Salmonella typhimurium: Cellular and Molecular Biology. American Society of Microbiology. Washington D. C.*, 1346-57.

Weidemann, A., G. Konig, D. Bunke, P. Fischer, J. M. Salbaum, C. L. Masters and K. Beyreuther (1989). "Identification, biogenesis, and localization of precursors of Alzheimer's disease A4 amyloid protein." Cell **57**: 115-26.

Weihofen, A., K. Binns, M. K. Lemberg, K. Ashman and B. Martoglio (2002). "Identification of signal peptide peptidase, a presenilin-type aspartic protease." Science **296**: 2215-8.

Wolfe, M. S., W. Xia, B. L. Ostaszewski, T. S. Diehl, W. T. Kimberly, D. J. Selkoe (1999). "Two transmembrane aspartates in presenilin-1 required for presenilin endoproteolysis and gamma-secretase activity." Nature **398**: 513-17.

Woods, D. F. and P. J. Bryant (1991). "The discs-large tumor suppressor gene of Drosophila encodes a guanylate kinase homolog localized at septate junctions." Cell **66**: 451-64.

Wootton, J. C. and M. H. Drummond (1989). "The Q-linker: a class of interdomain sequences found in bacterial multidomain regulatory proteins." Protein Eng **2**: 535-43.

Xia, W., J. Zhang, D. Kholodenko, M. Citron, M. B. Podlisny, D. B. Teplow, C. Haass, P. Seubert, E. H. Koo and D. J. Selkoe (1997). "Enhanced production and oligomerization of the 42-residue amyloid beta-protein by Chinese hamster ovary cells stably expressing mutant presenilins." J Biol Chem **272**: 7977-82.

Xia, W., W. J. Ray, B. L. Ostaszewski, T. Rahmati, W. T. Kimberly, M. S. Wolfe, J. Zhang, A. M. Goate and D. J. Selkoe (2000). "Presenilin complexes with the C-terminal fragments of amyloid precursor protein at the sites of amyloid beta-protein generation." Proc Natl Acad Sci U S A **97**: 9299-304

Xu, X., Y. C. Shi, W. Gao, G. Mao, G. Zhao, S. Agrawal, G. M. Chisolm, D. Sui and M. Z. Cui (2002). "The novel presenilin-1-associated protein (PSAP) is a pro-apoptotic mitochondrial protein." J Biol Chem **277**:48913-2

Yang, D. S., Tandon, A., Chen, F., Yu, G., Yu, H., Arawaka, S., Hasegawa, H., Duthie, M., Schmidt, S. D., Ramabhadran, T. V., Nixon, R. A., Mathews, P. M., Gandy, S. E., Mount, H. T., George-Hyslop, P., and P. E. Fraser (2002) "Mature glycosylation and trafficking of nicastrin modulate its binding to presenilins." J Biol Chem **277**: 28135-42

Yu, G., F. Chen, G. Levesque, M. Nishimura, D. M. Zhang, L. Levesque, E. Rogaeva, D. Xu, Y. Liang, M. Duthie, P. H. St George-Hyslop and P. E. Fraser (1998). "The presenilin 1 protein is a component of a high molecular weight intracellular complex that contains beta-catenin." J Biol Chem **273**: 16470-5.

Yu, G., M. Nishimura, S. Arawaka, D. Levitan, L. Zhang, A. Tandon, Y. Q. Song, E. Rogaeva, F. Chen, T. Kawarai, A. Supala, L. Levesque, H. Yu, D. S. Yang, E. Holmes, P. Milman, Y. Liang, D. M. Zhang, D. H. Xu, C. Sato, E. Rogaev, M. Smith, C. Janus, Y. Zhang, R. Aebersold, L. S. Farrer, S. Sorbi, A. Bruni, P. Fraser and P. St George-Hyslop (2000). "Nicastrin modulates presenilin-mediated notch/glp-1 signal transduction and betaAPP processing." Nature **407**: 48-54.

Yue, B. G., P. Ajuh, G. Akusjarvi, A. I. Lamond and J. P. Kreivi (2000). "Functional coexpression of serine protein kinase SRPK1 and its substrate ASF/SF2 in *Escherichia coli*." Nucleic Acids Res. **28**: E14.

Zhang, J., D. E. Kang, W. Xia, M. Okochi, H. Mori, D. J. Selkoe and E. H. Koo (1998). "Subcellular distribution and turnover of presenilins in transfected cells." J Biol Chem **273**: 12436-42.

Zheng, B., J. B. Clarke, W. H. Busby, C. Duan and D. R. Clemmons (1998). "Insulin-like growth factor-binding protein-5 is cleaved by physiological concentrations of thrombin." Endocrinology **139**:1708-14.

Zumbrunn, J. and B. Trueb (1996). "Primary structure of a putative serine protease specific for IGF- binding proteins." FEBS Lett **398**: 187-92.

7 Appendix

7.1 Table of figures